THE

LONDON, EDINBURGH, AND DUBLIN

PHILOSOPHICAL MAGAZINE

AND

JOURNAL OF SCIENCE.

[SIXTH SERIES.]

NOVEMBER 1924.

LXXVI. *On the Impact of a Solid Sphere with a Fluid Surface and the Influence of Surface Tension, Surface Layers, and Viscosity on the Phenomenon.* By G. ERIC BELL, *B.Sc., Physics Research Laboratory, University College, Nottingham* *.

[Plate XV.]

THE phenomena attending impact with fluid surfaces were first studied by Worthington †, who traced by means of instantaneous photography the course of events after the impact. He showed that splashes fall into two fairly clearly defined classes, one in which no air is drawn into the liquid, which he calls a "smooth" or "airless" splash, and the other in which a large air-cavity is produced, which he calls a "rough" or "basket" splash. If the falling body be a sphere, quite clean and free from grease, the splash is smooth for low impact-velocities but becomes rough if the velocity is increased, the transition from one to the other being quite sudden. Traces of grease and dust make this "critical velocity" much less, and it is also less if an oil is used instead of water. Worthington attempts an explanation of the effect of dust, and also of the different effect in the case of oil, and shows that any factor which renders the surface shearable produces a rough splash.

* Communicated by Prof. E. H. Barton, F.R.S.

† Worthington, Phil. Trans. Roy. Soc., A 193. (1897) and A 225. (1900).

Mallock * develops a simple mathematical theory of the shape of the cavity produced, confining his attention to the case of the impact of a solid sphere with a fluid surface. This theory gives the general shape of the cavity, but does not agree exactly with experiment, and there appear to be contributing factors of which he does not take account.

The object of the present research is to examine the phenomena in more detail, with special reference to the effect of surface-layers on the impinging ball, and the surface tension and viscosity of the liquid, and to try to extend Mallock's theory.

Experimental Procedure.

The general method of experiment is similar to that of Worthington and Mallock, but differs slightly from either. The apparatus is shown diagrammatically in fig. 1. The Leyden-jar battery L has its inner coating connected to one pole of a Wimshurst machine, its outer coating, together with the other pole of the machine, being earthed. The inner coating is then connected to two spark-gaps A and B in series, and finally to earth. The Wimshurst machine is run at a steady rate by means of a small electric motor, and serves to charge up the jars. M and M′ are two small electromagnets connected through a key K to a battery of cells. On depressing the key K, the electromagnets release respectively a large ball which falls between the electrodes of the first spark-gap A, and a small ball which falls into the liquid in the tank T.

When the large ball falls through the spark-gap A the resistance of the whole circuit is reduced and the potential-difference established serves to cause a spark to leap across the second gap B. By suitably arranging the height through which the large ball falls, the splash caused by the other one may be photographed at any time.

The balls employed are Hoffmann steel balls, of diameters 1 inch and 5/16 inch. The secondary spark-gap B has magnesium electrodes, and produces a very brilliant, highly actinic spark, casting a shadow of the splash which is recorded on the photographic plate P.

As steel balls are used, it is possible to suspend them from the poles of the magnets directly, thus simplifying the arrangements and also avoiding any constraints such as would cause the balls to rotate.

* Mallock, Proc. Roy. Soc. xcv. (1918).

Imperial "Special Rapid" plates (H & D 250) were used, developed with Tabloid "Rytol" or a special developer recommended by the makers of the plates.

The timing caused a certain amount of trouble at first, but by reducing the strength of the magnets by means of the rheostats R and R′ so that they only just supported the balls,

Fig. 1.

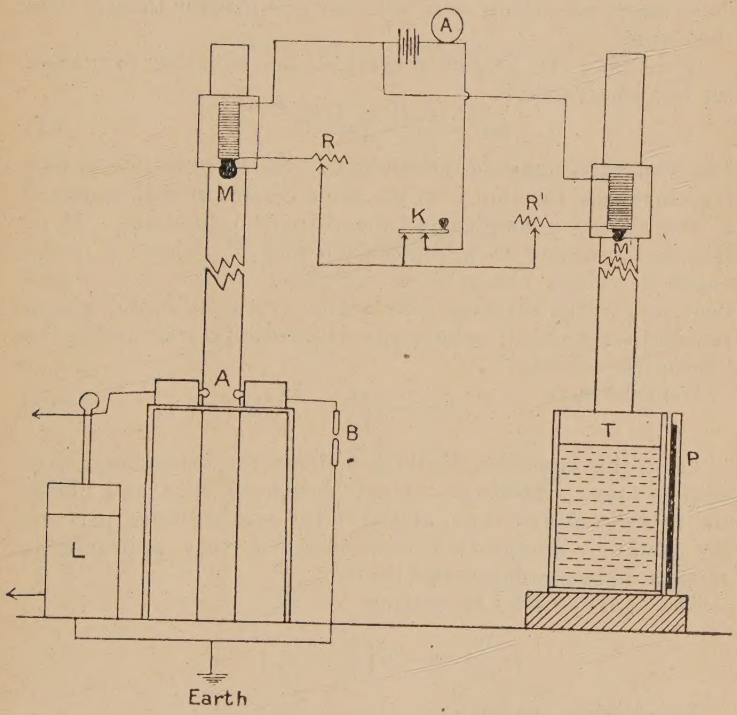

Diagram of Apparatus.

and keeping the electrodes, especially those of the large gap A, clean and polished, this difficulty was overcome and photographs taken under similar conditions "reproduced" with accuracy.

By this means a large number of photographs have been obtained, showing the effect of coating the ball with surface-layers of different substances, of using different liquids, and of changing the viscosity of the liquid.

Mallock's Theory and Comparison with Experimental Results.

Consider a sphere of density ρ falling normally with velocity v into a fluid of unit density. As long as the cavity remains open to the surface the sphere is influenced by (1) a hydrodynamic resistance, Av^2, proportional to the square of the velocity, (2) a hydrostatic pressure proportional to the depth, Bx, and (3) an acceleration C, upwards or downwards according as to whether ρ is greater than or less than unity.

If we take the axis of x vertical, the equation to motion for this small time is

$$\dot{v} = -Av^2 - Bx + C. \quad . \quad . \quad . \quad . \quad . \quad . \quad (1)$$

The constants may be eliminated. So long as the cavity remains open, the shot is in the same condition as if mounted at the end of a weightless tube of its own diameter. It is, therefore, subject to a retardation $g(x'/h)$, where h is the depth at which the tube, as weighted by the shot, would float, and x' the distance from a new origin at h, and also a retardation $g(v_1^2/v_0^2)$, where v_1 is the velocity at x' and v_0 the "terminal velocity."

We thus have

$$\dot{v} = -g\left(\frac{x'}{h} - \frac{v_1^2}{v_0^2}\right). \quad . \quad . \quad . \quad . \quad . \quad (2)$$

From this equation, Mallock deduces the space-time curve step by step. However, we may integrate once and obtain the velocity at any time, and also, for special cases, perform the complete integration and obtain a very approximate relation between depth and time.

The equation may be written

$$v_1 \frac{dv_1}{dx'} = -g\left(\frac{x'}{h} - \frac{v_1^2}{v_0^2}\right).$$

Integrating, we have

$$v_1^2 = Ce^{-\frac{2g}{v_0^2}x'} - \frac{v_0^2}{h}\left(x' - \frac{1}{2}\frac{v_0^2}{g}\right).$$

Inserting the initial conditions, that the sphere is at the surface when $t=0$, with a velocity v_s, i. e., at $t=0$, $x'=-h$, and $v=v_s$, we have

$$v^2 = e^{-\frac{2g}{v_0^2}(h+x')}\left\{v_s^2 - \frac{v_0^2}{h}\left(h + \frac{v_0^2}{2g}\right)\right\} - \frac{v_0^2}{h}\left(x' - \frac{v_0^2}{2g}\right). \quad . \quad (3)$$

For water, and liquids of similar viscosity (of the order ·01) the "terminal velocity" v_0 is very high (for a steel

sphere 5/16 in. diameter v_0 is of the order 2000 cm. per sec.) and the equation of motion (2) may be simplified to

$$v_1 \frac{dv_1}{dx} = -\frac{g}{h}x', \quad \ldots \ldots \quad (4)$$

giving on integration

$$x' = \mathrm{A} \sin \sqrt{\frac{g}{h}}t - \mathrm{B} \cos \sqrt{\frac{g}{h}}t,$$

or

$$x' = \mathrm{A} \sin pt - \mathrm{B} \cos pt \quad \text{where } p^2 = g/h,$$

and

$$v_1 = \frac{g}{h}\{\mathrm{A} \cos pt + \mathrm{B} \sin pt\}.$$

Inserting the initial conditions that at $t=0$, $x' = -h$ and $v_1 = v_s$, we have

$$x' = v_s \frac{h}{g} \sin pt - h \cos pt. \quad \ldots \ldots \quad (5)$$

Fig. 2.

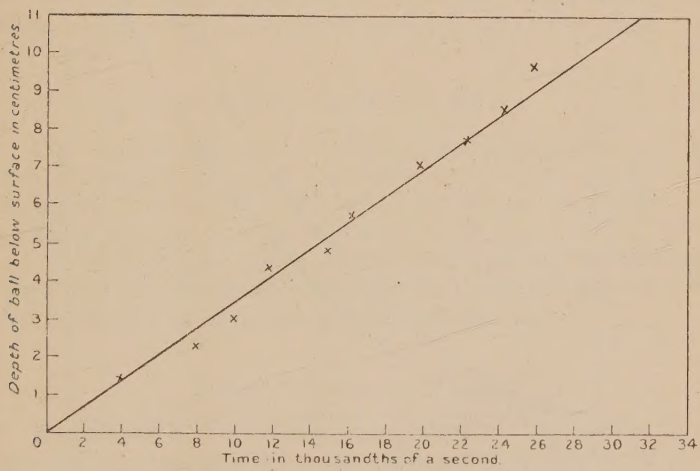

Space-time Graph for Sphere in Water.

Thus, for the very limited time for which the assumed conditions are valid, the space-time curve is a straight line. That this is substantially true is evident from fig. 2, which gives the experimentally determined space-time curve for a steel sphere dropping into water.

Unfortunately, the equation to motion (2) cannot be integrated completely in its general form, and for viscous liquids

such as glycerine (v_0 for pure glycerine at a temperature of 17° C. is of the order 23 cm./sec. for a steel ball 5/16 in. diameter) indirect methods must be used in order to obtain the space-time curves.

Fig. 3 shows the curves for glycerine, density 1·26 and viscosity 10. The velocity space-curve has been deduced from equation (3) for an initial velocity of 300 cm. per sec., and the space-time curve deduced from it.

Fig. 3.

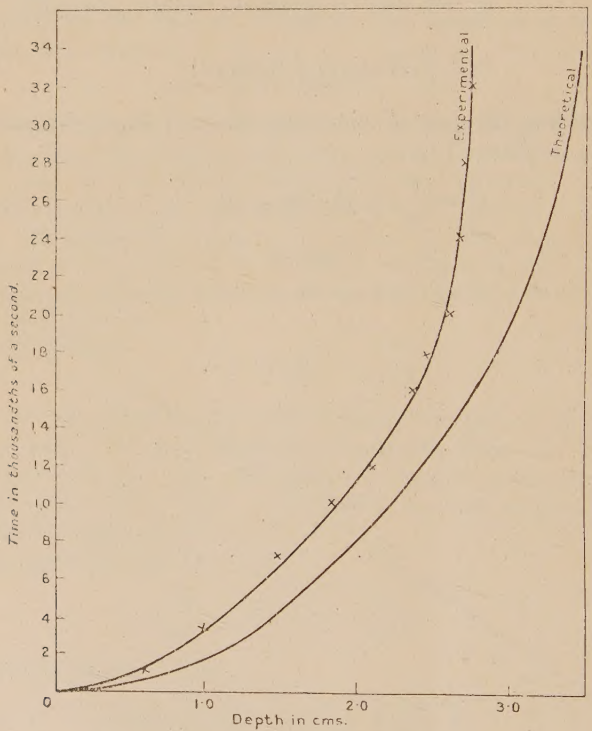

Space-time Graph for Sphere in Glycerine.

The curve marked "experimental" has been deduced from the measurement of a large number of photographic records, after correction for the refraction of the light on passing through the tank. The agreement between the two is as good as can be expected. The ball appears to fall more slowly than demanded by the theory, probably because the impact introduces conditions near the surface which have not been considered.

Shape of the Cavity.

Mallock also deduces an expression for the shape of the cavity at any time. He assumes that, after the impact, two forces are operative on the liquid, one giving it an outward flow, whose radial component is some function of the velocity v_1, and the other a hydrostatic pressure, giving the surface a velocity inwards.

If η and ξ are the coordinates of a point on the surface of the cavity at any time t_x, η being the distance of the point from the surface of a cylinder traced by the circumference of the shot and ξ its depth, we have

$$\eta = \int_{t_\xi}^{t_{x'}} [f(v_1) - \sqrt{2g\xi}]dt, \quad . \quad . \quad . \quad . \quad (6)$$

the integration limits being the time at which the shot passed the point, and the time under consideration.

Mallock remarks that many forms of $f(v_1)$ may be found which fit the curve fairly well, but as none have a theoretical basis he takes $f(v_1)$ as some constant of v_1, say θv_1, obtaining the result

$$\eta = (t_x - t_\xi)(\theta v - \sqrt{2g\xi}). \quad . \quad . \quad . \quad . \quad (7)$$

Fig. 4 shows the curves deduced from this equation, giving the theoretical shape of the cavity at the time given, $t=0$ being the time at which the ball is just below the surface.

These figures may be compared with those of Pl. XV, which gives reproductions of the actual photographs, allowance being made for the magnification and distortion due to the refraction of light passing through the tank.

Influence of Surface Tension

Equation (7) shows that the shape of the cavity does depend to some extent on the nature of the liquid, in particular on its viscosity, since the time of the descent (t_x & t_ξ) and also θv the velocity of radial outflow depend on the viscosity, but no account is taken of the influence of surface-tension.

A detailed comparison of photographs of splashes taken under different conditions seems to show that surface-tension does play a rather important part. The cavity formed when the ball is dropped into turpentine, although of the same general shape as when dropped into water, is slightly wider.

The viscosities of the two liquids are nearly the same, but the surface-tension of turpentine is only 27·3 dynes per cm. against the 72·4 dynes per cm. of water. The same thing is apparent in the case of the ball falling into paraffin oil, although the photographic record is too weak to reproduce.

Fig. 4.

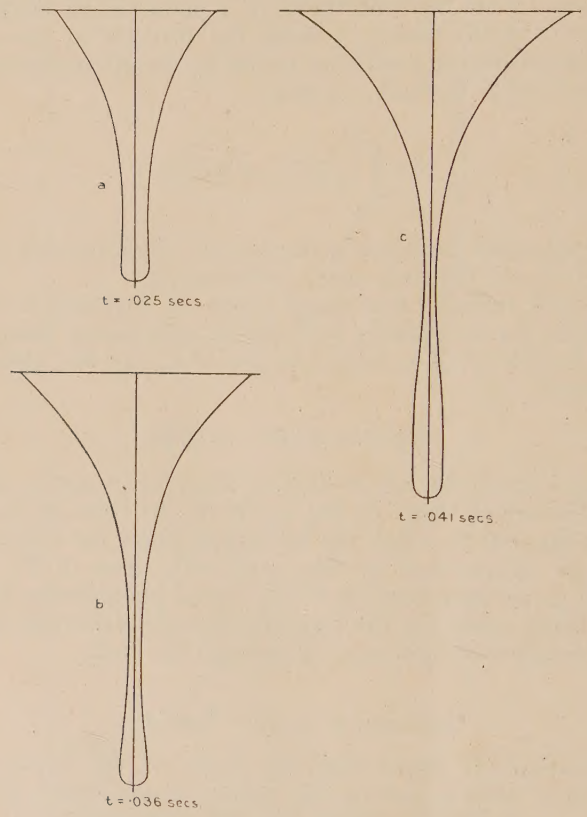

Shape of Cavity deduced from Mallock's Theory.

The shape of the air-cavity at the times given deduced from Mallock's theory for a steel ball $\frac{5}{16}$ inch diameter falling into water with a velocity under the surface of 300 cm. per sec.

It will further be seen that the cavity is wider when the ball is coated with a thin oil-layer. The mouth of the cavity formed when the ball is coated with paraffin oil and turpentine is much wider than when coated with (solid) paraffin-wax.

This is probably due to the fact that in the first case the cavity is lined with a thin layer of a substance of lower surface-tension. Worthington (*loc. cit.*) noted that when a liquid drop is allowed to fall into a liquid, the cavity is lined with the liquid of the drop itself, thus providing an *a priori* justification for this explanation.

It thus appears that, in addition to the two forces of which Mallock takes account, there is a third one due to surface-tension. This causes a pressure over the walls of the cavity of magnitude $2T\left(\frac{1}{R}+\frac{1}{r}\right)$, where r and R are the radii of curvature, the direction of the pressure being such as to tend to cause the cavity to collapse. Thus, paraffin oil and turpentine having low surface-tensions, this force tending to close the cavity will be less, and the cavity at any time wider, than in the case of a liquid of higher surface-tension.

Influence of Surface Layers.

It will be seen from the photographs that surface-layers on the ball have a very pronounced effect on the surface-disturbance, in addition to their effect on the shape of the cavity.

Referring to Pl. XV., figs. 1 (*a*, *b*, & *c*) are shadowgraphs of the splash occurring when the ball is wet with paraffin oil, and falls into water. In figs. 2 (*a*, *b*, & *c*) the ball has been coated with a thin layer of paraffin-wax, in figs. 3 (*a*, *b*, & *c*) it has been wet with water, and in figs. 4 (*a*, *b*, & *c*) with turpentine.

Figs. 5 (*a*, *b*, & *c*), 6 (*a*, *b*, & *c*) and 7 (*a*, *b*, & *c*) show the result of the impact of a sphere wet with turpentine, paraffin oil, and water respectively falling into turpentine.

In the cases shown in figs. 8 (*a*, *b*, & *c*) a layer of paraffin oil 1·4 cm. thick has been floated on the surface of the water, and the ball wet with paraffin oil.

In all these cases the velocity of the ball just below the surface was 300 cm. per sec., and the resulting splash "rough" in each case. With this velocity a perfectly smooth, clean, and well-polished ball invariably gave a smooth splash.

When the ball is wet with water and falls into either water or turpentine, the cavity closes over very quickly, as is shown in figs. 3 & 7. The figures in this case do not reproduce so accurately as in the other cases, owing to the fact that it is extremely difficult to get a film of water to adhere evenly.

The general shape of the cavity does not vary much, except

for such slight differences as are accounted for by varying surface-tensions.

When the ball is wet with paraffin oil and falls into turpentine, the result is very curious, the cavity collapsing very quickly at the top, in much the same way as when the ball is wet with water and falls into either water or turpentine.

Finally, in one series of experiments a layer of paraffin oil 1·4 cm. thick was floated on the surface of the water and the ball wet with paraffin oil. The object of this was to observe the effect at the interface of two liquids. As will be seen from the photographs, the ball appears to penetrate into the second liquid without dragging the first liquid after it.

The difference in the surface disturbance under varying conditions is more noticeable.

The ball wet with paraffin oil gives very similar surface effects to the ball coated with paraffin wax, both being quite different from the case in which the surface of the ball is wet with turpentine. When the ball is wet with turpentine and falls into turpentine, the surface-disturbance is very similar to that when the ball wet with turpentine falls into water, and also to the case of a ball wet with paraffin oil falling into paraffin oil.

A slight, though remarkable difference exists, however, between the surface-disturbances shown in figs. 5 & 8 and the other cases, for it appears that when the ball is coated with the same liquid as that upon which it impinges, the upshot rim tends to close in more rapidly at the top.

Influence of Viscosity.

Figs. 9–11 show the effect of the impact of a clean and well-polished steel ball 5/16 in. diameter with the surface of a glycerine-water mixture of different viscosities.

In the first series, figs. 9 (*a*, *b*, & *c*) the viscosity of the glycerine and water mixture was 4·5 and the shape of the cavity appears to be very little different from the previous examples. The neck tends to form earlier and of course the ball falls more slowly. A glycerine and water mixture of viscosity 9 gives the effects shown in figs. 10 (*a*, *b*, & *c*). Again we have a very similar effect, although the surface conditions are quite different from those produced when liquids of low viscosity are used.

With increasing viscosity, however, the characteristics of

the cavity alter fundamentally, and with viscosity 12 we obtain the effect shown in figs. 11 (*a*, *b*, & *c*). It will be noticed that the cavity is always much narrower, and that the liquid appears to cling to the upper surface of the ball. The very pronounced neck has almost disappeared, although there is still a minimum diameter. Instead of opening out quickly below the neck as previously occurred, we see that the lower part of the cavity is nearly cylindrical, and that it retains this form for a comparatively long time. When finally the cavity collapses, it does so from the bottom, gradually, not suddenly collapsing from the neck as is the case for low viscosities.

Mallock's theory fits the experimental curves fairly well up to viscosity 9, but the author has been unable to deduce from theory the shape shown in figs. 11. It seems probable that the expression for radial outflow θv is not applicable,—possibly some more complicated function of v could be found which would make equation (7) apply. In general terms the theory appears valid, for the numerical value of $f(v)$ of equation (6) will almost certainly decrease with increase of viscosity, thus making η smaller, and also making it become negative sooner.

The Striæ on the Figures.

On all the photographs obtained using liquids of very low viscosity there appear nearly horizontal striæ, as is clearly seen in the figures of Plate XV.

Examination of the photographs shows that

(1) The striæ are always nearly horizontal.
(2) They never appear in the liquid below the air-cavity.
(3) They extend on either side of the cavity for some distance.

The origin of these is not at all clear, but it is possible that they may be due to some kind of waves—probably compressional. Such waves would produce places of alternate compression and rarefaction, accompanied by corresponding changes in refractive index. Regular variations of refractive index would have a focussing effect, and thus account for the comparatively clear definition and brilliance of the bright lines.

The explanation is only tentative. At first it was thought that the striæ were due to reflexion from the plate-holder and elsewhere ; all parts of the apparatus were then painted

dead-black and a new plate-holder constructed having a face of the dead-black matt paper in which plates are usually wrapped, but this did not eliminate the markings. Further, the fact that the depth to which the striæ extend in the liquid is related to the depth of the air-cavity tends to show that the markings are due to some disturbance in the liquid and not to fortuitous circumstances.

Other possible explanations have been considered and abandoned. It is known that if a large bubble be allowed to ascend in the liquid contained in a fairly wide tube, it assumes a more or less cylindrical form with hemispherical ends, and that the "walls" of the bubble are covered with beautiful small ripples. However, since the markings appear in the liquid outside the cavity, this explanation of the striæ observed does not seem to hold.

Summary.

In this paper the phenomena attending the impact of a solid sphere with a fluid surface are studied, with special reference to the effect of (1) the surface-tension of the liquid, (2) surface-layers on the ball, and (3) the viscosity of the liquid. It is shown that the theory given by Mallock holds fairly well for liquids of low viscosity, but evidence is given that surface-tension should be introduced into the theory. Surface-layers affect both the shape of the air-cavity and also (in a more pronounced manner) the surface-disturbance. The effect on the shape of the cavity is such as is accounted for by varying surface-tension, but no explanation can be given for the varying surface-conditions. When liquids of high viscosity are used the shape of the cavity changes fundamentally, and Mallock's theory in its simplified form does not appear to be applicable. Finally the nature and origin of certain striæ which appear on the photographs is discussed, and a tentative explanation given.

In conclusion the author desires to thank Prof. E. H. Barton, D.Sc., F.R.S., for his kindly interest, aid, and criticism, the Department of Scientific and Industrial Research for a grant by the aid of which the research has been carried out, and the Imperial Plate Company, Cricklewood, for technical advice on the manipulation of their plates under these difficult conditions.

Fig. 1 Fig. 2 Fig. 3 Fig. 4 Fig. 5 Fig. 6 Fig. 7 Fig. 8 Fig. 9 Fig. 10 Fig. 11.

a

b

c

	Fig. 1	Fig. 2	Fig. 3	Fig. 4	Fig. 5	Fig. 6	Fig. 7	Fig. 8	Fig. 9	Fig. 10	Fig. 11
Coated with	paraffin oil.	paraffin wax.	water.	turpentine.	turpentine.	paraffin oil.	water.	paraffin oil.	clean.	clean.	clean.
Falling into	water.	water.	water.	water.	turpentine.	turpentine.	turpentine.	paraffin oil & water.	glycerine: $\eta = 4{\cdot}5$.	glycerine: $\eta = 9$.	glycerine: $\eta = 12$.

LXXVII. *The Determination of Molecular Diameters from Surface-Tension Measurements.* *By* SERGIUS MOKROUSHIN *.

THE methods for determination of molecular dimensions may be divided into (1) kinetic or dynamic, and (2) statistical methods. Values of molecular diameter from the kinetic theory of gases depend upon the kinetic energy of the molecules (Jäger, *Handbuch der Physik*, Winkelmann, 'Wärme,' p. 761, 1906), and especially upon the distances of approach one to another at the time of collision. The greater the momentum of a molecule the nearer will it approach another during the period of collision. For this reason the molecular diameters as determined by Lenard from ionization measurements are less than those found from measurements of viscosities of gases (Timiriaseff, 'Kinetic Theory of Matter,' p. 161, 1923). Lenard (*Ueber Kathodenstrahlen*, Nobel Vorlesung, 1906) found that when molecules are subjected to bombardment by electrons, the diameters so calculated continually decrease as the electron velocity is increased and become ultimately of the order of 10^{-12} cm., *i. e.* one ten-thousandth of the average value found from viscosity measurements.

The surface-tension method allows us to determine a value of the molecular diameter in a liquid or gas, and makes it independent of the determination of mean free path resulting from collisions. Naturally this method must be referred to statistical methods and to those involving the use of van der Waals's equation of state (Lewis, 'A System of Physical Chemistry,' Kinetic Theory, p. 13), in which 6/7 of the term b appears to be the volume actually occupied by the molecules themselves, and whence, knowing the Avogadro number, we may easily determine the molecular diameter.

Statistical methods depend upon the determination of molecular forces of attraction observable when the distances between molecules become less than 10^{-7} cm. (Langmuir, Lewis, *l. c.* p. 762). Consequently we may consider this value as the order of magnitude of the largest radius of the sphere of attraction of one molecule for another, or, as the diameter of the molecule.

We may regard the surface of a liquid as a unimolecular layer, since it has been shown by Lord Rayleigh ('Nature,' xlii. p. 43, 1890) that the thickness of an oil film spread on

* Communicated by Prof. F. G. Donnan, F.R.S.

water is of the order of $1{\cdot}6\times10^{-7}$ cm., and by Devaux (Journ. Phys. iii. (4) p. 450, 1904) that films of paraffin and metal sulphides give thicknesses of the same order. This has been more definitely shown by Langmuir (Journ. Amer. Chem. Soc. xxxix. p. 1848, 1917). Hence we may assume that the surface-tension is equal to the force of attraction of one molecule for another. On the other hand, we know that the latent heat of vaporization has to be used in overcoming the forces of cohesion (the "disgregation" of Clausius), and for the performance of external work by the gas (Graetz, *Handbuch der Physik*, Winkelmann, 'Wärme,' p. 1087).

The internal heat of vaporization is given by the equation

$$Q = \lambda_i + p(v_1 - v), \quad . \quad . \quad . \quad . \quad . \quad (1)$$

where λ_i = internal latent heat of vaporization,

p = pressure of vapour,

v = volume of liquid,

v_1 = volume of vapour formed.

Since v is small compared with v_1 when the temperature is far from the critical point, we may express equation (1) as

$$Q = \lambda_i + pv_1. \quad . \quad . \quad . \quad . \quad . \quad . \quad (2)$$

Then if v_1 is the volume per gram molecule, we have by the Clapeyron equation

$$Q = \lambda_i + RT, \quad . \quad . \quad . \quad . \quad . \quad . \quad (3)$$

where R is the universal gas constant = 1·985 cals., and T = absolute temperature of vaporization.

Then if we assume that the internal latent heat of vaporization is used in increasing the surface-energy in the process of change of state, *i. e.* increasing the free surface of the molecules, we have

$$Q = \sigma(S - S_0) + RT, \quad . \quad . \quad . \quad . \quad (4)$$

where σ = surface-tension,

S = surface of molecules of vapour,

S_0 = free surface of vaporization of liquid.

The term S_0 being small compared with S, we may write

$$Q = \sigma S + RT, \quad . \quad . \quad . \quad . \quad . \quad . \quad (5)$$

whence $$\sigma S = Q - RT, \quad . \quad . \quad . \quad . \quad . \quad . \quad . \quad (6)$$

or expressing in C. G. S. units we have

$$\sigma S = 4{\cdot}189 \times 10^7 (Q - RT),$$

where $4{\cdot}189 \times 10^7$ ergs is the mechanical equivalent of heat. The molecular surface in a vapour, $S = \pi d^2 N$ where N is the Avogadro number, $= 6{\cdot}85 \times 10^{23}$ (Perrin, Lewis, *l. c.* p. 29). Hence the molecular diameter may be easily determined from the equation

$$d = \sqrt{\frac{4{\cdot}189 \times 10^7}{\pi N}} \cdot \sqrt{\frac{Q - RT}{\sigma}}, \quad . \quad . \quad (7)$$

or since $\sqrt{\frac{4{\cdot}189 \times 10^7}{\pi N}}$ is a constant $= 4{\cdot}41 \times 10^{-9}$, we may write

$$d = K \sqrt{\frac{Q - RT}{\sigma}} \quad . \quad . \quad . \quad . \quad . \quad . \quad . \quad . \quad (8)$$

Table I. shows some molecular diameters, calculated by means of this equation, compared with determinations by other methods.

TABLE I.

Molecular diameters $\times 10^8$.

Substance.	Ionization, Lenard.	Viscosity of Gases, Sutherland [1].	Equation of State, Van der Waals [2].	Diffusion Coefficient in Aqueous Solution, Svedberg [3].	Kinetic Theory and Capillary Constant, Jäger [4].	Equation (8).
N_2	1·00	2·95	6·7	—	—	4·94
H_2	0·63	2·17	4·7	1·6	—	4·18
O_2	—	2·71	6·1	4·6	—	4·6
H_2O.....	1·02	—	—	—	5·1	5·12
Cl_2	—	3·74	—	5·0	—	5·24
Br_2	—	—	—	7·6	—	5·82

[1] Sutherland, Phil. Mag. xix. p. 25 (1910).
[2] Lewis, 'A System of Physical Chemistry,' Kinetic Theory 13.
[3] Svedberg, *Z. phys. Chem.* lxvii. p. 105 (1909).
[4] Jäger, *Handbuch der Physik*, Winkelmann, 'Wärme,' p. 767.

Jäger (*l. c.*) determined the value of molecular diameter, as we have done, as a function of the surface energy, but he connected this surface energy not with the latent heat of vaporization, but with the kinetic energy of the vapour molecules, assuming that every particle in the change of state divides into at least two particles, and that the surface energy increases in this way and becomes equal to the kinetic energy of the particles or molecules. The diameter for water determined by Jäger, $5{\cdot}10 \times 10^{-8}$ cm., is the same as that obtained in this paper, $5{\cdot}12 \times 10^{-8}$ cm.

By application of the Trouton Rule (according to which $\frac{Q}{T_{boil}} = \text{constant} \sim 21$), we may easily calculate the molecular diameter at the boiling-point. Equation (8) then takes the form $d = K\sqrt{\frac{19T}{\sigma}}$, and putting $K\sqrt{19} = K_1$, we have

$$d = K_1\sqrt{\frac{T}{\sigma}}, \quad . \quad . \quad . \quad . \quad . \quad . \quad (9)$$

where $K_1 = 1{\cdot}92 \times 10^{-8}$.

From equation (4) it follows that the latent heat of vaporization depends upon the value of the free surface of a liquid, and diminishes as the surface increases. Moullerigne (*Journ. Phys.* v. (3) p. 159, 1896) draws attention to the dependence of latent heat of vaporization upon the form of the surface.

I would like to point out that, owing to difficulties of obtaining reference literature, it is possible that reports of investigations of this type may have appeared and not been seen by me.

In conclusion I wish to express my deepest gratitude to Professors A. V. Thoubnikoff and R. E. Makovetzky for their kind interest and valuable information.

Laboratory of Physical Chemistry,
University of Oural, Ekaterinburg,
May 5th, 1923.

LXXVIII. *On the Determination of the Frequencies of the Resonant Tones of some Compound Resonators used in Acoustical Instruments.* By E. T. Paris, *D.Sc., F.Inst.P.**

§ 1. *Introduction.*

RESONANCE, or "tuning," is employed in nearly all instruments used for measuring the amplitude of sound waves in air. Sensitive Rayleigh disk instruments, for example, are generally made with double resonators, and depend for their sensitiveness largely on the response of a resonator to the particular tone which it is desired to measure †. Other well-known tuned instruments are the phonometer designed by the late Professor A. G. Webster ‡, and the selective hot-wire microphone §. In the phonometer, tuning is performed by means of a single (variable) Helmholtz resonator, while in the hot-wire microphone it is accomplished by a single or double resonator according to the degree of sensitiveness required.

It is clearly important that means should be available for calculating the frequencies of resonators used in such instruments, and, conversely, for determining the dimensions of resonators which are required to respond to given tones. The formula for the natural frequency of a Helmholtz resonator (as used in the phonometer and the singly-resonated hot-wire microphone) is well known and has stood the test of experience. The theory has also been given of some of the more usual forms of double resonator employed in Rayleigh disk instruments and hot-wire microphones ‖. There remains, however, a number of other resonators—some double and some of a more complicated kind—which have been found serviceable in the construction of acoustical instruments, but which have so far received little attention from a theoretical point of view. It is the purpose of the present paper to give a brief description of

* Communicated by Prof. H. W. Porter, D.Sc., F.R.S., F.Inst.P.

† See, for example, the description of the "Microtonometer" by Professor C. V. Boys in 'The Dictionary of Applied Physics,' iii. p. 723; or the instrument figured by F. R. Watson, 'Acoustics of Buildings,' p. 93 (1923).

‡ Details are given in 'Nature,' cx. pp. 42–45 (1922); and Proc. Roy. Inst. xxiii. pp. 406–411 (1924).

§ W. S. Tucker and E. T. Paris, Phil. Trans. A, ccxxi. pp. 389–430 (1921).

‖ Rayleigh, 'Theory of Sound' (2nd ed.), ii. pp. 189–192, and Phil. Mag. xxxvi. pp. 365–376 (1918); E. T. Paris, Proc. Roy. Soc. A, ci. pp. 391–410 (1922).

these resonators and the ways in which they are employed, and to show how equations can be derived from which their resonance frequencies are calculable by the use of graphical methods. Although the work is mainly theoretical, a few experiments are described which illustrate the application of some of the theoretical formulæ.

§ 2. *Extension of the Theory of the Boys Double Resonator.*

The Boys double resonator is a combination of a Helmholtz resonator with a stopped pipe. The Helmholtz resonator is attached to the pipe as shown diagrammatically in fig. 1 or fig. 2, and the sound-detecting apparatus (Rayleigh disk or hot-wire grid) is placed in the short neck leading from the pipe into the Helmholtz resonator (*c*, figs. 1 & 2). The

Fig. 1.

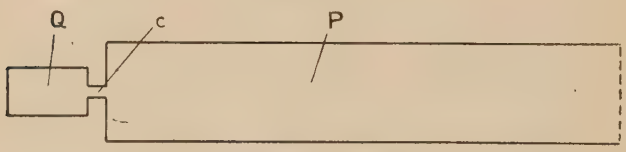

Boys Resonator ($m=1$).

Fig. 2.

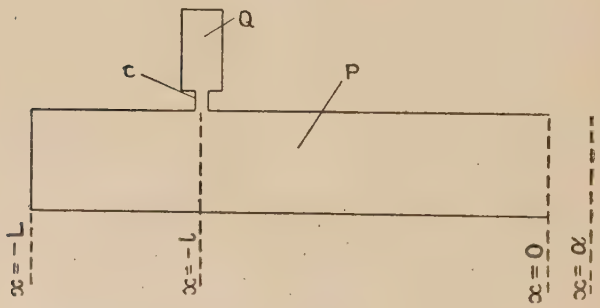

Boys Resonator ($m < 1$).

advantage of the arrangement is that when the resonator responds to a sound of suitable frequency the air in the neck oscillates with an amplitude which may be hundreds of times greater than the amplitude in the original wave. This type of resonator was first used by Boys in the construction of Rayleigh disk instruments.

The particular variety of Boys double resonator shown in fig. 1, in which the Helmholtz resonator (Q) is attached at

the closed end of the pipe (P), has already received attention in connexion with its application in the construction of doubly-resonated hot-wire microphones. The frequencies of the resonant tones are given by values of n which satisfy the equation *

$$\tan\frac{\pi n}{2n_0} = -\frac{2\pi\sigma}{ac}n_1\left(\frac{n}{n_1}-\frac{n_1}{n}\right), \quad . \quad . \quad . \quad (1)$$

where n_0 is the number of vibrations per second in the fundamental resonant tone of the pipe ; n_1 is the number of vibrations per second in the fundamental resonant tone of the Helmholtz resonator † ; c is the hydrodynamical conductance of the neck of the Helmholtz resonator ; and a is the velocity of sound in air. The values of n obtained in particular cases by a graphical solution of (1) have been found to be in good agreement with observation.

The form of resonator to which it is now desired to direct attention is that shown in fig. 2, which differs from that shown in fig. 1 in that the Helmholtz resonator is attached to the pipe at some distance from the closed end. This kind of resonator is important on account of its usefulness in the construction of extremely sensitive instruments, such as Boys's microtonometer. In connexion with hot-wire microphones, it is employed in cases where instruments are required which are to be very sensitive over a narrow range of frequencies and are to be used with an amplifier and telephones or vibration-galvanometer. (For the "bridge" method of using the hot-wire microphone, the form described in the next section is more suitable.)

In order to obtain an equation from which the frequencies of the resonant tones can be calculated, we proceed as follows. The loss of acoustical energy from the resonator—due to viscous forces and the escape of sound from the mouth of the resonator—is left out of account, and those frequencies are sought which are compatible with a stationary motion of the air contained within the walls of the resonator and a surface of no pressure variation at the mouth.

It is convenient to suppose that the pipe is straight ; although the subsequent work would need no serious modification if the pipe were curved, provided that the cross-sectional area remained the same throughout its length. Thus, let the axis of the pipe be parallel to the axis of x, and

* Proc. Roy. Soc. A, ci. p. 396 (1922). A slight alteration is made in the notation.

† The overtones of the Helmholtz resonator are left out of account because of their relatively high frequencies.

let the open end lie in the plane $x=0$, and the closed end in the plane $x=-\mathrm{L}$. The dimensions of the orifice of the Helmholtz resonator being small compared with the length of the pipe, the position of the resonator can be defined with sufficient accuracy by saying that the orifice lies in the plane $x=-l$ (fig. 2). It will be assumed that the motion of the air inside the pipe takes place parallel to the axis of x except near the orifice of the Helmholtz resonator, say from $x=-l+\beta$ to $x=-l-\beta$. Let ϕ_1 be the velocity-potential of the motion from the open end to $x=-l+\beta$, and ϕ_2 the velocity-potential from $x=-l-\beta$ to $x=-\mathrm{L}$. Also let α be the correction for the open end, and let $x'=x+\alpha$, $\mathrm{L}'=\mathrm{L}+\alpha$, $l'=l+\alpha$, etc., so that x', L', l', etc., are reduced lengths of the pipe. In accordance with the assumed stationary nature of the motion, the general expressions for ϕ_1 and ϕ_2 can be written

$$\left.\begin{aligned}\phi_1 &= (\mathrm{A}_1 \sin kx' + \mathrm{B}_1 \cos kx') \cos kat,\\ \phi_2 &= (\mathrm{A}_2 \sin kx' + \mathrm{B}_2 \cos kx') \cos k(at+\theta),\end{aligned}\right\} \quad . \quad (2)$$

where A_1, A_2, B_1, B_2, and θ are constants as yet undetermined, and $k=2\pi/\lambda$, λ being the wave-length.

The condition to be satisfied at $x'=0$ ($x=\alpha$), there being no escape of energy from the pipe, is that there shall be no variation of the pressure, so that

$$(\partial\phi_1/\partial t)_{x'=0} = 0,$$

and hence $\mathrm{B}_1=0$. At the closed end, ϕ_2 must be such that the velocity is zero, that is

$$(\partial\phi_2/\partial x')_{x'=-\mathrm{L}'} = 0,$$

so that

$$\mathrm{B}_2 = -\cot k\mathrm{L}' \,.\, \mathrm{A}_2.$$

The expressions for ϕ_1 and ϕ_2 thus become

$$\left.\begin{aligned}\phi_1 &= \mathrm{A}_1 \sin kx' \,.\, \cos kat,\\ \phi_2 &= -\mathrm{A}_2 \operatorname{cosec} k\mathrm{L}' \cos k(x'+\mathrm{L}') \,.\, \cos k(at+\theta).\end{aligned}\right\} \quad (3)$$

It remains to put in the conditions to be satisfied by ϕ_1 and ϕ_2 in that part of the pipe which is near to the orifice of the Helmholtz resonator (*i. e.* from $x'=-l'+\beta$ to $x'=-l'-\beta$). In order to do this, use will be made of a method of approximation which is frequently of service in such cases. The method consists in assuming that the irregular motion due to the presence of the Helmholtz resonator is confined to a volume the dimensions of which

are so small compared with the wave-length that the actual motion at any instant is the same as it would be if the fluid occupying this volume were incompressible*. Let σ be the cross-sectional area of the pipe, and dq/dt the rate (c.c. per sec.) at which fluid is passing into the Helmholtz resonator. Then one of the conditions to be satisfied by ϕ_1 and ϕ_2 in the neighbourhood of the orifice of the resonator is (on the above assumption)

$$\sigma\left\{\left(\frac{\partial\phi_1}{\partial x'}\right)_{x'=-l'+\beta}-\left(\frac{\partial\phi_2}{\partial x'}\right)_{x'=-l'-\beta}\right\}=\frac{dq}{dt}. \quad . \quad (4)$$

Now β is small compared with the wave-length (at most comparable with the end correction), and therefore, if those cases are excluded in which the Helmholtz resonator is close to the open end of the pipe, the above equation may be simplified by neglecting β in comparison with l'. The simplified approximate condition is

$$\sigma\left(\frac{\partial\phi_1}{\partial x'}-\frac{\partial\phi_2}{\partial x'}\right)_{x'=-l'}=\frac{dq}{dt}. \quad . \quad . \quad . \quad (5)\dagger$$

The other condition which must be fulfilled in the neighbourhood of the Helmholtz resonator is the continuity of the pressure, and is expressed by

$$\partial\phi_1/\partial t=\partial\phi_2/\partial t \text{ when } x'=-l'. \quad . \quad . \quad . \quad (6)$$

From this condition we see that $\theta=0$; and since all adjacent potentials of the type (2) with which we shall have occasion to deal must satisfy a condition of the type (6), the arbitrary phase-angle θ will be assumed to be zero in all cases.

Let ψ be the velocity-potential inside the Helmholtz resonator, and Q the volume of the resonator. Then

$$dq/dt=c(\phi_{-l'}-\psi), \quad \psi=(a^2/\mathrm{Q})\int q\,dt, \quad . \quad (7)$$

where $\phi_{-l'}$ is the limiting value of ϕ_1 or ϕ_2 when $x'\to -l'$, and c is the conductance of the orifice. Also let

$$4\pi^2 n_1^2=a^2c/\mathrm{Q},$$

so that n_1 is the number of vibrations per second in the fundamental tone of the resonator, and let $2\pi n=ka$.

* Rayleigh, 'Theory of Sound' (2nd ed.), ii. p. 66.

† A condition of this form is given by Rayleigh to indicate the method to be followed in the case of a pipe with lateral openings (Sci. Papers, i. p. 50).

Then we find from (7) :

$$\frac{dq}{dt} = \frac{c}{1-(n_1^2/n^2)}\,\phi_{-l'}. \quad . \quad . \quad . \quad . \quad . \quad (8)$$

From (3) and (5) we have

$$A_2 = A_1 \sin kl' \sin kL' \sec k(L'-l'),$$

and substituting the values of ϕ_1 and ϕ_2 from (3) in (5) and using the value of A_2 just given, we obtain

$$dq/dt = \sigma k A_1 \{\cos kl' - \sin kl' \tan k(L'-l')\}. \quad . \quad (9)$$

Equating this value of dq/dt to that given in (8), and putting in the value of $\phi_{-l'}$ obtained from (3), we find, as the equation for determining the frequencies of the resonant tones,

$$-\frac{c}{1-(n_1^2/n^2)} \sin kl' = \sigma k \{\cos kl' - \sin kl' \tan k(L'-l')\}$$

for

$$\frac{1}{\cot kl' - \tan k(L'-l')} = -\frac{2\pi\sigma}{ac} n_1 \left(\frac{n}{n_1} - \frac{n_1}{n}\right). \quad . \quad . \quad (10)$$

Let $l' = mL'$. Then, if n_0 is used to denote the fundamental frequency of the pipe, we have

$$L' = a/4n_0, \quad kL' = \pi n/2n_0, \quad \text{and} \quad kl' = m\pi n/2n_0,$$

and equation (10) may be rewritten in the following form, which is more convenient for the purpose of calculation :

$$\frac{1}{\cot(m\pi n/2n_0) - \tan\{(1-m)\pi n/2n_0\}} = -\frac{2\pi\sigma}{ac} n_1 \left(\frac{n}{n_1} - \frac{n_1}{n}\right).$$
$$. \quad . \quad . \quad (11)$$

In order to find the resonant tones graphically, write Y_1 for the left-hand side of (11) and Y_2 for the right-hand side, and plot values of Y_1 and Y_2 as ordinates against values of n/n_0 as abscissæ. The curves $y = Y_1$ and $y = Y_2$ will intersect with one another at a number of points, and the abscissæ of these points give the values of n/n_0 at which the resonant tones occur. To find the effect of changing l' (or mL'), *i. e.* the distance of the resonator from the open end of the pipe, the Y_1 curves may be plotted for a number of selected values of the parameter m. The curves $y = Y_1$ when $m = 1$, $m = \frac{3}{4}$, $m = \frac{2}{3}$, and $m = \frac{1}{2}$, and n/n_0 is between 0 and 4, are shown in fig. 3.

When m is unity, Y_1 is simply the tangent of $\pi n/2n_0$. The position of the resonant tones and the way in which they

are affected by the tuning of the Helmholtz resonator have already been discussed *.

As an example of the shift in the position of the resonant tones caused by varying m, let $n_1 = n_0$ (that is, let the Helmholtz resonator be tuned to the fundamental of the pipe) and let $2\pi\sigma n_1/ac = 8$. The curve $y = Y_2$ is shown at AA^1 in fig. 3. The intersections with the Y_1 curves indicate that for each value of m there is one resonant tone below n_0 (between $0{\cdot}8\, n_0$ and $0{\cdot}9\, n_0$) and another tone above n_0 (between $1{\cdot}1\, n_0$ and $1{\cdot}3\, n_0$). We see also that for this value of $2\pi\sigma n_1/ac$ a

Fig. 3.

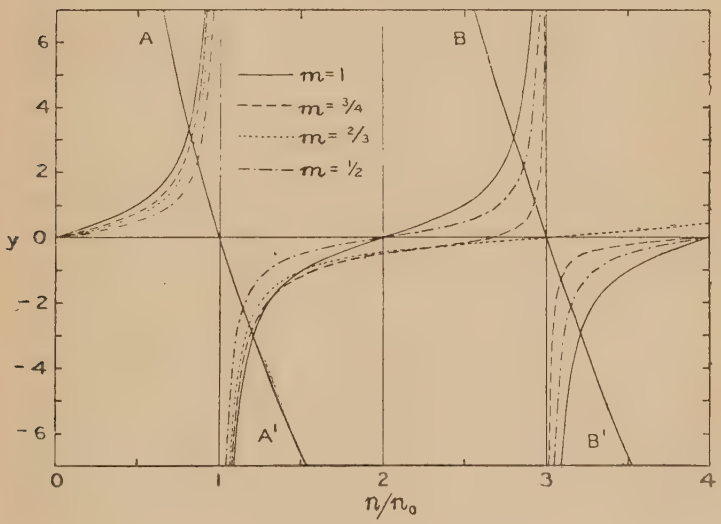

Graphical Solution of Equation (11).

decrease in the value of m causes each of these tones to move inwards towards n_0. By choosing a smaller value for $2\pi\sigma n_1/ac$, however, the slope of the curve AA^1 can be diminished in the region under consideration, and by this means the interval from the tone next above n_0 to the one below it can be increased. If $2\pi\sigma n_1/ac$ is so small that the intersections indicating the frequencies of the upper tone lie between $n = 1{\cdot}5\, n_0$ and $n = 2\, n_0$, then a decrease in m no longer produces a decrease in the frequency of the upper tone in every case. It can easily be seen from the figure that if N is the frequency of the upper tone when $m = 1$, then the frequency is raised if m is decreased to $\frac{3}{4}$, is lowered

* Proc. Roy. Soc. A, ci. pp. 400, 401 (1922).

slightly when m is further decreased to $\frac{2}{3}$ (but still remains above N), and falls below N when $m=\frac{1}{2}$.

In addition to the lowest pair of tones, there is a series of tones whose frequencies are not far removed from those of the overtones natural to the pipe. These are also given by the intersections of the Y_2 curve, of which AA^1 (fig. 3) is a portion, with the Y_1 curve. When n is great, Y_2 approaches the value $-(2\pi\sigma/ac)n$ asymptotically, and it is evident that the intersections take place to the right of the asymptotes to the Y_1 curve at $n/n_0=3$, $n/n_0=5$, $n/n_0=7$, etc., so that the overtones of the compound resonator are all higher than those natural to the pipe.

The form of the Y_1 curve when $m=\frac{2}{3}$ is exceptional and demands special attention. Unlike the other curves, it does not pass from $+\infty$ to $-\infty$ as n/n_0 passes through the value 3, and consequently one mode of vibration in the neighbourhood of $3n_0$ appears to be lost. The reason for this is that when $m=\frac{2}{3}$ the orifice of the Helmholtz resonator is situated at a loop of the first overtone of the pipe, and its presence in this position has no effect on the motion within the pipe when $n=3n_0$. In the theoretical treatment it has been assumed that the motion in the orifice (measured by dq/dt) does not vanish for any of the resonant modes of vibration of the combination, whereas modes are actually possible in which $dq/dt=0$, namely those which occur when the orifice is situated at a loop of one of the overtones characteristic of the pipe. In order to complete the solution when $m=\frac{2}{3}$, we must regard the vertical lines $n/n_0=3$, $n/n_0=9$, $n/n_0=15$, etc., as portions of the Y_1 curve, remembering that $dq/dt=0$ for all modes whose frequencies are given by intersections with these lines.

A similar state of affairs occurs whenever the orifice is at a loop of one of the overtones of the pipe, *i. e.* whenever m has a value r/s such that r is an even integer and s is an odd integer greater than r.

These results are illustrated in fig. 3, where BB' is a portion of the Y_2 curve drawn for the particular case when $n_1=3n_0$, that is when the Helmholtz resonator is tuned to the first overtone of the pipe. The value of $2\pi\sigma n_1/ac$ is taken to be 22, and fig. 3 shows that the tones on each side of $3n_0$ are most widely separated when $m=1$. When $m=\frac{3}{4}$ the interval from the upper to the lower tone is considerably diminished, and as m approaches the value $\frac{2}{3}$ the interval approaches unity until when $m=\frac{2}{3}$ there is but one tone, viz. $n=3n_0$. In this case, however, $dq/dt=0$ as explained above. After m has passed through the value $\frac{2}{3}$ the two

tones move apart, and when $m=\frac{1}{2}$ they are again well separated.

The above remarks indicate the general nature of the effects to be observed when the Helmholtz resonator is tuned to the fundamental or to the first overtone of the pipe. The position of the resonant tones can be found in a similar manner for any tuning of the component resonators, but there are some special cases which call for attention.

These special cases are all associated with the occurrence of a loop at $x'=-l'$, and in order to investigate them, it will be convenient to regard the compound resonator under consideration as a *triple* resonator consisting of the following components:—

(i) An *open* pipe extending from $x'=0$ to $x'=-l'$;

(ii) A *stopped* pipe extending from $x'=-l'$ to $x'=-\mathrm{L}'$;

and (iii) The Helmholtz resonator.

We first note that all the Y_1 curves cross the axis $y=0$ at certain places, and that if the Helmholtz resonator is tuned to the value of n where the crossing occurs, its frequency appears unaltered as one of the resonance frequencies of the combination. For example, if $n_1=2n_0$, the frequency $2n_0$ appears as one of the resonance frequencies of the combination when $m=1$ or when $m=\frac{1}{2}$.

In these cases the intersections between the Y_1 and Y_2 curves lie on the axis $y=0$; that is to say, the tuning of the Helmholtz resonator is such that its frequency n_1 is a root of $\mathrm{Y}_1=0$ treated as an equation in n. It can be shown from equation (11) that the roots of $\mathrm{Y}_1=0$ are those values of n which would produce in the open-pipe component (i), or in the stopped-pipe component (ii), or possibly in both, a vibration which would have a loop at $x'=-l'$. These values of n are therefore the resonance frequencies of the components (i) and (ii). There are two cases to be considered:—

(*a*) Let n' be the frequency of the fundamental (or one of the overtones) of the component (i). Then this will be one of the resonance frequencies of the compound resonator if either the Helmholtz resonator or the component (ii) is also tuned to n'. In the former case there will be no vibration whatever in that part of the pipe which lies between the Helmholtz resonator and the stopped end at $x'=-\mathrm{L}'$, this being one of those cases in which sound is sometimes said to be "absorbed" by a resonator *, so that the component (ii)

* *Cf.* Rayleigh, 'Theory of Sound' (2nd ed.), ii. p. 210.

is idle *. In the latter case the orifice of the Helmholtz resonator is at a loop of one of the overtones of the stopped pipe L', and hence (as described above) the component (iii) is idle, that is $dq/dt=0$.

(*b*) Let n'' be the frequency of the fundamental (or one of the overtones) of the component (ii). Then this will be one of the resonance frequencies of the compound resonator if either the Helmholtz resonator or the component (i) is also tuned to n''. In the former case, theory indicates that there should be no vibration at all in the component (i). In practice this is evidently impossible, but it suggests that in special cases a small vibration of the right frequency in (i) may be sufficient to maintain a comparatively large oscillation between (ii) and the Helmholtz resonator. The case when (i) and (ii) are in tune has already been dealt with.

§ 3. *Experimental Results.*

The experiments described in this section illustrate the application of equation (11). Before giving details of the experimental method, it may be well to point out that the theoretical equations are in a form which is suitable for the calculation of the resonant tones of a compound resonator partly from the *frequencies* of its components and partly from their *dimensions*. It is, of course, possible to express the frequencies of the components in terms of their dimensions ; but the equations then take on a more complicated form, and the agreement between calculated and observed values would depend not only on the theory given in the present paper, but also on the accuracy of the usual formulæ for calculating the hydrodynamical conductance of an orifice and the correction for an open end. It has been thought best to leave questions as to the accuracy of such formulæ to be answered by special investigations, and to accept the observed frequencies of the components as part of the data for calculating the tones of a compound resonator.

The frequencies of the resonant tones were determined experimentally with the aid of a hot-wire microphone grid mounted in the neck leading from the pipe into the Helmholtz resonator. The resonator to be tested was laid on the ground at a distance of about one metre from an electrically-driven siren of the Seebeck pattern, the speed of which could be controlled by means of a rheostat in series with the armature of the motor. The siren was mounted on a table, and

* The circumstances here contemplated are, of course, ideal. In practice there is always some loss of energy from the pipe, and the absence of vibration in (ii) would not be complete.

its revolutions per minute were indicated by an Elliot speed-counter attached by flexible shafting to the axle of the motor. The microphone grid formed one arm of a Wheatstone bridge, and the response of the resonator was measured by the deflexion of a microammeter with suitable series and shunt resistances. The deflexion of the microammeter was in all cases very closely proportional to the change in ohmic resistance suffered by the hot-wire grid. The deflexions were observed for a series of selected readings of the speed-counter, and from these readings curves were constructed showing the relation between deflexion and vibrations per second in the fundamental tone of the siren *. All observations were made out-of-doors.

The error of the speed-counter was found by a stroboscopic method with the help of a tuning-fork, the period of which had been determined from a chronometer by means of a Bull photographic recorder.

The deflexions observed in this method are approximately proportional to the square of the maximum velocity occurring in the neck of the Helmholtz resonator †, that is to

$$\{(1/A) \mid dq/dt \mid\}^2,$$

where A is the cross-sectional area of the neck and $\mid dq/dt \mid$ is the amplitude of the flow in c.c. per second. They are therefore approximately proportional to the *energy* of the vibration in the neck of the resonator. Certain resonant tones, however, would escape notice if this method only were to be relied on, namely those in which $dq/dt=0$, as for example those which occur when a Helmholtz resonator is placed at a loop of one of the resonant tones of a stopped pipe. Allowance for this fact must be made in interpreting the experimental results.

A resonator was made similar to that shown diagrammatically in fig. 2. The pipe P was an iron tube, 10·2 cm. in diameter (internal), and closed at one end by a brass plate ·5 cm. thick. The walls of the tube were ·6 cm. thick, and the length—measured from the open end to the inside face of the brass plate—was 120·3 cm. The frequency of the fundamental tone of the pipe was determined by ear,

* The microphone grids and their mounting and the method of plotting "resonance curves" is described in greater detail in Phil. Trans. A, ccxxi. pp. 391–393 & 395–398 (1921). The siren used in the present experiments was of the "circular hole" pattern previously used in the experiments with double resonators described in Proc. Roy. Soc. A, ci. p. 347 (1922).

† Phil. Trans. A, ccxxi. p. 410 (1921). See also R. C. Richards, Phil. Mag. xlv. pp. 926–934 (1923).

the method being as follows :—The pipe was laid on the ground in front of the siren, and the ears of an observer were connected by means of stethoscopes and rubber tubing to a nipple at the closed end of the pipe. The speed of the siren was then gradually increased until the frequency of the note passed through that value at which maximum resonance occurred in the pipe, the observer noting the speed-counter reading when the resonance appeared to him to be loudest. The mean of several observations gave the fundamental frequency of the pipe as $66\frac{1}{2}$ vibrns. per sec. at 10° C., and hence the reduced length L′ was 127 cm. (the velocity of sound in air being taken as 337·6 metres per sec. at 10° C.).

The pipe was provided with brass fittings so that a Helmholtz resonator could be attached at the closed end (as in fig. 1) or in a position $\frac{1}{4}$ L′, $\frac{1}{3}$ L′, or $\frac{1}{2}$ L′ from the closed end, these positions corresponding respectively to the four cases when $m=1$, $m=\frac{3}{4}$, $m=\frac{2}{3}$, and $m=\frac{1}{2}$. The end of the orifice of the Helmholtz resonator when in position was flush with the inside surface of the wall of the pipe. Two sets of observations were made, the first with a Helmholtz resonator tuned to the fundamental of the pipe, and the second with a resonator tuned to the first overtone of the pipe. The conductance of the orifice was found in each case by attaching it to a container of known volume and measuring the resonance frequency in the usual way with a hot-wire microphone. The conductance was then calculated from the formula

$$c = 4\pi^2 N^2 Q/a^2,$$

N being the resonance frequency, Q the volume of the container, and a the velocity of sound.

In the first set of observations, the conductance of the orifice (a cylindrical tube 26·5 mm. long and 6·5 mm. in diameter) was found to be 0·133 cm. So that in equation (11) we have

$$\sigma = \pi(10{\cdot}2)^2/4 \text{ cm.}^2, \qquad c = 0{\cdot}133 \text{ cm.},$$

and $$n_1 = n_0 = 66\tfrac{1}{2} \text{ vibrns. per sec.}$$

Hence $$2\pi\sigma n_1/ac = 7{\cdot}60.$$

This is sufficiently close to 8 for the intersections of the Y_1 curves with AA^1 in fig. 3 to be used for the purpose of finding approximate values for the frequencies at which resonance peaks should occur in the experimental curves. The approximate values having been found, more exact values are obtained without difficulty by calculating a few

additional points in the neighbourhood of each approximate value. The calculated values of the lower and upper resonance frequencies (N_1 and N_2 vibrns. per sec. respectively) are shown in the second and third columns of Table I. They are given to the nearest half-vibration per second, which is as accurately as they could be determined experimentally. The observed values are shown in the fourth and fifth columns.

TABLE I.

($n_1 = n_0$.)

	Calculated.		Observed.	
m.	N_1.	N_2.	N_1.	N_2.
1	54	$80\frac{1}{2}$	$54\frac{1}{2}$	80
$\frac{3}{4}$	55	80	55	$79\frac{1}{2}$
$\frac{2}{3}$	$55\frac{1}{2}$	79	$55\frac{1}{2}$	78
$\frac{1}{2}$	$57\frac{1}{2}$	$76\frac{1}{2}$	$57\frac{1}{2}$	$75\frac{1}{2}$

It will be seen that on the whole the observed values correspond very well with those predicted by theory, although there is evidence of a systematic error in the calculated value of N_2, this being always $\frac{1}{2}$ or 1 vibration greater than the observed value. The resonance curves for the cases when $m=1$ and $m=\frac{1}{2}$ are reproduced in fig. 4. The curves for $m=\frac{3}{4}$ and $m=\frac{2}{3}$ were intermediate in form between those shown in fig. 4, and as m was increased, the height of the peak due to the upper tone decreased, while that due to the lower tone increased, equality occurring for some value of m between $\frac{2}{3}$ and $\frac{1}{2}$. It is perhaps somewhat surprising to find that the response is so large when $m=\frac{1}{2}$, and some interesting questions arise as to the sensitiveness of instruments made with this type of resonator. A discussion of these questions, however, would necessitate taking into account the losses occurring in the resonator, and would lie outside the scope of the present paper.

The effects to be observed when the Helmholtz resonator is tuned to a note in the region of the first overtone of the pipe are more striking than those just described. The resonator employed in this part of the experiment had an orifice 6·5 mm. in diameter and 21 mm. long. The frequency was 205 vibrns. per sec., and the conductance of the orifice ·167 cm., so that we have $2\pi\sigma n_1/ac = 18{\cdot}7$. As before, we use the intersection of the Y_1 curves in fig. 3 with the Y_2 curve BB′ (which is constructed for the case when

$2\pi\sigma n_1/ac=22$) to obtain approximate values of the resonance frequencies, and then find more exact values by calculating a few additional values in the neighbourhood of the approximations, using the proper value of $2\pi\sigma n_1/ac$. The calculated and observed frequencies are shown in Table II.

Fig. 4.

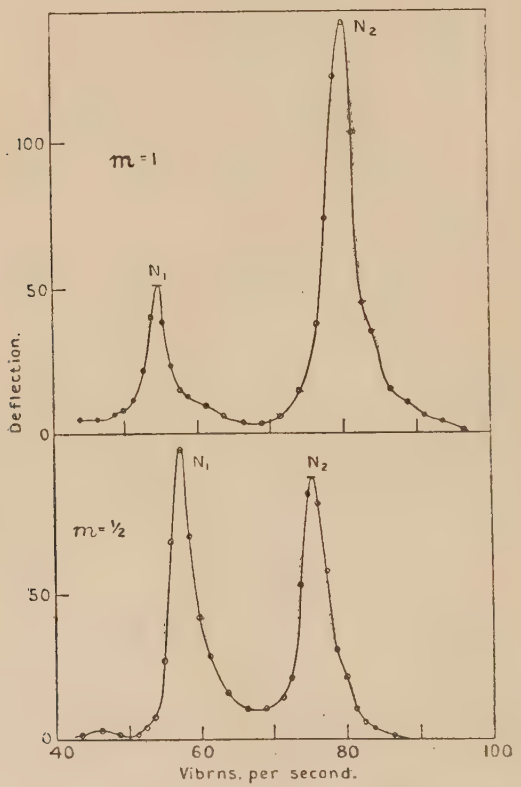

Resonance Curves for Boys Resonator ($n_1=n_0=66\frac{1}{2}$ vibrns. per sec.).

TABLE II.

($n_1=205$, $n_0=66\frac{1}{2}$.)

	Calculated.		Observed.	
m.	N_2.	N_3.	N_2.	N_3.
1	186	217	185	216
$\frac{3}{4}$	196	209	195	207
$\frac{2}{3}$	205		200	
$\frac{1}{2}$	191	213	190	212

The agreement here is also satisfactory, although the calculated frequencies are all a little greater than those observed. The resonance curves are shown in fig. 5. It will be seen that the changes in the shape of the curve are

Fig. 5.

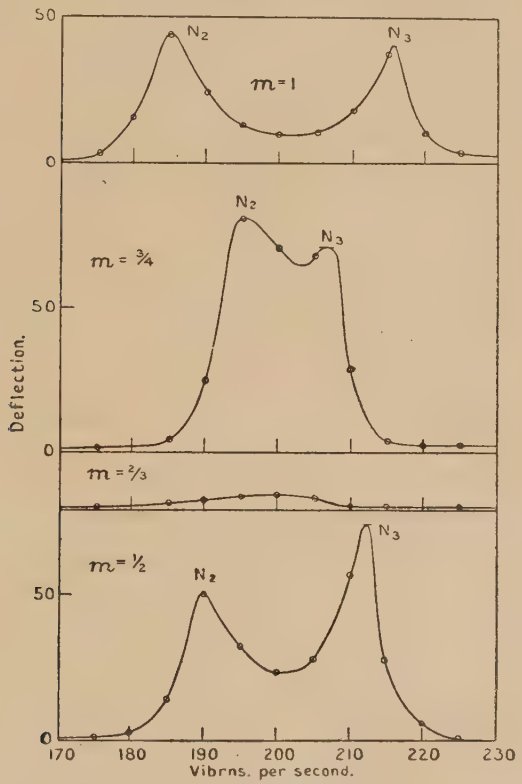

Resonance Curves for Boys Resonator ($n_1=205$, $n_0=66\frac{1}{2}$).

very marked, the most sensitive position for the Helmholtz resonator being when $m=\frac{3}{4}$. When $m=\frac{2}{3}$ the response is very small, the resonator being then at a loop of the first overtone of the pipe.

§ 4. *Combination of a Stopped Pipe with two Helmholtz Resonators.*

The kind of resonator dealt with in this section is shown diagrammatically in fig. 6, and is especially useful in the construction of hot-wire microphones which are to be

employed with the bridge method of measurement. In this method, in order to avoid "creeping" of the zero due to changing air-temperature or slow alterations in the battery, it is advisable whenever possible to use two microphone grids —one active and the other compensating—placed in opposite arms of a Wheatstone or battery bridge. If the grids are mounted in the necks of two Helmholtz resonators entering into the same stopped pipe (as in fig. 6), the compensation is very complete, and the arrangement has the additional advantage that when the microphone is used out-of-doors there is some compensation for the disturbing effect of wind.

Fig. 6.

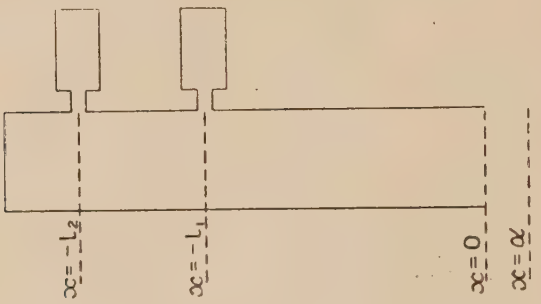

Combination of two Helmholtz Resonators and a Stopped Pipe.

Sensitive microphones of this type have been made for responding to sounds up to 512 vibrations per second, and have been found very effective for measuring the sound reflected and transmitted by partitions of various materials.

In addition to the use indicated above, it will be obvious from what follows that with compound resonators of the type under consideration, microphones can be made which are sensitive to two distinct ranges of frequencies.

It is convenient to begin the theory with the consideration of the more general case of a compound resonator consisting of a number of Helmholtz resonators inserted at intervals in the side of a stopped pipe. For each Helmholtz resonator, say the sth member of the series (counting from that nearest to the open end of the pipe), let a linear quantity, γ_s, be chosen such that

$$\tan k\gamma_s = \frac{2\pi\sigma}{ac_s} n_s \left(\frac{n}{n_s} - \frac{n_s}{n}\right), \quad . \quad . \quad . \quad (12)$$

where n_s is the frequency of the sth resonator (vibrns. per sec.) and c_s is the conductance of the neck. Thus, if ϕ_s and ϕ_{s+1} be the potentials on each side of the sth resonator at

$x' = -l_s'$, we have, corresponding to equations (5) and (8),

$$\sigma\left(\frac{\partial\phi_s}{\partial x'} - \frac{\partial\phi_{s+1}}{\partial x'}\right)_{x'=-l_s'} = \frac{dq_s}{dt}, \quad . \quad . \quad . \quad (13)$$

$$\frac{dq_s}{dt} = \frac{c_s}{1-(n_s^2/n^2)}\phi_{-l_s'}. \quad . \quad . \quad . \quad . \quad (14)$$

Eliminating dq_s/dt from (13) and (14) and making the substitution indicated in (12), we find that one of the conditions to be satisfied by ϕ_s and ϕ_{s+1} when $x' = -l_s'$ is

$$\frac{1}{k}\left(\frac{\partial\phi_s}{\partial x'} - \frac{\partial\phi_{s+1}}{\partial x'}\right) = \cot k\gamma_s \cdot \phi_{-l_s'}, \quad . \quad . \quad (15)$$

while the other is

$$\partial\phi_s/\partial t = \partial\phi_{s+1}/\partial t. \quad . \quad . \quad . \quad . \quad . \quad (16)$$

If it happens that the sth resonator is at the closed end of the pipe, that is if $l_s' = \mathrm{L}'$, then equations (13) and (14) become

$$\sigma\left(\frac{\partial\phi_s}{\partial x'}\right)_{x'=-\mathrm{L}'} = \frac{dq_s}{dt}, \quad . \quad . \quad . \quad . \quad (17)$$

$$\frac{dq_s}{dt} = \frac{c_s}{1-(n_s^2/n^2)}\phi_{-\mathrm{L}'}, \quad . \quad . \quad . \quad . \quad (18)$$

and corresponding to (15) we have

$$\frac{1}{k}\left(\frac{\partial\phi_s}{\partial x'}\right)_{x'=-\mathrm{L}'} = \cot k\gamma_s \cdot \phi_{-\mathrm{L}'}. \quad . \quad . \quad . \quad (19)$$

Since

$$\phi_s = (\mathrm{A}_s \sin kx' + \mathrm{B}_s \cos kx') \cos kat, \quad . \quad . \quad (20)$$

(19) is equivalent to

$$\mathrm{A}_s \cos k\mathrm{L}' + \mathrm{B}_s \sin k\mathrm{L}' = \cot k\gamma_s(-\mathrm{A}_s \sin k\mathrm{L}' + \mathrm{B}_s \cos k\mathrm{L}'),$$

whence

$$\mathrm{A}_s - \mathrm{B}_s \cot k(\mathrm{L}' + \gamma_s) = 0$$

or

$$\mathrm{A}_s \cot k(\mathrm{L}' + \gamma_s + \pi/2k) + \mathrm{B}_s = 0. \quad . \quad . \quad . \quad (21)$$

Now, if there were no resonator at the closed end of the pipe, the condition to be fulfilled by ϕ_s would be

$$\left(\frac{\partial\phi_s}{\partial x'}\right)_{x'=-\mathrm{L}'} = 0, \quad . \quad . \quad . \quad . \quad . \quad (22)$$

whence

$$\mathrm{A}_s \cot k\mathrm{L}' + \mathrm{B}_s = 0. \quad . \quad . \quad . \quad . \quad . \quad (23)$$

Comparing (21) with (23), we see that the effect of placing

a resonator at the closed end of the pipe may be represented as the addition of a length $\Delta L'$ to the reduced length L', such that

$$\Delta L' = \gamma_s + (\pi/2k)$$
$$= \gamma_s + \tfrac{1}{4}\lambda. \quad . \quad . \quad . \quad . \quad . \quad . \quad . \quad (24)$$

In terms of the frequencies n and n_s, $\Delta L'$ is given by the formula :

$$\Delta L' = \frac{a}{2n}\left[\frac{1}{2} + \frac{1}{\pi}\tan^{-1}\left\{\frac{2\pi\sigma}{ac_s}\, n_s\left(\frac{n}{n_s} - \frac{n_s}{n}\right)\right\}\right]. \quad (25)$$

By means of the equations (15), (16), and (21) it is easy to write down the equation, the roots of which will give the frequencies of the resonant tones in any particular case. For example, let there be two Helmholtz resonators, one at $x' = -l_1'$, and another at $x' = -l_2'$, as in fig. 6. Following the same plan as before, we assume potentials ϕ_1 from $x' = 0$ to $x' = -l_1'$, ϕ_2 from $x' = -l_1'$ to $x' = -l_2'$, and ϕ_3 from $x' = -l_2'$ to $x' = -L'$, these having the general form for stationary waves given in (20). In addition to the condition at the open end ($x' = 0$), viz. $\partial\phi_1/\partial t = 0$ so that $B_1 = 0$, the conditions to be satisfied by ϕ_1, ϕ_2, and ϕ_3 are expressed by (i) two equations of the type (15) and (16) with $s = 1$, $x' = -l_1'$; (ii) two similar equations with $s = 2$, $x' = -l_2'$; and (iii) $\partial\phi_3/\partial x' = 0$ when $x' = -L'$. Substituting for ϕ_1, ϕ_2, and ϕ_3 expressions of the type (20), we thus obtain five equations from which the five constants A_1, A_2, B_2, A_3, and B_3 can be eliminated. The eliminant is :

$$\begin{vmatrix} -1 & 1 & -\cot kl_1' & 0 & 0 \\ \cot kl_1' + \cot k\gamma_1 & -\cot kl_1' & -1 & 0 & 0 \\ 0 & -1 & \cot kl_2' & 1 & -\cot kl_2' \\ 0 & \cot kl_2' + \cot k\gamma_2 & 1 - \cot k\gamma_2 \cot kl_2' & -\cot kl_2' & -1 \\ 0 & 0 & 0 & \cot kL' & 1 \end{vmatrix} = 0 \quad . \quad . \quad . \quad (26)$$

The values of n, or $ka/2\pi$, which satisfy this equation are the frequencies of the resonant tones. For graphical solution the equation may be written :

$$\frac{\cot kl_2' + T_2 \cot k(L' - l_2')}{1 - S_2 \cot k(L' - l_2')} = \frac{1 + S_1 \cot kl_1'}{S_1 - \cot kl_1'}, \quad . \quad (27)$$

where

$$\left.\begin{aligned} S_1 &= \cot kl_1' + \cot k\gamma_1, \\ S_2 &= \cot kl_2' + \cot k\gamma_2, \\ T_2 &= 1 - \cot k\gamma_2 \cot kl_2'. \end{aligned}\right\} \quad . \quad . \quad . \quad . \quad (28)$$

In (27) the right-hand side depends only on the position and tuning of the first resonator, while the left-hand side depends on the position and tuning of the second resonator and the reduced length of the pipe. If the second resonator is placed at the closed end of the pipe, *i. e.* if $l_2' = L'$, (27) reduces to

$$-\frac{T_2}{S_2} = \frac{1 + S_1 \cot kl_1'}{S_1 - \cot kl_1'} \quad . \quad . \quad . \quad . \quad . \quad (29)$$

This result can easily be deduced anew from the equations already given. Thus, instead of three equations expressing the conditions (ii) and (iii) given above, there is in this case one equation of the type (21) with $s=2$. With the two equations of condition (i) this makes three equations in all from which the constants A_1, A_2, and B_2 can be eliminated. The result is:

$$\begin{vmatrix} -1 & 1 & -\cot kl_1' \\ S_1 & -\cot kl_1' & -1 \\ 0 & \cot k(L' + \Delta L') & 1 \end{vmatrix} = 0, \quad . \quad (30)$$

in which $\Delta L'$ is written for $\gamma_2 + (\pi/2k)$ and, as before, S_1 for $\cot kl_1' + \cot k\gamma_1$.

Since $\cot k(L' + \Delta L') = S_2/T_2$, (30) is easily seen to be identical with (29).

Alternatively (30) can be written

$$\frac{1}{\cot kl_1' - \tan k(L' + \Delta L' - l_1')} = -\tan k\gamma_1, \quad . \quad (31)$$

a form which could have been obtained immediately from (10) by writing $L' + \Delta L'$ in place of L'. The equation corresponding to (11) is

$$\frac{1}{\cot(m\pi n/2n_0) - \tan\left[\{(1-m)\pi n/2n_0\} + \epsilon + (\pi/2)\right]} = -\frac{2\pi\sigma}{ac_1} n_1 \left(\frac{n}{n_1} - \frac{n_1}{n}\right), \quad (32)$$

where

$$\epsilon = \tan^{-1}\left\{\frac{2\pi\sigma}{ac_2} n_2 \left(\frac{n}{n_2} - \frac{n_2}{n}\right)\right\} \quad . \quad . \quad . \quad . \quad (33)$$

As an example of the use of these equations, we will consider the determination of the frequencies of the resonant tones by a graphical solution of (32). Let $m = \frac{3}{4}$, $n_2 = n_0$,

and $(2\pi\sigma/ac_2)n_2=8$. We first plot the values of

$$Y_1=\frac{1}{\cot(m\pi n/2n_0)-\tan[\{(1-m)\pi n/2n_0\}+\epsilon+(\pi/2)]} \quad (34)$$

against n/n_0. The resulting curve is shown in fig. 7 as far as $n/n_0=4$. As in the case of a stopped pipe with only one Helmholtz resonator (fig. 3), the curve is divided into a number of branches by asymptotes perpendicular to the axis $y=0$. These are shown by the broken lines in fig. 7. The

Fig. 7.

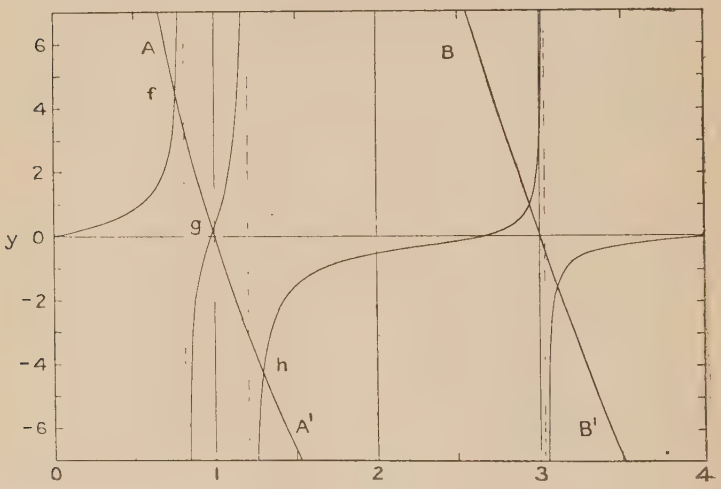

Graphical Solution of Equation (32).

position of the asymptotes is determined by the condition that the denominator of the right hand of (34) is equal to zero : *i. e.*,

$$\cot(m\pi n/2n_0)=\tan[\{(1-m)\pi n/2n_0\}+\epsilon+(\pi 12)],$$

from which we find that the condition is

$$\tan(\pi n/2n_0)=-\tan\epsilon,$$

or, by (33),

$$\tan\frac{\pi n}{2n_0}=-\frac{2\pi\sigma}{ac_2}n_2\left(\frac{n}{n_2}-\frac{n_2}{n}\right).$$

Now, the values of n which satisfy this equation are the frequencies of the resonant tones of the Boys resonator made from the pipe and the second resonator (n_2) alone (see equation (1)). Therefore the asymptotes of the Y_1 curve are the

lines $n/n_0=\mu_1$, $n/n_0=\mu_2$, etc., where μ_1, μ_2, etc., are such that $\mu_1 n_0$, $\mu_2 n_0$, etc., are the resonance frequencies of the Boys resonator at $x'=-l_1'$. Comparing this with the case discussed in the previous section, we see that the asymptotes in fig. 7 perform precisely the same rôle as do the asymptotes at $n/n_0=1, 3$, etc., in the simple case of a pipe combined with one resonator. In the latter case the asymptotes cut the axis $y=0$ at values of n/n_0, which give the frequencies of the stopped pipe alone.

As before, if m has certain values, the orifice of the resonator n_1 may be at a loop of the vibration within the pipe. This happens if m is such that $mL'=a/2\mu_n n_0$, where $\mu_n n_0$ is one of the resonance frequencies of the Boys resonator made from the pipe and the end resonator alone. Since L′ must exceed half a wave-length in order that a loop may occur within the pipe, μ_n must be greater than 2.

The line AA′ (fig. 7) is the curve found by plotting

$$Y_2 = -\frac{2\pi\sigma}{ac_1} n_1 \left(\frac{n}{n_1} - \frac{n_1}{n}\right)$$

against n/n_0 for the case when $n=n_0$ and $2\pi\sigma n_1/ac_1=8$. There are now three intersections with the Y_1 curve in the neighbourhood of n_0, at f, g, and h (fig. 7). In addition there are intersections (not shown in the figure) which give the frequencies of the overtones of the combination. The curve BB′ illustrates the case when the resonator n_1 is tuned to the first overtone of the pipe. There are now two resonant tones in the neighbourhood of $3n_0$ and two in the neighbourhood of the fundamental n_0. The intersections indicating the latter are not shown in the figure.

§ 5. *Experiments with a Stopped Pipe and two Helmholtz Resonators.*

The pipe used in these experiments was the same as that employed in the experiments described in § 3. One Helmholtz resonator (A) was placed at the stopped end of the pipe and another (B) in the side of the pipe. The resonator A was the same as that employed in the previous experiments, and was tuned to the fundamental of the pipe, so that in equation (33), which is subsidiary to (32), we have $n_2=66\frac{1}{2}$ vibrns. per second, $c_2=0{\cdot}133$ cm., and $2\pi\sigma n_2/ac_2 = 7{\cdot}60$. The resonator B was at a distance of one quarter of the reduced length of the pipe from the stopped end, so that in equation (32) we have $m=\frac{3}{4}$. Several experiments were made with different tunings of the resonator B, and the

results of three of them are shown in fig. 8. In each case there are two curves, one plotted from a hot-wire grid in A's orifice, and one from a hot-wire grid in B's orifice. These are shown in fig. 8 by the full and broken lines respectively *.

Fig. 8.

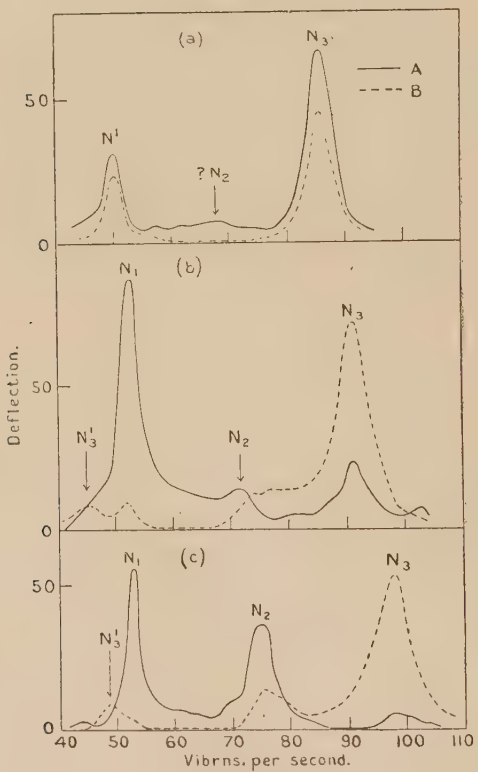

Resonance Curves for Combination of Stopped Pipe and two Helmholtz Resonators (A and B).

In the first experiment the frequency of B was $64\frac{1}{2}$ vibrns. per second and the conductance of its orifice 0·127 cm., so that $2\pi\sigma n_1 1 a c_1 = 7{\cdot}72$ in equation (32). For this tuning of B an inspection of fig. 7 shows that there should be three resonant tones, the exact values of the frequencies to be

* For the sake of clearness, observed points are not plotted in the figure, there being from forty to fifty points on each curve.

expected being shown under N_1, N_2, and N_3 in Table III. The resonance curves are shown at (*a*) (fig. 8), and it will be seen that, although N_1 and N_3 are well marked, the central tone N_2 is only feebly indicated in the curve for the resonator A, and probably not at all in the curve for the resonator B.

When the frequency of B is raised, however, the energy of the vibration at N_2 in the A resonator grows at the expense of those at N_3 in A and N_1 in B. This is shown by the curves at (*b*) (fig. 8). The tuning of B was here such that $n_1=81$ vibrns. per sec., $c_1=0{\cdot}127$ cm., and $2\pi\sigma n_1/ac_1 = 9{\cdot}70$. The small peak at N_3' is due to the impurity of the siren note, and is the response of B to the octave of the fundamental siren tone.

If the frequency of B is still further raised, the same process continues. The curves shown at (*c*) (fig. 8) are for the case when $n_1=93$ vibrns. per sec., $c_1=0{\cdot}127$ cm., and $2\pi\sigma n_1/ac_1=11{\cdot}1$. The vibration at N_2 in the A resonator is still more pronounced, while that at N_3 is inconsiderable. Similarly, practically all the energy in the B curve is concentrated into the peak at N_3. In this case also, B responds to the octave of the siren note at N_3'.

When n_1 is in the region of the first overtone of the pipe, the A curve is practically the same as that for $m=1$ in fig. 4, and the B curve is nearly that for $m=\frac{3}{4}$ in fig. 5. This was shown by an experiment in which $n_1=205$ vibrns. per sec., and $c_1=0{\cdot}167$ cm. The resonance curves for this experiment are not reproduced, but the observed and calculated resonance frequencies are included in Table III.

TABLE III.

($n_2=n_0=66\frac{1}{2}$.)

	$2\pi\sigma n_1/ac_1$	Calculated.			Observed.		
		N_1.	N_2.	N_3.	N_1.	N_2.	N_3.
$64\frac{1}{2}$	7·72	50	$65\frac{1}{2}$	86	50	?$67\frac{1}{2}$	$85\frac{1}{2}$
81	9·70	$52\frac{1}{2}$	$72\frac{1}{2}$	92	$52\frac{1}{2}$	$71\frac{1}{2}$	91
93	11·1	$52\frac{1}{2}$	76	$99\frac{1}{2}$	53	75	98
205	18·7	$53\frac{1}{2}$	79	197	54	$79\frac{1}{2}$	194

In the case when $n_1=205$, the fourth tone (N_4) was observed at 206 vibrns. per second, corresponding to a calculated value of 210 vibrns. per second.

§ 6. *Combination of Helmholtz Resonator and Conical Horn.*

Compound resonators consisting of a Helmholtz resonator combined with a conical horn have been used for the purpose of producing sensitive hot-wire microphones. A simple arrangement of this kind is shown diagrammatically in fig. 9. If the horn is made sufficiently large compared with the wave-length of the incident sound, the instrument is directive in its action, the greatest response being obtained when the mouth of the horn is directed towards the source of sound. If, however, the mouth of the horn is less than half a wave-length in diameter, the directive action is not very marked, and the sensitivity of the instrument appears to depend on the resonant properties of the combination rather than on the sound-collecting power of the conical horn.

Fig. 9.

Conical Horn and Helmholtz Resonator.

No attempt will be made in the present paper to give a complete theory of this type of instrument, but attention will be confined to methods of calculating the resonance frequencies in the special case when the directive properties are not well marked—that is, when the diameter of the conical horn can be treated as small compared with the wave-length. Some modifications of the simple form of resonator shown in fig. 9 will also be dealt with.

The theory of this type of resonator probably shows many similarities to that of such instruments as the phonodeik of D. C. Miller * and the Low-Hilger "audiometer" †. The essential feature of these instruments—which are primarily

* 'The Science of Musical Sounds,' pp. 78–87 (1916).

† *Alias* the "Optical Sonometer." See F. Twyman and J. H. Dowell, Journ. of Sci. Instruments, Preliminary Number, pp. 254–255 (May, 1922).

intended for the examination of wave-form—is a light diaphragm mounted near the vertex of a conical horn. The diaphragm and horn form a compound resonator, analogous to that consisting of a horn and Helmholtz resonator, which generally exhibits very pronounced resonance frequencies.

The first arrangement to be considered is that shown in fig. 9. The conical horn is truncated at the narrow end and closed by a flat plate, through a hole in which is inserted the orifice of the Helmholtz resonator.

In order to find the resonant tones, we assume a stationary vibration of the air within the cone. If the vertex of the cone is taken as the origin, the general expression for the stationary vibration is

$$\phi = \frac{1}{r}(\mathrm{A}\sin kr + \mathrm{B}\cos kr)\cos kat, \quad . \quad . \quad (35)$$

where r is the distance measured from the vertex. Let the closed end of the cone be at $r=\mathrm{R}_0$ (see fig. 9) and the open end at $r=\mathrm{R}$, and let $\mathrm{R}'=\mathrm{R}+\alpha$, where α is the end correction. Also let $\mathrm{L}'=\mathrm{R}'-\mathrm{R}_0$.

The condition to be satisfied by ϕ at the open end is

$$(\partial\phi/\partial t)_{r=\mathrm{R}'} = 0,$$

whence

$$\mathrm{B} = -\mathrm{A}\tan k\mathrm{R}',$$

so that

$$\begin{aligned}\phi &= (\mathrm{A}/r)(\sin kr - \tan k\mathrm{R}'\cos kr)\cos kat \\ &= (\mathrm{A}\sec k\mathrm{R}'/r)\sin k(r-\mathrm{R}')\cos kat. \quad . \quad . \quad (36)\end{aligned}$$

The condition to be satisfied at the closed end of the pipe is that the total flux across a portion of spherical surface of radius R_0 drawn inside the pipe is equal to the total flux into the Helmholtz resonator. If Ω is the solid angle of the cone, this condition is expressed by the equation :

$$\left\{\Omega r^2 \frac{\partial\phi}{\partial r}\right\}_{r=\mathrm{R}_0} = \frac{dq}{dt}. \quad . \quad . \quad . \quad . \quad . \quad (37)$$

Finally, if c is the conductance of the neck of the Helmholtz resonator and Q is its volume, we have

$$\frac{dq}{dt} = c(\phi_{0\mathrm{R}} - \psi), \quad \psi = (a^2/\mathrm{Q})\int q\,dt. \quad . \quad . \quad (38)$$

Putting $4\pi^2 n_1^2 = a^2 c/\mathrm{Q}$, we have, from (38),

$$\frac{dq}{dt} = \frac{c}{1-(n_1^2/n^2)}\phi_{\mathrm{R}_0}. \quad . \quad . \quad . \quad . \quad . \quad (39)$$

Whence, eliminating dq/dt,

$$\left\{\Omega r^2 \frac{\partial \phi}{\partial r}\right\}_{r=R_0} = \frac{c}{1-(n_1^2/n^2)}\phi_{R_0}. \quad . \quad . \quad (40)$$

It is evident from (40) that in the expression for ϕ given in (36) we may put $A \sec kR'$ equal to unity, so that the potential inside the cone may be taken to be

$$\phi = (1/r)\sin k(r-R')\cos kat. \quad . \quad . \quad . \quad (41)$$

Substituting this value of ϕ in (40), we obtain, as the equation for the frequencies of the resonant tones,

$$\Omega\{\sin kL' + kR_0 \cos kL'\} = -\frac{c}{1-(n_1^2/n^2)}\frac{\sin kL'}{R_0}$$

or

$$\frac{1}{1+kR_0 \cot kL'} = -\frac{\Omega R_0}{c}\left(1-\frac{n_1^2}{n^2}\right). \quad . \quad (42)$$

Whence, corresponding with equation (1), § 2,

$$\frac{1}{(a/2\pi nR_0)+\cot(2\pi nL'/a)} = -\frac{2\pi\Omega R_0^2}{ac} n_1\left(\frac{n}{n_1}-\frac{n_1}{n}\right). \quad (43)$$

The length L′ is an acoustical length, and includes an end-correction which varies with the solid angle of the cone. The frequency equation for a cone closed at $r=R_0$ is

$$\tan kL' + kR_0 = 0. \quad . \quad . \quad . \quad . \quad . \quad (44)$$

So that, if n_0 is the observed fundamental frequency of the cone, we have

$$L' = \frac{a}{2\pi n_0}\left\{\tan^{-1}\left(-\frac{2\pi n_0 R_0}{a}\right)\right\}. \quad . \quad . \quad (45)$$

From (43) we easily return to the case of the Boys double resonator, with a parallel pipe. (43) is, in fact, more general than equation (1), § 2, and includes the parallel pipe as a special case. In order to return to the case of the parallel pipe, let $\Omega \to 0$ and $R_0 \to \infty$ in such a way that the product ΩR_0^2 remains finite and equal to the cross-sectional area at the closed end of the pipe. In these circumstances the first term in the denominator of the left side of (43) becomes negligible, and the equation may be rewritten in the form

$$\tan\frac{2\pi nL'}{a} = -\frac{2\pi\sigma}{ac} n_1\left(\frac{n}{n_1}-\frac{n_1}{n}\right). \quad . \quad . \quad (46)$$

At the same time L′ becomes equal to $a/4n_0$ in accordance with (45), so that (46) is wholly equivalent to equation (1).

The solution of (43) may be effected graphically, as in the case of (11) and (32). As with the parallel pipe (fig. 3, $m=1$), the Y_1 curve, representing the left-hand side of (43), is divided into a number of branches by asymptotes perpendicular to the line $y=0$, these cutting it at points corresponding to the resonance frequencies of the cone without the Helmholtz resonator. The curve is non-periodic owing to the presence of the term $a/2\pi n R_0$ in the denominator of Y_1. A numerical example of the solution of (43) is given in § 7.

If the resonator is placed so that its orifice enters through the side of the conical pipe an equation for the resonant tones can be deduced analogous to (11), § 2. This case is of some practical importance, since an attempt has been made to use auxiliary resonators in this way in order to remove objectionable resonances from conical horns such as those used in "loud-speakers" and gramophones *.

Let R_1 be the distance of the orifice of the resonator from the vertex, and let R_0 and R′ have the same meanings as before. Also let ϕ_1 and ϕ_2 be potentials of the general form (35), ϕ_1 being the potential from $r=R'$ to $r=R_1$, and ϕ_2 the potential from $r=R_1$ to $r=R_0$. From the condition that $\partial\phi_1/\partial t=0$ when $r=R'$ and $r^2(\partial\phi_2/\partial r)=0$ when $r=R_0$, we find that suitable expressions for ϕ_1 and ϕ_2 are

$$\left.\begin{aligned}\phi_1 &= -\frac{1}{r}\frac{A}{\cos kR'}\sin k(R'-r)\cos kat,\\ \phi_2 &= +\frac{1}{r}\frac{A_2}{\sin k(R_0+\rho_0)}\cos k(r-R_0-\rho_0)\cos kat,\end{aligned}\right\} \quad . \quad (47)$$

where ρ_0 is a linear quantity such that $\cot k\rho_0=kR_0$.

The conditions to be satisfied when $r=R_1$ are

$$\left.\begin{aligned}\partial\phi_1/\partial t &= \partial\phi_2/\partial t,\\ \Omega r^2\left(\frac{\partial\phi_1}{\partial r}-\frac{\partial\phi_2}{\partial r}\right) &= \frac{c}{1-(n_1^2/n^2)}\phi_{R_1}.\end{aligned}\right\} \quad . \quad . \quad (48)$$

From the first of these conditions we find that

$$A_2 = -\frac{\sin k(R'-R_1)\sin k(R_0+\rho_0)}{\cos kR'\cos k(R_1-R_0-\rho_0)}A_1,$$

* I am indebted for this information to Mr. P. Rothwell. The work is referred to in a letter to 'Nature,' Feb. 24th, 1923, pp. 254-255, but a full account has not been published.

so that the expressions for ϕ_1 and ϕ_2 may now be written,

$$\left.\begin{aligned}\phi_1 &= -\frac{1}{r}\sin k(\mathrm{R}'-r)\cos kat,\\ \phi_2 &= +\frac{1}{r}\frac{\sin k(\mathrm{R}'-\mathrm{R}_1)}{\cos k(\mathrm{R}_1-\mathrm{R}_0-\rho_0)}\cos k(r-\mathrm{R}_0-\rho_0)\cos kat.\end{aligned}\right\} \quad (49)$$

By substituting these values in the second of conditions (48) and rearranging the terms, we obtain the equation for determining the resonant tones in the standard form,

$$\frac{1}{\cot k(\mathrm{R}'-\mathrm{R}_1)-\tan k(\mathrm{R}_1-\mathrm{R}_0-\rho_0)} = -\frac{2\pi\Omega\mathrm{R}_1^2}{ac}n_1\left(\frac{n}{n_1}-\frac{n_1}{n}\right). \quad . \quad . \quad . \quad (50)$$

As a check on this result we may note that if R_1 is put equal to R_0, (50) becomes identical with (43).

If, instead of being truncated at $r=\mathrm{R}_0$ the cone is continued as far as the vertex, we have $\mathrm{R}_0=0$, and hence

$$k\rho_0 = \cot^{-1}(k\mathrm{R}_0) = \pi/2,$$

so that (50) becomes

$$\frac{1}{\cot k(\mathrm{R}'-\mathrm{R}_1)+\cot k\mathrm{R}_1} = -\frac{2\pi\Omega\mathrm{R}_1^2}{ac}n_1\left(\frac{n}{n_1}-\frac{n_1}{n}\right). \quad (51)$$

One other arrangement may be noted—namely, that made by placing one Helmholtz resonator at $r=\mathrm{R}_1$ and another at $r=\mathrm{R}_0$, the cone being closed at $r=\mathrm{R}_0$, except for the orifice of the resonator. Let n_1 be the frequency and c_1 the conductance of the orifice of the resonator at $r=\mathrm{R}_1$, and n_2, c_2 the frequency and conductance of the orifice of the one at $r=\mathrm{R}_0$. Let ϕ_2 be the potential between $r=\mathrm{R}_1$ and $r=\mathrm{R}_0$. If the cone were completely closed at $r=\mathrm{R}_0$, the condition to be satisfied by ϕ_2 would be

$$\left\{\Omega r^2\frac{\partial\phi_2}{\partial r}\right\}_{r=\mathrm{R}_0} = 0. \quad . \quad . \quad . \quad . \quad . \quad (52)$$

Whence, since

$$\phi_2 = (1/r)(\mathrm{A}_2\sin kr+\mathrm{B}_2\cos kr)\cos kat,$$

$$\mathrm{A}_2\cot k(\mathrm{R}_0+\rho_0)-\mathrm{B}_2 = 0, \quad . \quad . \quad . \quad . \quad (53)$$

where, as before, ρ_0 is a linear quantity such that

$$\cot k\rho_0 = k\mathrm{R}_0.$$

When there is a resonator at $r = \mathrm{R}_0$, we have, instead of (52),

$$\left\{\Omega r^2 \frac{\partial \phi_2}{\partial r}\right\}_{r=\mathrm{R}_0} = \frac{c}{1-(n_2^2/n^2)}\phi_{\mathrm{R}_0}, \quad \ldots \quad (54)$$

from which we find

$$\mathrm{A}_2(1-k\mathrm{R}_0\cot k\mathrm{R}_0) + \mathrm{B}_2(\cot k\mathrm{R}_0 + k\mathrm{R}_0)$$

$$= -\frac{c_2}{1-(n_2^2/n^2)}\frac{1}{\Omega \mathrm{R}_0}(\mathrm{A}_2 + \mathrm{B}_2\cot k\mathrm{R}_0). \quad . \quad (55)$$

Let

$$\cot k\gamma = \frac{c_2}{1-(n_2^2/n_2)}\frac{1}{\Omega k\mathrm{R}_0^2}.$$

Then (55) may be rewritten in the form,

$$\mathrm{A}_2\{1-k\mathrm{R}_0(\cot k\mathrm{R}_0 + \cot k\gamma)\}$$

$$+\mathrm{B}_2\{k\mathrm{R}_0 + (\cot k\mathrm{R}_0 + k\mathrm{R}_0\cot k\mathrm{R}_0\cot k\gamma)\} = 0,$$

or

$$\mathrm{A}_2\cot k\mathfrak{R} - \mathrm{B}_2 = 0, \quad \ldots \quad (56)$$

where

$$\cot k\mathfrak{R} = \frac{k\mathrm{R}_0(\cot k\mathrm{R}_0 + \cot k\gamma) - 1}{k\mathrm{R}_0 + \cot k\mathrm{R}_0 + k\mathrm{R}_0\cot k\mathrm{R}_0\cot k\gamma}. \quad (57)$$

Comparing (56) with (53), we see that the equation for determining the resonant tones can be found by writing $\mathfrak{R}$ in place of $(\mathrm{R}_0 + \rho_0)$ in (50). If $k\mathrm{R}_0$ is small, we have approximately

$$k\mathrm{R}_0\cot k\mathrm{R}_0 = 1,$$

and in this case

$$\cot k\mathfrak{R} = \cot k(\Gamma + \rho_0) \quad \ldots \quad (58)$$

if

$$\cot k\Gamma = \cot k\mathrm{R}_0 + \cot k\gamma.$$

In the application of equations (50), (51), and similar forms it is necessary to bear in mind that if R_1 has certain values, the Helmholtz resonator in the side of the cone may be situated at a loop of one of the overtones of the cone, or

cone and resonator combination. The remarks in § 2 concerning the effect on the position of the resonant tones when the Helmholtz resonator is at a loop of one of the overtones of a parallel pipe apply *mutatis mutandis* to the case of the conical pipe.

§ 7. *Experiment with Conical Horn and Helmholtz Resonator.*

In order to test equation (43), a conical horn was made from "Fibre Sheet" about 1 mm. thick. The slant length of this horn was 122 cm., the diameter of the wide end 30·5 cm., and of the narrow end 10·6 cm., so that $R_0=65$ cm. The narrow end of the horn was closed with a flat plate of brass, into the middle of which could be screwed the neck of a Helmholtz resonator,

The fundamental resonance frequency (n_0) of the cone was found to be $99\frac{1}{2}$ vibrns. per sec. Putting these values of n_0 and R_0 in (45), we find that $l'=132$ cm.

Two experiments were performed. In the first one a Helmholtz resonator of frequency $93\frac{1}{2}$ vibrns. per sec., with an orifice of conductance ·127 cm., was attached to the cone. We have in this case $2\pi\Omega R_0^2/ac=12·1$, the air-temperature at the time of the experiment being 4°·5 C. The resonance frequencies in the neighbourhood of the fundamental calculated from (43) are 84 and 101 vibrns. per sec. The observations showed that there was one resonant tone of frequency 87 vibrns. per sec. and another of frequency between 98 and 103 vibrns. per sec. There was some doubt as to the exact position of the upper tone, since the upper peak in the resonance curve was not of a simple kind, but was itself divided into two peaks, one at 98 and the other at 103 vibrns. per sec. It seemed probable that this was due to a vibration in the wall of the horn, which was of a somewhat flimsy nature.

In the second experiment a Helmholtz resonator tuned to 205 vibrns. per sec., with an orifice of conductance ·167 cm., was used. This frequency is close to the first overtone of the horn, namely about 210 vibrns. per sec. The frequencies at which resonance would be expected to occur, calculated from (43), are 192 and 218 vibrns. per sec., while the observed frequencies were 190 and 215 vibrns. per sec.

These results are sufficient to show that equation (43) is

substantially true, although (for the reason stated) the agreement between the calculated and observed values in the first part of the experiment was not very satisfactory.

§ 8. *Summary.*

Theoretical expressions are obtained by means of which the resonance frequencies of several types of compound resonator employed in acoustical instruments can be calculated by the use of graphical methods. The types of resonator discussed are:—

(1) The Boys double resonator, consisting of a Helmholtz resonator combined with a stopped pipe. The theory previously given is extended to the case when the Helmholtz resonator is at some distance from the stopped end of the pipe, and the relation between the resonance frequencies and the distance of the Helmholtz resonator from the stopped end is discussed. This type of resonator is used in the Rayleigh disk and hot-wire instruments.

(2) A compound resonator made from two Helmholtz resonators and a stopped pipe. This kind of resonator is used in hot-wire microphones which are to be employed with the "bridge" method of measurement, or which are to be sensitive throughout two distinct ranges of frequencies.

(3) A combination of Helmholtz resonator and conical horn used for hot-wire microphones, and analogous to the diaphragm and horn combination in the phonodeik and similar instruments.

Experiments are described which show a satisfactory agreement with the theoretical results.

§ 9. *Conclusion.*

The work described in this paper was performed in the Acoustical Research Section of the Signals Experimental Establishment, Woolwich, and is one of the investigations carried on in that Section with the assistance of the Department of Scientific and Industrial Research.

Signals Experimental Establishment,
Woolwich,
May 1924.

LXXIX. *Studies on the Deformation of Tungsten Single Crystals under Tensile Stress.* *By* The Research Staff of the General Electric Co., Ltd.* (*Work conducted by* F. S. Goucher.)

[Plates XVI.–XXIV.]

Summary.

A combined X-ray and microscopic study is made of the deformed single crystals—in particular the fractured crystals—which are produced by the extension and fracture of fine tungsten wires composed of crystals, many of which occupy locally the complete volume of the wire.

The deformation may be accounted for in all cases by slip on the (112) planes and in the [111] direction, with the single exception of a crystal subject to special constraints which slipped as well on the (100) planes and in the [100] direction. The [111] direction represents the line of densest packing of atoms for this type of lattice structure—the body-centred—the [100] direction being next in order. The results are therefore in accord with the direction of easiest slip in the case of single crystals of metals involving other types of lattice.

Marked distortions of the crystal planes occur in the direction of slip equivalent to changes in inclination of the plane to this direction of from 10°–20° without any corresponding change in the atomic spacing; which leads to the view that such distorted crystals are no longer "single crystals" in the strict sense, and that such distortion is the cause of hardening due to slip.

The most favourable crystal orientation for extension by slip is such that two sets of 112 planes are symmetrical to the stress, each making an angle of 35° with the direction of stress; in agreement with the most prevalent orientation in drawn tungsten wires and rolled tungsten foils.

The most favourable orientation for slip on one set of planes is about 40° to the direction of stress, which accounts for the stability of crystal orientation when two sets of (112) planes are symmetrical to the stress.

(1) *Introduction.*

In a previous paper† experiments were described dealing with the strength of tungsten single crystals under such conditions that the crystals always fractured in the form of wedges approximately symmetrical to the axis of the specimen and the direction of stress. This condition was obtained by the use of fine wires, so treated that many crystals

* Communicated by the Director.

† Phil. Mag. Aug. 1924, p. 229.

occupied locally the complete volume of the wire. On submitting such wires to tensile stress, deformation occurred only in certain of these large crystals, and chance ensured that at least one of these would have an orientation very near to that offering the minimum resistance to deformation and fracture.

It was shown by means of X-ray analysis that the crystals after deformation were still single crystals, and that the crystal orientation was the same within 10° for all fractured crystals. It was assumed that, in common with single crystals of other metals, viz. aluminium *, zinc †, and tin ‡, deformation takes place by a process of slip on definite crystal planes. The crystal orientation with respect to the symmetrical wedge forms was such that the (112) planes were indicated as the slip planes, the direction of slip being the [111] direction. It was stated that experiments were in hand which definitely established this. It is the object of the present paper to describe these experiments. They include, in addition to a further study of the crystal forms by means of X-rays, a microscopic study of the etching pits produced in these crystals which throws some light on the mechanism of their deformation.

Information in regard to the exact mechanism of deformation of these crystals is desirable because of the interpretation of the strength measurements and their co-ordination with other physical properties as already described. Further, the determination of the slip plane and direction of slip is of interest because as yet no such determination has been made in the case of a metal having the body-centred type of lattice structure.

(2) *The Crystal Forms.*

The crystal forms studied were the fractured crystal wedges and the deformed crystals produced in the fractured wires in the manner described in detail in the previous paper. To minimize the experimental difficulties of X-ray analysis, angle measurements, and microscopic examination, only the largest wires—0·20 mm. in diameter—were used. The temperature at which these wires were fractured was about 3000° K. unless otherwise stated, the stress being about 1 kg./mm.^{2} and the time of fracture about 1 minute.

Photographs showing exterior views of typical crystal

* G. I. Taylor and C. F. Elam, Proc. Roy. Soc. A, vol. cii. p. 643 (1923).

† Mark, Polanyi, Schmid, *Zeit. f. Phys.* xii. (1922).

‡ Mark, Polanyi, *Zeit. f. Phys.* xviii. (1923).

forms are shown in figs. 1–3 (Pl. XVI.), taken at a magnification of 50. Figs. 1 and 2 show two views of the same wire in perpendicular directions. They show a markedly symmetrical wedge-shaped fracture, and a partially formed wedge, slightly asymmetrical to the wire axis. It is to be noted that the edge of the wedge shown in fig. 2 is not a true representation of the form of this edge because at the moment of fracture an arc takes place—the wire being heated electrically—causing the metal near the end of the wedge to melt. Fig. 3 shows another wedge form often obtained; such wedges are shorter than those shown in figs. 1 and 2 and have a larger wedge angle.

Etched sections of such wires cut parallel to the wire axis so as to show the wedge forms are shown in figs. 4, 5, and 6, taken at a magnification of 70. The specimens were mounted in hard glass which has a coefficient of expansion very nearly equal to that of tungsten, and which has the advantage that the specimen can be seen during the course of grinding. The etching was carried out in boiling hydrogen peroxide, the etching time being two minutes. Fig. 4 shows a typical long wedge slightly asymmetrical; fig. 5 a partially formed wedge; and fig. 6 a typical short wedge such as that shown in fig. 3. In all cases it is clear that deformation has taken place in large crystals occupying the full wire diameter.

These crystal forms suggest that deformation has taken place by a process of slip on crystal planes in all cases, and in the particular case shown in fig. 5 it appears to have occurred almost entirely on one set of planes perpendicular to the plane of the section.

(3) *Direct Determination of Slip Plane and Direction of Slip.*

Since the direction of slip and the inclination of the slip plane can be directly measured in the case of certain forms, it only remains to determine the crystal orientation by means of X-ray analysis in order to identify the slip plane and the direction of slip for this particular case.

Such a determination has been made for the crystal form shown in the photograph (fig. 7, Pl. XVII.) (× 50); the plane of slip is practically perpendicular to the plane containing the wire axis and the direction of slip, and the inclination of this plane to the wire axis is very nearly 40°.

The wire was mounted in hard glass as before, and a section cut as nearly as possible through the slipped portion of the crystal; this section was an elongated ellipse with its major axis inclined at about 7°—determined by careful measurement—to the direction of slip, and its minor axis

approximately perpendicular to the wire axis and the direction of slip. A determination of the crystal orientation with respect to the plane of this section was made by means of an X-ray spectrometer (such as that used in the measurements described in the previous paper).

The results of this analysis show that a set of (112) planes is inclined to the plane of the section at very nearly the same angle as the measured plane of slip. These (112) planes are, however, distorted; the nature of the distortion is such as to affect the inclination of the planes, but not apparently the atomic spacing. There is no variation in inclination of these planes in directions parallel to the minor axis of the section, but there is a variation in the direction of the major axis. The mean inclination of these planes with respect to the direction of the major axis was found to be 6°, and the inclination of these planes with respect to the minor axis was about 2°, which agrees very well with the inclination of the measured plane of slip to these two directions. It is therefore considered as established that the (112) planes are the planes of slip in this case.

Some of the X-ray photographs used in the determination are shown in fig. 8, Nos. II, III, and IV (Pl. XVII.). They were taken with a small Debye camera—3 cm. radius,—the specimen being mounted at the axis which was perpendicular to the direction of the X-ray beam. No. I shows the positions of (110), (100), and (112) reflexions, obtained from undistorted crystals, when the corresponding planes approximately intersect the spectrometer axis, and is merely given as a standard of reference. No. II shows a (112) reflexion obtained with the specimen in question mounted so that its minor axis intersects the spectrometer axis: it shows a spot of normal size and pattern characteristic of an undistorted crystal. No. III shows the corresponding reflexion obtained when the major axis of the specimen intersects the spectrometer axis; the reflected spot is markedly elongated. Such a spot is equivalent to the effect of gradually inclining an undistorted crystal to the spectrometer axis through an angle of about 10°, as calculated from the constants of the spectrometer. No. IV shows the effect of actually inclining the minor axis from its position as shown in II to one making an angle of 10° with the spectrometer axis. The distortion giving rise to the elongation need not, of course, be a uniform bending, and preliminary measurements on this point indicate that it is not, but rather of the nature of a buckling up of the planes in the direction of slip.

The direction of slip along such a (112) plane was not determined in the case of this crystal, but other crystals having exactly the same form were examined for crystal orientation by cutting sections perpendicular to the slip plane and parallel to the wire axis, and examining them in the X-ray spectrometer. A number of these were studied, and all showed a (110) set of planes to be within a few degrees parallel with such a section. This limits the direction of slip to the [111] direction, viz. along the diagonal of the unit cube of the tungsten lattice. The dimensions referred to are more easily visualized by reference to the photographs of the model shown in figs. 9 and 10 (Pl. XVIII.). Fig. 9 shows the arrangement of atoms in a unit cube of the tungsten lattice which is of the body-centred type. The vertical plane of the model is a (110) plane, viz. the plane passing through atoms 1 2 3 4 5. A (112) plane is a plane passing through atoms 7, 8, and intersecting half the distance between 1 and 2. This is shown better in the model (fig. 10), which contains more atoms, the model being oriented so that the (112) planes are in the line of vision and are those parallel to the black lines ; the atoms through which the lines are drawn lie in the [111] directions.

(4) *Wedge Forms—Theoretical.*

The possibility of explaining the form of the fractured crystals by slip on two sets of planes both inclined to the wire axis was briefly discussed in the previous paper. The crystal orientation with respect to the wedge forms was found to be such as to render it highly probable that the (112) planes were the planes of slip, the direction of slip being the [111] direction, and the direct determination of these in the case just discussed supports this view. It is proposed to test this supposition further by a comparison of the theoretical form assumed by a cylindrical specimen when slip occurs on two sets of planes inclined symmetrically to its axis with that actually found in the case of these wedges. Such a comparison should indicate the inclination of the planes of slip.

The manner of formation of a symmetrical wedge by means of slip on two sets of planes is best understood by considering successive stages of the process as illustrated in the series of diagrams shown in fig. 11.

Fig. 11, I, represents a section of a test-specimen which is perpendicular to two sets of slip planes parallel to A D and B C respectively, and each inclined at an angle θ to the axis of the specimen. II–V represent successive slips on alternate conjugate planes, with the result that the crystal is

extended and at the same time reduced in diameter in the plane of the section. If the slips are small enough in comparison with the dimensions of the specimen, and if there is, on the average, as much slipping on one set of planes as on the other, it is easy to see that a completely symmetrical fracture may be produced. It should be noted that no reason is assumed for the alternation of the slipping; this will be discussed later.

Fig. 11.

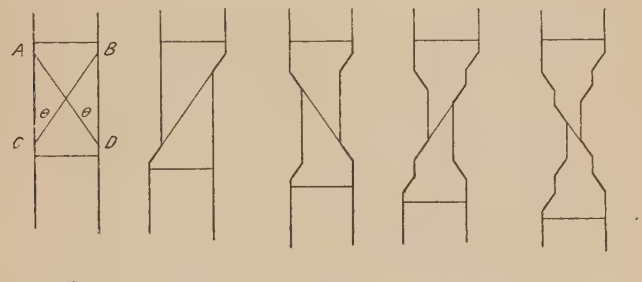

It was shown in the previous paper that there is a perfectly definite relation between the resultant angle of such a symmetrical wedge and the angle θ. This relation will hold for any section of a cylindrical specimen cut parallel to its axis and perpendicular to the planes of slip, and it should therefore be possible to determine the complete form of a fractured cylinder for any given value of θ.

Fig. 12.

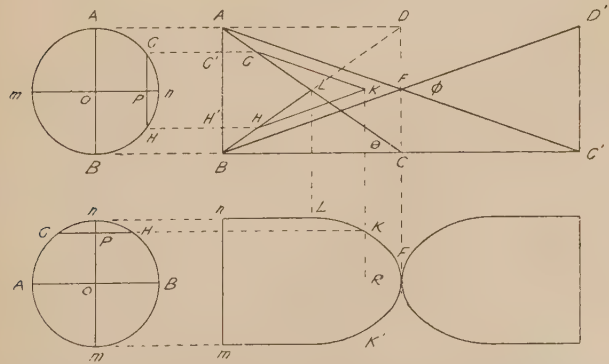

Let A B C D, fig. 12, represent a section through the axis of the cylinder of diameter A B. Let A C and B D represent the directions of two sets of slip planes in the cylinder perpendicular to the section. It was shown previously that

before fracture can occur the crystal must extend an amount C C′, such that C C′ = B C. Then A C′ and B D′ will represent the contour of this section at the time of fracture, provided an equal amount of slipping has occurred on both sets of planes, the angle ϕ being given by the relation

$$\phi = 2\tan^{-1}(\tfrac{1}{2}\tan\theta) \quad . \quad . \quad . \quad . \quad . \quad (1)$$

Any other section of the cylinder at a distance O P from the axis and parallel to it will have assumed the form G′ G K H H′, of which the angle G K H = ϕ; there is obviously no slipping within the portion G′ G L H H′. The locus of K for all such sections is shown in the projection as the curve L K F, which is a portion of an ellipse; the outline of the two wedges is completed in the projection as shown. The two surfaces of the wedge will themselves be portions of cylinders the axes of which are inclined to the axis of the specimen.

Models have been constructed which illustrate the form assumed by a cylindrical specimen when deformed by symmetrical slip on two sets of planes. These were built up in accordance with the principle of alternate slip as illustrated in fig. 11, the angle of the slip planes with the axis of the cylinder being chosen as 35° to correspond to the (112) planes, and the extent of slipping regulated to give an angle of 39° as calculated from the theory. Photographs of these models are shown in figs. 13–16 (Pl. XVIII.). Fig. 13 shows a wedge in process of formation; figs. 14 and 15 show two views of a completed wedge taken in perpendicular directions; and fig. 16 shows the other view of the model shown in fig. 13.

(5) *Wedge Forms—Measurements.*

A determination of the wedge angle ϕ for a large number of the fractured crystals was made by photographing the wedge forms at a magnification of 100, and measuring the mean angle between the wedge surface throughout the main portion of the wedge. The curved shoulders of the wedge where the crystals are first reduced in diameter, and the irregular tips sometimes formed at the moment of fracture through the formation of an arc or an evident distortion of the thin part of the wedge, were in all cases neglected.

The results of such measurements are given in Table I. They clearly divide themselves into two groups; Group I, long wedges with a mean angle of 39° and a deviation from the mean of not more than 2°; Group II, short wedges with any angle from 50°–60°.

TABLE I.—Wedge Angles.

Group I. Measured Angle. ϕ		Group II. Measured Angle. ϕ	
41°	38°	51°	52°
39	39	53	55
38	38	50	55
37	36	55	54
39	40	55	60
37	39	53	57
		52	56
Mean = 38° 24′		Mean = 54° 12′	

Substituting the mean value $\phi = 38° 24'$ in equation (1) of the last section, we get

$$\theta = 34° 51',$$

which agrees well with the angle made by the (112) planes with the wire axis when the crystal orientation is symmetrical with this axis.

It therefore appears that this contour of the 39° wedges is accounted for by slip on the (112) planes, and in the [111] direction as before. The form of the other wedges having larger angles is still unexplained. This, as we shall see later, is due to unsymmetrical slip on the same set of planes and in the same direction.

It was thought desirable to check the wedge shape of the 39° wedges in other dimensions—in particular the theoretical contour of the wedge-edge as constructed in fig. 12, and as shown in the models. A symmetrical wedge comparatively free from end distortions and having comparatively straight wedge surfaces—such a one as shown in fig. 1 (Pl. XVI.)—was mounted in hard glass, and a series of sections made in planes perpendicular to the wire axis. Each section was photographed to show the contour, some of these being shown in the series I–VI (fig. 17, Pl. XIX.) (×150).

The horizontal dimensions of these sections as measured from the photographs were compared with the theoretical

values on the same scale as shown in fig. 19. The dotted line represents the theoretical contour, and the crosses the corresponding observed dimensions in this direction. The vertical dimensions of the sections were used to locate the positions of the sections on the horizontal scale by plotting them on the line A B, O A being one-half the wire diameter as determined from the photograph VI in a vertical direction, and O B being of such a length that A B makes an angle $\frac{1}{2}\phi = 19° 28'$ with the direction of the horizontal axis. The theoretical contour was based on the wire diameter as determined from the horizontal dimension of photograph VI.

Fig. 19.

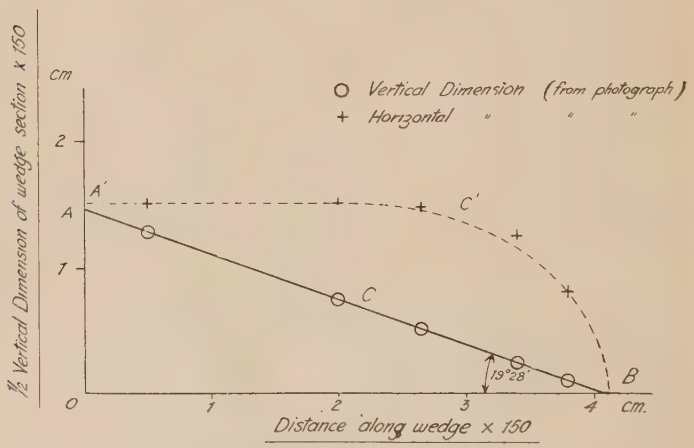

These measurements show that the wedge forms agree in other dimensions as well as wedge angle with the theoretical form, though even in this case there are evidences of some distortion, in particular section II, which is somewhat longer than the theoretical value.

(6) *Distortion of Crystal Planes by X-ray Analysis.*

Further evidence of distortion of these symmetrical wedge forms is shown by means of X-ray analysis. Measurements carried out in the manner described in section (3) show that the crystal planes are distorted in the direction of slip, but not in the perpendicular direction, the extent of the distortion being of the same order as that shown in the case of slip on one set of planes only. In this case the (110) planes were studied, sections being cut perpendicular to the wire

axis through the slipped portions of the wedge. Photographs such as those shown in fig. 18, I–IV (Pl. XVII.) were obtained.

Fig. 18, I, shows the effect of an undistorted (110) reflexion for the case of a symmetrical wedge deformed at 3000° K., the section being mounted so that its major axis —parallel to the wedge edge—intersected the spectrometer axis ; II shows the corresponding reflexion from the section mounted so that its minor axis intersects the spectrometer axis. Similar photographs were obtained with wedges deformed at 1000° K., of which III and IV are representative. The extent of the distortion amounts to about 10° in the case of photograph II and between 15° and 20° in the case of IV. It was shown that the distortion in the case of IV was of the nature of a smooth curve throughout the section, the curvature being convex outward, viz. toward the wedge edge. This was done by covering up half of the specimen, the corresponding half of the reflected beam being in this case obliterated.

(7) *Microscopic Examination.*

Having established the direction of the slip planes with respect to the symmetrical long wedge forms, it appeared desirable to examine microscopically sections of these wedges cut along various crystal planes in order to co-ordinate if possible the shape of the etching pits with the orientation of the crystal. If such a co-ordination could be made, it might be expected to throw light on the nature of the distortion and the mechanism of deformation giving rise to the short wedge forms, which are still to be explained.

Sections were prepared as nearly as possible parallel to the main crystal planes within long symmetrical wedge forms. These sections were etched for 2 minutes in boiling hydrogen peroxide, and then for 45 seconds in alkaline potassium ferricyanide ; they were then photographed under vertical illumination with a 3-mm. oil-immersion lens (N.A. 1·3).

The effects shown in photographs (figs. 20–23, Pl. XX.) (× 250) are typical of those obtained for the three main crystal planes, the (110), the (100), and the (112) planes. Figs. 20 and 21 show two views of a section cut nearly parallel to the (110) planes : such a section as would be obtained from the model shown in fig. 13 (Pl. XVIII.) when cut in a vertical plane perpendicular to the planes of slip. The photographs are mounted so that the axis of the wire is vertical in both

cases; fig. 20 is a view of the portion of the crystal through which the maximum amount of slip has taken place, and the lower part of fig. 21 is a view, near a grain boundary, of a portion of the same crystal which has not been deformed by slip. Both clearly show the same type of lamellæ with sharply-marked edges inclined at approximately 110° with each other, and each making the same angle with the wire axis; such markings correspond in direction with the intersection of two (112) planes with the plane of the section. It is notable that there is no evidence of any effect of slip on these markings.

Fig. 22 shows a section cut nearly parallel to a (112) plane near the tip of a symmetrical wedge: such a section as would be obtained from the model shown in figs. 14 and 15 (Pl. XVIII.) when cut parallel to one of the planes of slip. The photograph is mounted so that the wire axis lies in the vertical plane perpendicular to the plane of the section. The etching effects in this case are markedly different from those shown in figs. 20 and 21 (Pl. XX.), the heaviest markings being horizontal lines, though the absence of markings in the lower portion is particularly noticeable. These markings again correspond with the direction of the intersection of a (112) plane with the plane of the section, viz. the other slip plane inclined at 70° to the plane of the section.

The photograph shown in fig. 23 (Pl. XX.) was taken from a section cut nearly parallel to a (100) plane: such as would be obtained from the model (figs. 14 and 15, Pl. XVIII.) when cut parallel to its axis and parallel to the wedge edge. The etching pits appear to have no marked orientation with respect to the dimensions of the section. It should be noted that the intersection of the (112) planes with the plane of the section in this case has four-fold symmetry.

All these effects suggest that the etching reagents act more vigorously along the (112) planes than in any other direction, which is not surprising considering that this is the plane of slip, and therefore presumably of weakest bonding between atomic layers. The absence of markings in the lower part of the photograph (fig. 22, Pl. XX.) suggests that here, near the edge of the specimen, the etching reagent was able to clear off all the crystalline material along the (112) plane, which is evidently slightly inclined to the surface of the section.

On the strength of these results the examination was extended to various sections made from wedge forms, with the object of obtaining any information which might lead to a better understanding of the mechanism of their formation.

Photographs figs. 24–30 (Pls. XXI. & XXII.) were some of the most interesting of those obtained. These were taken at a magnification of 750 with the same lens as before.

Fig. 24 shows the central portion of the crystal shown in fig. 20 (Pl. XX.). It brings out the markings more clearly, and serves as a comparison for the photograph (fig. 25) showing the tip of the short wedge shown in fig. 6 (Pl. XVI.) taken at low magnification ; these photographs are mounted so that the wire axis is vertical in both cases. The markings shown in the photograph fig. 25 clearly suggest that the final fracture of this crystal has taken place by slip along a (112) plane from left to right, and it is to be noted that the angle made by this plane with the axis of the wire is about 40°.

Fig. 26 shows the tip of another such short-wedge form, but this time from a wire fractured at 1000° K. and under a load of 14 kg./mm.^{2} The photograph is again mounted so that the wire axis is vertical. The markings appear in every way the same as those shown in fig. 25, though there is evidence of greater distortion of the crystal. Again the final slip appears to have taken place along a (112) plane, the inclination of this plane to the direction of stress being, as before, about 40°. These two forms are indeed typical of all the short wedges examined, and, as we shall see, give the clue to a possible explanation of their formation.

Fig. 27 shows the tip of a very irregular wedge form, the photograph being mounted so that the wire axis is vertical. This form is such as to leave no doubt that slip has occurred in the direction of the etch markings. The photograph is of special interest because both the 70° angles and the 110° angles made by the (112) planes are to be seen. Marked curvatures of the planes are evident however, the planes having suffered a change of orientation of about 20° between successive slips in the last few large slips shown : such a distortion, though large, is not inconsistent with the results of X-ray analysis already given.

Fig. 28 (Pl. XXII.) shows a section of a wedge almost parallel to the (110) plane but perpendicular to the wire axis : such a section as that shown in fig. 17, III (Pl. XIX.), and similar to those used for X-ray analysis described in (6). The photograph is mounted so that the major axis is vertical. The markings are clearly similar to those obtained from other (110) sections, but—in agreement with the results of X-ray analysis—there is distinct evidence of distortion symmetrical with the major axis of the specimen.

The photographs figs. 29 & 30 were obtained from the

two sections described in (6), of which the distortions were compared in fig. 18, I–IV (Pl. XVII.). The 70° markings are predominant in these sections, their asymmetry about the vertical axis, particularly in fig. 30, being most marked.

The photograph fig. 31 (Pl. XXII.) is a view of one end of the section, described in (3), cut along the plane of slip; it is mounted so that the major axis of the section corresponding to the direction of slip is nearly vertical. The markings clearly resemble those shown in fig. 22 (Pl. XX.), and the evidence of distortion, especially near the bottom of the section, is clearly seen; further, this distortion appears to be symmetrical about the horizontal direction in agreement with the results of X-ray analysis.

(8) *Effect of Orientation on Mode of Deformation.*

The sharpness of the markings indicating the direction of the slip planes in the etched sections of these crystals suggests the possibility of determining by this means the crystal orientation in the various crystal forms produced by deformation.

A study of the effect of orientation on the shape of the deformed crystals, in particular those which have not fractured, should yield information concerning the relative tendency to slip under conditions of stress which are strictly comparable. Since these crystals were taken from test-wires which were actually fractured, the load, time of application of the load, and temperature were the same as were required for the fracture of the weakest crystal.

Sections were cut as nearly as possible parallel to the (110) planes perpendicular to the planes of slip in the case of a variety of typical crystal forms. These were prepared in the usual way and were photographed at two magnifications, one at 70 and the other at 250. The direction of the wire axis in the case of the latter was determined by comparison with the direction of the wire axis as shown by the former. Measurements were made on the high magnification photographs by drawing lines parallel to the etch markings and measuring the angles made by these lines with the direction of the wire axis; a mean of at least 10 readings was taken in the case of the best photographs. Four of these photographs are shown in figs. 32–35 (Pl. XXIII.), the photographs being mounted so that the wire axis is vertical in each case. Fig. 32 shows the somewhat drawn-out tip of a symmetrical long wedge; fig. 33, an unsymmetrical wedge; fig. 34, a

portion of a crystal which has slipped largely, but not entirely, on one set of planes ; fig. 35, one which has slipped almost entirely on one set of planes.

The results of the measurements clearly show that the orientation of the crystal with respect to the wire axis determines the form assumed by the crystal. The facts are represented diagrammatically in fig. 36. If we consider the line bisecting the angle between the two sets of slip planes as representing the inclination β of the crystal to the wire axis, then, as β increases from zero, the crystal

Fig. 36.

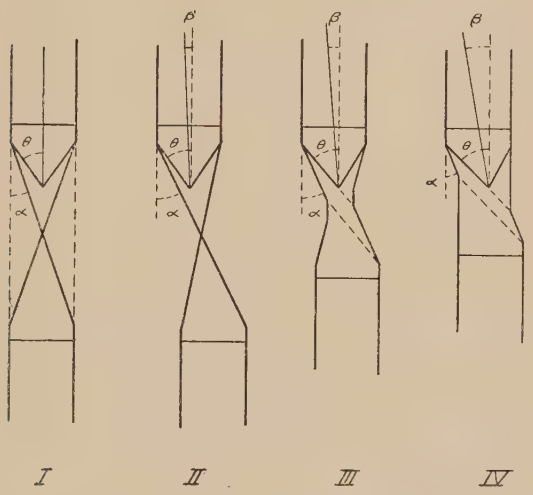

forms change from the symmetrical form shown in I to the asymmetrical forms shown in II, III and IV, a further increase resulting presumably in no deformation whatever. Such asymmetrical forms can only be produced by differences in the extent of slipping on the two sets of planes and the form shown in III indicates that the extent of slipping on the more oblique set of planes is greater than in any of the other forms since the obliquity of the surface here reaches a maximum.

The most favourable angle for slip on any one set of planes may, therefore, be determined by plotting the measured values of α—the angle between the more oblique crystal surface and the wire axis—against the corresponding values of θ—the angle made by the slip planes with the wire axis.

The results are shown in fig. 37 ; the triangle represents the relation between α as measured from the photograph fig. 7 (Pl. XVII.) and the mean values of θ as determined by X-ray analysis. Clearly α rises to a maximum, the corresponding value of θ being about 40°.

Fig. 37.

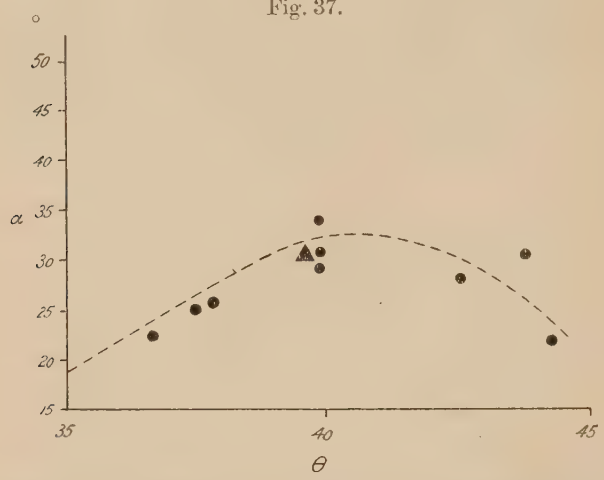

Though no great accuracy can be expected from such measurements, they are considered as sufficiently representative of the facts to warrant the general conclusion that the tendency for slip to occur on any one set of planes is greater the nearer the inclination of the set of planes with respect to the wire axis approaches an angle of about 40°.

(9) *The Mechanism of Wedge Formation.*

The effect of crystal orientation on the tendency to slip, coupled with the facts of crystal distortion, suggest the explanation of the formation of the crystal wedges, in particular the large angle short wedges which have not yet been explained.

The photographs figs. 25 & 26 (Pl. XXI.) clearly indicate that fracture occurred by a final slip practically on one plane inclined at an angle of about 40° to the wire axis. On the other hand, the inclination of the other surface forming the wedge angle shows that slip must have occurred previously on the conjugate set of planes, the inclination of which must have approached 40° at the time when slip took place. The suggested explanation is that the short wedges are produced

in crystals which are slightly inclined to the wire axis ; that, in consequence of this, slip in the beginning occurs mainly on one set of planes in the manner represented in diagram III (fig. 36) ; that the asymmetry of the form thus produced results in the re-orientation of the crystal in the region of reduced cross-sectional area, until the inclination of the conjugate planes is sufficiently favourable to result in slip, the most favourable angle being about 40°. This accounts for the large angle of these wedges, the total angle being 40° plus the angle produced by the succession of slips on the conjugate planes.

A similar process is no doubt involved in the formation of the long 39° wedges, the forms of which have been explained by assuming alternate slipping on two sets of conjugate planes symmetrically inclined to the wire axis in regions of progressively reduced cross-sectional area as represented in the series of diagrams shown in fig. 11. In the discussion of these wedge forms (4), however, no reason was given for the alternation of the slipping and the maintenance of the crystal stability during the process of deformation. The process of crystal distortion favouring slip on the alternate planes affords a possible explanation, especially since the amount of distortion required to change the balance in favour of slip on the conjugate planes need not be large. Fig. 27 (Pl. XXI.) shows clearly that such an action does actually occur in the case of this somewhat irregular long wedge form. In the photographs (fig. 24, Pl. XXI. and fig. 32, Pl. XXIII.) no evidence of the distortion appears, but it is to be expected that if the extent of slipping on each set of planes is small, the distortion would not be large, and, moreover, each successive distortion would tend to correct the previous one. It has been shown that the crystal wedges are distorted, the (110) planes—perpendicular to the wire axis—being convex toward the wedge edge. This can be accounted for by the effect of distortion due to the successive slips, if we assume that the slip planes tend to become distorted near their edges, the distortion reaching a maximum in the region where the overlapping is greatest. It would be expected that these planes would be pulled more nearly into the line of stress owing to the disturbance in the balance of forces due to overlapping. Under these conditions the crystal may be distorted momentarily, favouring slip in the conjugate planes until the process is reversed.

It should be pointed out, however, that such a crystal re-orientation is not necessary to explain the formation of these wedges, it being only necessary to assume that slipping,

once started on any plane, automatically stops, and that the next slip occurs in a new region of the crystal. Since slipping on one set of planes tends to reduce the volume of the crystal in which slips may occur on like planes of equal area, whereas it tends to increase the volume for conjugate planes of equal area (see diagrams, fig. 11), it follows that the probability of slip occurring in any volume of the crystal tends to favour the conjugate planes. The tendency for slip to be automatically limited finds a ready explanation in the distortion of the crystal planes in the direction of slip, especially near the edges, where there is a disturbance in the balance of forces due to overlapping ; such a distortion was shown to be produced in the zone of slip in the case of the crystal in fig. 7 (Pl. XVII.), which was deformed by slipping on one set of planes.

(10) *Special Case of Slip on* (100) *Planes.*

In the course of the investigation on the strength of these crystals, a freak case of fracture was observed which is of some significance. Figs. 38 and 39 (Pl. XXIV.) show two views of this fracture taken in perpendicular directions. They show that two wedge forms are produced which are inclined to each other at 90°. One of these wedge forms is very much like the long 39° wedge : such a wedge is shown in fig. 40 (Pl. XXIV.) for the sake of comparison. The other is of a much larger angle, measuring over 60°. A series of etched sections cut perpendicular to the wire axis and mounted with the proper relative orientation is shown in fig. 41, I–IV (Pl. XXIV.). They clearly show that the double wedge was formed from the same crystal, and that the cause of this formation lay in the groove, produced by a split in the wire in which the crystal was grown. The inclination of this groove was such as to prevent slip in the normal way. It was shown by X-ray analysis that the crystal section as shown in IV was nearly parallel to the (110) planes. This makes it practically certain that the narrow wedge was due to slip on (112) planes, and that the other wedge was produced by slip along (100) planes. The theoretical angle for this latter wedge would be 54°, but the actual angle is no doubt due, as in the case of short wedges, to asymmetrical slip accompanied by distortion. It may be observed that the force required to produce this fracture was larger than that required for a normal fracture, the breaking stress being 16 kg./mm.^{2} at 1200° K. as compared with 12 kg./mm.^{2} for a normal wire at the same temperature.

(11) *Discussion of Results.*

It has now been established that all of the deformed crystals studied, in particular the fractured crystal wedges, can be accounted for by a process of slip on the (112) planes and in the [111] direction, with the single exception of the specially constrained crystal, in which slip also occurred on the (1$\bar{0}$0) planes and in the [100] direction. All such deformed crystals showed distortions which affected the inclination of the crystal planes in the direction of slip, but which produced no marked change in the atomic spacings.

Further, it has been shown that the most favourable crystal orientation for extension and fracture is such that two sets of 112 planes are inclined at 35° to the wire axis, whereas the most favourable orientation for slip on one set of planes is such that the planes make an angle of about 40° with the wire axis.

The direction of slip, the [111] direction (viz. along the cube diagonal), is that of the densest packing of atoms for this type of crystal lattice (viz. the body-centred), the distance between the atoms along this line being smaller than along any other line of atoms in the crystal. The result is therefore in agreement with that obtaining in the case of the deformation of single crystals of other metals involving different lattice types, viz. zinc, tin, bismuth, and aluminium, as pointed out by Polanyi *. The one case in which slip occurred in the [100] direction (viz. along the cube edge) demonstrates the fact that slip can occur along other lines of atoms as well; further, it is to be noted that this direction is next in order to the [111] in the density of atoms. The nature of the constraints induced by the peculiar form of this crystal and the extra stress required to produce the deformation suggest that, under suitable conditions, a crystal could be made to slip in still other directions, and that such is in fact the case when a crystal is deformed as part of an aggregate.

The extent of the distortion produced by the deformation of these crystals is such that they can no longer be considered as "single crystals" in the strict sense. It follows both from the X-ray measurements and from the photographs that distortions of the crystal occur which would involve an atomic displacement of at least 10 per cent. in some cases, whereas no such displacement was observed; a displacement of 10 per cent. could easily be detected. It would appear

* Polanyi, *Zeit. f. Phys.* xvii. pp. 42–53 (1923).

that the crystal must be considered as made up of small, more perfect crystals with similar but not the same orientations. The mechanism of deformation, which satisfactorily accounts for the crystal forms, suggests that although the major portion of the slipping occurred before an appreciable amount of distortion took place,—with the exception of the slips near the point of fracture,—it is because of this distortion that slip is limited in extent along any one plane. If we take the view that slipping is merely a handing-on of atomic bonds, it is easy to see why a small curvature of the planes involving gaps or local changes in bonding in the chain of atoms would increase the resistance to slip.

The most favourable crystal orientation for extension and fracture is that which has been found to occur most frequently in worked crystal aggregates of tungsten, in particular drawn tungsten wire and rolled tungsten foils *. In both cases one set of (110) planes tends to set itself perpendicular to the direction of stress, and in the case of rolled foils the (100) crystal faces tend to lie in the plane of rolling. In the light of our experiments the reason for this becomes quite clear, in that extension can take place mainly by slip on the (112) planes inclined at 35° to the plane of rolling, and at the same time increase of width and some extension can take place by slip on the (100) planes. The fact that the tendency for slip to occur increases above 35° has been shown to account for the stability of crystals during deformation by extension when in this favoured crystal orientation. This is in agreement with the hypothesis put forward by Polanyi † to account for the stability of the favoured crystal orientations in worked metals. The fact that the most favourable angle for slip on one set of planes is about 40° and not 45° is worthy of note. Since the theoretical orientation for maximum shearing stress is 45°, the result would appear to indicate that the perpendicular component of stress is effective in producing slip in this case, but further experiments will be necessary in order to settle this point.

These experimental results demonstrating that the mechanism of fracture is in all cases the same are of importance in connexion with the interpretation of the strength measurements described in the previous paper. Discontinuities were found to occur in load-temperature curves at definite temperatures which were co-ordinated with variations in other

* Polanyi, *loc. cit.*
† Polanyi, *loc. cit.*

Fig. 1.

Fig. 2.

Fig. 3.

Figs. 1, 2, 3. Exterior view of fractured wires showing deformed crystals (×50).

Fig. 4.

Fig. 5.

Fig. 6.

Figs. 4, 5, 6. Etched sections of fractured wires showing deformed crystals (×70).

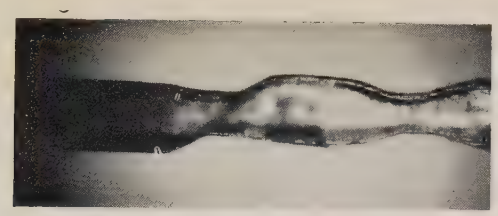

Fig. 7.

Fig. 7. Deformed crystal (left) which has slipped almost entirely on one set of planes (×50).

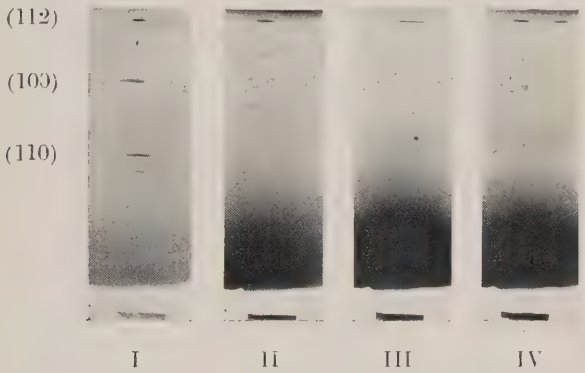

Fig. 8.

Fig. 8. X-ray photographs of (112) reflexions from planes of slip shown in crystal fig. 7 showing distortion of these planes.

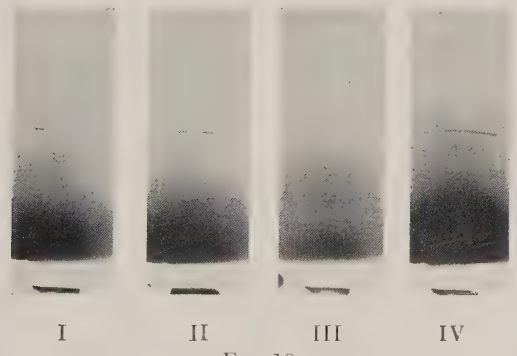

Fig. 18.

Fig. 18. X-ray photographs of (110) reflexions from sections of wedges perpendicular to wire axis showing distortion of these planes.

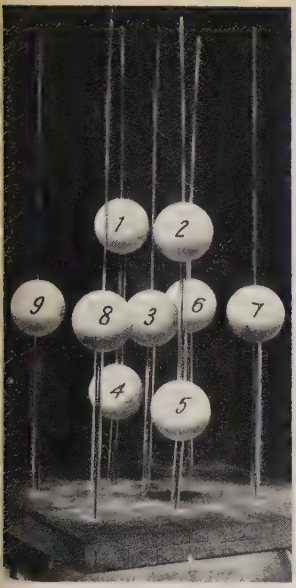

Fig. 9.

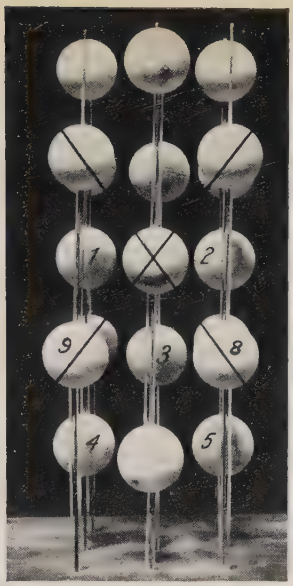

Fig. 10.

Fig. 13.

Fig. 9. Model of unit cube of tungsten lattice arranged with (110) plane—1245—vertical.

Fig. 10. Model showing arrangement of atoms in tungsten crystal and directions of (112) planes.

Fig. 14.

Fig. 15.

Fig. 16.

Figs. 13, 14, 15, 16. Models showing forms assumed by a cylinder when deformed by slip on two sets of planes symmetrically inclined to its axis.

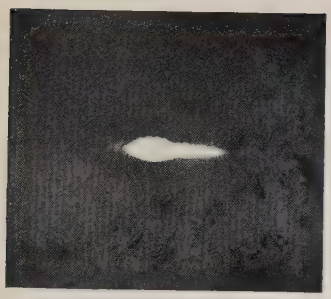

I

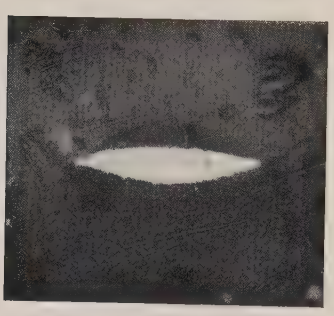

II

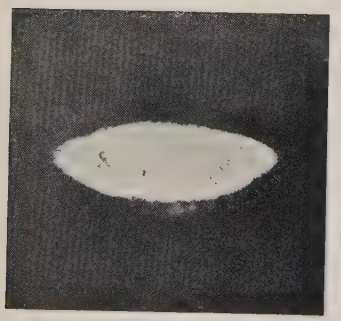

III

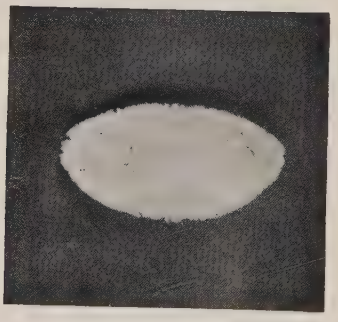

IV

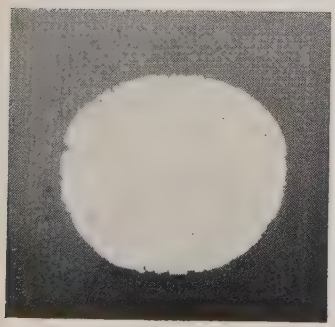

V

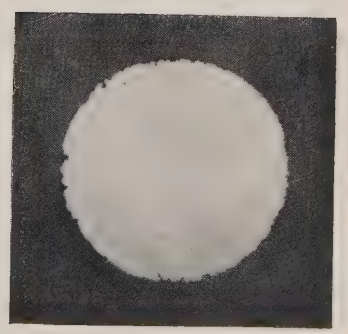

VI

Fig. 17.

Fig. 17, I–VI. A series of sections cut from a symmetrical wedge perpendicular to wire axis (×150).

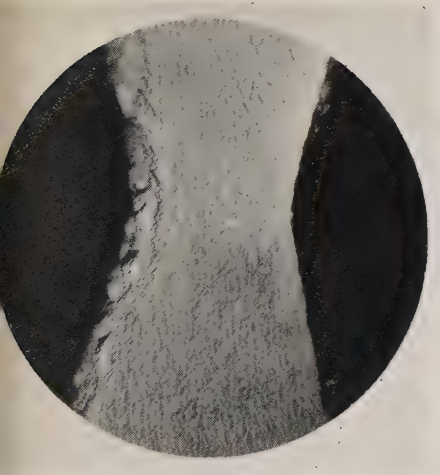

FIG. 20.

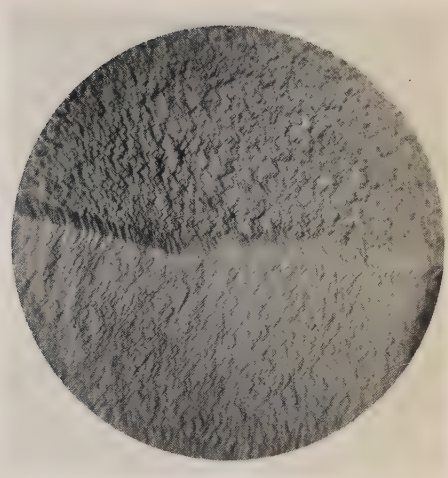

FIG. 21.

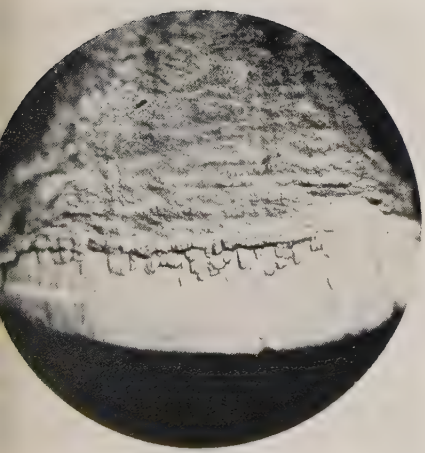

FIG. 22.

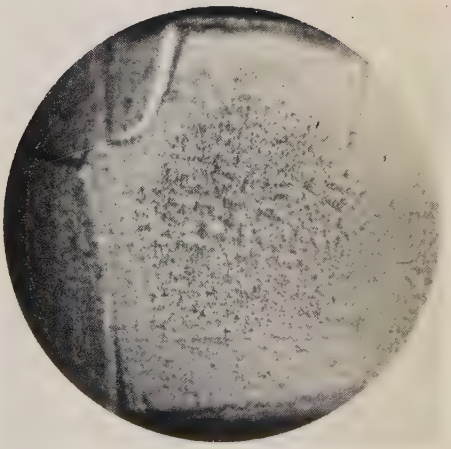

FIG. 23.

igs. 20, 21, 22, 23. Etched sections from wedge forms cut parallel to (110), (112), and (100) planes showing characteristic etching effects (× 250).

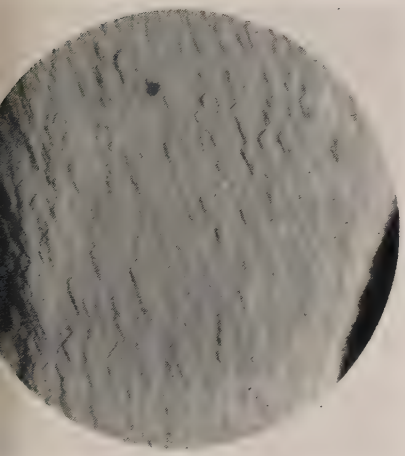

Fig. 24.

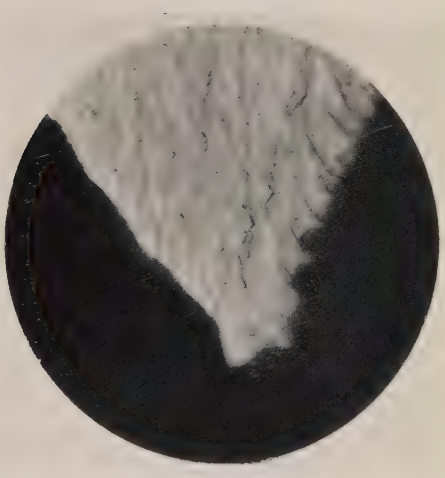

Fig. 25.

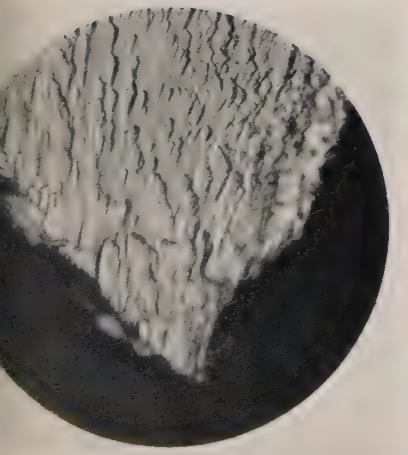

Fig. 26.

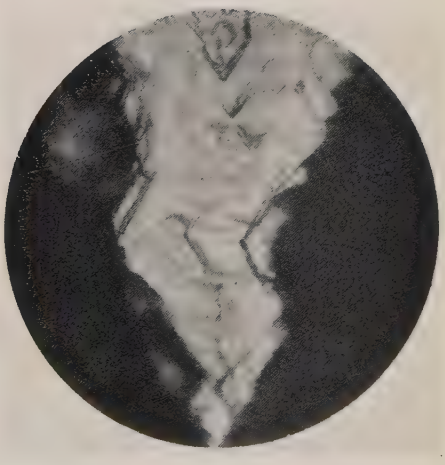

Fig. 27.

24, 25, 26, 27. Etched sections from wedge forms perpendicular to planes of slip showing distortions of slip planes (×750).

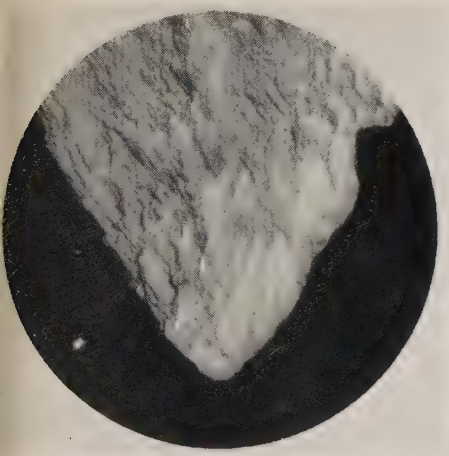

Fig. 28.

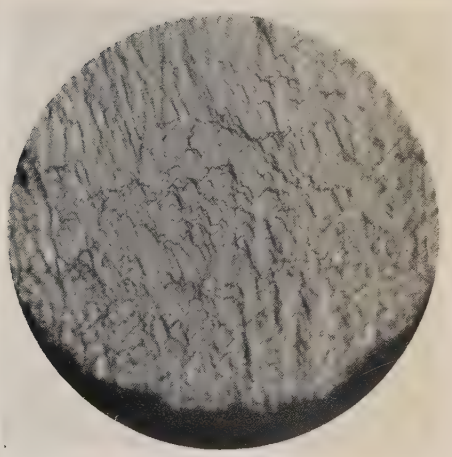

Fig. 29.

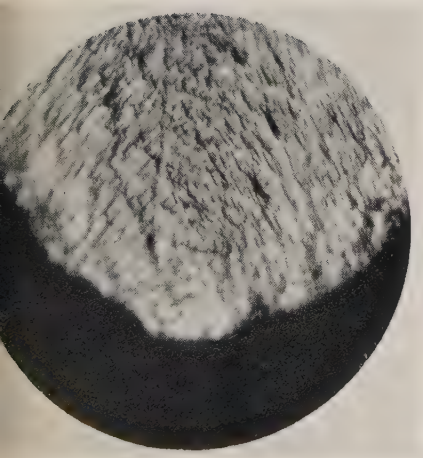

Fig. 30.

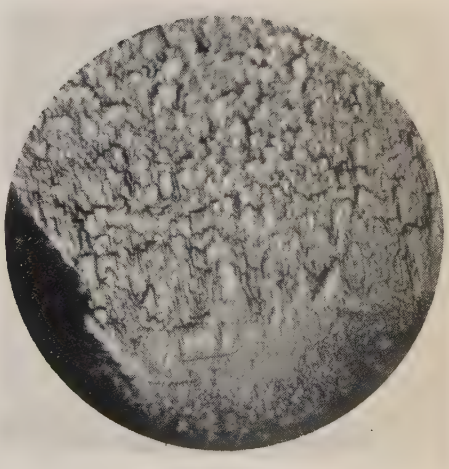

Fig. 31.

28, 29, 30. Etched sections from wedge forms perpendicular to wire axis showing distortions.
31. Section along slip plane showing distortion (×750).

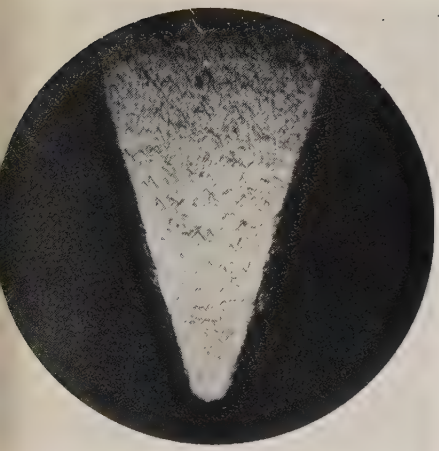

Fig. 32.

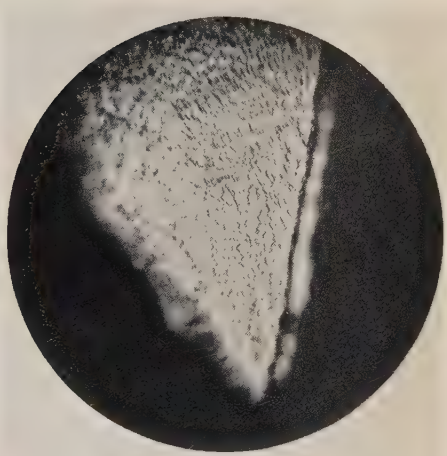

Fig. 33.

Fig. 34.

Fig. 35.

Figs. 32, 33, 34, 35. Etched sections from typical crystal forms showing crystal orientation (×250).

Fig. 38.

Fig. 39.

Fig. 40.

I

II

III

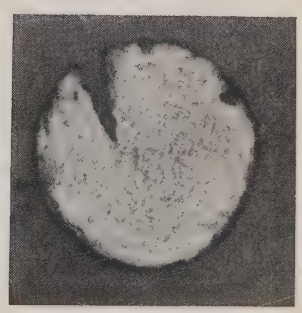

IV

Fig. 41.

Figs. 38, 39. An abnormal fracture showing two wedge forms inclined at right angles (×70).

Fig. 40. A normal fracture showing wedge angle (×70).

Fig. 41. A series of etched sections cut from abnormal wedge fracture showing that double wedge form was produced from same crystal.

physical properties, leading to the view that a new type of transformation was involved. The character of the curves in the neighbourhood of one of these discontinuities varied somewhat, depending apparently on the previous history of the wires in which the fractured crystals were grown. The present experiments establish that the measured forces have to do with the overcoming of atomic bonds of a perfectly definite type, and lend support to the view that this is merely a handing-on of atomic bonds—the atoms moving on to their new positions on the lattice; but they also show that the process is complicated by distortions which may very materially alter the strength measurements. It may well be that very slight differences in the perfection of the crystal before deformation will produce marked effect on the ability of the crystal to distort.

Research Laboratory of the
General Electric Company,
August 1st, 1924.

LXXX. *The Radioactivity of Basalts and other Rocks.* *By* J. H. J. Poole, *Sc.D.*, *and* J. Joly, *F.R.S.* *

IT has been shown in several recent papers that the geological history of the earth's crust depends very largely on the radioactivity of the sub-crustal magma. It is accordingly important to determine, as far as possible, what the absolute radioactive content of the magma actually is, since the time-interval between successive geological revolutions will depend on its value, and may be roughly estimated when the value is known. It is obviously impossible to deal with the problem directly, but, fortunately, it is now fairly well established that the magma is of a basic character, with a lower layer of possibly ultra-basic nature; and thus by determining the radioactivity of the basic and ultra-basic surface materials of the crust, we should be able to arrive at a very fair estimate of the radium content of the parent magma.

In order to measure the total radioactivity of a rock, it is necessary to determine both its radium and thorium contents. The effect due to the actinium series is so small that it is negligible in comparison with the probable errors in determining the small amounts of radium and thorium involved.

* Communicated by the Authors.

The actinium content of a rock has never, as far as we are aware, been directly determined, but can, of course, be approximately calculated from its radium content. In all the results given in this paper the radium content has been measured by the electric furnace method, and the thorium content by the solution method. To obtain as fair a mean value for the radioactivity of the underlying magma as possible, all available specimens from different localities have been dealt with. It may be remarked that the results show that this precaution is necessary, as the various basaltic outflows may differ appreciably in radioactivity. Thus, while the Hebridean outflow is rather below the average, the Coloradian is distinctly above it, and if we restricted our experiments to either we should obtain deceptive results.

Turning to the actual technique of the experiments, the method of procedure in determining the radium content of a rock by the electric furnace has been fully described in previous papers*. The method briefly consists in fusing about 8 g. of the powdered rock with 24 g. of mixed alkali carbonates in an electric tube furnace capable of giving a temperature of about 1100° C. The emanation which is liberated from the rock powder by the resulting chemical decomposition is transferred to an electroscope, where its effect on the rate of leak is measured. The effect of a known amount of radium emanation on the electroscope being previously determined, we can then calculate the amount of radium in the rock powder. For further details of the process the original papers may be consulted. The chief sources of uncertainty in the results may be summarized as follows. They are :—

(1) Exact value of constant of electroscope.
(2) Radioactive contamination of rock powder.
(3) Radioactive contamination of carbonates etc.
(4) Adsorption of radium emanation by soda-lime used for removal of CO_2.
(5) Incomplete washout of furnace.
(6) Presence of slight traces of water-vapour in the electroscope.
(7) Irregularity in the natural leak of the electroscope.

We will now deal with the methods adopted for reducing or eliminating these various sources of error.

Considering first the determination of the constant of the

* Joly, Phil. Mag. July 1911 and Oct. 1912.

electroscope, a new and improved method has been devised, 10 m.g. of uraninite of known uranium content were added to about 30 g. of radium-free borax glass, and the mixture fused, the melt being well stirred to ensure perfect mixing. The total weight of the melt was carefully ascertained, and hence we could calculate its uranium content per gramme. The melt was then ground up, sifted from finest powder, and stored in a glass tube for future use. When it was desired to standardize the electroscope, a suitable quantity of this powder was added to a rock powder, whose effect on the electroscope had already been determined, and the effect of the resulting mixture determined in the ordinary way. The net increase in the rate of leak of the electroscope over the rate of leak due to the rock powder alone will then be due to the radium content of the amount of the standardizing mixture used; and as this quantity is known, we can accordingly calculate what amount of radium corresponds to a gain in leak of one scale-division per hour. The advantages of this method are twofold—first, we can obtain very small quantities of uraninite without any very delicate weighings; and, secondly, the conditions under which the standardization experiment are conducted are practically identical with every other rock experiment. The object of having the rock present is that by its decomposition it may supply CO_2 to carry off the emanation from the melt. The amount of standardizing mixture used was so chosen that its radium content might be as nearly as possible the same as that of the class of rock which was being dealt with at the time. The constant of the electroscope was frequently determined by this method. Its value was found to vary from about 0·65 to about $0{\cdot}8 \times 10^{-12}$ g. of radium per scale-division per hour. This alteration in the value of the constant is probably to be attributed to differences in the size of grain of the soda-lime used in the absorption tubes, which would probably lead to different amounts of emanation being stopped by the tube. This point will be referred to again later. For some of the earlier experiments, in which the constant was determined by adding a weighed small quantity of uraninite directly to the rock powder, a rather lower value was obtained (0·5); but as the results, given by this constant, were subsequently confirmed when working with the higher constant, they have been included in the published values.

As far as the second error due to contamination of the rock powder is concerned, we may probably consider it as

eliminated. The rock was ground up immediately before an experiment in a room in which no radium had ever been handled ; and none of the various operators ever at any time during the course of the experiments came in contact with any possible source of contamination. The constancy of the results obtained is probably sufficient proof that no contamination could be taking place, as, if it had occurred, it would most certainly have led to much larger variations in the results from day to day. The possible contamination or, rather, radioactive impurity of the alkali carbonates is, however, a much more serious question, partaking as it does of the nature of a constant error, which will not be evident from mere inspection of the results. Several tests of the radium content of the carbonates were made, and although many of them gave null results, yet some seemed to indicate that they might contain small sporadic quantities of radium, which would vitiate the values obtained for the rock specimens. On this account a new method of dealing with the carbonates was adopted. Immediately before an experiment, the 24 g. of alkali carbonates were dissolved in water, boiled, and then evaporated to dryness in an evaporating basin. The carbonates are then immediately mixed with the rock powder in the usual way, placed in the platinum boat, and the experiment proceeded with in the ordinary fashion. The effect of this procedure is that any radium emanation the carbonates may contain is driven off in the preliminary boiling, and hence the radium content, if any, of the carbonates cannot affect the final result. In some cases, as has been described in previous papers, it is necessary to use small quantities of boracic acid to encourage a free evolution of CO_2, and this material, when used, is de-emanated in a similar fashion. This plan of de-emanating the chemicals was only adopted fairly late on in the series of experiments, and accordingly it was thought advisable to check some of the earlier results. The results obtained by the two different methods are shown in separate columns in the lists published. It will be seen that in most cases the agreement between the two is quite good, showing that on the average the radioactive impurity of the chemicals must be small.

The possibility of the soda-lime tube adsorbing some of the radium emanation is a troublesome one, and has not yet been overcome. The obvious way of dealing with the matter is to eliminate the soda-lime tube, and pass all the CO_2 directly into the electroscope. Unfortunately this would involve using too large an electroscope if we employ the usual 8 g. of rock powder ; and if we reduce this amount much, we shall

not be able to measure the increase in rate of leak with any accuracy. Any other plan of preventing the CO_2 from reaching the electroscope, such as freezing it out, would also labour under the same suspicion that it prevented some of the emanation also from reaching the electroscope. It is hoped in future, however, to make the electrical measurements more sensitive by using a Lindemann Electrometer, and hence to be able to use a smaller quantity of rock and deal with the total volume of CO_2 evolved. Meanwhile there is, of course, good reason to expect that the effect of the adsorption, if any, will be practically eliminated by the comparison method adopted for standardizing the electroscope.

As regards the possibility of the furnace not being completely washed out of emanation, this point had been tested previously by filling a second electroscope through the furnace immediately after the conclusion of an experiment. The second electroscope showed practically no increase in leak, showing that no emanation had been left in the furnace system. This test does not, of course, prove that the soda-lime had not adsorbed the emanation to a certain extent, as the latter would probably not be liberated by simply drawing air through the soda-lime tube. The effect of traces of moisture getting into the electroscope is troublesome, and on this account good drying tubes must be used, and the electroscope filled not too quickly. The danger is that there is usually a large amount of water evolved during the decomposition of the rock; and if even a small trace of this gets into the electroscope, it will give a spuriously high result if the latter is read immediately. However, we can fairly easily discriminate between this water-vapour effect and the true radioactive effect by rating the electroscope immediately after the transference and also three hours later. If the effect is truly radioactive, the net gain in leak should show about a 30-per-cent. increase at the end of three hours, but if it is partially due to water-vapour, there may be no increase, or even possibly a slight decrease at the end of the three hours. Thus experiments in which the correct increase is not shown have been excluded. It is, however, quite easy to avoid this error by renewing the drying materials fairly frequently.

The irregularities sometimes observed in the natural leak of the electroscope were found to be due to two causes. One is the effect of light on the sulphur insulation of the gold-leaf system, which is quite large, and the other the accumulation of slight traces of radioactive products in the atmosphere of the laboratory unless a good circulation of air is maintained. The result is that the electroscope must be kept

in the dark as much as possible and the room kept well ventilated. When these precautions were observed, the natural rate of leak remained quite sufficiently constant. It was found also that under these conditions there was no advantage in filling the electroscope with air drawn in directly from outside the building.

Turning next to the consideration of the thorium content, this was determined, as has already been mentioned, by the solution method. The details of this method have already been published in the 'Philosophical Magazine' for May 1909. The solutions used were prepared from the melts obtained from the experiments with the electric furnace. These melts were carefully ground up and then treated with pure water. After standing for at least 6 hours, the resulting mixture was filtered. The filtrate is discarded, as it contains no thorium, and the residue dissolved in dilute pure HCl and then made up to a convenient bulk with water. It is usually possible to obtain a perfectly limpid rock solution by this method; but if too concentrated HCl is used, or if the decomposition is not complete owing to the furnace not having reached a sufficiently high temperature, we are apt to get a cloudy solution, owing to the presence of gelatinous silica. Previous experiments have, however, shown that this cloudiness has no very marked effect on the value obtained for the thorium content of the solution.

The amount of thorium in the solution is determined by boiling it in a constant current of air, which is subsequently passed through a reflux condenser and set of drying tubes into an electroscope whose rate of leak any thorium emanation liberated from the solution will affect. In order to eliminate the radium emanation, the solution is previously boiled for about twenty minutes in an open flask. The electroscope is standardized in the ordinary way by using a solution containing a known amount of thorium. It is obvious that the constant of the electroscope will depend on the velocity of the air-current, and it is easy to show that there is a certain value of this velocity which will give the lowest value of the constant. Thus, if we let N_0 = number of thorium emanation atoms escaping from the solution per second, V = velocity of air-stream in c.c. per sec., a = volume of condenser etc., b = volume of condenser and electroscope, and λ = the radioactive constant for thorium, we see that, when a steady state has been attained, N, the number of atoms breaking up per second in the electroscope, will be equal to

$$N_0\left[e^{-\frac{\lambda a}{V}} - e^{-\frac{\lambda b}{V}}\right].$$

This quantity will be a maximum when

$$e^{-\frac{\lambda a}{V}} \cdot \frac{\lambda a}{V^2} - e^{-\frac{\lambda b}{V}} \frac{\lambda b}{V^2} = 0$$

or

$$ae^{-\frac{\lambda a}{V}} = be^{-\frac{\lambda b}{V}},$$

which gives

$$V = \frac{\lambda(b-a)}{\log b - \log a}.$$

The value for the volume of the condenser system which has to be inserted in this expression is not the actual total volume, but only that fraction of it which is not occupied by water-vapour. As this fraction is not known, we can only calculate approximately what the best value of the air-current should be. Putting in, however, $a = 50$ c.c., which from the dimensions of the actual apparatus would appear to be a fairly reasonable value, V comes out to be about 3 c.c. per sec. In practice the best value of V was determined by trial, and about 4 c.c. per sec. was found to give the best results, so the agreement with the theoretical value is satisfactory. The method used of obtaining a steady current of air through the electroscope has been previously fully described. The only alteration made was to employ a glass capillary tube as an air-leak instead of a stopcock, as it was felt that the former was more likely to be constant in value.

The chief uncertainty in the thorium determinations arises from the small increase in leak which the solution gives in many cases. The method adopted was to measure the natural leak of the electroscope immediately before and after the rock solution. The air-supply was taken from outside the building, as the air in the laboratory is usually slightly more ionized, due to gas burners etc. The danger of the solution becoming contaminated with thorium is much less than in the case of the radium determinations, as we are dealing with so much smaller quantities in the latter case. It is highly improbable that any of the more active elements of the thorium family could be accidentally introduced, since no mesothorium preparations have ever been used in this laboratory. For a fuller description of the experimental details and the precautions adopted, the reader may refer to the earlier papers, as no important alterations have been made in the method.

In the following tables, column II. contains results obtained with the use of de-emanated carbonates.

The figures in the columns must be multiplied by 10^{-12} in the case of radium and by 10^{-5} in the case of thorium, the results being the quantities found per gram of rock.

In obtaining the mean values, the figures given in column I. have had to be employed in most cases. It will be seen from the results that, if de-emanated carbonates had been used in every case, the mean values would probably be reduced by about $0{\cdot}1 \times 10^{-12}$; not a very important alteration. It may be noticed that no thorium could be detected in the carbonates.

Basic Rocks.

Western European.

Rock.	Radium Content. I.	Radium Content. II.	Thorium Content.
Basaltic Lava, Iceland, near Hafna, Jordun.	0·65		0·50
Vesicular Basalt, Iceland	1·00		0·45
Basalt, Arthur's Seat, Edinburgh	1·12		1·00
Ditto	1·40		
Basalt, Staffa	0·96		0·90
Basalt with Tachylite, Tobermory, Mull.	0·96		0·60
Basalt, Squire Hill, Belfast	0·62		0·69
Ditto	0·75		0·56
Ditto	0·47		
Basalt, Blackhead, Co. Antrim	0·87	0·56	0·34
Basalt, near Clegan, Co. Galway	1·1		0·24
Basalt, Giant's Causeway, Co. Antrim.	0·50		0·17
Basalt, Lintz, Rhenish Prussia	1·50		1·26
Laminated Basalt, Striegan, Silesia	0·89		0·60
Basalt, Pholberg, Saxony	1·63		1·15
Ditto	1·72	1·60	
Basalt, Siebengeberge	1·17		1·10
Ditto	1·10		
Basalt, Vogelgiberge	1·72		1·10
Basalt, Drachenfels, Bonn	1·30		0·98
Gabbro, Baxenstein, Radanthal, Hartz.	1·10		0·25
Vesicular Basalt, Gravenoire Volcano, Clermont.	1·25	1·19	1·12
Basalt, Murat-le-quaire	1·38		0·87
Pyroxene Basalt, Les Sources de Royat, Clermont.	1·68 1·03		0·82
Basalt, Mt. Rognon	1·03		0·56
Rowley Rag Basalt, near Birmingham.	1·13		0·71
Mean Value (*a*) Hebridean Basalts	0·77		0·49
(*b*) Other European Basalts	1·30		0·84

U.S.A. (Western States).

Rock.	Radium Content. I.	Radium Content. II.	Thorium Content.
Vesicular Basalt, Chaffee Co., Colorado.	1·80	1·70	1·70
Olivine Basalt, Jefferson Co , Colorado	1·86		2·40
Olivine Basalt Porphyry, Border Co., Colorado.	1·46		0·80
Ditto	1·55		
Hornblende Basalt, Chaffee Co., Colorado	2·70		3·00
Ditto	2·75		
Olivine Plagioclase Basalt, Huerfane, Co. Colorado.	1·00		1·50
Ditto	1·24		
Olivine Basalt, Mt. St. Helen's, Washington.	1·44	1·40	0·65
Gabbro, Nye, Montana	1·12		0·56
Mean Value.....	1·69		1·52

U.S.A. (Eastern States).

Diabase, Somerset Co., New Jersey ...	1·18		0·60
Diabase, Upper Mt. Clair, New Jersey.	1·12	0·80	0·83
Ditto	1·57		
Diabase, Columnar, Mt. Toru, Massachusetts.	0·85	0·71	0·60
Hornblende Gabbro, Albermarle Co., Virginia.	0·87		0·32
Ditto	0·83		
Quartz Diabase, Suffern, New York ...	1·22		0·90
Mean Value	1·09		0·65

Atlantic Islands.

Stony Lava, St. Helena	1·81		1·0
Basalt, St. Helena	0·93	0·91	0·62
Basalt, Ascension	0·76		0·43
Ditto	0·97		
Olivine Basalt, Madeira	1·38		1·07
Basalt, Tenerife, Canary Islands	2·77	2·63	1·78
Basalt, Flores, Azores	1·40		0·84
Basalt, Cape Verde Islands	0·86		0·64
Olivine Basalt, Fernando Noronha ...	1·20		0·56
Ditto ...	1·04		
Mean Value	1·31		0·87

Indian Ocean Islands.

Basalt, Christmas Island	1·05	0·94
Basalt, Island of Rodriguez	0·76	0·56
Basalt, Kerguelen Island	0·77	0·45
Mean Value	0·86	0·65

Pacific Islands.

Rock.	Radium Content. I.	Radium Content. II.	Thorium Content.
Basaltic Lava, Hawaiian Islands	1·25		0·28
Ropy Lava, Kilauea	0·96		0·30
Vesicular Basalt, Hawaiian Islands ...	1·10		0·37
Olivine Basalt, Juan Fernandez	1·06	0·96	0·32
Mean Value	1·09		0·32

Deccan Basalts.

Index No			
20/861, Loc. Kasara-Igatpure		0·91	0·62
20/855, Bombay, Nagpur Ry.		0·75	0·43
20/851		0·60	0·37
20/853		0·80	0·52
20/850		0·82	0·56
20/852		0·72	0·24
Mean Value		0·77	0·46

South African Dolerite.

Karoo Dolerite, Teviot Borehole (1225 feet deep), Cape Province.	1·75		0·58
Karoo Dolerite, near Victoria, West Cape Province.	1·25		0·62
Karoo Dolerite, Cape Province	1·50		0·80
Karoo Dolerite, Teviot Borehole (1025 feet deep), Cape Province.	1·25		0·79
Mean Value	1·44		0·70

Ultra-basic Rocks.

Rock.	Radium Content. I.	Radium Content. II.	Thorium Content.
Picrite, Cornwall		0·43	0·60
Picrite, Inchcolen, Firth of Forth ...		0·50	0·34
Palæopicrite, Highweek, Devonshire ..		0·44	0·32
Do. Nassau		0·50	0·32
Limburgite, Kaiserstahl, Baden		1·20	1·40
Ditto		1·14	
Ditto		1·22	
Limburgite, Stoppelskuppe, Eisenach.		1·06	0·75
Do. Hassenberg, Markliss, Lausitz.		1·08	1·32
Lherzolite, Pyrenees		0·56	0·30
Do. Piedmont		0·39	0·30
Amphibole Peridotite, Schreisheim, Baden.		0·99	0·58

Ultra-basic Rocks (*continued*).

Rock.	Radium Content. I.	Radium Content. II.	Thorium Content.
Biotite Peridotite, Harzburg		0·35	0·10
Wehrlite, Frankenstein, Odenwald ...		0·46	0·20
Hornblende Olivine Peridotite, Syracuse, New York.		1·75	1·58
Cumberlandite Peridotite, Rhode Island.	1·08		0·21
Dunite, Krombal, Styria		0·52	0·30
Dunite, Dun Mts., New Zealand		0·42	0·37
Eulysite, Tunaberg, Sweden		0·74	0·13
Augitite, Bohemia		1·40	1·37
Theralite, Sohla Mahren		0·96	1·12
Mean Value		0·80	0·61

Intermediate Rocks.

Rock.	Radium Content. I.	Radium Content. II.	Thorium Content.
Andesite, San Juan Co., Colorado ...		2·70	1·10
Andesite Porphyry, Massachusetts ...	1·40		0·25
Granodiorite, Minnesota	3·15		1·57
Diorite, Sassi, Finland	3·06		0·47
Anorthosite, Wichita Mts., Oklahama.	1·75		0·10
Anorthosite, New York	1·52		0·28
Mica Dacite, Border Co., Colorado ...	2·70		0·47
Mean Value	2·26		0·61

Acid Rocks.

(Mostly Archæan Granites.)

Rock.	Radium Content. I.	Radium Content. II.	Thorium Content.
Rapakivi Granite, Finland.....	5·77		5·70
Ditto	6·65		6·00
Granite, Sornas, Finland	3·98		1·75
,, Hango, Finland	5·77		2·75
,, Zirkala, Finland	5·07		2·03
,, Haltula, Finland	4·72		1·75
,, Hanga Udd., Finland...	4·62		2·25
,, Tyterlaks, Finland	4·81		1·37
,, Kajaloki, Finland	2·45		1·88
,, Orwen, Finland.....	2·97		0·75
,, Kuru, north of Tammerfors, Finland.	7·00	6·30	4·00
,, Fustila, Finland	4·64		8·20

Acid Rocks (*continued*).

Rock.	Radium Content. I.	Radium Content. II.	Thorium Content.
Kugel Granite, Finland	2·88		0·86
Granite, Flannan Islands, W. of Lewis	1·75		0·90
Granite, Loch Michard, Sutherland	1·58		0·51
Granite, Cape Wrath, Sutherland	2·27		1·73
Mica Gneiss, north of Tammerfors, Finland.	1·75		1·00
Adergneiss, Teisks, Finland	2·97		0·75
Hornblende Orthogneiss (Lewisian), Tiree.	1·20		0·64
Granogneiss, Island of Coll	1·84		0·52
,, Ballyhaugh, Island of Coll	1·66		1·97
Orthogneiss, Tiree	1·60		1·63
Mean Value	3·54		2·31

Broadford Sill, Skye.

Base (Basaltic)	0·96		0·50
10 ft. from base (Granophyric)	1·62		0·75
6 ft. from top (Granophyric)	1·49		0·52
Top (Basaltic)	1·03		0·37

Broadford Dyke, Skye.

North Margin of Dyke (dark-coloured)	0·79		0·52
Centre of Dyke (light-coloured)	1·05		0·94
Ditto	1·75		1·08

Dyke east of Broadford.

Easterly light-coloured margin	1·05		0·30
Central dark-coloured portion	1·92		0·64
Westerly light-coloured margin	1·05		0·62

The general means for basaltic rocks are as follows:—

		Radium.	Thorium.
All basalts, dolerites, gabbros	(58)	1·19	0·77
Hebridean basalts	(6)	0·77	0·49
European ,,	(15)	1·30	0·84
Deccan ,,	(6)	0·77	0·46
Western U.S.A. basalts	(7)	1·69	1·52
Atlantic Islands	(8)	1·31	0·87
Indian Ocean Islands	(3)	0·86	0·65
Pacific ,, ,,	(4)	1·09	0·32
Eastern U.S.A.	(5)	1·09	0·65
S. African	(4)	1·44	0·70

Results previously available as determined by similar methods of analysis (Phil. Mag. October 1912 and April 1915) :—

	Radium.	Thorium.
All basalts, dolerites, gabbros (31)	1·28	0·51
Hebridean basalts (11)	0·50	0·38
Basalts, Deccan and Antarctic (14)	2·0	0·84
Diabases and dolerites (8)	1·0	0·22
Gabbros and norites (5)	1·3	0·50
General basalts (18)	1·4	0·63

On similar rocks, but determined by the Wet Method, the radium content was as follows :—

	Gabbros and Norites.	Dolerites and Diabases.	Basalts.
Strutt [1]	0·63 (1)	0·59 (2)	0·44 (8)
Farr and Florance [2]	0·33 (2)	0·59 (3)	0·81 (1)
Buchner [3]	0·70 (1)	0·87 (2)	0·50 (1)
Fletcher [4]	...	...	0·71 (5)

[1] Strutt, Proc. R. S. lxxvii. & lxxxiv.
[2] Farr & Florance, Phil. Mag. Nov. 1909.
[3] Buchner, *Konink. Akad. Wet. Amsterdam*, Oct. 1910 and April 1911.
[4] Fletcher, Phil. Mag. July 1910 and Jan. & June 1911.

Comparing the new results with the previous results obtained by similar procedure, there is little difference noticeable. Thus 58 basalts, dolerites, and gabbros give for the radium content 1·19 (recent), and 31 similar rocks formerly give 1·28. In the thorium content on the same specimens we have: recent 0·77 and former 0·51. The radium results by Wet Method are hardly comparable; they have been shown by direct comparison to give somewhat lower values. The published results show values ranging from 0·33 to 0·87 for rocks of basaltic origin.

The chief matter of interest is the values to be ascribed to the plateau basalts. Daly, Washington, and others have shown that there is close chemical resemblance between the chemical composition of the plateau lavas, and among these, the Deccan, Thulean (Hebridean), and Oragonian (Western U.S.A.) are specifically cited by Washington. The radioactive constituents are closely alike in quantity in the case of the Hebridean and Deccan, but the basalts from the Western U.S.A. show appreciably greater quantities both of

radium and of thorium. If the latter specimens are authentically derived from the plateau basalt, this is difficult to account for.

The point is of interest, for as we would naturally infer the plateau basalts to represent the general basaltic substratum of the earth's surface, the evaluation of their average radioactivity is of importance. On the other hand, the lavas of the oceanic islands might be expected to proceed from pockets in the lava forming the ocean-floor which possibly do not take part in the phenomena of the cyclical changes and deformation of the earth's surface crust.

In short, we want to know, so far as may be attainable, what quantities of radioactive materials are to be taken into account in forming an estimate of the time-periods involved in the evolution of heat in the substratum. This is the most important constant connected with the geological influence of radioactivity. It is hoped to continue the present investigation, with a view to derive, if possible, further light on this point as well as on the subject of small errors possibly entering into the existing procedure.

The ultra-basic rocks are somewhat lower in the mean than the basalts. These rocks have, hitherto, not been systematically investigated.

A point of interest is the high values noticeable in the case of certain of the granites of Finland. There appears to be no doubt of the reliability of these results ; they apply to areas where intense thermal conditions prevailed in remote times.

A comparison of the results for acid, intermediate, and basic rocks shows that the relation first found by Lord Rayleigh is sustained.

We have to thank Dr. J. J. Sederholm for the specimens from Finland and for information most kindly supplied therewith. We desire to acknowledge also the kindness of Professor Harold S. Palmer in sending lavas from Hawaii, and of the Trustees of the British Museum in supplying specimens from the oceanic islands.

LXXXI. *Crystal Structure and Absorption Spectra.—The Cobaltous Compounds. By* Robin Hill *and* Owen Rhys Howell *.

[Plate XXV.]

THE red and blue colours of the cobaltous compounds have attracted much attention and many theories have been advanced to account for them and for the change from one to the other.

Von Babo (*Jahresber.* 1857, p. 72) appears to have been the first to observe the change in colour of cobalt solutions on heating and on the addition of alcohol or of certain salts. He thought the transformation from red to blue was due to dehydration of the cobalt salt. Schiff (Liebig's *Ann. Chem.* cx. p. 203, 1859) was of the same opinion. Gladstone (Journ. Chem. Soc. x. p. 79, 1858; *ibid.* xi. p. 36, 1859) after examining the spectra of cobalt solutions, and Vogel (*Ber.* xi. p. 913, 1878) after a more extended investigation, also inferred that the difference in colour was due to a difference in hydration. Russell (Proc. Roy. Soc. xxxii. p. 258, 1881) studied the absorption spectra of various cobalt solutions and of fused cobalt salts, and he concluded that the change in colour was due to the presence of hydrates. Tichborne (Chem. News, xxv. p. 133, 1872), Potilitzin (*Ber.* xvii. p. 276, 1884; *Bull. Soc. Chim.* (3) vi. p. 264, 1891), Lescoeur (*Ann. Chim. Phys.* (6) xix. p. 547, 1890; *ibid.* (7) iv. p. 213, 1895), Étard (*Comptes Rendus*, cxiii. p. 699, 1891; *ibid.* cxx. p. 1057, 1895), Charpy (*Comptes Rendus*, cxiii. p. 794, 1891), and Wyrouboff (*Bull. Soc. Chim.* (3) v. p. 460, 1891; *ibid.* vi. p. 3) studied the formation and range of stability of the hydrates of different cobalt salts. They argued from their results that the change in colour on heating was best explained by a change from one hydrate to another.

Hartley (Trans. Roy. Dub. Soc. (2) vii. p. 253, 1900; Journ. Chem. Soc. lxxxiii. p. 401, 1903) made a very exhaustive investigation on the absorption spectra of cobalt solutions at different dilutions and at different temperatures. He found that those salts which are anhydrous, or are not dehydrated below 100°, or do not change colour when dehydrated, give solutions whose absorption spectra do not change on heating. Hydrated salts, however, give solutions whose absorption spectra undergo a marked change on

* Communicated by the Authors.

heating, and a similar change is generally produced by the addition of salts which act as dehydrating agents. Hartley therefore concluded that the change in colour is essentially an hydration phenomenon. Jones and Uhler (Amer. Chem. Journ. xxxvii. p. 126, 1907) have examined the absorption spectra and electrical conductivities of cobalt solutions in the presence of varying amounts of different salts. They found that "the blue and red colours correspond, respectively, to wide and narrow bands; or, in terms of the theory, to small hydration and relatively large hydration."

This theory of hydration is sufficient to account for the colour changes within its limited application. It is, however, not sufficiently embracing in that it makes no attempt to account for the colour of anhydrous compounds and of solids.

Berch (*Wien. Akad. Sitzungsber.* (2) lvi. p. 724, 1867), thinking he observed a transformation of the red $CoCl_2 6H_2O$ to blue without change of composition, proposed to account for the change in colour of cobalt salts by postulating that there are two modifications of the hexahydrate, one red and the other blue. Potilitzin (*loc. cit.*) showed that the observation was incorrect and thus disproved the theory. Not only has this view no experimental justification, but it contributes nothing towards an explanation of the cause of the colour.

Ostwald (*Grundlinien der anorg. Chem.* p. 620; *Lehrbuch der allgem. Chemie*) believes the red colour is due to the cobalt ion and the blue colour to the un-ionized salt. Whereas this may explain the change in colour from red to blue on the addition of certain salts to cobalt solutions, by consequent depression of the ionization of the cobalt salt, it fails to explain why some salts are ineffective in bringing about the change. It also fails to account for the change in colour on heating, since the ionization of the salt undergoes very little change in the process.

Engel (*Bull. Soc. Chim.* (3) vi. p. 239, 1891; see also Le Chassevent and Le Chatelier, *ibid.* (3) vi. pp. 3, 84, 209, 1891) considers that no general theory can explain all the colour changes. Each one must have a separate interpretation. The change in colour of cobalt chloride solution on the addition of hydrochloric acid or metallic chlorides is due to the formation of double chlorides in solution.

Donnan and Bassett (Journ. Chem. Soc. lxxxi. p. 939, 1902) from a study of the coloured solutions, chiefly their behaviour on electrolysis, concluded that "the blue colour is largely due to complexes such as $\overline{CoCl_4}$ or $\overline{CoCl_3}$," while the red colour is due to "the cobalt atom outside the immediate

sphere of the chlorine atoms." The colour of a solution containing cobalt and another metal is consequently determined by the relative tendencies of the two metals to form complex anions. If the cobalt has the greater tendency, the solution is blue; if the other metal has the greater tendency, the solution is red.

Hantzsch and Shibata (*Zeit. anorg. Chem.* lxxiii. p. 309, 1912) determined the apparent molecular weight and the absorption spectrum of cobalt thiocyanate in various solvents. From the manner of ionization thus determined, they concluded that the blue solutions contained *complexes* such as $Co[Co(SCN)_4]$ in which the cobalt atom in the complex is associated with four groups, and the red solutions contained complexes such as $Co[Cl_4(HgCl_2)_2]$ or $[Co(SCN)(H_2O)_5]SCN$ in which the cobalt atom in the complex is associated with six groups.

The interest of the present authors was aroused in this subject by a chance observation through a direct vision spectroscope that the absorption spectra of cobalt spinel, cobalt blue, and the blue solution of cobalt oxide in potash were so very similar. In the present communication an account is given of the absorption spectra in the visible region of a number of cobaltous solutions and of pigments derived from divalent cobalt. The latter are an important class of compounds which do not appear to have been investigated hitherto in this way, nor does any attempt appear to have been made to account for the colour of cobalt solutions by comparing them with the solid compounds.

Working along these lines, we have concluded that the blue colour is due to the direct association of the cobalt atom with four atoms or groups, and that the red colour is due to its direct association with six atoms or groups. We were led to this belief before we were aware of the paper by Hantzsch and Shibata (*loc. cit.*), who assign similar values to the number of groups forming their complexes. As will appear, our idea of the nature of the four and six associations is entirely different and is applicable generally. Thus, whereas the hypothesis of Hantzsch and Shibata can hardly be used to account for the colour of the pigments, our own idea of the association in solution is founded on the constitution of these. Again, Hantzsch and Shibata assume that the addition of a metallic salt to a solution of a cobalt salt results in the formation of a complex between the two salts; we show that the function of the added salt is simply to force the cobalt atom from one type of association to the other.

Experimental.

Preparation of Pigments.—A number of compounds in which cobaltous oxide is combined with certain colourless oxides are well known pigments. The essential method of preparation consists in heating a mixture of the oxides to obtain a homogeneous non-fused mass. It is, however, advantageous to use the sulphates, because on warming they melt in their water of crystallization giving a perfect mixture, and on further heating evolve sulphur dioxide yielding a friable and completely oxidized mass. Our method of preparation, therefore, consisted in making a mixture of the requisite quantities of the sulphates (or stannic oxide and silica where these enter the composition) and heating, gently at first and finally at about 1200° for half an hour.

As ordinarily prepared for pigments, these compounds are too intensely coloured for examination. We therefore prepared "diluted" colours in which the cobalt is replaced by other suitable metals such as magnesium or zinc. In each case a series was prepared. The compound at the one end of the series, containing no cobalt, was used as a "blank"; the compound at the other end of the series, containing the maximum possible amount, was prepared to see if it was of the same nature as the intermediate compounds, and it was compared with the corresponding commercial "artist's" colour. One of the intermediate compounds of suitable intensity was selected for examination.

The following is a list of the pigments prepared, together with the composition of the "diluted" compound examined:—

Thénard's Blue or Cobalt Blue	(*a*)	$CoOAl_2O_3$	$3?\ MgOAl_2O_3$
,, ,,	(*b*)	$CoOAl_2O_3$	$32\ BeOAl_2O_3$
,, ,,	(*c*)	$CoOAl_2O_3$	$32\ ZnOAl_2O_3$
Cerulean Blue	(*a*)	$CoOSnO_2$	$32\ MgOSnO_2$
,, ,,	(*b*)	$(CoO)_2SnO_2$	$32(MgO)_2SnO_2$
,, ,,	(*c*)	$(CoO)_2SnO_2$	$32(ZnO)_2SnO_2$
Cobalt o-silicate	(*a*)	$(CoO)_2SiO_2$	$4(MgO)_2SiO_2$
,, ,,	(*b*)	$(CoO)_2SiO_2$	$32(ZnO)_2SiO_2$
Rinmann's Green		$CoO\ 256ZnO$	
Cobalt Pink		$CoO\ 8MgO$	

Preparation of Solutions.—The coloured solutions were made by adding the requisite quantity of a concentrated standard solution of cobalt sulphate to a solution of the potassium salt saturated at room temperature, or to hydrochloric acid saturated with the necessary metallic chloride.

The corresponding "blank" solution was made up in the same way using water instead of the cobalt solution. Both solutions were allowed to stand in order that the precipitated potassium sulphate and suspended particles might settle.

The "cobalt thiocyanate in ether" was made by extracting a solution containing a known amount of cobalt, treated with potassium thiocyanate, with ether containing 5 per cent. of amyl alcohol until colourless, and making up the extracts to a known volume.

The concentration of each solution is given in brackets after it and is expressed as gram atoms of cobalt per litre.

Instrument.—All the measurements were made by means of a Nutting photometer with a Hilger Wavelength Spectroscope.

The pigments were examined by reflected light. Small boxes were made of cardboard in the form of a cube with two of its adjacent faces missing. One of these boxes was placed immediately against each of the photometer apertures with one of the open sides next the aperture and the other open side up. The inside of one of the boxes was covered with a thick layer of the pigment and the other with a corresponding "blank," both prepared by mixing with 5 per cent. gum arabic solution to the necessary consistency. The source of light was a powerful half-watt lamp placed immediately above the photometer box.

For the examination of the liquids the optical arrangement of the instrument as ordinarily employed was slightly modified by using as a light source a disk of opal glass placed in front of a 200 candle-power half-watt lamp, and by inserting a lens in each of the two beams (formed on division) to bring the image of the light source into the plane of the rhomb, a suggestion kindly made by Dr. Hartridge. With this arrangement the relative intensities of the three fields did not vary with the position of the eye at the eyepiece; moreover, the coincidence in the junction of the fields was rendered more perfect owing to elimination of diffraction.

Cell.—It was deemed advisable, where the solubility of the substance allowed, to examine a thin layer of concentrated cobalt solution in preference to a thick layer of dilute solution, for the following reasons:—

(*a*) The effect of any impurities in the potassium salt used for making the solutions is of less account.

(*b*) The effect of oxidation or of other changes in the coloured solution is greatly reduced.

(*c*) The loss of light due to suspended particles is of less consequence.

A special cell was therefore designed and constructed as shown in fig. 1. A and C are two pieces of plate glass 6 cm. × 3·7 cm. × 7 mm. A has two holes each 1 cm. diameter bored through it, their centres being 2·3 cm. apart. B is a piece of window glass the same size as A and C, but only 2 mm. thick, and has a square hole 2·6 cm. × 9 mm. cut in the middle. A B and C are put together face to face as shown, the faces in contact being smeared with a very little vaseline. The whole is held in a wooden frame made of two pieces D and E. D has a square hole 4·6 × 2 cm. cut in it

Fig. 1.

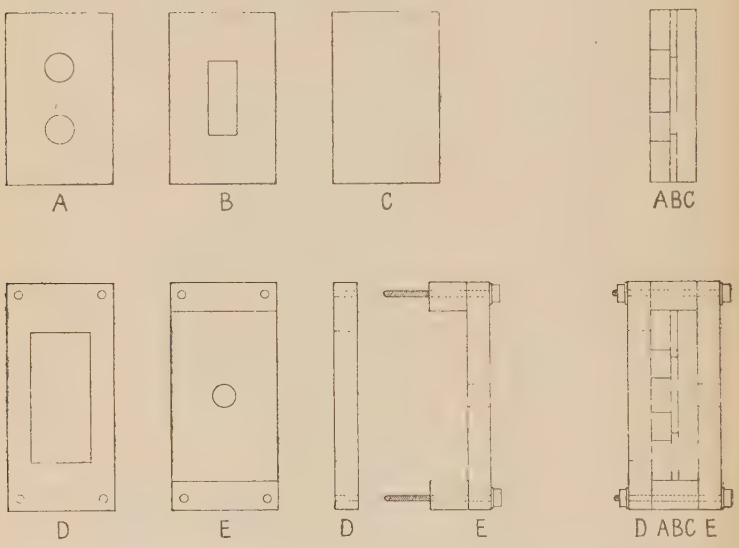

giving sufficient clearance to the two holes in A. E is provided with four small bolts as shown ; it has a hole 8 mm. diameter bored through the middle. The assembled cell is placed in E, D is placed over it, and the whole screwed up.

The holes in A are provided with rubber stoppers carrying glass tubes, the lower leading to a stoppered flask containing the solution for examination and the upper to a receiver. The solution is blown over, filling the cell. The tubes are so arranged that the beam of light is uninterrupted ; it enters A between the two holes, traverses the layer of liquid and emerges through the hole in E which gives a beam of the requisite size without any stray light.

Two such cells were mounted side by side on a stand, the distance between them being such that the two emerging beams coincided with the apertures of the photometer box. One was filled with the cobalt solution and the other with the "blank."

Method of Plotting.—All the curves are plotted with wavelengths in Ångström units as abscissæ and fraction of light absorbed as ordinates.

Blue Compounds.

The crystal structure of spinel ($MgO\,Al_2O_3$, or $Mg\,Al_2O_4$) has been elucidated by means of X-rays by W. H. Bragg (Phil. Mag. (2) xxx. p. 309, 1915), who showed that each magnesium atom is surrounded by *four* oxygen atoms. In this connexion it may be noted that Dickinson (Journ. Amer. Chem. Soc. xliv. p. 774, 1922) has shown from an X-ray examination of the crystal structure of the double alkali cyanides of cadmium and mercury ($K_2Cd(CN)_4$ and $K_2Hg(CN)_4$) that the groups $Cd(CN)_4$ and $Hg(CN)_4$ play the same part in the structure as the MgO_4 group in spinel.

The magnesium atoms in spinel may be partly replaced by cobalt, giving the blue cobalt spinel. We are indebted to Mr. A. Hutchinson, F.R.S., for a piece of the artificial gem which we used for examination.

It will be seen that the curves for cobalt spinel (fig. 2 F) and cobalt blue (fig. 2 E) are almost identical, the only difference in their form being that the maxima in the case of the spinel are sharper than in that of the cobalt blue, since the former is examined by transmitted light and the latter by reflected light, where some is scattered. It is therefore reasonable to conclude that the structure of cobalt blue is identical with that of cobalt spinel. Since cobalt spinel is a solid solution, it follows that in both cases the cobalt atom replaces the magnesium atom without change in structure and is therefore surrounded by four oxygen atoms.

The absorption curve for cobalt blue with beryllium as diluent (fig. 2 D) is of precisely the same nature as with magnesium as diluent. On treating this substance with concentrated acids the cobalt is readily dissolved, leaving a perfectly white residue of beryllium aluminate (crysoberyl). It follows that cobalt aluminate and beryllium aluminate are non-miscible and that the absorption spectrum of this pigment is due to the cobalt aluminate itself contained in it. Since the same absorption spectrum is obtained with cobalt blue, confirmatory evidence is thus obtained that in this

compound cobalt and magnesium are interchangeable without change in structure.

Zinc is known to form a spinel with the same structure as magnesium spinel, and it may be replaced by cobalt yielding a blue pigment just as magnesium is so replaceable. The

Fig. 2.

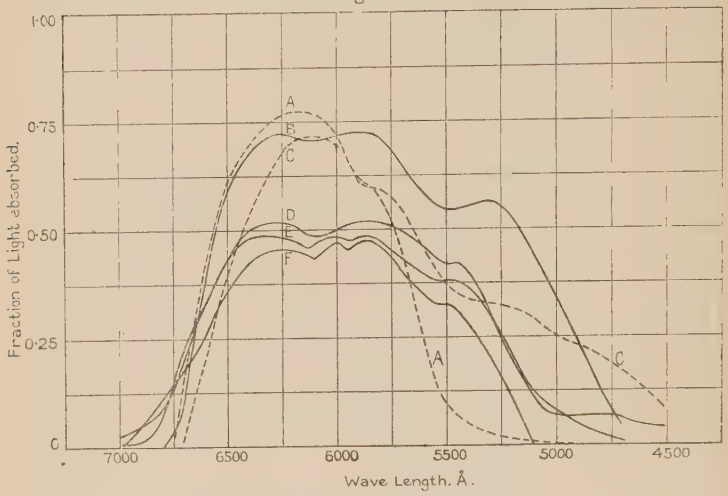

A. *Cobalt thiocyanate in ether.* $\left(\frac{1}{20,000}\right)^*$.

B. *Cobalt oxide in potassium hydroxide.* $\left(\frac{1}{40}\right)$.

C. *Cobalt thiocyanate in potassium thiocyanate.* $\left(\frac{1}{40}\right)$.

D. *Cobalt Blue* (*b*). $CoO\,Al_2O_3\;32BeO\,Al_2O_3$.

E. *Cobalt Blue* (*a*). $CoO\,Al_2O_3\;32MgO\,Al_2O_3$.

F. *Cobalt Spinel.*

* *Examined in 10 cm. tube.*

absorption spectrum of this compound (fig. 3 E) is strictly comparable with that of cobalt blue with magnesium as diluent (reproduced again for comparison in fig. 3 G). The absorption bands are exactly similar. The compound is of a more violet shade than the corresponding magnesium one. This is particularly noticeable in artificial light, the magnesium compound retaining more of the blue colour than the zinc compound. This fact is interesting because it is stated that zinc oxide is added in the manufacture of commercial cobalt blue. Its effect is not to introduce a tinge of green into the blue colour as is popularly supposed, but only to help in forming the spinel structure. The curves bring out

this point and show that the effect on the absorption spectrum of introducing zinc for magnesium is extremely slight, thus clearly revealing the CoO_4 group as a distinct entity.

Cerulean blue is stated to be a compound of cobalt oxide and stannic oxide. It has been investigated by Hedvall (*Arkiv. Kem. Min. Geol.* (18) v. p. 1, 1914), who prepared

Fig. 3.

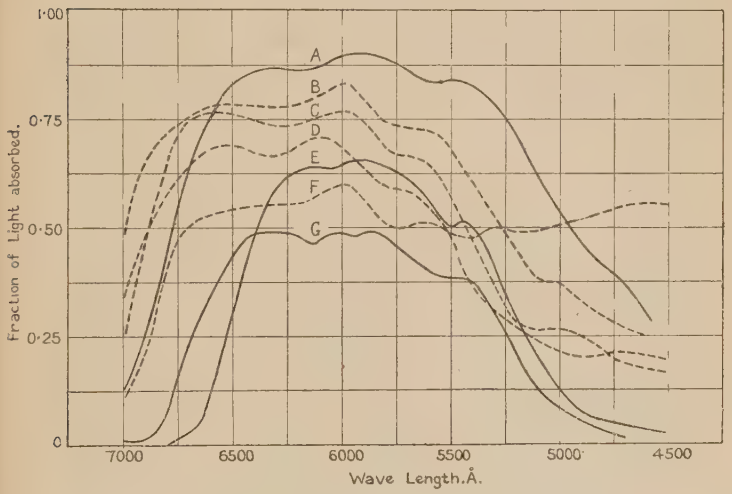

A. *Cobalt ortho-silicate* (*b*). $(CoO)_2SiO_2$ $32(ZnO)_2SiO_2$.
B. *Cerulean Blue* (*b*). $(CoO)_2SnO_2$ $32(MgO)_2SnO_2$.
C. *Cerulean Blue* (*a*). $CoO\,SnO_2$ $32MgO\,SnO_2$.
D. *Rinmann's Green.* $CoO\,256ZnO$.
E. *Cobalt Blue* (*c*). $CoO\,Al_2O_3$ $32ZnO\,Al_2O_3$.
F. *Cerulean Blue* (*c*). $(CoO)_2SnO_2$ $32(ZnO)_2SnO_2$.
G. *Cobalt Blue* (*a*). $CoO\,Al_2O_3$ $32MgO\,Al_2O_3$.

cobalt ortho-stannate Co_2SnO_4 which he found was green, but that if more stannic oxide was used the product became bluer in proportion to the excess employed. We first tried using calcium as a diluent in this case and obtained a semi-fused greyish-blue mass. It was obvious that the compound was of a totally different type; calcium cannot replace cobalt without change in structure of the compound.

By introducing an equivalent amount of magnesium for cobalt in the ortho-stannate, however, a perfectly blue product is obtained which corresponds exactly in colour and intensity with the artist's pigment "cerulean blue." It is seen that this compound (fig. 3 B) has precisely the same

absorption spectrum as one having double the amount of stannic oxide (fig. 3 C). It therefore follows that in both cases the cobalt is present as the ortho-stannate ; the function of the excess of stannic oxide must be the same as that of the magnesium oxide.

By introducing zinc instead of magnesium, a dull green compound is obtained. This would appear to correspond more nearly to the green pure ortho-stannate, since the atomic weight of zinc is approximately the same as that of cobalt. It will be seen, however, that the absorption spectrum of this compound (fig. 3 F) is exactly similar to that of the other two stannates with an additional absorption in the violet.

The absorption spectrum of cobalt oxide in zinc oxide (fig. 3 D) is of exactly the same shape as in the case of the stannates. The compound was examined against zinc oxide as a "blank." The zinc oxide was prepared under the same conditions as the pigment and was a distinct yellow. Although the pigment is a bright green (Rinmann's Green) its absorption spectrum examined in this way is precisely the same as that of the perfectly blue stannates. Further, the absorption spectra of all these compounds are exactly like those of the cobalt blues, the only difference being that they are a little more extended.

Now the crystal structure of zinc oxide has been elucidated by W. L. Bragg (Phil. Mag. xxxix. p. 647, 1920) by X-ray measurements, and he showed that the zinc atom is surrounded by *four* oxygen atoms. The cobalt atom replacing the zinc is consequently similarly situated, and there seems no doubt, therefore, that in all these compounds the cobalt atom is surrounded by four other atoms.

Cobalt hydroxide is readily soluble in hot concentrated potassium hydroxide, yielding an intense *blue* solution from which it crystallizes in *pink* microscopic crystals (de Schulten, *Compt. Rend.* cix. p. 266, 1889). It may be noted that magnesium hydroxide similarly dissolves in and crystallizes from hot concentrated potash (de Schulten, *ibid.* ci. p. 72, 1885). The absorption spectrum of the cobalt solution (fig. 2 B) is of exactly the same character as that of cobalt spinel and cobalt blue, so that the cobalt atom appears to be similarly enveloped in all cases. It is suggested that in the solution of cobalt oxide in potash the cobalt atom is also surrounded by four groups, probably hydroxyls.

The persistence of a definite association of groups or a molecular structure in solution just as in solids seems to be very real.

The absorption spectrum of cobalt thiocyanate in potassium thiocyanate (fig. 2 C) bears a marked resemblance to that of the oxide in potash. The second and third bands are depressed but correspond exactly with those of the latter.

In the case of the thiocyanate in ether (fig. 2 A) the second band has almost disappeared and the third completely. A difference is to be expected since this is a solution of a simple cobalt salt ; the cobalt atom is uncharged. The close similarity of this curve to that of the thiocyanate in potassium thiocyanate is therefore all the more striking.

Both in the blue solids and blue solutions, therefore, the cobalt atom is in immediate association with *four* atoms or groups.

Red Compounds.

The structure of magnesium oxide has been investigated by Wyckoff (Amer. Journ. Sci. i. p. 138, 1921), who found it was of the same type as that of rock-salt; the magnesium atom is surrounded by *six* oxygen atoms. Cobalt replaces the magnesium in the oxide, giving a *red* compound. The cobalt atom is here surrounded by six oxygen atoms and the absorption spectrum (fig. 4 F) is of an entirely different type from that of the blue pigments. It is suggested that just as in the blue compounds the colour is due to the association of the cobalt atom with four groups, so also in the red compounds the colour is due to its association with six.

Although the absorption spectrum of potassium cobaltocyanide $K_4Co(CN)_6$ has not been examined owing to the rapidity with which it decomposes water, it is interesting to note that the solution is pink and that the compound is described as violet-red crystals. Here the cobalt atom is known to be associated with six cyanogen groups.

The chloride, sulphate, and nitrate of cobalt give practically identical absorption spectra (fig. 4 A) at the dilution used, and the form of the curve is exactly similar to that of cobalt oxide in magnesium oxide. It follows that the cobalt atom is associated with six groups in these solutions. Since the salts are almost completely ionized, it would appear that the cobalt atom is in direct association with six molecules of water.

The absorption spectra of the formate (fig. 4 E), oxalate (fig. 4 D), and tartrate (fig. 4 C) in the corresponding potassium salts are all strictly comparable with each other and with those of cobalt oxide in magnesium oxide and the aqueous solutions of the chloride, sulphate, and nitrate. It

therefore appears that the cobalt atom is similarly associated with six groups in these solutions also.

The cobalt ortho-silicate with magnesium as diluent is *red* and gives a very similar absorption spectrum (fig. 4 B) to that of cobalt oxide in magnesium oxide. With zinc as diluent, however, the compound is *blue* and gives an absorption spectrum (fig. 3 A) absolutely comparable with that of

Fig. 4.

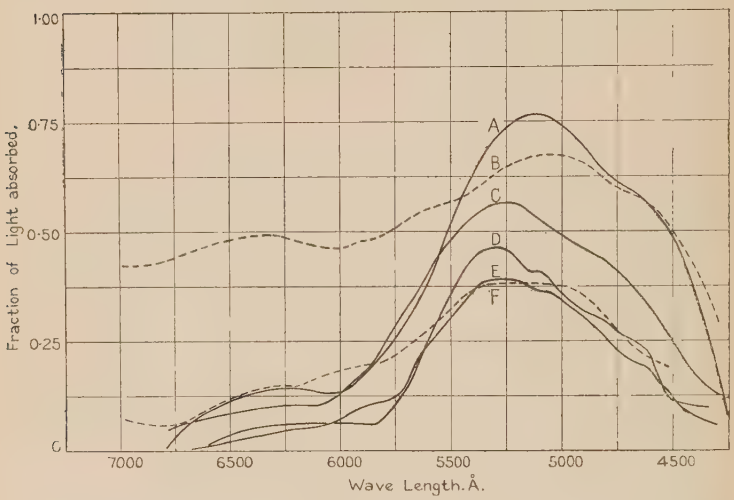

A. *Cobalt chloride, sulphate, or nitrate.* $\left(\frac{1}{50}\right)^{*}$.

B. *Cobalt ortho-silicate (a).* $(CoO)_2SiO_2$ $4(MgO)_2SiO_2$.

C. *Cobalt tartrate in potassium tartrate.* $\left(\frac{1}{10}\right)$.

D. *Cobalt oxalate in potassium oxalate.* $\left(\frac{1}{10}\right)$.

E. *Cobalt formate in potassium formate.* $\left(\frac{1}{10}\right)$.

F. *Cobalt Pink.* $CoO\ 8MgO$.

* *Examined in 10 cm. tube.*

cobalt blue. It is evident that the two compounds are of entirely different structure. It would appear that in the former the cobalt atom replacing the magnesium is associated with six groups. In the latter, the zinc atom which has a strong tendency towards association with *four* groups is so situated and the cobalt atom replacing it takes the same structure, yielding a blue compound.

The absorption spectrum of cobalt in concentrated hydrochloric acid (fig. 5 A) is of very similar shape to that of cobalt oxide in zinc oxide (fig. 3 D) but shifted bodily into the red. It is therefore probable that the cobalt atom is similarly situated and associated with four atoms (or groups), possibly chlorine. The behaviour of the solution on the addition of other salts confirms this.

Fig. 5.

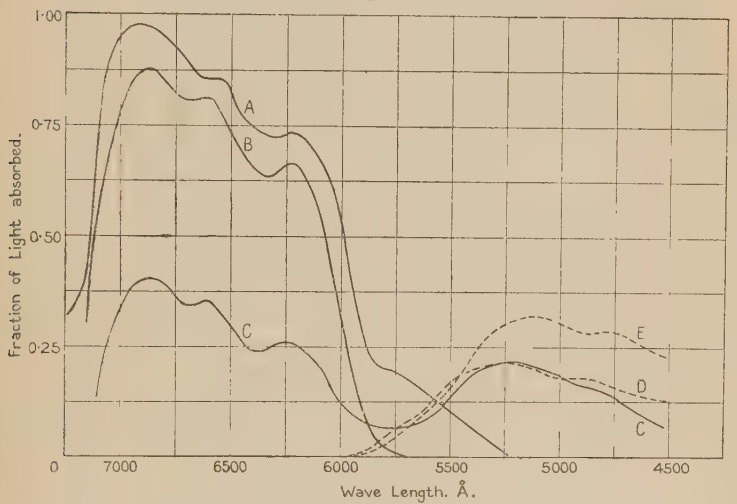

A. *Cobalt chloride in hydrochloric acid.* $\left(\frac{1}{5000}\right)^*$.
B. *Cobalt chloride in* $HCl + MgCl_2$. $\left(\frac{1}{100}\right)$.
C. *Cobalt chloride in* $MgCl_2$ *alone.* $\left(\frac{1}{10}\right)$.
D. *Cobalt chloride in* $HCl + ZnCl_2$. $\left(\frac{1}{10}\right)$.
E. *Cobalt chloride in* $ZnCl_2$ *alone.* $\left(\frac{1}{5}\right)$.

* *Examined in 10 cm. tube.*

The addition of magnesium chloride to the solution causes no change of colour, and the absorption spectrum (fig. 5 B) is almost identical. The addition of zinc chloride, however, changes the colour from blue to red, and the absorption spectrum (fig. 5 D) becomes exactly comparable with that of cobalt oxide in magnesium oxide. In other words, the cobalt atom which was previously associated with *four* atoms is now associated with *six*. The change would appear to be

due to the superior tendency of the zinc to associate with four atoms : there is a redistribution of the structure, whereby the zinc atom takes to itself four groups and the cobalt atom, as a result, has six forced upon it.

The same distribution occurs with zinc chloride alone in the absence of hydrochloric acid, and a precisely similar absorption spectrum is shown (fig. 5 E). With magnesium chloride alone in the absence of hydrochloric acid, however, a particularly interesting result is obtained. Although the solution remains blue, the absorption spectrum (fig. 5 C) shows that both the red and blue compounds are present together. The curve is composed of two distinct parts, the one being the typical curve obtained with the blue compounds and the other that with the red. Since the intensity of the blue compounds is far greater than that of the red, it will be seen from the curve that very little blue is present compared with the red, although the solution looks blue. In the case of magnesium, therefore, which is not strictly limited to an association with four groups, as is zinc, the general structure as regards the cobalt atoms has not been displaced to one form alone ; in fact, both are seen to be present in equilibrium.

Some representative spectra are reproduced in the Plate, and we are indebted to Mr. F. J. Stoakley for invaluable aid in preparing the photographs.

Summary.

1. By examining and comparing the absorption spectra of solutions with those of solid compounds of known crystalline structure, the nature of the association of the atoms in solution can be elucidated.

2. The cobalt atom in the solid *blue* compounds is associated with *four* other atoms or groups. The same arrangement accounts for the colour of the blue solutions.

3. Similarly, in the solid *red* compounds and in the red solutions the cobalt atom is associated with *six* other atoms or groups.

4. The blue compounds are more soluble than the red ; the latter usually separate from solution.

5. The maximum absorption of the blue compounds is much greater than that of the red.

6. Constitutions are given to the well known cobaltous pigments.

We are deeply indebted to Mr. C. T. Heycock for placing at our disposal the necessary apparatus in the Goldsmiths'

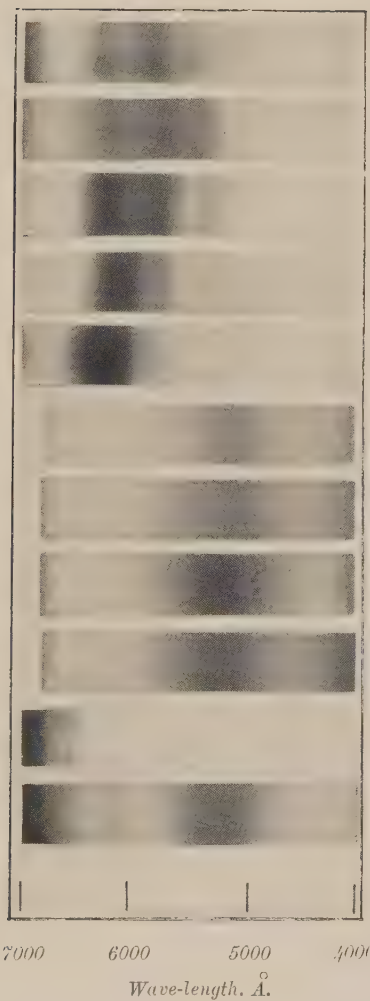
Cobalt Spinel.
Cobalt Blue (a).
$Co(OH)_2$ in KOH.
$Co(CNS)_2$ in KCNS.
$Co(CNS)_2$ in ether.
Cobalt Pink.
Cobalt o-silicate (a).
$CoCl_2$ in water.
$CoCl_2$ in $HCl+ZnCl_2$.
$CoCl_2$ in $HCl+MgCl_2$.
$CoCl_2$ in $MgCl_2$.
7000
6000
5000
4000
Wave-length. Å.

Laboratory for the preparation of the pigments, and to Professor T. M. Lowry for giving us exceptional facilities for making the spectroscopic measurements. One of us (O. R. H.) is indebted to the Royal Commissioners for the Exhibition of 1851 and the other (R. H.) to the Board of Scientific and Industrial Research, for grants held during this investigation.

University Chemical Laboratory,
Cambridge.

LXXXII. *The Damping of Torsional Vibrations in Air at Reduced Pressures.* *By* Ruby V. Wagner, *M.Sc.* *

THE Law of Maxwell, that the viscosity of a gas is independent of the pressure, is known to hold only within certain limits of pressure, and to break down completely at exhaustions greater than about 1/60 atmosphere. A convenient method of investigating the relation between the viscosity and the pressure is by observation of the damping of torsional vibrations at different pressures, the logarithmic decrement for such vibrations being a function of the viscosity. This method was employed by Crookes, Maxwell, and others, various forms of vibrating body being used.

In the experiments of Crookes † a mica vane was suspended in a vertical plane and made to oscillate about its vertical diameter, the damping being observed at pressures ranging from atmospheric to $\cdot 02 \times 10^{-6}$ atmosphere.

A different arrangement was used by Maxwell ‡ in the experiments made to test the validity of his law. He suspended a circular disk in a horizontal plane between two fixed plates, the disk oscillating in its own plane about the axis of the suspension, thus exposing a larger surface to the frictional forces.

Experiments were made with similar apparatus by Kundt and Warburg §, and the deviations from the law at higher

* Communicated by Prof. W. Wilson, Ph.D. The experimental work described in this paper formed the subject of a thesis approved for the M.Sc. degree of the University of London.

† Crookes, Phil. Trans. clxxii. p. 387.

‡ Clerk Maxwell, Scientific Papers, ii. p. 1.

§ Kundt and Warburg, Pogg. *Ann.* clv. p. 340 (1875).

exhaustions were examined. In their earlier work no accurate measurements of pressure were made, and the apparent diminution in the gas viscosity was ascribed entirely to the sliding of the gaseous layers over the oscillating body, the coefficient of slip being inversely proportional to the pressure, and thus producing the same effect as a reduction in the viscosity.

A modified form of this apparatus was used by Hogg *, who showed that the decrease in viscosity is a real effect, and that the reduction in damping cannot be accounted for entirely by the slip. He used a McLeod gauge for measurements of pressure, and obtained curves for various gases.

More recently experiments have been carried out † in which the stationary deflexions of a body, caused by the rotation of a neighbouring body, were measured at different pressures. This method is open to the objection that for high exhaustions large speeds of rotation are necessary, and these set up irregular conditions in the gas and increase the disturbing effects of slight deviations from parallelism etc.

In the experiments here described the measurement of the logarithmic decrement was preferred, a hollow aluminium cylinder being used as oscillating body in place of the mica or glass disks of earlier experiments. This cylinder is very light, and the damping due to the suspension should be very small in comparison with that due to air friction.

A hollow aluminium cylinder was suspended by a bifilar silk suspension between two concentric brass cylinders, an air-gap of about 2 mm. separating the oscillating body from each of the stationary ones. The oscillations were started magnetically, and the damping observed by means of a beam of light reflected on to a scale by a small concave mirror above the cylinder.

When the pressure is such that the mean free path of the molecules is small compared with the distance between the cylinders, the relation between the logarithmic decrement and the viscosity can be calculated as for a liquid. The equation to the oscillation is

$$I\frac{d^2\theta}{dt^2}+\left(2\pi a^3 h\mu\frac{d_1+d_2}{d_1 d_2}\right)\frac{d\theta}{dt}+\eta\theta=0, \quad . \quad . \quad (1)$$

* J. L. Hogg, "On Friction in Gases at Low Pressures," Amer. Acad. Proc. xlii. no. 6, pp. 115–146 (July 1906); xlv. no. 1, pp. 3–17 (Aug. 1909).

† Timiriazeff, "Ueber die Innere Reibung Verduennter Gase," *Ann. der Phys.* xl. pp. 971–991. Langmuir, Phys. Rev. April 1913.

where I = moment of inertia of the system,
a = radius of oscillating cylinder,
h = height of oscillating cylinder,
μ = coefficient of viscosity,
$d_1 d_2$ = distance between the oscillating and each of the stationary cylinders,
η = the torsion constant.

The logarithmic decrement

$$\lambda = \frac{\pi^2 a^3 h \mu (d_1 + d_2)}{\sqrt{\eta I} \cdot d_1 d_2}, \quad \ldots \ldots \quad (2)$$

i. e. $$\lambda = A \frac{d_1 + d_2}{d_1 d_2} \mu, \quad \ldots \ldots \quad (2\,a)$$

i. e. $$\lambda \propto \mu.$$

At low pressures, when the mean free path is comparable with the distance d, it cannot be assumed that the velocity of the gas layer is the same as that of the solid in contact with it, and allowance must be made for the slip. Maxwell defines the coefficient of slip as the quantity $\beta = \frac{\mu}{\sigma}$, where μ = the coefficient of viscosity and σ = coefficient of external friction, *i. e.* the force required per unit area of plane to maintain a uniform relative velocity of 1 cm./sec.

The resistance to the moving body is then the same as if the fixed surface was moved back a distance 2β, and allowance can be made for the slip by writing $(d + 2\beta)$ instead of d, the quantity β being inversely proportional to the pressure (Kundt and Warburg).

The decrement λ is then no longer proportional to the viscosity, for, substituting $(d + c/p)$ for d in the expression $(2\,a)$, c being a constant, and p = pressure,

$$\lambda = A \mu p \left(\frac{1}{p d_1 + c} + \frac{1}{p d_2 + c} \right).$$

The suspended cylinder A (fig. 1) was of thin aluminium sheeting, 0·5 mm. thick, radius 2·05 cm., height 2·5 cm., with struts across the top as in the figure (fig. 2), the struts and cylinder being cut from a spun cylindrical aluminium box, so that there were no joints. At the centre of the

cross formed by the struts a small hole was pierced, into which was fitted a thin aluminium rod (*b*, fig. 2) about 2·5 cm. long, and shaped into a hook at the upper end. This rod was held in place by a small nut below the struts, and to it was fixed a small concave mirror (*c*), at the back of which was attached a very small piece of magnetized watch-spring.

Fig. 1.

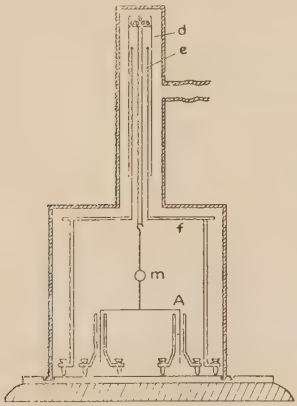

Fig. 2.

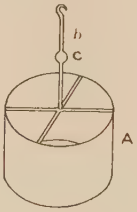

The bifilar suspension (fig. 3) was the same as that used in the White pattern of the Kelvin quadrant electrometer. *e* is a conical screw which can be moved in or out of its socket, thus separating or approaching the screws *c*, *d*, round which the fibre passes. By turning the pins *a*, *b*, the suspension can be lengthened or shortened, and the points of suspension can be moved forwards or backwards by means of the same screws. The silk fibre passed round the hook on *b* (fig. 2), which was grooved to prevent slipping.

Fig. 3.

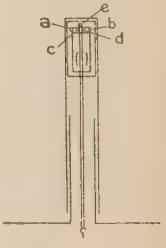

The upper part of the bifilar was fixed to a hollow brass cylinder (*d*, fig. 1) sliding over a second cylinder *e*, about 1 cm. diameter and 10 cm. long, through which the fibres passed. This cylinder was supported on a circular brass plate *f* standing on three legs with screw feet, the plate having a hole at the centre, 1 cm. in diameter, to allow the suspension to pass through. The bifilar could be made of suitable length by sliding the outer cylinder up or down, and final adjustments were made by means of the

pins *c*, *d*. The bifilar was arranged to give a convenient period of oscillation, that finally used being 18 secs.

The stationary cylinders were also of brass, and stood on three legs with screw feet. The oscillating cylinder projected by about 2 mm., above and below the two brass cylinders, which were of equal height. This arrangement facilitated the adjustments and setting for parallelism, and made it possible to view the oscillating cylinder after the case was sealed down.

The containing chamber was entirely of brass, and cylindrical in shape, as shown in fig. 1. In the lower part a plate-glass window 3·5 cm. by 6·5 cm. was sealed on to a ground rim with Faraday cement. The exit tube was in the upper part of the case, so that the oscillating system was in some measure protected in case of a sudden inrush of air.

The base consisted of a brass plate, in which grooves were cut for the screw feet, the plate being fixed to a wooden base, and the whole standing on a slate slab projecting from the wall.

The cylinders were placed in position, and the bifilar so arranged that the addition of the small magnet produced no change in the zero reading. There was therefore no twist on the bifilar in the position of rest. The necessary adjustments of level were made by means of the screw feet.

The general arrangement of the apparatus was as indicated in fig. 4. B, C are drying tubes filled with phosphorus pentoxide, which could readily be renewed by opening the tubes *h*, *k*. The tube D contains vegetable charcoal, and E, F are McLeod gauges. G leads to a Fleuss-Geryk oil-pump.

The joint to A was sealed with Faraday cement, and a pressure tubing sleeve was found satisfactory at the pump, as the tap T_2 was kept closed at higher exhaustions. The brass case and window were sealed down with cement. The tube H was drawn into a capillary and sealed off. Dry air was admitted when necessary through the wash-bottle K containing concentrated sulphuric acid.

As a preliminary precaution, the apparatus was repeatedly evacuated and filled with dry air. It was then sealed up, evacuated to about 0·2 mm., and the charcoal in D alternately strongly heated and cooled *in vacuo*. The oil-pump was worked by an electric motor, and pressures from atmospheric to 0·15 mm. could be obtained. Pressures below these were obtained by immersing the charcoal tube D in liquid oxygen. By means of the tap T_1 the charcoal tube

could be placed in communication with the rest of the apparatus for any requisite length of time, and the exhaustion proceeded with by stages, pressures between 0·015 cm. and 0·00001 cm. being readily obtained.

The use of liquid oxygen has an advantage over that of liquid air in that the temperature of the boiling liquid remains constant, whereas in the case of liquid air a fresh supply, being richer in nitrogen, will have a lower temperature than a quantity that has been standing for some hours *.

Fig. 4.

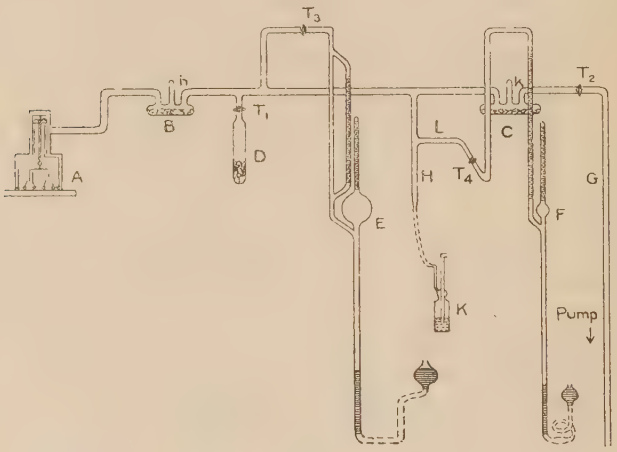

For measurements of pressure between 76 cm. of Hg and 1 cm. Hg, the McLeod gauge F was replaced by an ordinary manometer. Pressures below 1 cm. were read by means of a McLeod gauge with a bulb of about 30 c.c capacity ; and for pressures below 0·015 cm., a McLeod with a 500 c.c. bulb was used. The upper readings of the gauge F could also be taken with the manometer, and the lower readings of F with the McLeod E, so that the readings on the various gauges could be made to overlap, and continuity was ensured. The decrement was measured at pressures ranging from atmospheric to 0·00001 cm. Hg.

The required pressure was obtained by means of the pump or liquid oxygen, and the taps T_1, T_2 were closed. The apparatus was then left for about ten minutes. (This was

* J. L. Hogg, Amer. Acad. Proc. xlv. (Aug. 1909).

found necessary, as otherwise the pressure in A was not the same as that indicated by the gauge at the lower pressures, and unreliable readings resulted.) The pressure was then read on the McLeod gauge. The oscillations were started by bringing up a small magnet to the case A, and 20 complete oscillations read by means of a lamp and scale at a distance of 1 metre from A. The decrement was calculated from these. The pressure reading was then again taken, and if it varied from the earlier measurement, the readings were discarded.

The experiments were carried out at room temperature, which was read at intervals, and accordingly it was desirable to cover as large a pressure range as possible each day. The small changes in temperature during the day did not appreciably affect the results, and except at the highest exhaustions, curves obtained on days when the temperatures differed by 1° or 2° C. coincided.

Two distinct sets of readings were taken. In one case the outer brass cylinder only, and in the second case both outer and inner brass cylinders, were used.

The results obtained are indicated in the accompanying tables and curves, the curves being drawn from readings taken on different days and selected so that, as far as possible, the temperature was constant throughout. For the section below 0·001 cm. two sets of readings only were used, when the temperature was the same as for the other readings. The logarithmic decrement $= l \times \log_e 10$, and the ordinates in the curves represent l.

The entire range can be shown most conveniently by plotting logarithms of pressures as abscissæ, and values of l as ordinates (curve 1). Sections are shown in the following curves (pp. 856, 857).

(A) *For the case when the outer brass cylinder only was used.*

Kundt and Warburg state * that as long as the layer of gas has thickness greater than fourteen times the mean free path, the retarding force does not vary by more than 1/1000 part of its value. In the curves obtained, however, the decrement is seen to fall off quite decidedly from 76 cm. to about 30 cm. Hg. This effect was noted by Crookes in the case of all gases except hydrogen.

* Kundt and Warburg, Phil. Mag. July 1875.

Between 30 cm. and 1·5 cm. the decrement is constant, then falls off slowly to 0·15 cm. and more rapidly afterwards. At about 0·015 cm. the mean free path becomes approximately equal to the distance between the cylinders, and the

TABLE (Curve A).

P. (cms. Hg).	λ.	log P.
77·15	·03787	1·88733
73·75	·03778	1·86777
66·35	·03751	1·82184
55·05	·03699	1·74075
47·85	·03659	1·67989
42·35	·03635	1·62685
33·95	·03615	1·53085
26·8	·03598	1·42813
14·35	·03583	1·15686
8·75	·03589	·94201
4·05	·03578	·60745
1	·03555	·00000
·644	·03553	$\bar{1}$·96567
·3434	·0352	1·53577
·2002	·0349	$\bar{1}$·20140
·1357	·03452	1·13268
·06763	·03305	2·83014
·02882	·02991	2·45983
·02236	·02879	2·3496
·01548	·02621	2·18986
·01409	·02553	2·14895
·01146	·02367	2·05922
·01112	·02340	$\bar{2}$·04621
·00968	·02244	3·98588
·00732	·0204	3·86392
·00678	·0198	$\bar{3}$·83108
·00442	·0164	$\bar{3}$·64561
·00298	·0136	$\bar{3}$·47420
·00220	·01221	$\bar{3}$·34242
·00140	·00933	$\bar{3}$·14516
·001115	·00845	$\bar{3}$·04725
·00076	·0070	$\bar{4}$·88080
·00059	·0055	$\bar{4}$·76938
·00041	·00536	4·61287
·00034	·00483	$\bar{4}$·53148
·00016	·00389	4·20412
·000078	·00315	5·89209
·000053	·00304	$\bar{5}$·72428
·000034	·00264	5·53148
·0000184	·00251	5·26482
·000011	·00242	$\bar{5}$·04287

TABLE (Curve B).

P. (cms. Hg).	*l*.	log P.
76·53	·04250	1·88384
60·73	·04240	1·78341
36·2	·04225	1·55871
28·73	·04221	1·45834
8·13	·04207	·91009
5·53	·04206	·74273
2·63	·04197	·41996
·77366	·04192	$\bar{1}$·88855
·53159	·04180	1·72558
·28009	·04155	1·44730
·19276	·04109	$\bar{1}$·28502
·06945	·03915	$\bar{2}$·84167
·04769	·03821	$\bar{2}$·67839
·03143	·03652	$\bar{2}$·49723
·01989	·03532	$\bar{2}$·29859
·01616	·03356	$\bar{2}$·20845
·01294	·03044	$\bar{2}$·11206
·01099	·02842	$\bar{2}$·04107
·00973	·02710	$\bar{3}$·98833
·00680	·02397	$\bar{3}$·83277
·00421	·01937	$\bar{3}$·62467
·00356	·01807	$\bar{3}$·55189
·00282	·01596	$\bar{3}$·45025
·00224	·01392	$\bar{3}$·35025
·00175	·01199	$\bar{3}$·24304
·00124	·00974	$\bar{3}$·09202
·00069	·00697	$\bar{4}$·83885
·000616	·00659	$\bar{4}$·78958
·00053	·00601	$\bar{4}$·72428
·000316	·00462	$\bar{4}$·49969
·00023	·00427	$\bar{4}$·36173
·000156	·00348	$\bar{4}$·19312
·000068	·00307	$\bar{5}$·83505
·000064	·00286	$\bar{5}$·80618
·000052	·00259	$\bar{5}$·71600
·000036	·00233	$\bar{5}$·55630
000019	·00217	$\bar{5}$·27875
·000015	·00212	$\bar{5}$·18184

Values for Curve 3 B (calculated).

P. (cms. Hg).	*l*.
·0136	·0295
·0103	·0274
·00921	·0265
·0076	·025
·00584	·0225
·0044	·0200
·00339	·0175
·00255	·015
·00129	·01
·000729	·00697

Curve 1.

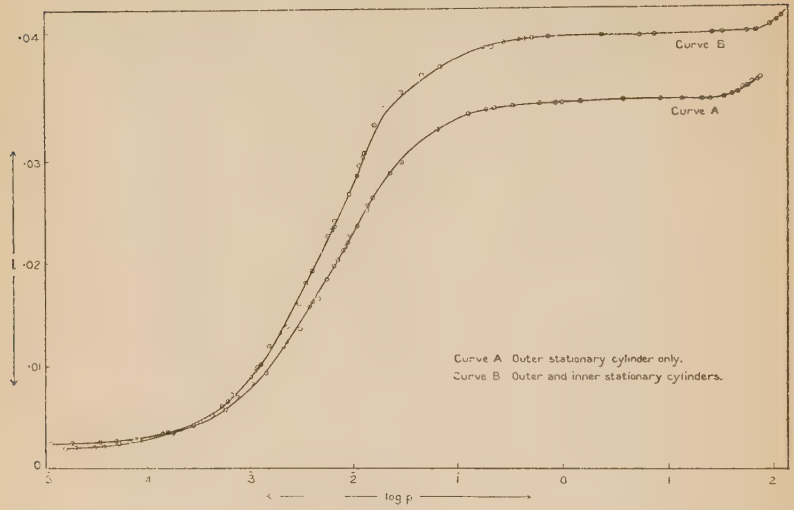

Curve 2.

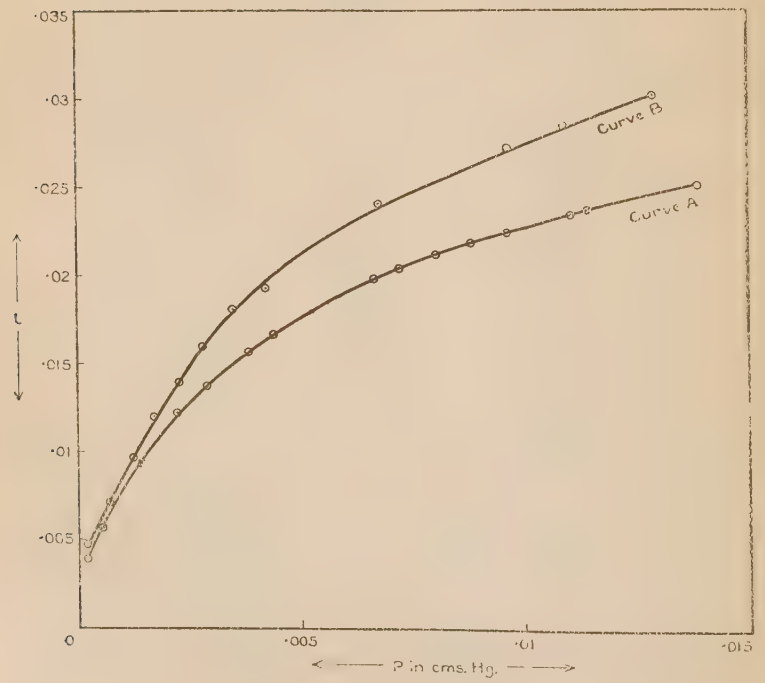

Curve 3.

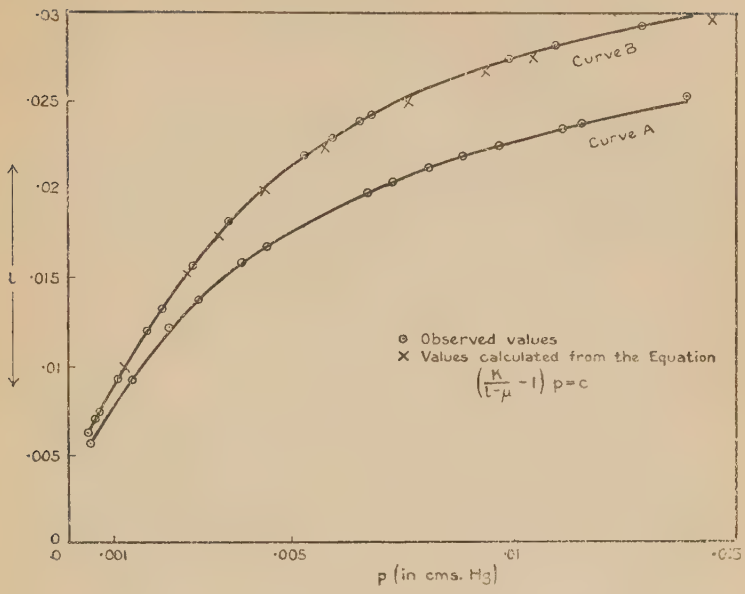

Curve 4.

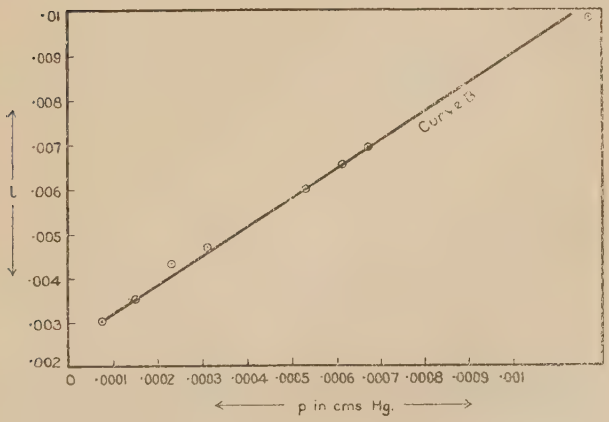

decrement then falls off very rapidly (curve 2). In the logarithmic curve there is a point of inflexion, and the decrement appears to approach a constant value, about ·05 of its value at atmospheric pressure. This residual damping will be due to the friction in the silk fibre, and possibly in a

very small degree to electromagnetic effects. Hogg takes the limiting value for l, as determined from his curves, to indicate the damping due to causes other than air friction, and allows for the viscosity of the suspension etc. in this way.

Below about 0·0007 cm. the decrement is proportional to the pressure. This fact has been utilized * in the construction of gauges for the measurement of low pressures in cases where the use of a McLeod is undesirable. A gauge of the decrement type was first suggested by Sutherland †, and various types have since been developed ‡.

(B) *For the case when the outer and inner brass cylinders were used.*

In this case, only a very slight decrease in the damping was observed at pressures just below atmospheric, and the decrement remained almost constant down to a pressure of about 1·5 cm. Attempts were made to find whether the decrease noticeable in curve A occurred at slightly higher pressures in curve B. The brass case was soldered to the base with Wood's fusible alloy, and the window wired on to the case. A manometer and pump were connected to the oscillation apparatus, and the readings thus carried up to about 130 cm. Hg. A slight increase in the decrement was found as indicated in Curve 1.

The region between 0·015 cm. and 0 0005 cm. is shown in curve 2. The earlier equations of Maxwell and Sutherland were modified by Hogg to the expression

$$\left\{\frac{k}{l-\mu}-1\right\}p=c,$$

where k and c are constants,

l = the total logarithmic decrement,

μ = the decrement due to the suspension etc.,

which Hogg took as the lowest value of l obtained in his experiments, the constants being calculated from the curves.

This equation holds very accurately for curve B for pressures below 0·015 cm., suitable values, as determined

* P. E. Shaw, Proc. Phys. Soc. Lond. xxix. pp. 171–175. Langmuir, Phys. Rev. April 1913.

† Sutherland, Phil. Mag. Feb. 1897.

‡ S. Dushman, "Production and Measurement of High Vacua."

from the curves, being given to the constants k and c. The calculated and observed values are shown in curve 3, the values taken for the constants being

$$k = \cdot 0372, \qquad c = \cdot 0047, \qquad \mu = \cdot 002.$$

At pressures below ·001 cm. the mean free path becomes greater than the distance d. Collisions between the molecules are infrequent, and they travel to and fro between the oscillating and stationary cylinders, the angular momentum of the oscillating cylinder being thereby reduced. The loss of momentum will be proportional to the number of molecules present, *i. e.* to the pressure, and to the mean molecular velocity, which is constant as long as the temperature is constant. The logarithmic decrement will accordingly be proportional to the pressure*. This was found to be the case, the linear relation holding for pressures about ·0007 cm.

Curve B crosses curve A in curve 1 at about ·0002 cm. It would appear that at these and lower pressures a large proportion of the damping is due to the suspension, and the two curves would be expected ultimately to coincide. It was unfortunately not possible to employ the same suspension in the two sets of readings; for curve B a new suspension was used, which was adjusted so that the decrement at atmospheric pressure was the same as for the previous suspension under the same conditions. The difference between the two suspensions would show more markedly at high exhaustions, and the fact that the lowest value of l in curve B is greater than in curve A can be accounted for by this difference.

LXXXIII. *A Note on the Theory of Artificial Telephone and Transmission Lines.* *By* The Research Staff of the General Electric Co., Ltd.† (*Work conducted by* A. C. Bartlett.)

A UNIFORM telephone line of length l having inductance L, resistance R, capacity C, and leakage S per unit length can be replaced, as far as measurements at the two ends are concerned, by various simple networks, of

* Dushman, "Production and Measurement of High Vacua," Part 4, General Electrical Review, Sept. 1920.

† Communicated by the Director.

which one is illustrated in fig. 1,

Fig. 1.

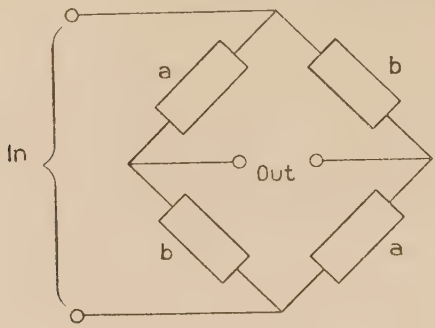

where

$$a = Z_0 \coth \frac{Pl}{2},$$

$$b = Z_0 \tanh \frac{Pl}{2},$$

$$Z_0 = \sqrt{R + jpL} \Big/ \sqrt{S + jpC},$$

$$P = \sqrt{R + jpL} \,.\, \sqrt{S + jpC},$$

$$p = 2\pi f,$$

f being the frequency.

In other networks of this kind impedances appear which are represented by hyperbolic sines and cosecants in addition to tangents and cotangents. The methods discussed in this note have not, so far, proved applicable to such networks.

The elements of these networks such as $Z_0 \tanh \frac{Pl}{2}$ can be represented at any given frequency by a resistance in series with either a capacity or an inductance, but such a representation is not correct at all frequencies.

In practice, when a long artificial line has to be simulated, it is usually split up into a number of short lengths $\frac{l}{n}$. In this case $\frac{Pl}{2n}$ is small so that

$$Z_0 \tanh \frac{Pl}{2n} = Z_0 \,.\, \frac{Pl}{2n}$$

$$= (R + jpL) \,.\, \frac{l}{2n},$$

which is a resistance $\frac{Rl}{2n}$ in series with an inductance $\frac{Ln}{2n}$; the values are independent of frequency, provided $\frac{l}{n}$ is sufficiently small.

The purpose of this note is to put forward an alternative method which does not require the line to be split into small sections; its interest is perhaps theoretical rather than practical. It depends on the expansion of $Z_0 \tanh \frac{Pl}{2}$ and $Z_0 \coth \frac{Pl}{2}$ either as an infinite continued fraction or as an infinite series such that the terms of the fraction or series can be represented by simple arrangements of resistances, inductances, and capacities.

First we have

$$\tanh x = \frac{x}{1 + \frac{x^2}{3 + \frac{x^2}{5 + \dots}}},$$

$$Z_0 \tanh \frac{Pl}{2} = \frac{Z_0 \frac{Pl}{2}}{1 + \frac{P^2l^2}{3.4 + \frac{P^2l^2}{5.4 + }}}$$

$$= \frac{1}{\frac{2}{Z_0 Pl} + \frac{1}{\frac{3.2Z_0}{Pl} + \frac{1}{\frac{5.2Z_0}{Z_0 Pl} + }}},$$

and so on.

But this represents the impedance of the network,

Fig. 2.

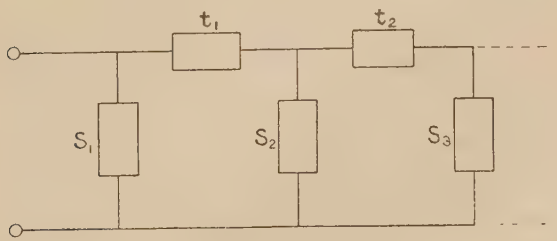

where

$$S_n = \frac{Z_0 Pl}{2(4n-3)},$$

$$t_n = \frac{Z_0}{Pl}.2(4n-1).$$

Now

$$Z_0 P l = l(R + jpL),$$

and is therefore a resistance lR in series with an inductance lL; and

$$Z_0/P l = \frac{1}{l(S + jpC)},$$

a capacity lC shunted by a leak lS.

Thus $Z_0 \tan \frac{Pl}{2}$ can be represented by the network,

Fig. 3.

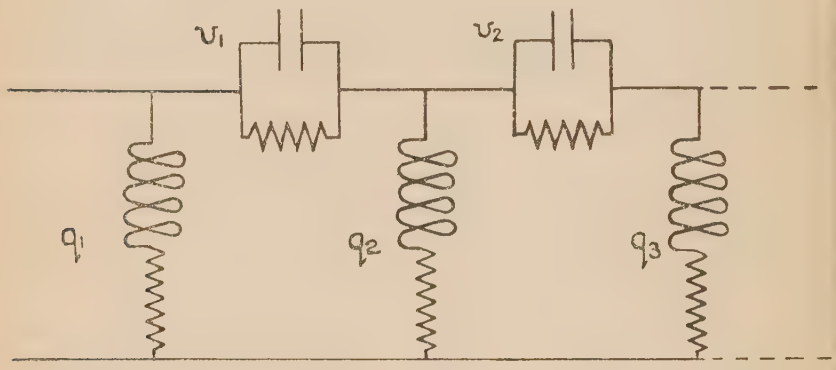

the shunt elements being given by

$$q_n = \frac{l}{2(4n-3)} \cdot (R + jpL);$$

the series elements by

$$v_n = \frac{2(4n-1)}{l(S + jpC)}.$$

Second we have

$$\tanh u = \sum_{n=1}^{n=\infty} \frac{8u}{(2n-1)^2\pi^2 + u^2}.$$

Thus $Z_0 \tanh \frac{Pl}{2}$

$$= \Sigma \sqrt{\frac{R + jpL}{S + jpC}} \cdot \frac{4l \sqrt{R + jpL} \cdot \sqrt{S + jpC}}{(2n-1)^2\pi^2 + l^2(R + jpL)(S + jpC)}$$

$$= \Sigma \frac{1}{\frac{(2n-1)^2\pi^2}{4l(R + jpL)} + \frac{(S + jpC)l}{4}}.$$

But the expression under the Σ is the impedance of the network,

Fig. 4.

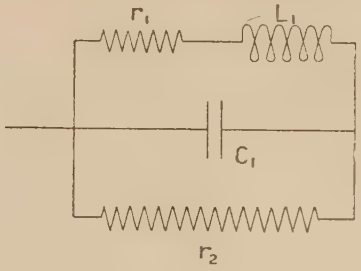

where

$$r_1 = \frac{4lR}{(2n-1)^2\pi^2},$$

$$L_1 = \frac{4lL}{(2n-1)^2\pi^2},$$

$$c_1 = \frac{l}{4}c,$$

$$r_2 = \frac{4}{lS}.$$

Thus $Z_0 \tanh \frac{Pl}{2}$ can be represented by an infinite series of such networks connected in series.

The other elements of the network of fig. 1 can be treated by applying the foregoing analysis to the admittance instead of to the impedance.

$Z_0 \coth \frac{Pl}{2}$ is equivalent to the following network if the series expansion is used,

Fig. 5.

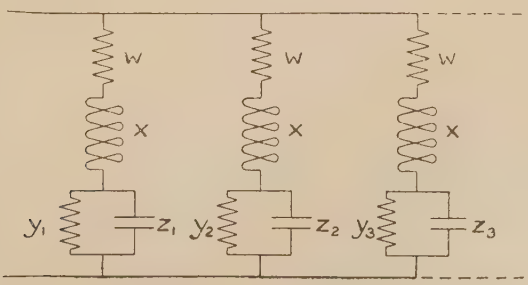

where

$$w = \frac{Rl}{4},$$

$$x = \frac{lL}{4},$$

$$y_n = \frac{1}{4lS} \cdot (2n-1)^2\pi^2,$$

$$z_n = \frac{4lC}{(2n-1)^2\pi^2}.$$

If the continued fraction expansion is used, it is equivalent to

Fig. 6.

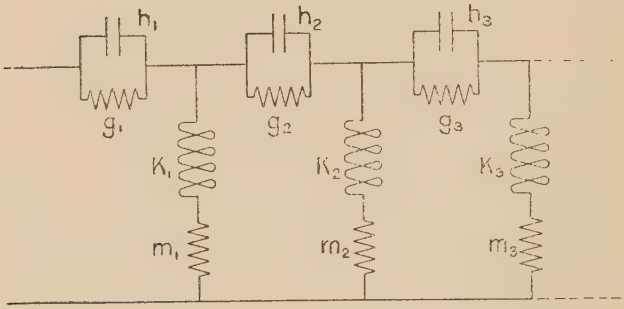

where

$$h_n = \frac{lC}{2.(4n-3)},$$

$$g_n = \frac{2(4n-3)}{lS},$$

$$k_n = \frac{lL}{2(4n-1)},$$

$$m_n = \frac{Rl}{2(4n-1)}.$$

Thus all the elements of the "bridge" type of network shown in fig. 1 can be expanded into convergent forms that are physically realizable, and any desired approximation can be obtained by taking a sufficient number of terms.

We have not succeeded in obtaining similar expansions for the impedance $Z_0/\sinh Pl$ and $Z_0 \sinh Pl$ that occur in the Π and T types of artificial line illustrated in fig. 7.

Fig. 7.

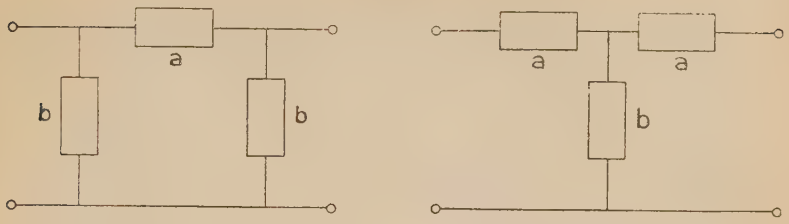

Π Section.

$$a = Z_0 \sinh Pl.$$
$$b = Z_0 \coth \frac{Pl}{2}.$$

T Section.

$$a = Z_0 \tanh \frac{Pl}{2}.$$
$$b = Z_0 / \sinh Pl.$$

In connexion with this it is interesting to note that $Z_0 \tanh \frac{Pl}{2}$ and $Z_0 \coth \frac{Pl}{2}$ have definite physical meanings, being the impedances of a line of length $\frac{l}{2}$ short circuited and open circuited respectively at the far end, whereas $Z_0 \sinh Pl$ and $Z_0/\sinh Pl$ have no such definite meaning.

Note added later.

The expansion

$$\coth x = \frac{1}{x} + \Sigma \frac{2x}{x^2 + n^2\pi^2}$$

can also be used and gives networks of the same general form for

$$Z_0 \coth \frac{Pl}{2} \text{ and } Z_0 \tanh \frac{Pl}{2}.$$

Thus both

$$Z_0 \coth \frac{Pl}{2} \text{ and } Z_0 \tanh \frac{Pl}{2}$$

can be expanded either in the form of a ladder network or as an infinite sequence of impedance elements connected in parallel or as an infinite sequence of impedances connected in series.

LXXXIV. *On Air-waves of Finite Amplitude. By* W. B. Morton, *M.A., and* Amy I. Woods, *M.A., M.Sc., Queen's University, Belfast* *.

Introduction.

THE classical memoir on this subject is that published in 1910 by the late Lord Rayleigh †. In it a thorough examination is made of the conditions under which it is possible for a disturbance of finite amplitude to be propagated through a gas without change of type. After a summary and criticism of the earlier work of Poisson, Stokes, Earnshaw, Rankine, and Hugoniot, the conclusion is reached, by combining arguments of a mechanical and thermodynamic kind, that such propagation is only possible when the influence of dissipative forces is taken into account and when the wave is one of compression, bringing a higher density to a region of the gas. Further, the wave is of a very special type; an assigned ratio of initial and final pressures must be accompanied by a definite ratio of densities also, and therefore of temperatures, and there must be a definite relative velocity of the two masses of gas which are separated by the wave.

Lastly, the possibility of the physical existence of the wave is conditional on the existence of a solution, satisfying the terminal conditions, of a certain rather complicated differential equation, involving the variation of the specific volume along the wave. An equation, exactly equivalent to this, but using the velocity as dependent variable, was arrived at independently by Mr. G. I. Taylor ‡ in a paper read at the same meeting of the Royal Society.

In the earlier part of Lord Rayleigh's paper the effects of heat-conduction and viscosity are considered separately, but both are taken into consideration in the final discussion which leads to the equation. It does not appear to be necessary to make the separation, since the two magnitudes are linked together by the theory of gases.

Lord Rayleigh established the existence of the required solution by a closely-reasoned and rather difficult argument, based on an interpretation of the differential equation as an equation of motion of a particle. By way of confirmation he worked out two special cases arithmetically by the method of Runge. It seemed possible to discuss this matter in a

* Communicated by the Authors.

† Proc. Roy. Soc. lxxxiv. p. 247 (1910); Collected Papers, v. p. 573.

‡ Proc. Roy. Soc. lxxxiv. p. 371 (1910).

somewhat broader way by means of the graphical method of "isoclines," of which an account is given by M. D'Ocagne in his book 'Calcul Graphique et Nomographie'*, where Massau is named as the originator of the method. This is done in the first part of the present paper.

In the second part the physical characteristics of the "Rayleigh wave" are examined in some detail. It seems worth while to do this in spite of the very special nature of this type of motion, and the improbability of the precise balance of terminal states, needed for its unchanging advance, being attained in practice. Actual explosion waves have often been photographed. Probably the observation of a wave has not been extended through a sufficiently great distance to permit of the detection of change of form. It does not appear impossible that by some kind of adjustment the permanent type is approached as the wave proceeds. At any rate, this special type may present some features in common with the more general case of a wave initiated in an arbitrary manner.

I. The Rayleigh-Taylor Equation.

In Lord Rayleigh's form the equation is

$$\mu' \frac{d}{dx}\left(\mu' \frac{dv^2}{dx}\right) + \mu' \frac{dv^2}{dx}\left\{ \frac{3(\gamma+1)}{8\gamma} \cdot \frac{v_1+v_2}{v} - \tfrac{3}{2} - h \right\} = \tfrac{3}{4}h(\gamma+1)(v_1-v)(v-v_2)$$

(*loc. cit.*, eqn. 98).

v is the volume of unit mass, decreasing, as the wave passes, from v_1 to v_2; γ is the ratio of specific heats and h the constant $c\mu/k$, where c is the specific heat at constant volume, μ the viscosity, and k the conductivity; μ' is the viscosity divided by the mass-velocity m, i. e. the mass which crosses unit area per second at any point, when the wave is made stationary in space by superposing the proper backward velocity on the gas as a whole. For the discussion which follows it is convenient to adopt a transformation of the equation differing slightly from Lord Rayleigh's. We shall put

$$-\mu' dv^2/dx = v_2^2 \eta, \qquad v = v_2 \xi, \qquad v_1/v_2 = s,$$

so that ξ is the specific volume expressed as a multiple of its ultimate value and s is used, as in Rayleigh's paper, for the ratio of the final to the initial density. The dependent variable η is the rate of increase of ξ^2 in the small distance μ',

* P. 149. See also an article by Brodetsky in the 'Mathematical Gazette,' 1919-20.

measured in the direction in which the wave is travelling. Rayleigh's (ξ, U) correspond to our ($v_2^2\xi^2$, $-v_2^2\eta$). The equation now takes the form

$$\frac{d\eta}{d\xi} = \frac{A\xi(\xi-1)(s-\xi)}{\eta} - B(\xi-c),$$

where

$$A = \tfrac{3}{2}h(\gamma+1),$$

$$B = 3+2h,$$

$$c = 3(\gamma+1)(s+1)/4\gamma(3+2h).$$

The required solution is one for which η runs through positive values from zero at $\xi=1$ to zero at $\xi=s$, and s may have any value from unity to the upper limit $(\gamma+1)/(\gamma-1)$. The terminal points (1, 0) and $(s, 0)$ are "singular points" at which the value of dy/dx becomes indeterminate. When the origin is transferred to such a point and terms of the second order are neglected the differential equation assumes in general the form

$$dy/dx = (ax+by)/(a'x+b'y).$$

By putting $y=mx$ a quadratic equation

$$b'm^2+(a'-b)m-a = 0$$

is found whose roots determine two special directions at the point. The arrangement of the curves which satisfy the differential equation depends on the nature of the roots of this quadratic *.

The analysis is a good deal simplified in the present case owing to the special values, $a'=0$ and $b'=1$. We have

$$dx/y = dy/(ax+by) = d(y-mx)/(b-m)y+ax.$$

If m is a root of $m^2-bm-a=0$ then $a=-m(b-m)$, and $(b-m)$ is the other root, and so

$$d(y-m_1x)/m_2(y-m_1x) = d(y-m_2x)/m_1(y-m_2x),$$

giving as approximate integral near the origin the equation

$$(y-m_1x)^{m_1} = C(y-m_2x)^{m_2}.$$

When the roots m_1 m_2 are real and have the same sign the point is a "node." An infinite number of solution-curves pass through the point, arranged like a family of parabolas having a common tangent which has the special direction of

* See Picard, *Traité d'Analyse*, iii. p. 206.

smaller slope. When the roots are real with opposite signs the point is a "col." The curves are then like a family of hyperbolas with common asymptotes and two solution-curves only leave the point, one in each of the special directions. When the roots are complex the singular point is a "focus" and the solution-curves wind round it in the manner of a spiral. For purely imaginary roots we have a "centre," the arrangement round it being similar to the case of concentric ellipses.

Nature of the singular points.

It is necessary first to settle the character of the terminal points in the present case. When the reductions are effected the quadratics are found to be :

$$\text{at } \xi = 1, \quad m^2 - \mathrm{B}(c-1)m - \mathrm{A}(s-1) = 0,$$

$$\text{at } \xi = s, \quad m^2 + \mathrm{B}(s-c)m + \mathrm{A}s(s-1) = 0.$$

It is seen at once that the former point is always a "col," but the nature of $\xi = s$ requires some consideration. This is the more necessary because Lord Rayleigh, in his numerical work, took for the constant h the value of ·4, in accordance with Maxwell's law of the inverse fifth power for molecular repulsions. The values given by Meyer and Jeans for actual gases are in the neighbourhood of ·6. One would like to be assured of the possibility of the wave for any values of the constants h and γ. If the roots of the second quadratic are real the point is a node, because the constant term is essentially positive. The condition for this is

$$\mathrm{B}^2(s-c)^2 - 4\mathrm{A}s(s-1) > 0,$$

which has to hold for all values of s from unity to $(\gamma+1)/(\gamma-1)$. For $s=1$ the left-hand side is a complete square, and when the other extreme value is put for s, and B and A replaced by their values, the expression again reduces to a complete square, viz.

$$4(\gamma+1)^2(h-\tfrac{3}{4})^2/(\gamma-1)^2.$$

Therefore the expression is positive for all intermediate values of s, provided the quadratic in s has not two real roots lying in the interval.

Written out in full the equation is

$$\{64\gamma^2h^2 - 48(2\gamma^2-\gamma+1)\gamma h + 9(3\gamma-1)^2\}\, s^2 + 6(\gamma+1)\{8(2\gamma-1)\gamma h - 3(3\gamma-1)\}\, s + 9(\gamma+1)^2 = 0.$$

There are three critical values of h in ascending order of magnitude (when $\gamma > 1$),

$$h_1 = 3(3\gamma-1)/8\gamma(2\gamma-1),$$
$$h_2 = 3/4\gamma,$$
$$h_3 = 3\{2\gamma^2-\gamma+1-2(\gamma-1)\gamma^{1/2}(\gamma+1)^{1/2}\}/8\gamma.$$

For $h=h_1$ the coefficient of s changes sign,
for $h=h_2$ the discriminant of the equation vanishes,
for $h=h_3$ the coefficient of s^2 changes sign.

For $0 < h < h_1$ the coefficients are $+ - +$, roots imaginary,
$h_1 < h < h_2$,, ,, $+ + +$, ,, ,,
$h_2 < h < h_3$,, ,, $+ + +$, roots real and both negative,
$h_3 < h$,, ,, $- + +$, roots real and of opposite sign.

Therefore in no case do both roots lie in the interval between the extreme values of s. We conclude that $\xi=1$ is always a col and $\xi=s$ always a node. It remains to show that one of the infinite numbers of solution-curves at $(s, 0)$ runs, through positive values, to the point $(1, 0)$.

Geometrical discussion of the equation.

A general idea as to the configuration in the plane of $(\xi\eta)$ of the curves which satisfy the differential equation is obtained by considering the "isoclines" along with the "inflexion-locus." An isocline is the locus of points at which $d\eta/d\xi$ has an assigned value, p. The inflexion-locus passes through the points where $d^2\eta/d\xi^2$ vanishes; on opposite sides of it the solution-curves have their concavities turned in opposite directions. At the intersection of the inflexion-locus with an isocline p, the isocline itself has the slope p *.

In the present case the isoclines are the cubic curves

$$A\xi(\xi-1)(s-\xi) = \eta\{B(\xi-c)+p\}.$$

They all pass through the three singular points $\xi=0, 1, s$ on the ξ-axis. This axis itself is the isocline $p=\infty$; the solution-curves cross it everywhere at right angles. Special importance attaches to the curve $p=0$,

$$\eta = A\xi(\xi-1)(s-\xi)/B(\xi-c).$$

* See D'Ocagne, *loc. cit.* p. 153.

This has $\xi=c$ as asymptote. It will be found later that essential differences arise according as this does or does not lie in the section between $\xi=1$ and $\xi=s$.

There are three special values of p for which the cubic breaks up into a straight line through one of the singular points and a parabola through the other two. These are

$$p = \mathrm{B}c, \quad \xi = 0, \quad \text{and} \quad \mathrm{B}\eta = \mathrm{A}(\xi-1)(s-\xi);$$
$$p = \mathrm{B}(c-1), \quad \xi = 1, \quad \text{and} \quad \mathrm{B}\eta = \mathrm{A}\xi(s-\xi);$$
$$p = \mathrm{B}(c-s), \quad \xi = s, \quad \text{and} \quad \mathrm{B}\eta = -\mathrm{A}\xi(\xi-1).$$

The equation of the inflexion-locus is

$$\mathrm{B}\eta^3 + \mathrm{A}\{3\xi^2-2(s+1)\xi+s\}\eta^2 - \mathrm{AB}(\xi-c)\xi(\xi-1)(s-\xi)\eta + \mathrm{A}^2\xi^2(\xi-1)^2(s-\xi)^2 = 0.$$

There is a node at each singular point and the tangents to the two branches of the curve have the "special directions."

In order to examine the disposition of the branches with respect to the tangents it is necessary to take into account terms of the third degree, when the equation is referred to the double point as origin. The terms of second and third degree may be written

$$(y-m_1x)(y-m_2x) = u_3.$$

To find the side of the tangent $y=m_1x$ on which the curve lies, it is only necessary to consider the sign of

$$y-m_1x = u_3/(y-m_2x) = u_3(m_1)x^2/(m_1-m_2),$$

where $u_3(m)$ means that the values $x=1$, $y=m$ have been inserted in u_3.

In the present case, when account is taken of the quadratic equation satisfied by m_1, m_2, it is found that the expression for $u_3(m)$ can be written in the forms

$$-\mathrm{B}(1-c)m\{\mathrm{B}m+\mathrm{A}(2-s)\}/\mathrm{A}(s-1) \quad \text{at } \xi=1;$$
$$\mathrm{B}(s-c)m\{\mathrm{B}m+\mathrm{A}(2s-1)\}/\mathrm{A}s(s-1) \quad \text{at } \xi=s.$$

Thus at $\xi=1$ critical values of s are those which make $c=1$ or $m=-\mathrm{A}(2-s)/\mathrm{B}$. The former value is given at once by the meaning of the constant c as

$$s = \{\gamma(9+8h)-3\}/3(\gamma+1) = s_1,$$

say. For $\gamma=1{\cdot}41$, $h={\cdot}4$, s_1 is $1{\cdot}96$, and more generally it can be seen that the value lies within the range with which we are concerned.

The other critical value is found by inserting the given value of m in the quadratic equation which gives the special

directions and solving the equation so obtained for s. In this case it is found on examination that for the actual range of values of γ and h the roots do not correspond to values of s occurring in the question. One root is negative and the other positive but less than unity. Therefore s_1 is the only critical value found at $\xi=1$. It has been met with already, as the value for which the asymptote $\xi=c$, of the zero isocline, passes within the range, from $\xi=1$ to $\xi=s$, inside which the relevant solutions of the differential equation lie.

At $\xi=1$ the slopes $m_1\, m_2$ have opposite signs; we are concerned only with the positive value, and the above examination shows that the corresponding branch of the inflexion-locus lies below the tangent for $s<s_1$ and above for $s>s_1$.

Near the other terminal point, $\xi=s$, the critical cases are given by $s=c$ and $m=-\mathrm{A}(2s-1)/\mathrm{B}$.

It is found that the former condition leads to a value of s which is the reciprocal of that found above for $c=1$ and which therefore is less than unity and irrelevant. On the other hand, the quadratic for s got by using the second condition has one root lying in the range of the problem. Its expression in terms of γ and h is lengthy and need not be written out here. We shall call it s_2. The value for $\gamma=1{\cdot}41$ and $h={\cdot}4$ is $2{\cdot}24$. At this point both the tangents have negative slopes, so that both branches of the inflexion-locus lie in the region $1<\xi<s$, $\eta>0$, with which we are concerned. For $s<s_2$ both branches are below the tangents, for $s>s_2$ the curve lies above the tangent of smaller slope and below that of greater slope. Examples of these different configurations will be seen in the diagrams which follow.

Another point of some importance is the relation to the special directions of the isocline of zero slope, where it passes through the singular points. Its equation is

$$\eta = \mathrm{A}\xi(\xi-1)(s-\xi)/\mathrm{B}(\xi-c),$$

so $$d\eta/d\xi = \mathrm{A}(s-1)/\mathrm{B}(1-c) \quad \text{at } \xi=1,$$

and $$= -\mathrm{A}s(s-1)/\mathrm{B}(s-c) \text{ at } \xi=s.$$

When these values are inserted in the quadratics for m they make the left-hand side reduce to m^2. It follows that the zero isocline lies outside the angle formed by the lines $y=m_1x$, $y=m_2x$ drawn in the direction of positive x.

Discussion of particular cases.

Lord Rayleigh evaluated the coefficients of his equation, putting $\gamma=1{\cdot}41$, $h={\cdot}4$. This value of γ leads to $5{\cdot}88$ as the maximum s. By what appears to be an oversight

Lord Rayleigh replaces this by 6, which corresponds to $\lambda = 1{\cdot}40$, but the effect of this difference on the numerical values of the coefficients is negligible. It should be noted that there is nothing in the purely mathematical aspect of the question to indicate the existence of this upper limit to s. It arises physically, from the consideration of the pressure. The formal solution of the differential equation with $\gamma = 1{\cdot}41$ and $s = 6$ would lead to infinite and negative pressures in the wave.

Fig. 1.

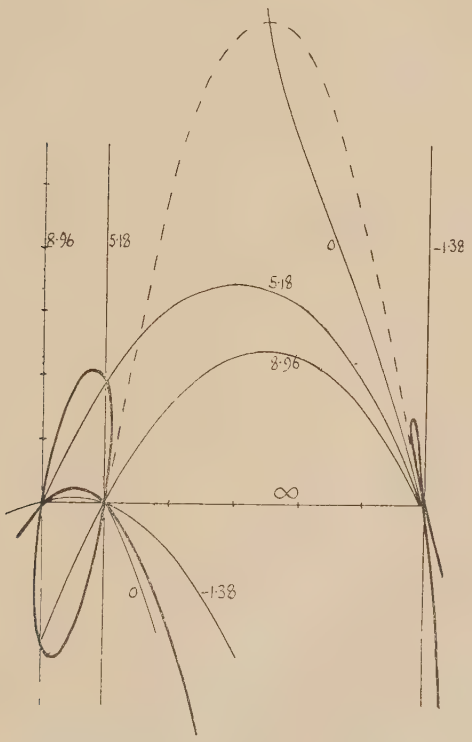

$S = 6$

Lord Rayleigh worked his way from point to point by Runge's method, beginning at the col $\xi = 1$ and starting off along the special direction of positive slope. He found that the path led to the node at $\xi = 6$. Evidently this process could not have been applied in the reverse direction.

It is convenient to begin with the extreme case $s = 6$. The distribution of the loci is shown on fig. 1, which is extended to the origin in order to complete the run of the

curves. The isocline for $p=0$ is drawn, having its asymptote along $\xi=c=2{\cdot}36$, and also the special isoclines which break up into a straight line and parabola. The inflexion-locus is drawn with a heavier line. It will be noticed that it passes through the intersections of line and parabola on the special isoclines. As already mentioned, the axis is the isocline $p=\infty$. The broken curve is the solution of the equation plotted from Lord Rayleigh's numbers. The special directions are the tangents to the inflexion-locus at the singular points.

Fig. 2.

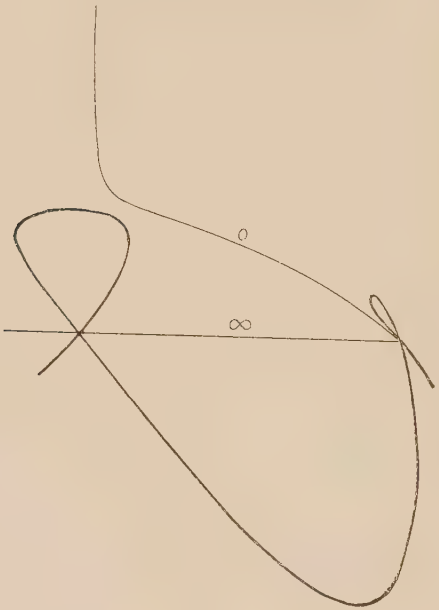

S = 2

A study of these curves will make evident the existence of the required solution-curve. A family of curves leaves the singular point (6, 0) all touching the special direction of smaller inclination to the axis and running in a region where $d^2\eta/d\xi^2$ is negative, *i. e.* the concavity is downwards. Since the locus $p=0$ makes a still smaller angle with the axis, the curves, in the domain of positive η, encounter the locus and turn downwards before they meet the inflexion-locus, so

one curve of the family passes downward through each point of the axis between (1, 0) and (6, 0), and we reach the required solution-curve as a limit. There is, of course, the same sort of ultimate discontinuity as is found in bringing hyperbolas up to the asymptotes.

From a physical point of view one would expect that any doubt as to the existence of a solution would attach to the larger values of s; this is the opinion expressed by Lord Rayleigh. It is therefore somewhat surprising to find that when the diagram is modified in the way of diminishing s, the matter becomes not more, but less obvious. Progressive changes in the configuration of the field take place in the manner described below, and may

Fig. 3.

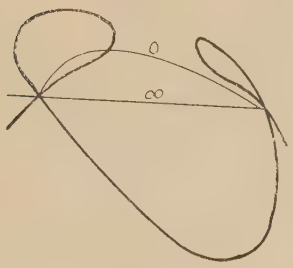

$S = 1{\cdot}7$

Fig. 4.

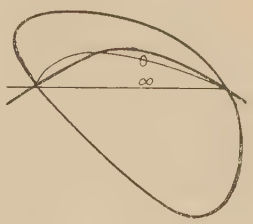

$S = 1{\cdot}6$

be followed in figs. 1–4, which have been drawn for $s = 6, 2, 1{\cdot}7, 1{\cdot}6$.

It will be enough to consider the zero isocline and the inflexion-locus. When s becomes less than 1·96 there is no asymptote to $p = 0$ between the terminal points, the curve then runs in an arc from one point to the other.

At $s = 2{\cdot}24$ and $s = 1{\cdot}96$ respectively, the inner sides of the loops on the inflexion-locus pass across the tangents, but notwithstanding this, the loops at first persist, the branch of the curve crossing back over the tangent. (See fig. 3 for $s = 1{\cdot}7$.) With continued decrease of s the two loops approach each other, as if by a mutual attraction. For some value between 1·7 and 1·6 they meet, and this is followed by a complete change in the configuration, as shown on fig. 4. In this tangled arrangement of the two loci it is not so easy to follow the course of the solution-curves. We shall use

fig. 5 for $s=1{\cdot}5$, on which the air-wave solution, calculated by Runge's method, has been inserted as a broken line.

Consider the curves which cross $p=0$ between the singular point A and the highest point B, where it intersects the inflexion-locus. These at first turn upwards until they meet the inflexion-locus where the curvature is reversed, the slope then decreases and becomes zero again at some point on BC,

Fig. 5.

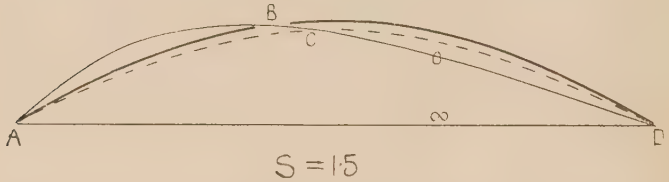

and thence the curves, remaining concave downwards, run into the node D, between the broken line and the inflexion-locus. On the other hand, the curves which rise perpendicularly from the axis bend over to meet the zero isocline at points between CD and reach the node without encountering the inflexion-locus, filling up the region between the broken line and the zero isocline. The curve required for the wave-solution is the limiting one which separates these two sets.

II. Properties of the Wave.

Summary of the Physical Theory.

In the following outline of the argument by which the differential equation is reached the equations are numbered as in Lord Rayleigh's paper. The motion is supposed to be stationary. The velocity of the air is abruptly decreased from the constant value u_1 to the constant u_2 in passing the wave. Conservation of mass gives $u_1/v_1=u_2/v_2=m$ (the "mass-velocity"). By means of this the specific volume v may be substituted for the velocity u in the equation of motion. When this is done the integral found is

$$p+m^2v-\tfrac{4}{3}m\mu\frac{dv}{dx}=\text{constant}$$

$$=p_1+m^2v_1=p_2+m^2v_2, \quad . \quad (87)$$

which enables p, and also θ the absolute temperature, at any point, to be expressed in terms of v.

If the air in travelling a distance dx undergoes a small

change of condition specified by dp, dv, it must have received heat of amount given (in mechanical units) by

$$(\gamma-1)dQ = \gamma p\,dv + v\,dp.$$

By use of (87) this can be expressed in terms of v only. Now dQ is made up of dQ_1, heat passing into the unit mass by conduction, and dQ_2, heat generated by viscosity. The latter part is equal to

$$\tfrac{4}{3}m\mu\left(\frac{dv}{dx}\right)^2 dx. \quad . \quad . \quad . \quad . \quad . \quad . \quad (92)$$

Subtracting this from the expression for dQ the remainder is found to be a complete differential and its integration gives for the total heat received by conduction between the initial state v_1 and the value v

$$(\gamma-1)Q_1 = \gamma(p_1+m^2v_1)v - (\gamma+1)\tfrac{1}{2}m^2v^2 + \tfrac{4}{3}m\mu v\frac{dv}{dx} + \text{const.}$$

But the total heat conducted into the gas in passage from the one uniform condition to the other is nil. Expressing this fact we get the important relation

$$(p_1+m^2v_1) = (p_2+m^2v_2) = (\gamma+1)m^2(v_1+v_2)/2\gamma. \quad (86)$$

By means of it the expression for the conducted heat can be put into the form

$$(\gamma-1)Q_1 = \tfrac{1}{2}(\gamma+1)m^2(v_1-v)(v-v_2) + \tfrac{4}{3}m\mu v\frac{dv}{dx}. \quad (96)$$

The last step is to connect Q_1 with the temperature $\theta = pv/R$ as given by (87) through the equation of conduction in the form

$$mQ_1 = k\,d\theta/dx. \quad . \quad . \quad . \quad . \quad . \quad (74)$$

This gives the differential equation required.

Relation between terminal states.

From eqn. (86), putting s, as before, for $v_1/v_2 = \rho_2/\rho_1$,

$$p_2/p_1 = \{(\gamma+1)s-(\gamma-1)\}/\{(\gamma+1)-(\gamma-1)s\},$$

$$\theta_2/\theta_1 = \{(\gamma+1)s-(\gamma-1)\}/s\{(\gamma+1)-(\gamma-1)s\}.$$

The pressure and temperature ratios are infinite for $s=(\gamma+1)/(\gamma-1)$. On account of the limited range of s it is convenient to take it, rather than the pressure-ratio, as the variable defining the amplitude of the wave.

Rate of propagation.

The plan of making the wave stationary, although it is adapted to the mathematical investigation of the motion, does not lend itself to a clear physical conception. For this it is better to consider one of the two regions of air as being at rest. There is then a choice between two alternatives. We may think of a wind of high-pressure air moving with velocity (u_1-u_2) into a region of low-pressure quiescent air, its front advancing through the latter at rate u_1. Or we may imagine a moving mass of low-pressure air with velocity (u_1-u_2) piling itself up against a block of high-pressure air as it comes to rest, the thickness added per second being u_2. In either case the process will continue indefinitely only when there is the special adjustment of pressure-ratio to density-ratio given above. We shall adopt the former conception as more like what happens in an explosion-wave, and we shall find the velocity of propagation u_1 in terms of the ordinary velocity of sound in the quiescent low-pressure gas, which will be denoted by $u_1'=(\gamma p_1 v_1)^{1/2}$.

Equation (86) gives

$$m^2 = 2\gamma s p_1/v_1\{(\gamma+1)-(\gamma-1)s\},$$

$$\therefore \quad u_1/u_1' = m_1 v_1/(\gamma p_1 v_1)^{1/2} = [2s/\{(\gamma+1)-(\gamma-1)s\}]^{1/2}$$

and $$u_2/u_1' = [2/s\{(\gamma+1)-(\gamma-1)s\}]^{1/2}.$$

It will be seen that u_2 has a minimum value for

$$s = (\gamma+1)/2(\gamma-1)$$

and that both velocities become u_1' for $s=1$.

On fig. 6 the velocities, the pressure-ratio, and the temperature-ratio are plotted against s, for $\gamma=1{\cdot}40$. For convenience the ratios p_1/p_2, θ_1/θ_2 less than unity, are taken instead of their reciprocals. The vertical distance between the two velocity-curves gives the wind-velocity in the high-pressure region.

Variation of $pv\theta$ within the wave.

Once η has been determined as a function of ξ from the differential equation, by an arithmetical or geometrical method, it becomes possible to examine the state of affairs inside the narrow layer of transition which constitutes the wave.

In the first place (p, θ) are immediately connected with v.

For from equations (86) (87) we obtain

$$p/p_1 = \{(\gamma+1)(s+1)\xi - 2\gamma\xi^2 - \tfrac{4}{3}\gamma\eta\}/\xi\{(\gamma+1)s-(\gamma-1)\},$$

and θ/θ_1 is the same expression multiplied by r/v_1 or ξ/s. It remains to connect v or ξ with distance measured along the direction of propagation. This can be done by mechanical or arithmetical quadrature. By definition

$$dx/d\xi = -2\mu'\xi/\eta.$$

Fig. 6.

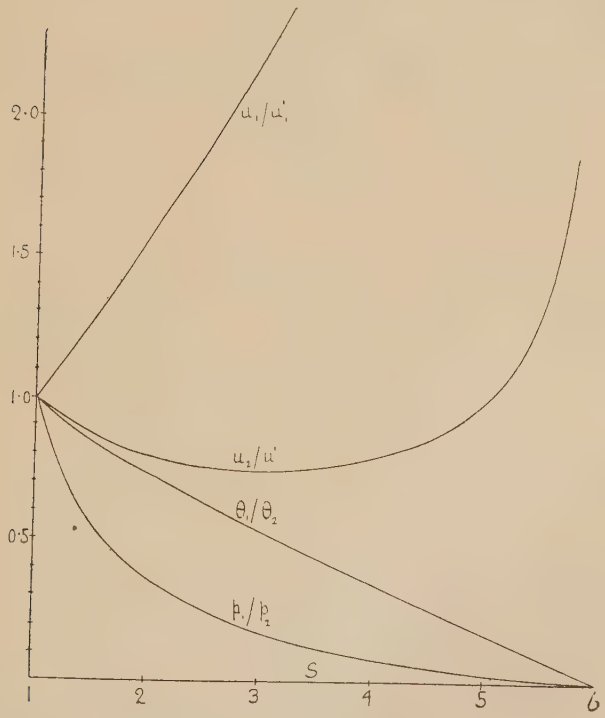

The length $\mu' = \mu/m$ will depend on the temperature at the point and on s. To get a definite unit, μ' must be expressed in terms of μ_1 the viscosity at temperature θ_1 and the limiting value of mass-velocity, m_1, applicable to sound-waves in the initial condition of the gas. The length

$$\mu_1/m_1 = \text{viscosity / sound-velocity} \times \text{density}$$

has been shown by Lord Rayleigh to be of very small size, of the order $\frac{1}{3} \times 10^{-5}$ cm. for air under ordinary conditions.

If we write $\mu/\mu_1 = f'(\theta/\theta_1)$ and use the expression already found for m as a function of s which gives

$$m/m_1 = [2s/\{(\gamma+1)-(\gamma-1)s\}]^{1/2},$$

we have

$$dx/d\xi = -2f(\theta/\theta_1) \cdot [\{(\gamma+1)-(\gamma-1)s\}/2s]^{1/2} \cdot (\xi/\eta) \cdot (\mu_1/m_1).$$

The expression on the right can be plotted against ξ, and the integral curve then gives us the power to associate each value of ξ with a value of x, in terms of the length-unit μ_1/m_1. The origin of x is of course arbitrary.

This work has been carried out for the two cases $s=1{\cdot}5$ and $s=5$, $\gamma=1{\cdot}41$. Runge's process was used to find η for values of ξ at intervals of ·02 and ·2 respectively. The

Fig. 7.

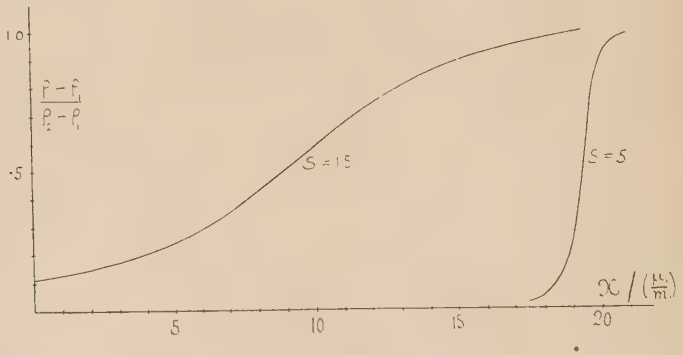

theoretical law for variation of viscosity was taken, by which $f'(\theta/\theta_1) = (\theta/\theta_1)^{1/2}$. A Coradi Integraph was used. The results are shown on fig. 7. In order to compare the two cases the quantity plotted is the fractional rise in density $(\rho-\rho_1)/(\rho_2-\rho_1)$. It will be seen that the larger increase of density takes place in a much shorter distance. The difference is still more marked when one considers the time rather than the distance, because the five-fold condensation-wave travels at about four times the speed of the other.

It is interesting to notice that the difference between the two graphs is purely one of horizontal scale. By multiplying the abscissæ of the curve for $s=5$ by 11 it can be brought into coincidence with the other. This is shown on fig. 8, where the calculated points for $s=5$ and $s=1{\cdot}5$ are marked with a circle and cross respectively.

It does not seem worth while to reproduce the curves for the pressure, which are of the same general character as these. In connexion with the temperature, however, a point of some physical interest arises.

Fig. 8.

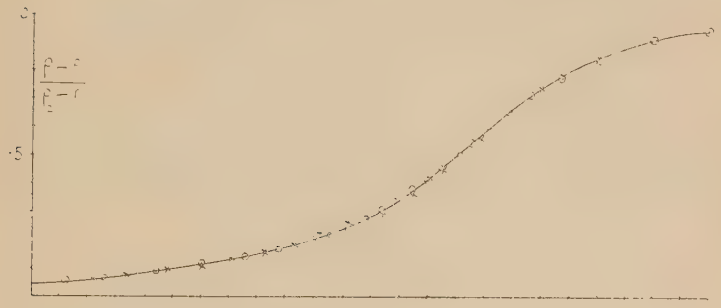

Analysis of the temperature-rise.

There are three different causes which bring about the heating of the gas:—

(1) The adiabatic compression, which alone is operative on the ordinary theory of sound.
(2) Conduction: the gas at first gains heat from warmer parts and then loses an equal amount to colder parts.
(3) Viscosity.

The question of the relative importance of these three factors naturally suggests itself. It can be answered by carrying the analysis of Lord Rayleigh a little farther, if we assume the specific heat c to be independent of the temperature. Denote by θ_a, θ_c, θ_v the temperatures which would be produced by the action of the three causes separately so that the actual rise $(\theta-\theta_1)$ at a point is the sum of $(\theta_a-\theta_1)$ $(\theta_c-\theta_1)$ $(\theta_v-\theta_1)$.

The formulæ already given furnish $(\theta-\theta_1)$ and $(\theta_c-\theta_1)$. The adiabatic heating is known, and so all three contributions can be separated.

We have

$$\theta_c-\theta_1=Q_1/c=(\gamma-1)Q_1/R=(\gamma-1)Q_1\theta_1/p_1v_1,$$

which gives, by use of (96) and the expression for m^2,

$$(\theta_c-\theta_1)/\theta_1 = \gamma\{(\gamma+1)(s-\xi)(\xi-1)-\tfrac{4}{3}\eta\}/s\{(\gamma+1)-(\gamma-1)s\},$$

while

$$\theta/\theta_1=\{(\gamma+1)(s+1)\xi-2\gamma\xi^2-\tfrac{4}{3}\gamma\eta\}/s\{(\gamma+1)-(\gamma-1)s\}:$$

on subtraction the term in η disappears, and we obtain

$$(\theta-\theta_c)/\theta_1=$$

$$(\gamma-1)\{\gamma\xi^2-(\gamma+1)(s+1)\xi+(\gamma+1)s+s^2\}/s\{(\gamma+1)-(\gamma-1)s\}$$

This expression combines the temperature-increases due to compression and viscosity. The former of these is given by

$$\theta_a/\theta_1=(v_1/v)^{\gamma-1}=(s/\xi)^{\gamma-1}.$$

Fig. 9.

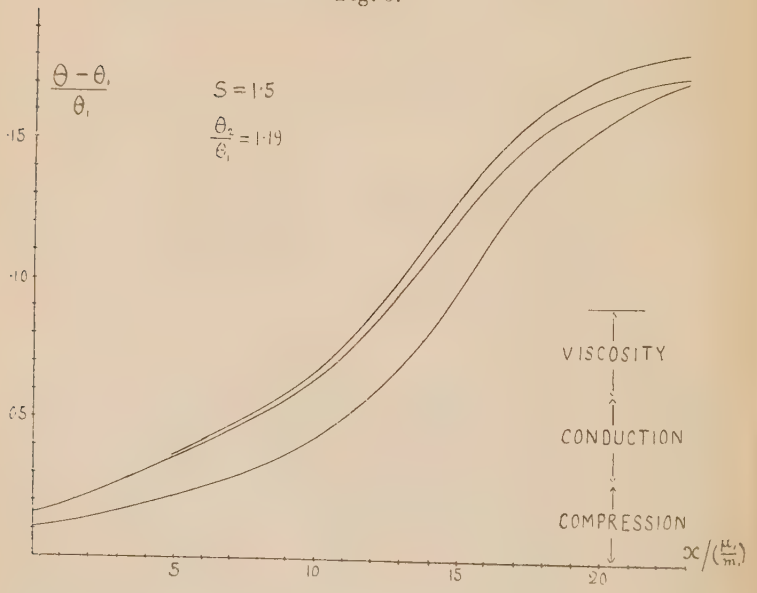

Thus the adiabatic and the viscosity effects separately are found to be functions purely of the density at the point.

The calculations have been carried out for the two cases $s=1{\cdot}5$ and $s=5$, and the results are displayed on figs. 9 and 10. The horizontal scale of distance is opened up tenfold in the latter diagram.

The ordinate of the highest curve gives the actual temperature and the three segments into which it is divided by the other curves show how the total rise of temperature is made up, the order upwards being the adiabatic, conductivity, and

Fig. 10.

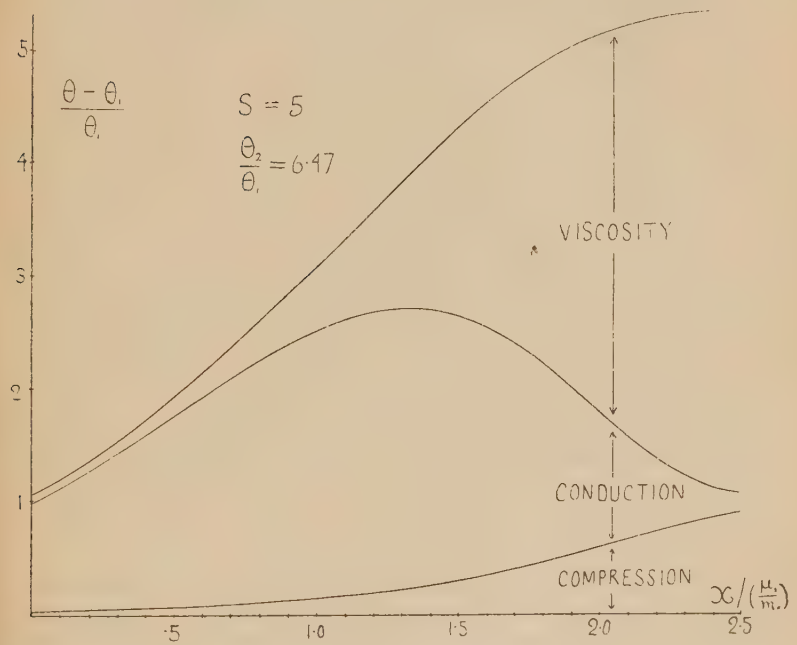

viscosity parts. The central segment disappears at the limits of the wave. The diagrams present a striking contrast. For the wave of small amplitude the greater part of the heating is due to the adiabatic compression. This was to be expected: but it is rather remarkable how with a high degree of compression the relation is reversed. The greater part of the permanent heating is then due to the action of viscosity.

LXXXV. *Stability of the Atom.* *By* Prof. D. N. Mallik, *B.A., Sc.D., F.R.S.E., Muslim University, Aligarh, India* *.

Summary.

Larmor has shown that in a permanently stable system of "electrons" (*e. g.* a system of electrons and a nucleus forming an atom) the vector sum $|e\dot{v}|$ is constantly zero, the radiation of energy per unit time being $\frac{2}{3}\frac{e^2\dot{v}^2}{c}$, where $\dot{v}$ is the acceleration of an electron and c the velocity of light. These expressions are shown to be also deducible by direct integration of the field equation of the electron theory and to be alone consistent with the electron theory of dispersion. The principle of [permanent] stability thus established is proved then (on certain assumptions) to be the necessary consequence of the quantum conditions postulated by Sommerfeld in the case of a [Bohr] atom of Hydrogen.

It is thus shown that the non-emission of radiation by a Bohr atom of Hydrogen and the usual quantum conditions as well as the proper choice of coordinates are all consistent with the classical theory interpreted in terms of quantum ideas. A tentative attempt is then made to extend the theory to more complex atoms.

Stability of the Atom.

1. In the usual presentation of Bohr's theory of spectral series it is stated that in the stationary states no radiation is assumed to take place from the atoms themselves in contradistinction to the classical electromagnetic theory or ordinary electrodynamics.

It should be observed, however, that in all cases of dynamical stability of a permanent type, there should not be any such radiation, and accordingly any theory that is to be consistent with the principle of conservation of energy must proceed on postulates suitable for the purpose. The principle that in a permanent dynamical system there should not be any radiation of energy was, in fact, clearly stated by Larmor, who was probably the first to investigate the mechanism of molecular radiation. For he says ('Æther and Matter, p. 225):—

"It thus appears that when the orbital motions in a molecule are so constituted that the vector sum $|e\dot{v}|$ of the

* Communicated by the Author.

accelerations of all the electrons (*i. e.* positive and negative charges) with due regard to their signs is constantly null, there will be no radiation or very little abstracted from it, and therefore this steady motion will be permanent. The condition that is thus necessary for absence of dissipation by radiation limits the number of types of motions otherwise steady in the molecules that can be permanent."

3. In order to analyse this statement further we may seek, in the first place, to derive the conditions specified above on the general electron theory and then see if this can be made to fit in with Bohr's theory.

4. We have, if (α, β, γ) be the magnetic force,

$$\dot{\alpha} = -4\pi c^2\left(\frac{\partial h}{\partial y} - \frac{\partial g}{\partial z}\right),$$

where $$4\pi(\dot{f}+\dot{\mathrm{A}}) = \left(\frac{\partial \gamma}{\partial y} - \frac{\partial \beta}{\partial z}\right),$$

A, B, C being the electric moment of electric charges due to a distribution of electrons of volume density ρ

$$= -\rho\{(x-x_0), (y-y_0), (z-z_0)\} \quad \text{per unit volume,}$$

and $$\frac{\partial \mathrm{A}}{\partial x} + \frac{\partial \mathrm{B}}{\partial y} + \frac{\partial \mathrm{C}}{\partial z} = -\rho = -\left(\frac{\partial f}{\partial x} + \frac{\partial g}{\partial y} + \frac{\partial h}{\partial z}\right).$$

Hence we have

$$\ddot{\alpha} = c^2\left[\nabla^2\alpha - \frac{\partial}{\partial \alpha}\left(\frac{\partial \alpha}{\partial x} + \frac{\partial \beta}{\partial y} + \frac{\partial \gamma}{\partial z}\right)\right) + 4\pi\left(\frac{\partial \rho \dot{z}}{\partial y} - \frac{\partial \rho \dot{y}}{\partial x}\right)\Big].$$

If $$\frac{\partial \alpha}{\partial x} + \frac{\partial \beta}{\partial y} + \frac{\partial \gamma}{\partial z} = 0$$

(magnetic permeability = 1),

we have

$$\ddot{\alpha} = c^2\left(\nabla^2\alpha + 4\pi\left(\frac{\partial \dot{\mathrm{C}}}{\partial y} - \frac{\partial \dot{\mathrm{B}}}{\partial z}\right)\right).$$

This gives

$$\alpha = \frac{4\pi c^2}{\mathrm{D}^2 - c^2\nabla^2}\left(\frac{\partial \dot{\mathrm{C}}}{\partial y} - \frac{\partial \dot{\mathrm{B}}}{\partial z}\right), \quad \text{where } \mathrm{D} \equiv \frac{d}{dt},$$

$$= \frac{4\pi c^2}{2\mathrm{D}}\left[\frac{1}{\mathrm{D} + c\nabla} + \frac{1}{\mathrm{D} - c\nabla}\right]\left(\frac{\partial \dot{\mathrm{C}}}{\partial y} - \frac{\partial \dot{\mathrm{B}}}{\partial z}\right),$$

$$= \left(n\frac{\partial}{\partial y} - m\frac{\partial}{\partial z}\right)\frac{4\pi c^2}{2\mathrm{D}}\left[\frac{1}{\mathrm{D} + c\nabla} + \frac{1}{\mathrm{D} - c\nabla}\right]\mathrm{F}(t),$$

where $\dot{\mathrm{A}}, \dot{\mathrm{B}}, \dot{\mathrm{C}} = (l, m, n)\,\mathrm{F}(t)$.

But

$$\frac{1}{2\mathrm{D}}\left\{\frac{1}{\mathrm{D}+c\nabla}+\frac{1}{\mathrm{D}-c\nabla}\right\}\mathrm{F}(t)$$

$$=\frac{1}{2\mathrm{D}}\left[e^{-ct\nabla}\int^{t}e^{ct'\nabla}\,\mathrm{F}(t')\,dt'+e^{ct\nabla}\int e^{-ct'\nabla}\,\mathrm{F}(t')dt'\right]$$

$$=\frac{1}{\mathrm{D}}\int[\cosh c(t-t')\nabla]\,\mathrm{F}(t)\,dt$$

$$=\frac{1}{4\pi}\frac{1}{c^2}\int\frac{\mathrm{F}\left(t-\frac{r}{c}\right)}{r}\,d\tau,$$

since $c(t-t')=r$, if $d\tau=$element of volume.

[Rayleigh's 'Sound,' vol. ii. ch. xiv.]

$$\therefore\quad \alpha=\left(n\frac{\partial}{\partial y}-m\frac{\partial}{\partial z}\right)\int\frac{\mathrm{F}\left(t-\frac{r}{c}\right)}{r}\,d\tau$$

$$=\left(n\frac{\partial}{\partial y}-m\frac{\partial}{\partial z}\right)\frac{\phi\left(t-\frac{r}{c}\right)}{r},$$

where $ev=\phi(t)$.

$=e(\dot{x},\,\dot{y},\,\dot{z})$.

Therefore, if $\mathrm{H}=(\alpha,\beta,\gamma)$ and θ the inclination of r to the direction of electronic motion,

$$\mathrm{H}=\sin\theta\frac{\partial}{\partial r}\left(\frac{\overline{ev}}{r}\right),$$

where $\overline{ev}$ is the value of ev at $t-\frac{r}{c}$,

$$=-\sin\theta\left(\frac{ev}{r^2}+\frac{e\dot{v}}{cr}\right)_{t-\frac{r}{c}}.$$

5. Again, if the electric force is

$$(\mathrm{X},\,\mathrm{Y},\,\mathrm{Z})=4\pi c^2(f,\,g,\,h),$$

where

$$\ddot{f}+\frac{d}{dt}(\rho\dot{x})=\mathrm{V}^2\nabla^2(f+\mathrm{A})$$

$$=c^2\nabla^2 f$$

(V = velocity in any medium),

we have

$$\ddot{\mathrm{X}}=c^2\nabla^2\mathrm{X}-4\pi c^2\frac{d}{dt}(\rho\dot{x});$$

whence

$$X = \frac{1}{2D}\left[\frac{1}{D-c\nabla} + \frac{1}{D+c\nabla}\right]\left\{-4\pi c^2 \frac{d}{dt}(\rho\dot{x})\right\},$$

i. e.

$$X, Y, Z = -(l, m, n)\left(\frac{e\dot{v}}{r}\right)_{t-\frac{r}{c}}$$

[writing $l \,.\, F(t) = \dfrac{d}{dt}(\rho\dot{x})$ and proceeding as in (4)].

6. Hence, for an isolated electron, the radiation of energy, in accordance with Poynting's theorem,

$$= \frac{1}{4\pi}\int \frac{e^2\dot{v}^2}{r^2 c}\sin^2\theta\, dS \quad \text{over an infinite sphere}$$

$$= \frac{2}{3}\cdot\frac{e^2\dot{v}^2}{c}.$$

Now the quantum condition for radiation of frequency ν is

$$W - W' = \nu h,$$

where W is the total energy,

which in this case becomes (in accordance with quantum ideas)

$$\frac{2}{3}\cdot\frac{e^2\dot{v}^2}{c}\Delta t = \frac{1}{3}\frac{e^2}{c}\dot{v}\Delta v.$$

If the change in the potential energy of the electron is ΔV,

$$W - W' = \frac{1}{2}\Delta m v^2 + \Delta V$$

$$= \frac{1}{3}\frac{e^2}{c}\dot{v}\Delta v = \nu h.$$

7. These conditions can evidently be satisfied on a suitable postulate as to the operation of the *field*, although for such an [isolated] electron, the equation

$$\tfrac{1}{2}\Delta m v^2 = \nu h,$$

cannot be satisfied as has been pointed out by Jeans [Eighth Guthrie Lecture], so that if this were the only allowable equation, we should have to admit that an isolated electron cannot emit or absorb radiation.

8. Now the electromagnetic energy expresses the energy residing in the field, so that the fact that the total energy is made up of the energy of electronic system (including the case of an isolated electron) and the field is also clearly

brought out by the equation of art. 6. For the latter is included in V.

9. On this postulate by the application of Lagrange's theorem I have, in a recent paper *, obtained the equations of an electronic system which are sufficient to explain dispersion and aberration. They also lead to the expression for Lorentz transformations.

10. In the case of a system of electrons forming a permanently stable configuration we must have, in accordance with the above, the vector sum $|e\dot{v}| = 0$. This must then refer to the stationary states of Bohr's atom.

Now this condition is the same as

$$\frac{\int \ddot{\mathrm{A}}\, d\tau}{\int d\tau} = 0, \quad i.\,e. \text{ the mean value of } \ddot{\mathrm{A}} = 0,$$

but since it can be shown that the A's satisfy (for radiation) equations of the form

$$\ddot{\mathrm{A}} + p_0 \mathrm{A} = a_0 f,$$

neglecting terms depending on the induced magnetic field,

$$\text{and} \qquad \ddot{f} + \ddot{\mathrm{A}} = \mathrm{V}^2 \nabla^2 (f + \mathrm{A}),$$

where the quantities have their mean values over a specified region, (say) the volume of an atom, we easily find that no radiation will result if $(\ddot{\mathrm{A}}, \ddot{\mathrm{B}}, \ddot{\mathrm{C}}) = 0$.

11. We notice, incidentally, that this gives

$$\nabla^2 (f_0 g_0 h_0) = 0, \quad \text{where } f_0 = (f + \mathrm{A}), \text{ etc.},$$

which correlates to the usual equations of equilibrium of an elastic solid, viz.,

$$\nabla^2 (\omega_x, \omega_y, \omega_z) = 0,$$

so that

$$(f_0, g_0, h_0) \propto (\omega_x, \omega_y, \omega_z),$$

where $\omega_x, \omega_y, \omega_z$ may be defined as rotational strains of the medium or field, as in Maccullagh-Larmor theory of the æther or the steady rotation of a corpuscle about the nucleus or about the common centre of gravity of the nucleus and the corpuscles of the Bohr-Rutherford atom in a permanently stable configuration.

12. In order to examine whether this condition for a permanently stable configuration is implied in the Bohr-Sommerfeld theory, it would be useful to recall that this

* "Electron Theory of Aberration and Lorentz Transformations," Phil. Mag. Sept. 1924.

theory postulates, if account is taken of the motion of the nucleus, the two quantum conditions

$$\int_0^{2\pi}\left(mr^2\dot{\phi}\,d\phi+\mathrm{M}\mathrm{R}^2\dot{\phi}\,d\phi\right)=nh \quad . \quad . \quad . \quad (1)$$

and

$$\int\left(m\dot{r}\,dr+\mathrm{M}\dot{\mathrm{R}}\,d\mathrm{R}\right)_{\phi=0}^{\phi=2\pi}=n'h, \quad . \quad . \quad . \quad . \quad (2)$$

where m = mass of the electron,
M = mass of the nucleus,
r = distance of an electron from the common C.G.
R = distance of the nucleus from the same point,
ϕ = vectorial angle.

From (1) and (2), we have

$$(n+n')h=\int(mr^2+\mathrm{M}\mathrm{R}^2)\phi\,d\phi+\int(m\dot{r}\,dr+\mathrm{M}\mathrm{R}\,d\mathrm{R})$$
$$=\int(m\dot{x}\,dx+\mathrm{M}\dot{\mathrm{X}}\,d\mathrm{X})+\int(m\dot{y}\,dy+\mathrm{M}\dot{\mathrm{Y}}\,d\mathrm{Y})$$

in cartesians.

Now writing

$$\frac{r}{\frac{1}{m}}=\frac{\mathrm{R}}{\frac{1}{\mathrm{M}}}=\frac{\rho}{\frac{1}{m}+\frac{1}{\mathrm{M}}}\equiv\frac{\rho}{\frac{1}{\mu}},$$

we have

$$\int(mr^2+\mathrm{M}\mathrm{R}^2)\dot{\phi}\,d\phi=\int\mu\rho^2\dot{\phi}\,d\phi=2\pi p$$

if $\mu\rho^2\dot{\phi}=p=$ const. (for a central orbit); . . . (3)

similarly,

$$\int(m\dot{r}\,dr+\mathrm{M}\dot{\mathrm{R}}\,d\mathrm{R})=\int\mu\dot{\rho}\,d\rho,$$

the equation of the relative orbit being

$$\frac{l_0}{\rho}=1+\epsilon\cos\phi,$$

where ϵ is the eccentricity of the orbit, and l_0 the semi-latus rectum. We have, accordingly,

$$(n+n')h=2\pi p+\epsilon^2 p\int_0^{2\pi}\frac{\sin^2\phi}{(1+e\cos\phi)^2}d\phi$$
$$=\frac{2\pi p}{\sqrt{1-\epsilon^2}}. \quad . \quad . \quad . \quad . \quad . \quad . \quad . \quad . \quad . \quad (4)$$

Hence we conclude that quantum conditions are necessarily satisfied for all central [relative] orbits.

Moreover,

$$\frac{2\pi p'}{\sqrt{1-\epsilon^2}} = \int (m\dot{x}\,dx + \mathrm{M}\dot{\mathrm{X}}\,d\mathrm{X}) + \int (m\dot{y}\,dy + \mathrm{M}\dot{\mathrm{Y}}\,d\mathrm{Y})$$
$$= m\int (\dot{x}+\dot{\mathrm{X}})\,dx + m\int (\dot{y}+\dot{\mathrm{Y}})\,dy,$$

if $mx = \mathrm{MX}$, etc.

Differentiating this expression with regard to time, on the supposition that the orbit remains unchanged, we have, since

$$\frac{\mathrm{D}}{\mathrm{D}t}\int (\xi\,dx+\eta\,dy+\zeta\,dz)$$
$$= \int \left(\frac{\mathrm{D}\xi}{\mathrm{D}t}\,dx + \frac{\mathrm{D}\eta}{\mathrm{D}t}\,dy + \frac{\mathrm{D}\zeta}{\mathrm{D}t}\,dz\right) + \int (\xi\,d\xi+\eta\,d\eta+\zeta\,d\zeta)$$
$$= \int \left(\frac{\mathrm{D}\xi}{\mathrm{D}t}\,dx + \frac{\mathrm{D}\eta}{\mathrm{D}t}\,dy + \frac{\mathrm{D}\zeta}{\mathrm{D}t}\,dz\right) \text{ for a closed orbit,}$$

where

$$\frac{\mathrm{D}}{\mathrm{D}t} = \frac{\partial}{\partial t} + \xi\frac{\partial}{\partial x} + \eta\frac{\partial}{\partial y} + \zeta\frac{\partial}{\partial z}$$

and

$$\xi = \frac{\mathrm{D}}{\mathrm{D}t}(x+\mathrm{X}) \equiv (\dot{x}+\dot{\mathrm{X}})$$

(assuming * this operation permissible in this case),

$$0 = \int m(\ddot{x}+\ddot{\mathrm{X}})\,dx + \int m(\ddot{y}+\ddot{\mathrm{Y}})\,dy,$$

so that

$$\int m\left[(\ddot{x}+\ddot{\mathrm{X}})\frac{dx}{ds} + (\ddot{y}+\ddot{\mathrm{Y}})\frac{dy}{ds}\right] ds = 0,$$

$$m\int \left[(\ddot{x}+\ddot{\mathrm{X}})\frac{dx}{dn} + (\ddot{y}+\ddot{\mathrm{Y}})\frac{dy}{dn}\right] dn = 0$$

(ds, an element of arc, and dn, an element of normal).

Accordingly, since the coefficients of ds and dn must have the same sign throughout,

$$\dot{v}+\dot{\mathrm{V}} = 0,$$

where $\dot{v}$ and $\dot{\mathrm{V}}$ are the resultant accelerations of the electron and the nucleus respectively.

Thus, so long as we are confined to the Bohr orbit of the hydrogen atom, Larmor's condition $\lfloor e\dot{v} \rfloor = 0$ is satisfied.

13. Incidentally we observe that from (1), (2), and (4)

* This assumption is involved in Lorentz's theory, see art. 333, Poincaré's 'Electricité et Optique.'

we readily get the expression for the total energy (W) as required by theory.

For from the property of the elliptic orbit, we have

$$v^2 = \frac{\mathrm{E}e}{\mu}\left(\frac{2}{\rho} - \frac{1}{a}\right), \quad \ldots \ldots \quad (5)$$

where v is the velocity in the orbit, and a the semi-major axis ; also

$$\sqrt{\frac{\mathrm{E}e}{\mu}}\, l_0 = \frac{p}{\mu}, \text{ from (3)},$$

$$\text{or} \quad \frac{1}{a} = \frac{\mu \mathrm{E}e}{h^2} \cdot \frac{4\pi^2}{(n+n')^2}, \quad \ldots \ldots \quad (6)$$

which gives, remembering that

$$\mathrm{W} = \tfrac{1}{2}\mu v^2 - \frac{\mathrm{E}e}{\rho} = -\frac{\mathrm{E}e}{2a}, \text{ from (5)},$$

$$\mathrm{W} = \frac{-\mu(\mathrm{E}e)^2}{h^2} \frac{2\pi^2}{(n+n')^2}, \text{ from (6)},$$

where E is the charge of the nucleus.

14. The quantum conditions of art. 12 are postulates of Bohr's theory which thus seem to be capable of generalization, based on the present analysis.

For since in the case of the hydrogen atom we have $e[\ddot{v} + \ddot{\mathrm{V}}] = 0$, we have in *any closed orbit,*

$$\int (\ddot{x} + \ddot{\mathrm{X}})\, dx + \int (\ddot{y} + \ddot{\mathrm{Y}})\, dy = 0.$$

Integrating for an interval Δt in accordance with quantum ideas, we should have

$$\left[\int [(\dot{x} + \dot{\mathrm{X}})\, dx + (\dot{y} + \dot{\mathrm{Y}})\, dy]\right]_2^1 = (\mathrm{N}_1 - \mathrm{N}_2)h, \quad \text{say},$$

the integrations referring to two stationary orbits spanned in the interval Δt, *i. e.*

$$\left[\int m(\dot{x} + \dot{\mathrm{X}})\, dx + \int m(\dot{y} + \dot{\mathrm{Y}})\, dy\right] = \mathrm{N}_1 h,$$

for a particular stationary orbit (1);

$$\text{or} \quad \int (m\dot{x}\, dx + \mathrm{M}\dot{\mathrm{X}}\, d\dot{\mathrm{X}}) + \int (m\dot{y}\, dy + \mathrm{M}\dot{\mathrm{Y}}\, d\dot{\mathrm{X}}) = \mathrm{N}_1 h,$$

$$i.\,e. \quad \int (mr^2 + \mathrm{M}\mathrm{R}^2)\dot{\phi}\, d\phi + \int ((m\dot{r}\, dr + \mathrm{M}\dot{\mathrm{R}}\, d\mathrm{R}) = \mathrm{N}_1 h.$$

If the orbit is central the first is a *constant* $= 2\pi p$, say, which can be written $= nh$, in accordance with quantum ideas.

It follows accordingly (as in art. 12) that

$$\int (m\dot{r}\,dr + \mathrm{M}\dot{\mathrm{R}}\,d\mathrm{R})$$

is a *constant* and can be written on the same principle $=n'h$, so that $\mathrm{N}_1 = n + n'$.

15. One of Sommerfeld's reasons for taking r, ϕ as the variables is in one sense a purely analytical one: these coordinates allow the variables in the Hamilton-Jacobi differential equation of motion to be separated. He, however, also suggests a dynamical explanation, which may be generalized as follows:

The general quantum condition deduced from Larmor's condition being

$$\int (m\dot{x}\,dx + \mathrm{M}\dot{\mathrm{X}}\,d\mathrm{X}) + \int (m\dot{y}\,dy + \mathrm{M}\dot{\mathrm{Y}}\,d\mathrm{Y}) = \mathrm{N}h,$$

if we write $\mathrm{N} = n + n'$

and find two variables such that

$$\int \mathrm{F}(\phi)\,d\phi + \mathrm{F}(\psi)\,d\psi$$
$$= \int (m\dot{x}\,dx + \mathrm{M}\dot{\mathrm{X}}\,d\mathrm{X}) + \int m\dot{y}\,dy + \mathrm{M}\dot{\mathrm{Y}}\,d\mathrm{Y} = (n+n')h,$$

then, if on dynamical grounds we can prove that

$$\int \mathrm{F}(\phi)\,d\phi = \text{const.} = nh \text{ (say)},$$

it follows that

$$\int f(\psi)\,d\psi = n'h.$$

16. In three dimensions,

$$(x, y, z,\ \mathrm{X}, \mathrm{Y}, \mathrm{Z},\ r, \theta, \phi,\ \mathrm{R}, \theta, \phi)$$

for the hydrogen atom, we have

$$\int (m\dot{x}\,dx + \mathrm{M}\dot{\mathrm{X}}\,d\mathrm{X}) + \int (m\dot{y}\,dy + \mathrm{M}\dot{\mathrm{Y}}\,d\mathrm{Y}) + \int (m\dot{z}\,dz + \mathrm{M}\dot{\mathrm{Z}}\,d\mathrm{Z})$$
$$= \int m(\dot{x} + \dot{\mathrm{X}})\,dx + \int m(\dot{y} + \dot{\mathrm{Y}})\,dy + \int m(\dot{z} + \dot{\mathrm{Z}})\,dz$$
$$= \int (m\dot{r}\,dr + \mathrm{M}\dot{\mathrm{R}}\,d\mathrm{R}) + \int (mr^2 + \mathrm{M}\mathrm{R}^2)\dot{\theta}\,d\theta$$
$$+ \int (mr^2 + \mathrm{M}\mathrm{R}^2)\sin^2\theta\dot{\phi}\,d\phi$$
$$= \int \mu\dot{\rho}\,d\rho + \int \mu\rho^2\dot{\theta}\,d\theta + \int \mu\rho^2\sin^2\theta\dot{\phi}\,d\phi = \mathrm{N}h,$$

since $(\ddot{x} + \ddot{\mathrm{X}},\ \ddot{y} + \ddot{\mathrm{Y}},\ \ddot{z} + \ddot{\mathrm{Z}}) = 0$, for permanent stability. Again,

$$\mu\rho^2\dot{\theta} = p = \text{const.}$$

if the force is radial.

Let
$$\int \mu\rho^2 \dot{\theta}\, d\theta = n_1 h,$$
similarly
$$\mu\rho^2 \sin^2\theta\dot{\phi} = p' = \text{const.}$$
$$\therefore \quad \int \mu\rho^2 \sin^2\theta\dot{\phi}\, d\phi = n_2 h = 2\pi p'.$$
Accordingly (as in art. 12)
$$\int \mu\dot{\rho}\, d\rho = nh, \quad [\mathrm{N} = n + n_1 + n_2].$$
We have thus the *spatial* quantum conditions of Sommerfeld [p. 242, etc. 'Atomic Structure and Spectral Lines'].

These quantum conditions evidently impose a limitation on the inclination of the orbit of the electron to the invariable plane, conditioned by an external field which, however, must be such that the orbit is still practically central.

17. When we proceed to apply the theory to more complex atoms, we are confronted with serious difficulties arising from the fact that the nature of the configuration cannot be worked out in any of these cases on dynamical considerations.

We have, in fact, when there are N electrons and the nucleus,
$$\int (m \sum_{\mathrm{N}} \dot{r}_s\, dr_s + \mathrm{M}\dot{\mathrm{R}}\, d\mathrm{R}) + \int (m \sum_{\mathrm{N}} r_s^2 \dot{\phi}_s\, d\phi_s + \mathrm{MR}^2 \dot{\psi}\, d\psi)$$
$$= \int (m \sum_{\mathrm{N}} \dot{x}_s\, dx_s + \mathrm{M}\dot{\mathrm{X}}\, d\mathrm{X}) + \int (m \sum \dot{y}_s\, dy_s + \mathrm{M}\dot{\mathrm{Y}}\, d\mathrm{Y}),$$
where x_s, y_s, r_s, ϕ_s define the position of the sth electron, and X, Y, R, ψ that of the nucleus, according to the scheme
$$\Sigma mx = \mathrm{MX},$$
$$\Sigma my = \mathrm{MY}.$$
Now
$$\int [m \Sigma r_s^2 \dot{\phi}_s\, d\phi + \mathrm{MR}^2 \dot{\psi}\, d\psi] = \text{const.} = nh$$
in accordance with quantum ideas, if the orbits are central, so that
$$\int (m \Sigma \dot{r}_s\, dr_s + \mathrm{M}\dot{\mathrm{R}}\, d\mathrm{R}) + nh$$
$$= \int m \Sigma (\dot{x}_s + \dot{\mathrm{X}})\, dx_s + \int m \Sigma (\dot{y}_s + \dot{\mathrm{Y}})\, dy_s.$$

18. The conditions of permanent stability, however, are
$$\Sigma \ddot{x}_s + \ddot{\mathrm{X}} = 0, \qquad \Sigma \ddot{y}_s + \ddot{\mathrm{Y}} = 0.$$
for this gives vector sum
$$| \Sigma \overrightarrow{e\ddot{v}_s} + \mathrm{E}\ddot{\mathrm{V}} | = 0.$$

These conditions may be satisfied if we postulate

$$\int (m \Sigma \dot{r}_s \, dr_s + \mathrm{M}\dot{\mathrm{R}} \, d\mathrm{R}) = n'h \quad \text{(say)}$$

and $\qquad dx_1 = dx_2 = \ldots, \qquad dy_1 = dy_2 = \ldots$

as equations of constraints;

i. e. $\ddot{x}_s + \ddot{\mathrm{X}} = 0, \qquad \ddot{y}_s + \ddot{\mathrm{Y}} = 0$ (each term separately).

In this event, it is reasonable to suppose that the quantum condition will split up into

$$\int \left(m\dot{r}_s \, dr_s + \frac{\mathrm{M}}{\mathrm{N}} \dot{\mathrm{R}} \, d\dot{\mathrm{R}} \right) = n_s'h, \text{ etc.}$$

This, of course, will involve the supposition that there is no interaction between the electrons themselves and that each electron, together with the corresponding portion of the nucleus, behaves like a hydrogen atom. This is probably approximately true for the neutral helium atom.

19. Or, we may have the electrons arranged in groups; for each group we should have $dx_1 = \ldots = dx_s$, and a quantum condition of the type

$$\int \sum_p m\dot{r}_s \, dr_s + \frac{\mathrm{M}p}{\mathrm{N}} \dot{\mathrm{R}} \, d\mathrm{R} = n_p'h$$

(for a group of p electrons).

Separation of these groups according to the nature of the bonds between them and the nucleus as well as the magnitude of the interaction between the electrons will require further consideration.

20. For a number of electrons in three dimensions, we have (with obvious notation)

$$\begin{aligned} &\int (\Sigma m \dot{x}_r \, dx_r + \mathrm{M}\dot{\mathrm{X}} \, d\mathrm{X}) + \ldots\ldots + \ldots\ldots \\ &= \int \Sigma m (\dot{x}_r + \dot{\mathrm{X}}) \, dx_r + \ldots\ldots + \ldots\ldots \\ &= \int m \Sigma (\dot{r}_s \, dr_s + r_s^2 \dot{\phi}_s \, \delta\phi_s + r^2 \sin^2 \phi_s \dot{\psi}_s \, \delta\psi_s) \\ &\quad + \int \mathrm{M} (\dot{\mathrm{R}} \, d\mathrm{R} + \mathrm{R}^2 \, d\chi \cdot \dot{\chi} + \mathrm{R}^2 \sin^2 \chi \dot{\theta} \, d\theta). \end{aligned}$$

The condition for permanent stability will be satisfied if $(\ddot{x}_r + \ddot{\mathrm{X}}, \ \ddot{y}_r + \ddot{\mathrm{Y}}, \ \ddot{z}_r + \ddot{\mathrm{Z}}) = 0$, separately or in groups. Accordingly either of these expressions is constant $= \mathrm{N}h$, say, if the orbits are still central. But for a central orbit

$$\int (\Sigma m r_s^2 \dot{\phi}_s^2 \, \delta\phi_s + \mathrm{MR}^2 \dot{\chi} \, d\chi) = \text{const.} = n_1 h, \text{ say,}$$

and

$$2\pi\left[\Sigma m r_s^2 \sin^2\phi_s \dot{\psi}_s + \mathrm{M}\mathrm{R}^2 \sin^2\chi\dot{\theta}\right] = \text{const.} = n_2 h, \text{ say};$$

$$\therefore \quad \int (m\Sigma \dot{r}_s\, dr_s + \mathrm{M}\dot{\mathrm{R}}\, d\mathrm{R}) = \text{const.} = n_3 h,$$

so that

$$\mathrm{N} = n_1 + n_2 + n_3,$$

where n_1, n_2, n_3 may each split up into a number of quantum numbers.

In fact, if the independent coordinates defining the system are $p_1, p_2, \ldots p_r, \ldots$, there will be quantum conditions of the type

$$\int \left[m\Sigma (\dot{x}_r + \dot{\mathrm{X}}) \frac{\partial x_r}{\partial p_1} + \ldots\ldots + \ldots\ldots \right] dp_1 = n_{p_1} h, \text{ etc.}$$

This is of immediate application to the model of Helium atom as conceived by Landé and Bohr, and will be dealt with in a future paper.

21. Again, if $2\mathrm{T}$ = kinetic energy of the system,

$$2\mathrm{T} = \Sigma m(\dot{x}_r^2 + \dot{y}_r^2 + \dot{z}_r^2) + \mathrm{M}(\dot{\mathrm{X}}^2 + \dot{\mathrm{Y}}^2 + \dot{\mathrm{Z}}^2);$$

but since $\Sigma m \dot{x}_r = \mathrm{M}\dot{\mathrm{X}}$,

$$2\mathrm{T} = m\{\Sigma (\dot{x}_r + \dot{\mathrm{X}})\dot{x}_r + \Sigma (\dot{y}_r + \dot{\mathrm{Y}})\dot{y}_r + \Sigma (\dot{z}_r + \dot{\mathrm{Z}})\dot{z}_r\}.$$

$$\therefore \quad \frac{\partial \mathrm{T}}{\partial \dot{p}_r} = m\left\{ \Sigma (\dot{x}_r + \dot{\mathrm{X}}) \frac{\partial \dot{x}_r}{\partial \dot{p}_r} + \ldots\ldots + \ldots\ldots \right\}.$$

Now

$$\frac{\partial \dot{x}_r}{\partial \dot{p}_r} = \frac{\partial x_r}{\partial p_r};$$

$$\therefore \quad \frac{\partial \mathrm{T}}{\partial \dot{p}_r} = m\left\{ \Sigma (\dot{x}_r + \dot{\mathrm{X}}) \frac{\partial x_r}{\partial p_r} + \ldots\ldots + \ldots\ldots \right\}.$$

Thus the quantum conditions postulated are of the type

$$\int \frac{\partial \mathrm{T}}{\partial \dot{p}_r}\, dp_r = n_{p_r} h,$$

which may be shown to satisfy Larmor's conditions for permanent stability on a proper choice of constraints which must for the present be a matter of speculation.

A proof of this theorem, as well as several other postulates of quantum theory, will be given in a paper on "The Postulates of the Quantum Theory" which is ready for publication.

LXXXVI. *Curvature of the Spectral Lines in a Prism Spectroscope.* *By* G. Subrahmaniam, *M.A.*, *and* D. Gunniaya, *M.A.**

IT is a matter of common observation that the spectral lines obtained with a prism spectroscope are curved with their convex sides turned towards the red end of the spectrum. This, no doubt, forms an important difference between the dispersion spectra and the diffraction spectra. Excepting a few incidental references scattered here and there, no systematic quantitative relation between the details of the spectrometer and the resulting curvature of the spectral lines seems to have been found out. In view of the extensive use of rocksalt prisms and linear thermopiles for the examination of the infra-red region, such an investigation is well worth an attempt.

Fig. 1.

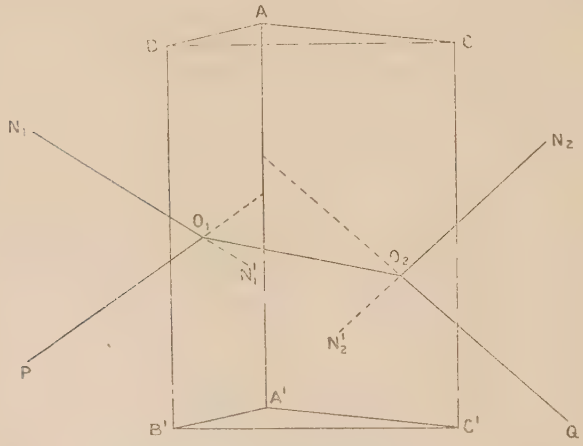

In what follows it is assumed that the curvature of the spectral lines arises from the obliquity of the incident rays to the principal plane of the prism, and that the several optical parts are "corrected." The accompanying diagram (fig. 1) represents a prism with its edge AA′ lying wholly in, and the principal plane perpendicular to, the plane of the paper. Let PO_1 be a ray not in the principal plane and θ the angle of incidence with the normal $N_1O_1N_1'$. The path of the ray O_1O_2 within the prism makes an angle θ' with the normal such that $\sin\theta = \mu \sin\theta'$. If ψ', ψ are angles of incidence

* Communicated by the Authors.

and emergence at the second surface $\sin\psi = \mu \sin\psi'$. Since the edge AA′ lies in both the refracting surfaces and the normals N_1N_1' and N_2N_2' are perpendicular to the edge, it follows (see Herman's 'Geometric Optics,' xxviii. p. 28) that the incident ray and the emergent ray are equally inclined to the edge. If the rays PO_1, O_1O_2, and O_2Q are projected on a great circle lying in the principal plane with reference to the edge of the prism as the pole, it is found that the actual deviation δ is related to the deviation δ' in the projected path by the equation :

$$\sin\frac{\delta}{2} = \sin\beta \,.\, \sin\frac{\delta'}{2},$$

where β is the inclination of the ray to the edge of the prism.

Obviously, therefore, δ' is always greater than δ except when $\beta = \frac{\pi}{2}$ when, however, the ray lies wholly in the principal plane and the two are equal. In the case of a prism placed in the minimum deviation, radiations from the centre of the slit lie, no doubt, in the principal plane, and

Fig. 2.

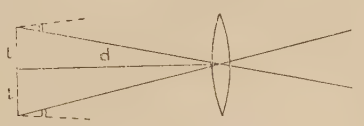

those from the extremities do not. If $2l$ is the length of the slit and d the distance of the collimating lens from the slit, the maximum possible divergence of the extreme ray is $\sin^{-1}\dfrac{l}{(d^2+l^2)^{\frac{1}{2}}}$, and therefore $\sin\beta$ under these conditions is $\dfrac{d}{(d^2+l^2)^{\frac{1}{2}}}$.

To take the following particular examples :—

(1) In the case of a spectrometer supplied by Adam Hilger & Co., length of the slit $2l = 1{\cdot}00$ cm. and $d = 30$ cm. about ; for a 60° angle prism of crown glass and for mean D line (5893×10^{-8} cm.)

$$\delta' - \delta = 0^\circ\ 1'\ 9''{\cdot}81,$$

and in consequence the resulting curvature of the D line is 0 0006785.

(2) With the same instrument, but with a 60° angle prism of flint glass and for mean D line

$$\delta' - \delta = 0^\circ\ 1'\ 30''{\cdot}23,$$

and the resulting curvature of the D line is **0·0008724.**

(3) In an infra-red spectrometer $2l = 2$ cm. and d the distance of the slit from the mirror is about 40 cm.; for a 60° angle prism of rocksalt and for the infra-red region $1{\cdot}420 \times 10^{-6}$ cm., $\mu = 1{\cdot}5213$

$$\delta' - \delta = 0^\circ\ 4'\ 0''{\cdot}13,$$

and the resulting curvature is **0·001163.**

H. H. The Maharaja's Research
Laboratories, Vizianagaram.

LXXXVII. *The Striated Discharge in Mercury Vapour.* By W. H. McCurdy, *M.A.*, 1851 *Exhibition Scholar, Princeton University* *.

Introduction.

DURING the past half century a large amount of work has been done on the problem of electrical discharges in rarefied gases. The various parts of the discharge have been studied independently, the Crookes dark space probably receiving most attention, since in this region of the discharge occurs the very interesting phenomenon of the high cathode fall of potential. Much less attention has been given to the negative glow, Faraday dark space, and positive column, which are the subject of this investigation.

Guided by certain theoretical considerations of space-charge and mobility, the experimental results to be described have led to a theory of the mechanism of current flow in the negative glow and Faraday dark space and an explanation of striations in the positive column, which seem satisfactorily to explain the essential features of the discharge.

In order to avoid confusion and unnecessary repetition, the following symbols will be used throughout the following discussion :—

μ_+ and μ_- are mobilities of positive ions and electrons respectively ; M and m are the masses of positive ion and electron ; $\bar{V}$ is the average velocity of the electrons, U_t is the terminal velocity of the positive ions, and Ω is the velocity of thermal agitation of the atoms, all three being expressed

* Communicated by Prof. K. T. Compton.

in equivalent volts ; l and L are the mean free paths of the electrons and the positive ions respectively ; E is the electric intensity ; c and C are the square root mean square velocities of the electrons and positive ions respectively.

Compton * gives, as the expression for the mobility of electrons,

$$\mu_- = 0{\cdot}815\frac{el}{mc}. \quad . \quad . \quad . \quad . \quad . \quad . \quad (1)$$

On the same assumptions, the mobility of the positive ions is found to be

$$\mu_+ = 1{\cdot}15\frac{el}{\mathrm{MC}}, \quad . \quad . \quad . \quad . \quad . \quad . \quad (2)$$

the difference in numerical factor in the two expressions being due to the fact that the masses of the positive ion and the atom are equal.

On the assumption of elastic collisions between the electrons and the gas molecules, Compton also finds that the terminal energy which an electron will attain, under the influence of an electric field, in the gas, is given by

$$eV_t = \tfrac{1}{2}e\left[\Omega + \sqrt{\Omega^2 + \frac{\mathrm{E}^2l^2\mathrm{M}}{1{\cdot}134m}}\right]. \quad . \quad . \quad . \quad (3)$$

On the assumption that the collisions between the positive ions and the gas molecules are as if between elastic spheres and that the law of conservation of momentum holds for the collisions, it is found that, on the average, the positive ion will lose half of its energy on collision if the molecules are considered to be at rest compared with the positive ions. If, however, as is actually more nearly the case, the ions are moving with a velocity U and the molecules with a velocity Ω, the average fraction of energy lost by a positive ion at a collision is given by

$$f = \tfrac{1}{2}\left(1 - \frac{\Omega}{\mathrm{U}}\right).$$

From this the terminal energy of the positive ions is found to be

$$eU_t = \tfrac{1}{2}e\left[\Omega + \sqrt{\Omega^2 + 4{\cdot}61\mathrm{L}^2\mathrm{E}^2}\right] \quad . \quad . \quad . \quad (4)$$

by the same reasoning as that by which Compton has obtained the terminal energy of the electrons.

From these equations it is possible by very simple processes to obtain any of the quantities that may be referred to in the course of the present work.

* Compton, Phys. Rev. xxii. p. 334 (1923).

Theory of the Positive Column.

Sir J. J. Thomson* has recently developed the mathematical theory of the striated positive column of the gaseous discharge. According to his theory, the condition for the occurrence of the striations in the positive column of the discharge is that the current density must be lower than a certain critical value which is determined by the rate of recombination of the electrons with positive ions, as well as other quantities which, so far as the author is aware, have not been determined. Consequently, to make further progress in the theory of the striated positive column it is necessary to approach the problem from a different angle.

In experiments on discharges in the so-called "noble gases," it has been found that a striated positive column cannot be obtained if the gas is carefully purified. The author has found the same to be true for mercury vapour, which is to be expected, since it is also a monatomic gas and would therefore be expected to be governed by the same laws. This criterion probably cannot be extended generally to include the multiatomic gases, although the author understands that work done under the supervision of Sir J. J. Thomson in the Cavendish Laboratory points to the conclusion that it is also true for nitrogen. In some of the earliest experiments on gaseous discharges, it was found that mixtures of gases produced the most beautifully striated positive columns†. Thus, in view of the fact that no striations occur in pure monatomic gases, it is natural to conclude that the striations are the direct result of the presence of impurities in the discharge.

In order to account for the striations in the positive column, it is necessary to find conditions which favour ionization at definite regions in the discharge. A shortening of the life of an excited atom will lead directly to this result. In the uniform positive column, atoms exist in every state of excitation, so electrons of almost any speed may produce partial or complete ionization. If, now, the life of an excited atom is diminished by the presence of impurities, it will have to receive the two amounts of energy, necessary to produce ionization, in rapid succession, assuming cumulative ionization. If this is to occur at any point in the positive column, the number of electrons available to supply the energy must be very large; consequently, in order to obtain a uniform positive column with impurities present, the current density

* Thomson, Phil. Mag. xlii. p. 986 (1921).

† J. J. Thomson, 'Conduction of Electricity in Gases.'

in the discharge would have to be large. If, however, the positions of ionization were so localized that a large proportion of the electrons had sufficient energy to produce ionization, considered as a cumulative effect, the probability of ionization would be greatly increased, and the discharge could be maintained at smaller current densities. On making an inelastic collision, the mobility of the electrons is increased, and, as a result, they are drawn at high velocity towards the anode, leaving a positive space-charge where the inelastic collision occurred. A corresponding negative space-charge must exist at some other place, and this will be on either side of the region of ionization. Few of the positive ions travel far before recombination ; so, to the cathode side of a region of ionization, a negative space-charge should be found, as there are fewer positive ions to neutralize the space-charge of electrons from the cathode or preceding striation. The resulting distribution of electric intensity tends to continue the ionization in the regions where it started. Thus we have a state which favours localization of ionization and resultant recombination and radiation ; in other words, a striated positive column.

The consequences of such a theory of the striations would include several points, which may be checked experimentally :—

1. A higher concentration of excited atoms should exist in the striations than in the space between them. By experiments on the absorption of spectral lines, it should be possible to determine the relative concentrations of excited atoms in different parts of the discharge. This work has been carried out by Compton, Turner, and McCurdy, and the results have been in accord with the theory. An account of this work will appear later.

2. If striations are due to an effect of impurities, these must be of such nature that the energy of an excited atom may be sufficient to transform them into some state of excitation. Franck * has found that excited mercury atoms will dissociate molecular hydrogen ; thus, if hydrogen is used to produce striations in mercury vapour, there should be a greater concentration of atomic hydrogen in the striations than in the regions between them. Any gas which has no critical potential below the lowest radiating potential of mercury should have no effect on the discharge in mercury vapour. Both of these points have been checked experimentally by Compton, Turner, and McCurdy. The presence of atomic hydrogen was detected by the reduction of oxides

* Franck, *Zeit. f. Phys.* xi. p. 761 (1922).

of metals and the occurrence of the mercury hydride band-spectra.

3. If the above theory is true, the potential difference between successive striations must be sufficient to give the electrons enough energy to produce ionization on travelling from one striation to the next. It was found that, in the case of hydrogen*, the potential difference between striations was somewhat greater than the ionization potential. Duffendack † found that, in hydrogen, an arc could not be maintained below the ionizing potential; thus cumulative ionization cannot occur in hydrogen. In order to ionize, the electrons must have fallen through a potential equal to the ionizing potential. Also, as collisions of electrons in hydrogen may not be perfectly elastic, the potential difference between striations may be greater than the ionizing potential. For mercury ‡ it has been found that the potential difference is about 5 volts. In this case, however, it was assumed that only excitation and not ionization occurred, the current being carried altogether by electrons emitted by the cathode. In the mercury discharge, however, when the current density is large, the density of excited atoms should be sufficient to make cumulative ionization possible. This would make a potential difference between striations of a little over 5 volts sufficient to produce the necessary ionization.

4. The next consequence of this theory is that the concentration of electrons and positive ions should be a maximum near the cathode side of a striation. The current density is the same at all points in the discharge. Thus the concentration of electrons, assuming that they carry practically all the current, should be inversely proportional to the velocity of drift, therefore directly proportional to the velocity of agitation. Also, the concentration of positive ions should be a maximum near the point where they are produced, since they disappear through recombination.

5. The last point to be considered is the distribution of velocities of the electrons. If ionization occurs in the striation, an excess of slow electrons should be found towards the anode side of the striation and in the space between striations. The closest approach to a Maxwellian distribution of velocities should occur just outside the cathode side of the striations, for there the time since the last inelastic collision is a maximum.

* McCurdy, Phil. Mag. xlvi. p. 531 (1923).
† Duffendack, Phys. Rev. xx. (6) p. 665.
‡ Grotian, *Zeit. f. Phys.* v. p. 148 (1921).

Theory of Faraday Dark Space and Negative Glow.

E. Brose * has pointed out that the distinction between the negative glow and Crookes dark space is more apparent than real. He shows that the spectral lines occurring in the negative glow extend out into the Crookes dark space, though with diminishing intensity. The same condition holds for the negative glow and the Faraday dark space. Consequently any theory applying to the negative glow should apply equally well to the Faraday dark space.

In the treatment of the positive column, it has been assumed that the current is due to the motion of electrons under the influence of the electric field. This cannot be true in the case of the negative glow and Faraday dark space, for, under such conditions, there would be no logical reason for the marked difference in the appearance of the two regions. Furthermore, a consideration of the efficiency of ionization shows that the number of positive ions produced by the electrons which have fallen through the cathode drop is too large to be received by the cathode without producing impossibly large currents or a space-charge too large to conform to Poisson's equation. The same conclusion may be drawn from the absence of a strong negative space-charge in this region. Very few positive ions would, under normal conditions, penetrate any great distance into the Faraday dark space from the positive column before being lost by recombination, as is proved by the uniformity of the positive column. Therefore, unless positive ions move from the negative glow towards the anode, there should be a negative space-charge in the Faraday dark space which increases from the positive column towards the cathode. This is not found to be the case.

The only alternative that can be postulated is that the current is carried by the diffusion towards the anode of the electrons and positive ions produced in large numbers in the negative glow. This alone cannot fully account for the conditions found in these regions, since the much more rapid diffusion of electrons would still cause a negative space-charge in the Faraday dark space. Therefore there must be an electric field tending to retard the flow of electrons and to accelerate that of the positive ions. A rough calculation of the field necessary to produce the observed results has been carried out; and although by no means rigorous, it shows that a very small field is sufficient to account for the observed

* Brose, *Ann. d. Phys.* lviii. p. 731 (1919).

conditions. This field would be automatically set up and adjusted by the mobilities and rates of diffusion.

The net current must be an electron current from the negative glow to the positive column, so, to get an estimate of the field which may exist, let us assume that the resultant current is the difference between an electron diffusion current in the positive direction and an electron conduction current in the negative direction. This will give an upper limit to the field which can exist and still allow the observed current to flow.

$$i = \mathrm{D}e\frac{d\mathrm{N}}{dx} - \mu_{-}\mathrm{N}e\mathrm{E},$$

where i represents the current density, D the coefficient of diffusion and N the electron density.

Since

$$\mathrm{D} = \frac{kT}{e}\mu = \tfrac{2}{3}\overline{\mathrm{V}}\mu, \qquad i = \mu e\left(\tfrac{2}{3}\mathrm{V}\frac{d\mathrm{N}}{dx} - \mathrm{EN}\right).$$

This must be positive; and also $\frac{d\mathrm{N}}{dx}$ is found experimentally to be of the same order of magnitude as N. Therefore E must be less than $\frac{2}{3}\overline{\mathrm{V}}$. This is of the order of 1 volt, so the electric field must be less than 1 volt per centimetre. It is quite possible that small gradients of this order might not be detected, since in measurements it is difficult to obtain very constant conditions.

Thus, to support the diffusion hypothesis, one should find a strong concentration of electrons and positive ions in the negative glow and Faraday dark space, and a strong concentration gradient diminishing towards the positive column, and, possibly, a negative potential gradient at the anode side of the negative glow.

The following work was carried out in an attempt to confirm the theories just advanced concerning both positive column and Faraday dark space. Mercury vapour was used, as the simplest possible conditions should exist with a monatomic gas. Also more critical data are known for mercury than for most of the other gases.

Method.

Several methods have been employed in the study of the discharge, the three most important of these being :—

1. The study of potential distribution by means of the deflexion of a beam of cathode rays developed by Aston*.

* Aston, Proc. Roy. Soc. A, lxxxiv. p. 526 (1911).

This method, however, is limited in application, since it can be used only at low pressures.

2. The Stark effect produced on lines of the spectrum emitted by atoms in an electric field *. This method is limited in application to the case of strong fields, since the effect is very small.

3. The use of an exploring electrode introduced into the path of the discharge, and a measurement of the potential which it acquires †. Objections have been raised against this method on the grounds that it may not take up the potential of the gas surrounding it, due to the inequalities of velocities of electrons and positive ions and also to non-uniform density of ions of the two signs.

The method selected for the following work is a modification of the one last named. It was first suggested by Langmuir ‡, and applied to the study of the uniform positive column of the mercury-vapour discharge.

If a wire is introduced into the path of a discharge and maintained at a potential negative to that of the surrounding gas, positive ions are accelerated towards it and electrons are repelled. The result is that the wire is surrounded by a positive space-charge sheath. The outside of this sheath is at the potential of the surrounding space, and the inside at that of the wire. The positive ion current to the wire is limited by space-charge, and may to a first approximation be considered as a space-charge current between concentric cylinders. As the potential of the wire is raised, electrons reach the wire against the field until, finally, enough electrons get in to just neutralize the positive ion current, but not enough to neutralize the positive space-charge around the wire, so the positive ion current is still limited by space-charge. This gives the apparent potential of the space as determined by the old exploring electrode and electrometer method, but actually the wire is still negative with respect to the gas. As the potential of the wire is still further raised, the electron current to it increases. This current should be expressible as a function of the potential difference between the outside and inside of the space-charge sheath by the following equation, if there is a Maxwellian distribution of velocities of the electrons:

$$I = N_0 e \sqrt{\frac{eV}{3\pi m}} \epsilon^{-\frac{3(V_0 - V)}{2V}} \quad . \quad . \quad . \quad . \quad (5)$$

* E. Brose, *loc. cit.*

† Thomson, Cond. in Gases, p. 530.

‡ Langmuir, Journal of Franklin Inst. Dec. 1923; Gen. Elec. Rev. xxvi. p. 731 (1923).

Therefore log I as a function of $V_0 - V$ should be a straight line, where I is the current density to the wire, and V_0 and V the potentials of the space and wire respectively.

When the wire is at the potential of the space, the law regulating the current to it changes. Above this no positive ions can reach the wire, so now the wire will be surrounded by a negative space-charge sheath. The thickness of this sheath will change more rapidly in the case of the electrons than for the positive ions, and as a result no simple relation can be expected to exist between the current and the applied potential. However, since a change in condition occurs as the potential of the space is passed, a "break" is found in the log I–voltage curve. The position of this "break" locates the true potential of the gas.

From these I.–V. curves (of the exploring electrode) it is possible to obtain some very interesting data.

Average Energy of Electrons.—Assuming a Maxwellian distribution of velocities of the electrons, it is readily seen from equation (5) that the average energy of the electrons may be determined directly from the current-voltage curves. Transforming the equation by taking the logarithms of both sides,

$$\log I = \log N_0 e \sqrt{\frac{e\bar{V}}{3\pi m}} - \tfrac{2}{3}\frac{V_0 - V}{\bar{V}} \quad . \quad . \quad . \quad (6)$$

Thus the slope of the curve log I as a function of V is connected with the average velocity in volts by the relation

$$\bar{V} = \frac{3}{2\tan\theta} \quad . \quad . \quad . \quad . \quad . \quad . \quad . \quad (7)$$

If the distribution is not according to Maxwell's law, the only method of determination of the average energy is by actual integration of the current curves. This process was carried out in a few cases.

Concentration of Electrons.—Although not in all cases is the distribution of speeds according to Maxwell's distribution law, still it is possible to obtain at least an approximate value for the electron concentration. From equation (5) it is observed that when $V_0 - V = 0$ the electron concentration as a function of the current is given by

$$N_0 = \frac{I}{e}\sqrt{\frac{3\pi m}{e\bar{V}}} \quad . \quad . \quad . \quad . \quad . \quad . \quad (8)$$

This serves as a ready means of obtaining the electron concentration, since all the quantities are either known or can be obtained from the curves.

Concentration of Positive Ions.—The determination of the positive ions is not so direct and simple as for electrons. More approximations have to be made in the calculation, and consequently the results cannot be expected to be quite so satisfactory. An approximate calculation may be carried out as follows :—

Assuming that the positive ion current to the wire at a known negative potential V with respect to the surrounding space is a positive ion space-charge current between coaxial cylinders, Langmuir's* space-charge equation

$$C = \frac{2\sqrt{2}}{9}\sqrt{\frac{e}{M}}\frac{V^{3/2}}{(-r\beta^2)}, \quad \ldots \quad (9)$$

where C is the current per unit length of the wire and r is its radius, may be used. From this it is possible to calculate the value of the quantity $(-\beta^2)$, and thus the radius of the outside surface of the space-charge sheath can be determined from the tables given by Langmuir. Thus, if a Maxwellian distribution is assumed, as has been done for electrons, it is possible to calculate the positive ion concentration directly. It is that concentration such that all positive ions striking the outer layer of the sheath contribute to the observed positive ion current. The equation involved is the same as that used for electrons with proper substitutions for the values of M and U. The method used for the determination of the energy of the positive ions is by calculation, using equation (4) for the terminal energy.

Correction to be applied to the potential determinations by the electrometer method.—This is found directly by taking the difference between the voltage of the point where zero current arrives at the wire and that where the "break" in the current-voltage curve occurs.

Apparatus.

A diagram of the apparatus used in this work is given in fig. 1. The main tube, of 1·5 inch diameter, was enclosed in an electric furnace which extended about twelve inches below the level of the mercury in the two small tubes marked A on the diagram. These tubes dipped into mercury wells so adjusted as to bring the level of the mercury almost to the base of the discharge-tube. The mercury in these served as a source of vapour for the discharge, and also as a

* Langmuir, Phys. Rev. xxii. p. 347 (1923).

means of connecting the filament F which served as cathode for the discharge. The object of using the hot cathode was to obtain currents of considerable magnitude without the use of very high potentials.

The filament F and anode B were fixed in a light glass frame which was movable inside the discharge-tube and so arranged that the length of the discharge could be easily adjusted by altering the position of the anode in the frame.

Fig. 1.

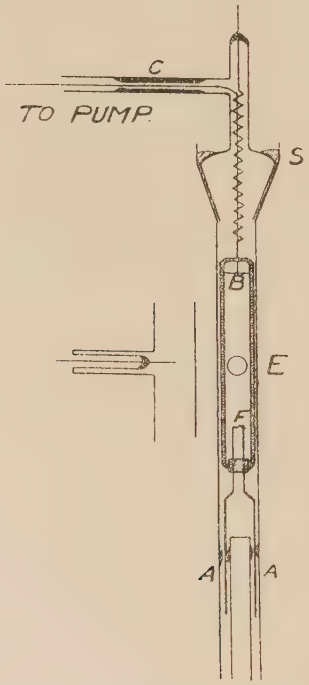

The anode was an iron disk, electrically connected through the spiral shown at the top of the tube, and the position of the frame was adjusted by means of the fine wire communicating through the capillary tube C with a winch not shown on the diagram. The capillary was inserted to allow as nearly constant pressure conditions in the discharge-tube as possible.

The exploring electrode was a piece of 4 mil tungsten wire,

and was covered with glass to within a few millimetres of the end and placed as near as possible to the centre of the discharge-tube.

The electrical connexions are shown in fig. 2. The resistance R_3 served as a potentiometer to vary the potential of the exploring electrode. The current to the electrode was measured on the microammeter A_3 and its potential by the voltmeter V_3.

Fig. 2.

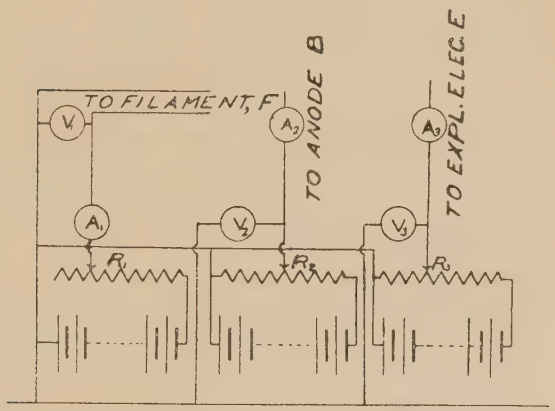

Readings of the current to the electrode were made at intervals of 0·5 volt from about 1 volt below the point where the current changed sign to several volts above. The results were plotted on semi-log. paper to make the calculations involved easier.

In plotting, only the electron current was wanted; therefore the positive ion current at a definite voltage below that of the space was added to the negative current as indicated by the ammeter, for this was considered to give the electron current near enough to the true value to satisfy other conditions of the work. Care was taken, however, to measure the positive ion current at a voltage sufficiently below that of the space to insure that no appreciable number of electrons reached the wire.

Results.

A set of four typical curves representing the current-voltage relation found in the various parts of a striation are shown in fig. 3.

The values of the potential distribution in a striation cannot be taken from fig. 3. It was necessary to so arrange the curves as to make them as distinct as possible rather than to give the distribution of potential over a striation.

Fig. 3.

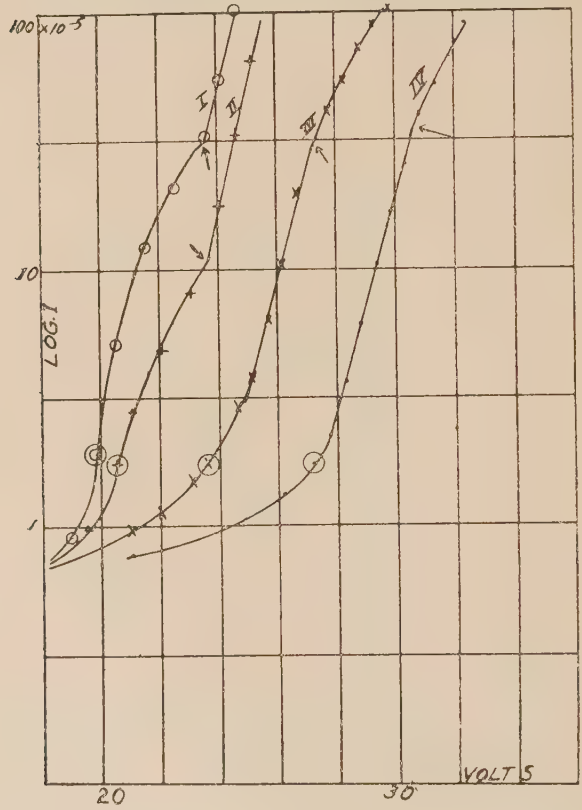

Curve No. I. was taken with the exploring electrode between two striations;
Curve No. II. at the anode side of a striation;
Curve No. III. in the middle of a striation; and
Curve No. IV. at the cathode side of the striation.

The circles represent the potential of the space as given by the old exploring electrode method. The arrows represent the true potential of the space.

It will be observed from the figure that the discontinuity giving the true potential of the space, indicated by the arrow, does not occur in the same direction in all cases.

The reason for this is not very clear. In order to determine whether or not the correct point was chosen, the potential of the space was determined also by means of a hot-filament exploring electrode, the true potential of the space being given by the highest potential which can be applied to the hot filament without stopping its thermionic emission. This method has been shown to give correct values, even in the electric field with no discharge flowing. The two methods checked within the experimental accuracy of the work.

Fig. 4 gives the general character of the distribution of potential in the discharge, and the broken curve gives the

Fig. 4.

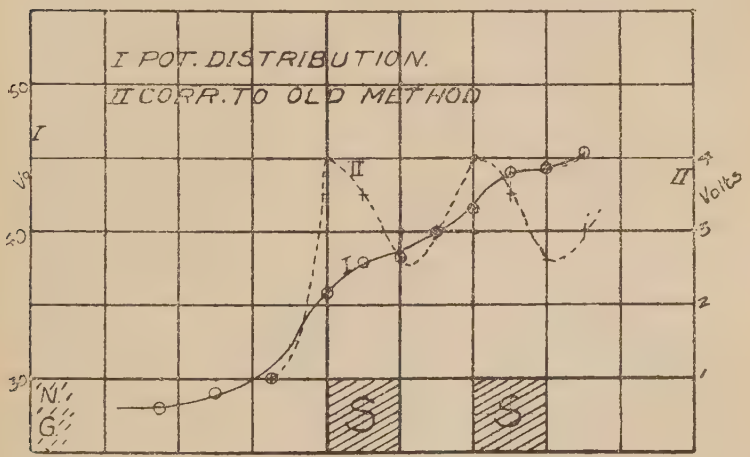

difference between the results of the current method and the usual, but less accurate, electrometer method of measuring potentials.

It will be observed that the potential distribution curves show the general characteristics of the distribution curves found in any work on gaseous conduction. They indicate a positive space-charge near the cathode face of the striations, and a negative space-charge between the striations. It will further be observed that the correction that must be applied to the electrometer determination of potential changes from place to place in the striations. It is a maximum near the cathode side of the striation and a minimum in the space between the striations. This is what would be expected

on the theory advanced to explain the striations and the processes occurring in the discharge.

Fig. 5 shows the variation in the concentration of the electrons and the positive ions at various points in the striations. In agreement with the theory, it is found that the concentration of both positive ions and electrons is a maximum near the cathode side of the striation and a minimum in the space between them. No claim to great accuracy is made regarding the numerical values of these concentrations, since too many approximations are necessary in the determinations. Still, as the conditions are comparatively constant,

Fig. 5.

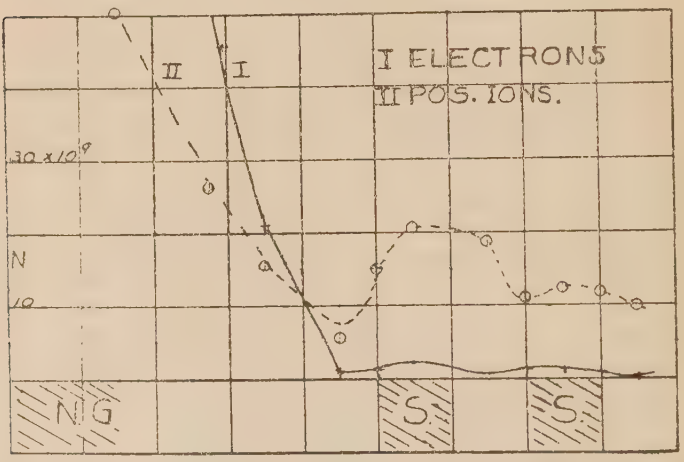

the relative values shown should be comparable and the order of magnitude of the results should be reliable. The positive ion concentration is in all cases too large, and some of the sources of error will be discussed later.

Table I. shows the numerical results of a typical run, and the energies of the electrons as calculated from the curves.

Discussion of Results.

As has been already pointed out, very small accuracy can be claimed for work of this nature. The discharge itself is too sensitive to small changes of conditions of the tube: also the assumptions which underlie the calculations of the quantities given cannot be accurately fulfilled. However, as an approximation to the true values, the results may be considered to be of some importance. The more important sources of error will be taken up separately.

TABLE I.

V.	V_0.	V_0-V.	$i+$.	$i-$.	$\bar{V}$.	N−.	r_s.	N+.	Position.
			$\times 10^{-6}$.	$\times 10^{-5}$.		$\times 10^{9}$.	$\times 10^{-2}$.	$\times 10^{9}$.	
54·5	57·4	2·9	4·9	1·5	1·2	·38	8·0	10·0	Between striations.
53·6	57·3	3·7	5·0	3·5	1·5	·75	7·4	11·8	Anode side of striation.
51·9	56·6	4·7	5·7	6·0	1·4	1·30	7·5	12·4	Middle of striation.
50·2	54·2	4·0	5·2	7·6	1·7	1·55	7·2	11·0	Cathode side of striation.
48·3	51·7	3·4	2·9	3·0	1·5	·65	8·5	5·6	1·3 mm. into F.D.S.
48·1	49·2	1·1	5·0	50	·40	21·0	5·4	15·5	13 mm. into F.D.S.
48·7	49·6	·9	7·2	100	·24	53·5	4·6	26·2	20 mm. into F.D.S.
48·9	50·0	1·1	55	250	·40	101·0	1·8	51·5	Anode side of negative glow.
48·8	50·1	1·3	475	470	·91	130·0	·9	900·0	Middle of negative glow.

Discharge at temperature 85°, mercury-vapour pressure = 0·12 mm.

Current in discharge was 12·5 mil amperes; potential across tube 86 volts.

V is potential of space by old method; V_0, the true potential of space; $i+$, the positive ion current to the wire at a known voltage below V_0; $i-$, the electron-current to the electrode at V_0; N−, the electron concentration; r_s, the radius of the sheath; and N+, the positive ion concentration.

Initial Velocities of the Positive Ions.—The positive ions on passing into the region of the space-charge sheath from the surrounding gas will have an initial velocity. The effect of this will be two-fold: (1) the positive ion current will somewhat exceed the value limited by Langmuir's original space-charge equation, which assumed zero initial velocity; and (2) all the ions that pass into the sheath may not reach the wire. In the determination of the positive ion density it was assumed that all ions reached the wire. An approximate calculation of the number of ions which fail to reach the electrode has been carried out based on the assumption that no collisions of the ions with gas molecules occur, which is the most unfavourable condition. If an ion passes into the positive ion sheath with a velocity U in a direction making an angle ϕ with the radius of the cylinder to the point, and the laws of (1) conservation of energy, (2) conservation of angular momentum are applied, it is found that the condition for the ion to reach the wire is given by the relation

$$\sin\phi < \frac{b}{a}\sqrt{1-\frac{V}{U}},$$

where V is the potential difference between the wire and the outside of the sheath, a and b the radii of the outside of the sheath and the wire respectively. From this it is seen at once that if V is of the order of 20 volts, and since U is of the order of 0·05 volt as calculated from the terminal velocity of the positive ions, all the ions will reach the wire provided that the ratio of the radii of the wire to the outside of the sheath is 1:20. If the sheath becomes larger than this, some of the ions which pass inside it will not reach the wire owing to their angular momentum. Care was taken in the calculations to see that this condition was satisfied.

The effect of the ends of the wire on the calculation of concentration.—If the radius of the sheath becomes large, the area of the two hemispherical ends which close the assumed cylindrical volume may become important. This factor was taken into consideration by assuming that the current density across the boundary of the sheath was the current to the wire divided by the total area of the sheath. This factor would also affect the calculation of the thickness of the sheath from the space-charge current equation. However, as the area of the ends was only about 20 per cent. of the area of the sides, this should not be an important source of error.

Velocity of Drift of the Positive Ions.—From the expressions

for the mobility and the terminal velocity of the positive ions it is found that, under the conditions applying to the discharge, the velocity of drift of the positive ions is comparable with that of thermal agitation. The above equations were based on the assumption of no velocity of drift. In order to arrive at an estimate of the error introduced by this, we may consider that the ions are made up of two groups:—

(1) Those which have a velocity of thermal agitation only, and
(2) Those which have a velocity of drift.

The relative numbers of ions in the two groups will be in the ratio of the velocities; the effective collecting areas of the two will be in the ratio of the area of the outside of the sheath to the area of the section of the sheath by a plane along the axis of the wire and at right angles to the axis of the tube—*i. e.*, in the ratio of $2\pi rL : 2rL$. This fact has been taken into account in the calculations of the concentrations given.

This, of course, cannot be considered to represent the actual facts of the case, for what really occurs is that the ions must be considered to have a Maxwellian distribution of velocities about a velocity of drift. However, statistically the two conditions would produce about the same results.

The effect of drawing the Positive Ions out of the Discharge.—The calculated value of the positive ion concentration is found still to be larger than that of the electrons after the above corrections have been made. A possible explanation of this may be found in the fact that all the positive ions which pass into the sheath are lost to the gas. Thus a negative space-charge should build up around the sheath, since electrons are reflected from the space by the electric field. This condition complicates the problem by the addition of an extra space-charge sheath between the wire and the undisturbed gas, and thus the positive ions which reach the wire do not arrive there simply by thermal motion, but are also drawn in by the electric field due to the negative space-charge. A mathematical treatment of this appears to involve so many unknown quantities that it is hopeless to attempt to obtain a satisfactory solution of the problem. However, it can readily be seen that the result will be a reduction in the positive ion concentration, though the amount of this reduction cannot readily be estimated.

Concentration of the Electrons.—The most obvious source of error in the determination of the concentration of the

electrons is the absence of an exact Maxwellian distribution of velocities. There seems to be no simple way of correcting for this factor, though it is probably not very important for small departures. Another source of difficulty is the fact that the glass covering of the exploring electrode becomes coated with a semi-conducting film after it has been in the discharge for some time. Successive runs under as nearly similar conditions as possible show that this error is not very serious.

A check on the electron concentration is possible on the assumption that the current in the positive column is totally one of conduction and carried entirely by the electrons. Making use of the mobility of the electrons as given above and the electric intensity as measured, it is possible to calculate the electron concentration necessary to account for the current. By carrying out a determination of this sort, it has been found that the result gives an electron concentration about three times that calculated from the other method. This agreement is probably as good as can be expected from work of this sort.

Summary.

The theory is advanced that the striations which occur in the positive column of the discharge in a monatomic gas under low pressure are due to the presence of impurities; and also that the current in the positive column of the discharge is due to the motion of electrons under the influence of the electric field, while that in the Faraday dark space and the negative glow is due to diffusion of electrons and positive ions produced in the negative glow by the fast electrons from the Crookes dark space.

The experimental results confirm the theories advanced in the following important respects:—

(1) The potential distribution in the discharge satisfies the theory as regards the distribution of space-charge.

(2) The concentration of the electrons is found to be a maximum near the cathode side of the striations. Also that of the positive ions, but the variation in the case is not so marked.

Further, it is found that the corrections that must be applied to the determination of potential in the discharge by the old exploding electrode method vary from point to point in the striations and are a maximum near the cathode side of the striation.

(3) A reverse field may exist in part of the negative glow,

but the concentration gradient of the electrons in the negative glow and Faraday dark space is found to be amply sufficient to account, by diffusion, for the currents observed in the discharge.

In conclusion, I wish to express my sincere thanks to Professor K. T. Compton, under whose supervision this work was carried out, for the interest he has taken and the assistance rendered throughout the course of the work; also to Dr. Irving Langmuir, who suggested the method for using the exploring electrode in advance of his publication, and who gave other valuable suggestions.

Palmer Physical Laboratory,
Princeton University.

LXXXVIII. *The Relations between Antisymmetric Tensors and Tensor-Densities.* *By* P. Du Val *.

THE object of this paper is to point out certain relations, not apparent in the usual treatment of the subject, between antisymmetric tensors and tensor-densities of various ranks. The four-dimensional case only will be discussed, though similar considerations apply to the tensor analysis in any number of dimensions.

§ 1. *Change of Coordinates.*

In the four-dimensional world let the coordinates, in two different systems, of the field-point be x_μ and x'_μ; let ${}^{\cdot}\mathrm{A}^\mu$, ${}^{\cdot}\mathrm{A}'^\mu$ be the components, in the same two systems, of a contravariant vector; then the law of transformation of vector-components with change of coordinates is

$$ {}^{\cdot}\mathrm{A}'^\mu = \frac{\partial x'_\mu}{\partial x_\alpha} {}^{\cdot}\mathrm{A}^\alpha, \quad \ldots\ldots \quad \text{(i.)} $$

where the summation convention gives one term on the right for each suffix α.

Similarly, if ${}^{\cdot}\mathrm{A}^{\mu\nu}$ be an antisymmetric contravariant tensor of the second rank,

$$ {}^{\cdot}\mathrm{A}'^{\mu\nu} = \frac{\partial x'_\mu}{\partial x_\alpha} \frac{\partial x'_\nu}{\partial x_\beta} {}^{\cdot}\mathrm{A}^{\alpha\beta}, $$

* Communicated by the Author.

where the summation on the right is with respect to α and β independently—*i. e.*, there is one term for each of the sixteen permutations $\alpha\beta$. Four of these terms vanish, however, and since ${}^{\cdot}A^{\alpha\beta} + {}^{\cdot}A^{\beta\alpha} = 0$, the equation becomes

$$ {}^{\cdot}A'^{(\mu\nu)} = \frac{\partial(x'_\mu, x'_\nu)}{\partial(x_\alpha, x_\beta)} \, {}^{\cdot}A^{(\alpha\beta)}, \quad . \quad . \quad . \quad . \quad . \quad \text{(ii.)} $$

where the enclosure of $(\alpha\beta)$ in brackets indicates that the summation is to give one term for each of the six such combinations. Only antisymmetric groups of suffixes will be enclosed in this way.

In the same way, if ${}^{\cdot}A^{\mu\nu\rho}$ be an antisymmetric contravariant tensor of the third rank,

$$ {}^{\cdot}A'^{(\mu\nu\rho)} = \frac{\partial(x'_\mu, x'_\nu, x'_\rho)}{\partial(x_\alpha, x_\beta, x_\gamma)} \, {}^{\cdot}A^{(\alpha\beta\gamma)}, \quad . \quad . \quad . \quad \text{(iii.)} $$

and if ${}^{\cdot}V^{\mu\nu\rho\sigma}$ be one of the fourth rank,

$$ {}^{\cdot}V'^{(\mu\nu\rho\sigma)} = \frac{\partial(x'_\mu, x'_\nu, x'_\rho, x'_\sigma)}{\partial(x_\alpha, x_\beta, x_\gamma, x_\delta)} \, {}^{\cdot}V^{(\alpha\beta\gamma\delta)}. $$

In this case, as there is only one component we may represent its magnitude (for a positive permutation of the suffixes 1 2 3 4) by ${}^{\cdot}V$, finding

$$ \begin{aligned} {}^{\cdot}V' &= \frac{\partial(x'_1, x'_2, x'_3, x'_4)}{\partial(x_1, x_2, x_3, x_4)} \, {}^{\cdot}V \\ &= D \, {}^{\cdot}V. \quad . \quad . \quad . \quad . \quad . \quad . \quad . \quad . \quad . \quad \text{(iv.)} \end{aligned} $$

The corresponding equations for antisymmetric covariant tensors are, of course,

$$ {}_{\cdot}A'_\mu = \frac{\partial x_\mu}{\partial x'_\alpha} \, {}_{\cdot}A_\alpha, \quad . \quad . \quad . \quad . \quad . \quad . \quad . \quad . \quad \text{(v.)} $$

$$ {}_{\cdot}A'_{(\mu\nu)} = \frac{\partial(x_\mu, x_\nu)}{\partial(x'_\alpha, x'_\beta)} \, {}_{\cdot}A_{(\alpha\beta)}, \quad . \quad . \quad . \quad . \quad \text{(vi.)} $$

$$ {}_{\cdot}A'_{(\mu\nu\rho)} = \frac{\partial(x_\mu, x_\nu, x_\rho)}{\partial(x'_\alpha, x'_\beta, x'_\gamma)} \, {}_{\cdot}A_{(\alpha\beta\gamma)}, \quad . \quad . \quad . \quad \text{(vii.)} $$

$$ {}_{\cdot}V'_{(\mu\nu\rho\sigma)} = \frac{\partial(x_\mu, x_\nu, x_\rho, x_\sigma)}{\partial(x'_\alpha, x'_\beta, x'_\gamma, x'_\delta)} \, {}_{\cdot}V_{(\alpha\beta\gamma\delta)}, $$

$$ \begin{aligned} {}_{\cdot}V' &= D^{-1} \, {}_{\cdot}V. \quad . \quad . \quad . \quad . \quad . \quad . \quad . \quad . \quad \text{(viii.)} \end{aligned} $$

It is clear, moreover, that a tensor density undergoes the same transformations as the corresponding tensor, and is in addition multiplied by D^{-1}. . . . . (ix.)

§ 2. *General Transformation of Linear Tensors.*

We now make the definition of a linear tensor of type r: we suppose r to be expressed in the two forms

$$r \equiv 4m+p \equiv -(4n+q),$$

where m and n are integers and $0 \geqslant p \geqslant 4$, $0 \geqslant q \geqslant 4$. This gives that $p+q=4$. If $p=1$, $q=3$, we call the tensor a displacement-tensor; if $p=q=2$, we call it a surface-tensor; if $p=3$, $q=1$, a space-tensor; and if $p=0$, $q=4$ or $p=4$, $q=0$, a scalar.

A linear tensor of the rth type has $\frac{4!}{p!\,q!}$ components, which may be distinguished by antisymmetric combinations either of p upper suffixes or of the remaining q lower suffixes. One more than the highest (positive or negative) multiple of 4 which occurs in r is indicated by the number of (upper or lower) dots which precede the symbol; thus, if $\mu \ldots \rho \ldots$ be a positive permutation of 1 2 3 4, with p suffixes $\mu \ldots$ and q suffixes $\rho \ldots$,

$${}^{m+1}\mathrm{A}^{\mu\ldots} = {}_{n+1}\mathrm{A}_{\rho\ldots}$$

is a linear tensor of type r. [Here ${}^{m+1}$ and ${}_{n+1}$ are used to indicate $m+1$ upper and $n+1$ lower dots; this will in general be unnecessary, as more than two dots do not ordinarily occur.] In any change of coordinates the corresponding transformation is

$$\left.\begin{aligned} {}^{m}\mathrm{A}'^{\mu\ldots} &= \mathrm{D}^{m}\frac{\partial(x'_{\mu}, \ldots)}{\partial(x_{\alpha}, \ldots)}\,{}^{m}\mathrm{A}^{\alpha\ldots}, \\ {}_{n}\mathrm{A}'_{\rho\ldots} &= \mathrm{D}^{-n}\frac{\partial(x_{\rho}, \ldots)}{\partial(x'_{\varepsilon}, \ldots)}\,{}_{n}\mathrm{A}_{\varepsilon\ldots}. \end{aligned}\right\} \quad . \quad . \quad . \quad \text{(x.)}$$

The equivalence of these two equations follows immediately from the identity

$$\frac{\partial(x_{\rho}, \ldots)}{\partial(x'_{\epsilon}, \ldots)} = \frac{\partial(x'_{\mu}, \ldots)}{\partial(x_{\alpha}, \ldots)} \Big/ \mathrm{D}.$$

It is easily seen that the equations (i.) ... (ix.) are all

cases of (x.), and hence that antisymmetric tensors and tensor densities of all ranks are by definition linear tensors, in accordance with the following table :—

Type.	Antisymmetric Tensors.	Antisymmetric Tensor-Densities.
+4	Contravariant, 4th rank.	
+3	„ 3rd rank.	
+2	„ 2nd rank.	
+1	„ 1st rank.	
0	Invariant.....	Contravariant, 4th rank.
−1	Covariant, 1st rank.....	„ 3rd rank.
−2	„ 2nd rank	„ 2nd rank.
−3	„ 3rd rank	„ 1st rank.
−4	„ 4th rank	Invariant-Density.
−5	.....	Covariant, 1st rank.
−6	.....	„ 2nd rank.
−7	.....	„ 3rd rank.
−8	.....	„ 4th rank.

§ 3. *The Grassmann Product.*

Clearly, in multiplying two linear tensors the summation will act differently according as we use upper or lower suffixes. It will thus be convenient to have a notation for products independent of the summation-convention and the position of the suffixes.

In general, we define the Grassmann product of two linear tensors as that obtained by writing the first with p_1 upper suffixes and the second with q_2 lower suffixes, and contracting ; if $p_1 < q_2$, we make the p_1 upper the same as the first p_1 lower suffixes ; if $p_1 = q_2$, we make each upper the same as the corresponding lower suffix : if $p_1 > q_2$, we make the q_2 lower the same as the last q_2 upper suffixes : both the p_1 and the q_2 suffixes being in brackets, so that the summation is by combinations of suffixes. The three types of products corresponding to $p_1 < q_2$, $p_1 = q_2$, $p_1 > q_2$ are called progressive, scalar, and regressive respectively.

The Grassmann product is conveniently represented by enclosing the two factors within square brackets, the suffixes being replaced by an upper dot for a displacement tensor, a lower dot for a space tensor, and one in an intermediate position for a surface tensor.

It is easily verified that the Grassmann product is commutative if at least one of the factors is a surface tensor ; but if neither is a surface tensor, the product

is anticommutative. Moreover, the product of three or four displacement or space tensors, or of two displacement or space tensors and one surface tensor, is associative.

Expressions for progressive products where both factors are written with upper suffixes, and for regressive where both are written with lower suffixes, are important.

I. Progressive:

$$[A^{\cdot}\,B^{\cdot}]^{(\mu\nu)} = -[B^{\cdot}\,A^{\cdot}]^{(\mu\nu)} = -\begin{vmatrix} A^{\mu} & A^{\nu} \\ B^{\mu} & B^{\nu} \end{vmatrix}, \quad . \quad . \quad . \quad \text{(xi.)}$$

$$[A^{\cdot}B_{\cdot}]^{(\mu\nu\rho)} = [B_{\cdot}\,A^{\cdot}]^{(\mu\nu\rho)} = A^{\mu}B^{\nu\rho} + A^{\nu}B^{\rho\mu} + A^{\rho}B^{\mu\nu}, \quad . \quad . \quad . \quad \text{(xii.)}$$

$$[A^{\cdot}\,B^{\cdot}\,C^{\cdot}]^{(\mu\nu\rho)} = -\begin{vmatrix} A^{\mu} & A^{\nu} & A^{\rho} \\ B^{\mu} & B^{\nu} & B^{\rho} \\ C^{\mu} & C^{\nu} & C^{\rho} \end{vmatrix}, \quad . \quad . \quad . \quad . \quad . \quad \text{(xiii.)}$$

$$[A^{\cdot}\,B^{\cdot}\,C^{\cdot}\,D^{\cdot}] = \begin{vmatrix} A^1 & A^2 & A^3 & A^4 \\ B^1 & B^2 & B^3 & B^4 \\ C^1 & C^2 & C^3 & C^4 \\ D^1 & D^2 & D^3 & D^4 \end{vmatrix}. \quad . \quad . \quad . \quad . \quad \text{(xiv.)}$$

II. Regressive:

$$[A_{\cdot}\,B_{\cdot}]_{(\mu\nu)} = -[B_{\cdot}\,A_{\cdot}]_{(\mu\nu)} = -\begin{vmatrix} A_{\mu} & A_{\nu} \\ B_{\mu} & B_{\nu} \end{vmatrix} \quad . \quad . \quad . \quad \text{(xv.)}$$

$$[A_{\cdot}B^{\cdot}]_{(\mu\nu\rho)} = [B^{\cdot}\,A_{\cdot}]_{(\mu\nu\rho)} = A_{\mu}B_{\nu\rho} + A_{\nu}B_{\rho\mu} + A_{\rho}B_{\mu\nu}, \quad . \quad . \quad . \quad \text{(xvi.)}$$

$$[A_{\cdot}\,B_{\cdot}\,C_{\cdot}]_{(\mu\nu\rho)} = -\begin{vmatrix} A_{\mu} & A_{\nu} & A_{\rho} \\ B_{\mu} & B_{\nu} & B_{\rho} \\ C_{\mu} & C_{\nu} & C_{\rho} \end{vmatrix}, \quad . \quad . \quad . \quad . \quad . \quad \text{(xvii.)}$$

$$[A_{\cdot}\,B_{\cdot}\,C_{\cdot}\,D_{\cdot}] = \begin{vmatrix} A_1 & A_2 & A_3 & A_4 \\ B_1 & B_2 & B_3 & B_4 \\ C_1 & C_2 & C_3 & C_4 \\ D_1 & D_2 & D_3 & D_4 \end{vmatrix}. \quad . \quad . \quad . \quad . \quad \text{(xviii.)}$$

In these formulæ the preceding dots are omitted, as the expressions are just the same whatever the arrangement of these may be.

§ 4. *Other Tensors.*

A tensor of type $(4m+p_1+p_2+\ldots-q_1-q_2-\ldots)$ is one which has components with $\Sigma(p)$ upper suffixes, of which the first group of p_1, the next group of p_2, etc., are each antisymmetric amongst themselves, and $\Sigma(q)$ lower suffixes, of which the first group of q_1, the next group of q_2, etc., are each antisymmetric amongst themselves; *i. e.*, if there are p_1 suffixes $(\mu\ldots)$, p_2 suffixes $(\rho\ldots)$, ..., q_1 suffixes $(\theta\ldots)$, q_2 suffixes $(\sigma\ldots)$, etc., then $\mathrm{T}^{(\mu\ldots)(\rho\ldots)\ldots}_{(\theta\ldots)(\sigma\ldots)\ldots}$, preceded by dots corresponding to one more than the highest multiple of 4 contained in $4m+\Sigma(p)-\Sigma(q)$, is such a tensor. It is transformed according to the law (*cf.* the law (x.)) :

$$\mathrm{T}'^{(\mu\ldots)(\rho\ldots)\ldots}_{(\theta\ldots)(\sigma\ldots)\ldots} = \mathrm{D}^m \frac{\partial(x'_\mu,\ldots)}{\partial(x_\alpha,\ldots)} \frac{\partial(x'_\rho,\ldots)}{\partial(x_\epsilon,\ldots)} \cdots \frac{\partial(x_\theta,\ldots)}{\partial(x'_\zeta,\ldots)} \frac{\partial(x_\sigma,\ldots)}{\partial(x'_\lambda,\ldots)} \cdots \mathrm{T}^{(\alpha\ldots)(\epsilon\ldots)\ldots}_{(\zeta\ldots)(\lambda\ldots)\ldots}. \quad \text{(xix.)}$$

We may, of course, replace any group of p_r upper suffixes by a lower group of the remaining $4-p_r$, and each lower group of q_r by an upper group of the remaining $4-q_r$, altering m so as to keep the sum $4m+\Sigma(p)-\Sigma(q)$ unchanged. In general, also, it will be necessary to distinguish the order of the suffix-groups, upper and lower together; thus $\mathrm{T}^{(\mu\ldots)\ (\rho\ldots)\ \ldots}_{(\theta\ldots)(\sigma\ldots)}$ is different from $\mathrm{T}^{(\mu\ldots)(\rho\ldots)\ \ldots}_{(\theta\ldots)(\sigma\ldots)}$, or from $\mathrm{T}_{(\theta\ldots)\ (\sigma\ldots)\ \ldots}^{(\mu\ldots)\ (\rho\ldots)}$, etc.

The n-ple product of two tensors is formed by taking the last n suffix-groups of the first, and the first n groups of the second, each with each, *i. e.* (if there are $m+n$ groups in the first tensor) the $(m+1)$th of the first with the 1st of the second, the $(m+2)$th of the first with the 2nd of the second, etc., and treating these pairs of groups separately as though to form a Grassmann product.

Thus, to take an instance at random, the double product of $\mathrm{T}^{(\mu\nu)\ (\alpha\beta\gamma)}_{(\rho\sigma)}$ and $\mathrm{E}_{\eta(\theta\phi)}$ is

$$[[\mathrm{T}\cdot\cdot\,\mathrm{E}\cdot]]^{(\mu\nu)\ (\alpha)}_{(\rho\sigma\eta)} = \mathrm{T}^{(\mu\nu)\ (\alpha\beta\gamma)}_{\rho\sigma}\mathrm{E}_{\eta(\beta\gamma)} + \mathrm{T}^{(\mu\nu)\ (\alpha\beta\gamma)}_{\sigma\eta}\mathrm{E}_{\rho(\beta\gamma)} + \mathrm{T}^{(\mu\nu)\ (\alpha\beta\gamma)}_{\eta\rho}\mathrm{E}_{\sigma(\beta\gamma)},$$

since the Grassmann product of $T_{(\rho\sigma)}$ and E_η is $T_{\rho\sigma}E_\eta + T_{\sigma\eta}E_\rho + T_{\eta\rho}E_\sigma$, and that of $T^{(\alpha\beta\gamma)}$ and $E_{(\theta\phi)}$ is $T^{(\alpha\beta\gamma)}E_{(\beta\gamma)}$.

A tensor of the second rank, whether contravariant or covariant, gives by repeated double multiplication into itself other tensors; take, for instance, any covariant tensor of the second rank, $.P_{\mu\alpha}$; from it we derive:

$$\left.\begin{aligned}
.P_{(\mu\nu)(\alpha\beta)} &= \tfrac{1}{2}[[.P_{\cdot\cdot}\,.P_{\cdot\cdot}]]_{(\mu\nu)(\alpha\beta)} \\
&= \begin{vmatrix} .P_{\mu\alpha} & .P_{\mu\beta} \\ .P_{\nu\alpha} & .P_{\nu\beta} \end{vmatrix}, \\
..P_{(\mu\nu\rho)(\alpha\beta\gamma)} &= \tfrac{1}{3}[[.P_{\cdot\cdot}\,.P_{\cdot\cdot}]]_{(\mu\nu\rho)(\alpha\beta\gamma)} \\
&= \begin{vmatrix} .P_{\mu\alpha} & .P_{\mu\beta} & .P_{\mu\gamma} \\ .P_{\nu\alpha} & .P_{\nu\beta} & .P_{\nu\gamma} \\ .P_{\rho\alpha} & .P_{\rho\beta} & .P_{\rho\gamma} \end{vmatrix}, \\
.. P_{\cdot} &= \tfrac{1}{4}[[.P_{\cdot\cdot}\,..P^{\cdot\cdot}]] = \tfrac{1}{6}[[.P_{\cdot\cdot}\,.P_{\cdot\cdot}]] \\
&= \begin{vmatrix} .P_{11} & .P_{12} & .P_{13} & .P_{14} \\ .P_{21} & .P_{22} & .P_{23} & .P_{24} \\ .P_{31} & .P_{32} & .P_{33} & .P_{34} \\ .P_{41} & .P_{42} & .P_{43} & .P_{44} \end{vmatrix},
\end{aligned}\right\} \text{(xx.)}$$

Now, by interchanging the two groups of suffixes of each of these, writing them with contravariant instead of covariant suffixes, and dividing by $..|P|$, we obtain a new series:

$$\left.\begin{aligned}
{}^{\cdot}Q^{\mu\alpha} &= \frac{..P_{(\beta\gamma\delta)(\nu\rho\sigma)}}{..|P|}, \\
{}^{\cdot}Q^{(\mu\nu)(\alpha\beta)} &= \frac{.P_{(\gamma\delta)(\rho\sigma)}}{..|P|}, \\
{}^{\cdot\cdot}Q^{(\mu\nu\rho)(\alpha\beta\gamma)} &= \frac{.P_{\delta\sigma}}{..|P|}, \\
{}^{\cdot\cdot}Q_{\cdot} &= \frac{1}{..|P|};
\end{aligned}\right\} \quad \ldots \quad \text{(xxi.)}$$

and these we find form a sequence of exactly the same kind as the P sequence ; to wit

$$\left.\begin{aligned}
{}^{\cdot}Q^{(\mu\nu)(\alpha\beta)} &= \tfrac{1}{2}\big[\big[{}^{\cdot}Q^{\cdot\cdot}\ {}^{\cdot}Q^{\cdot\cdot}\big]\big]^{(\mu\nu)(\alpha\beta)} \\
&= \begin{vmatrix} {}^{\cdot}Q^{\mu\alpha} & {}^{\cdot}Q^{\mu\beta} \\ {}^{\cdot}Q^{\nu\alpha} & {}^{\cdot}Q^{\nu\beta} \end{vmatrix}, \\
{}^{\cdot\cdot}Q^{(\mu\nu\rho)(\alpha\beta\gamma)} &= \tfrac{1}{3}\big[\big[{}^{\cdot}Q^{\cdot\cdot}\ {}^{\cdot}Q^{\cdot\cdot}\big]\big]^{(\mu\nu\rho)(\alpha\beta\gamma)} \\
&= \begin{vmatrix} {}^{\cdot}Q^{\mu\alpha} & {}^{\cdot}Q^{\mu\beta} & {}^{\cdot}Q^{\mu\gamma} \\ {}^{\cdot}Q^{\nu\alpha} & {}^{\cdot}Q^{\nu\beta} & {}^{\cdot}Q^{\nu\gamma} \\ {}^{\cdot}Q^{\rho\alpha} & {}^{\cdot}Q^{\rho\beta} & {}^{\cdot}Q^{\rho\gamma} \end{vmatrix}, \\
{}^{\cdot\cdot}|Q| &= \tfrac{1}{4}\big[\big[{}^{\cdot}Q^{\cdot\cdot}\ {}^{\cdot\cdot}Q_{\cdot\cdot}\big]\big] = \tfrac{1}{6}\big[\big[{}^{\cdot}Q_{\cdot\cdot}\ {}^{\cdot}Q_{\cdot\cdot}\big]\big] \\
&= \begin{vmatrix} {}^{\cdot}Q^{11} & {}^{\cdot}Q^{12} & {}^{\cdot}Q^{13} & {}^{\cdot}Q^{14} \\ {}^{\cdot}Q^{21} & {}^{\cdot}Q^{22} & {}^{\cdot}Q^{23} & {}^{\cdot}Q^{24} \\ {}^{\cdot}Q^{31} & {}^{\cdot}Q^{32} & {}^{\cdot}Q^{33} & {}^{\cdot}Q^{34} \\ {}^{\cdot}Q^{41} & {}^{\cdot}Q^{42} & {}^{\cdot}Q^{43} & {}^{\cdot}Q^{44} \end{vmatrix},
\end{aligned}\right\} \text{(xxii.)}$$

The relations between these two sets of tensors, considered as linear tensor operators, are important. If for instance, $.P_{\mu\alpha}{}^{\cdot}A^{\alpha} = .X_{\mu}$, $.P_{\mu\alpha}{}^{\cdot}B^{\alpha} = .Y_{\mu}$, $.P_{\mu\alpha}{}^{\cdot}C^{\alpha} = .Z_{\mu}$; $.P_{\mu\alpha}{}^{\cdot}D^{\alpha} = .W_{\mu}$, then also ${}^{\cdot}Q^{\mu\alpha}.X_{\alpha} = {}^{\cdot}A_{\mu}$, etc. ; moreover,

$$.P_{(\mu\nu)(\alpha\beta)}{}^{\cdot}\big[{}^{\cdot}A^{\cdot}\ {}^{\cdot}B^{\cdot}\big]^{(\alpha\beta)} = .\big[.X_{\cdot}.Y_{\cdot}\big]_{(\mu\nu)}$$

and

$${}^{\cdot}Q^{(\mu\nu)(\alpha\beta)}.\big[.X_{\cdot}.Y_{\cdot}\big]_{(\alpha\beta)} = {}^{\cdot}\big[{}^{\cdot}A^{\cdot}\ {}^{\cdot}B^{\cdot}\big]^{(\mu\nu)}, \text{ etc. ;}$$

$$..P_{(\mu\nu\rho)(\alpha\beta\gamma)}{}^{\cdot}\big[{}^{\cdot}A^{\cdot}\ {}^{\cdot}B^{\cdot}\ {}^{\cdot}C^{\cdot}\big]^{(\alpha\beta\gamma)} = .\big[.X_{\cdot}.Y_{\cdot}.Z_{\cdot}\big]_{(\mu\nu\rho)}$$

and

$${}^{\cdot}Q^{(\mu\nu\rho)(\alpha\beta\gamma)}.\big[.X_{\cdot}.Y_{\cdot}.Z_{\cdot}\big]_{(\alpha\beta\gamma)} = {}^{\cdot}\big[{}^{\cdot}A^{\cdot}\ {}^{\cdot}B^{\cdot}\ C^{\cdot}\big]^{(\mu\nu\rho)}, \text{ etc. ;}$$

$$..|P|\,{}^{\cdot}\big[{}^{\cdot}A^{\cdot}\ {}^{\cdot}B^{\cdot}\ {}^{\cdot}C^{\cdot}\ {}^{\cdot}D^{\cdot}\big] = .\big[.X_{\cdot}.Y_{\cdot}.Z_{\cdot}.W_{\cdot}\big]$$

and

$${}^{\cdot\cdot}|Q|.\big[.X_{\cdot}.Y_{\cdot}.Z_{\cdot}.W_{\cdot}\big] = {}^{\cdot}\big[{}^{\cdot}A^{\cdot}\ {}^{\cdot}B^{\cdot}\ {}^{\cdot}C^{\cdot}\ {}^{\cdot}D^{\cdot}\big]$$

Each Q-tensor is in fact the reciprocal of the corresponding P-tensor.

In the case of the metric tensor, $.g_{\mu\alpha}$ and $\cdot g^{\mu\alpha}$, the interchange of the two suffix-groups is inoperative, on account of the symmetry of the tensor. Between $.g_{(\mu\nu)(\alpha\beta)}$ and $\cdot g^{(\rho\sigma)(\gamma\delta)}$ the geometric mean $g_{(\mu\nu)(\alpha\beta)} = \frac{\cdot g_{(\mu\nu)(\alpha\beta)}}{\sqrt{-..|g|}}$ $= g^{(\rho\sigma)(\gamma\delta)} = \frac{\cdot g^{(\rho\sigma)(\gamma\delta)}}{\sqrt{-\cdot\cdot|g|}}$ is of importance; its type-number is 0.

§ 5. *Applications.*

The present discussion affects, of course, every branch and application of the tensor calculus; but some indication of its more striking applications may be of interest. Its chief interest certainly lies in the fact that it re-introduces into electrodynamics that similarity between electric and magnetic phenomena which does not fully appear in the usual tensor statement of the laws; since the tensor $\mathrm{F}_{\mu\nu}$ and the tensor-density $\mathbf{H}^{\mu\nu}$, on which Mie's electrodynamics rests, are both linear tensors of type -2; the tensor $\mathrm{F}_{\mu\nu\rho}+\mathrm{F}_{\mu\rho\mu}+\mathrm{F}_{\rho\mu\nu}$ and the vector density $(\mathbf{H}^{\mu\nu})_\nu$ being derived from them in exactly the same manner, by Grassmann multiplication with the symbolic vector of covariant differentiation—the tensor equivalent of Hamilton's operator, which we may conveniently write $.\nabla_\mu$. In fact, if $.\phi_\mu$ be the potential, Maxwell's equations become:

$$\left.\begin{aligned} .\mathrm{F}\cdot &= .[.\nabla.\ .\phi.]\cdot \\ .\mathrm{K}\cdot &= [.\nabla.\ .\mathrm{F}\cdot]\cdot = 0 \text{ identically,} \\ .\mathrm{C}\cdot &= .[.\nabla.\ .\mathrm{H}\cdot]\cdot \\ .\epsilon &= .[.\nabla.\ .\mathrm{C}\cdot] = 0 \text{ identically,} \end{aligned}\right\} \quad . \quad \text{(xxiii.)}$$

where the vanishing vector-density $\mathbf{K}^\mu$ has for time and space components the density and conduction flux of "magneticity," and the vanishing invariant density ϵ represents the departure from conservation of electricity.

Similarly, if the ponderomotive force be given by the covariant vector-density $\mathbf{P}_\mu$, we have

$$..\mathrm{P}. = ..[.\mathrm{F}\cdot\ .\mathrm{C}\cdot], \quad . \quad . \quad . \quad . \quad \text{(xxiv.)}$$

while the relation between field and induction is given by

$$d\,.\mathrm{L} = .[.\mathrm{H}\cdot d\,.\mathrm{F}\cdot], \quad \ldots \quad \text{(xxv.)}$$

where the invariant-density $\mathbf{L}$ is the density of the action-integral; this leads to the expression for $\mathbf{P}_\mu$ as the divergence of a mixed tensor-density $\mathbf{E}^\nu_\mu$,

$$\left.\begin{aligned} ..\mathrm{P}. &= ..[.\nabla.\,.\mathrm{E}'.]. \\ .\mathrm{E}^\nu_{\ \mu} &= .\mathrm{H}^{\nu\alpha}.\mathrm{F}_{\alpha\mu} + .\mathrm{L}\delta^\nu_{\ \mu}, \end{aligned}\right\} \quad \ldots \quad \text{(xxvi.)}$$

$\delta^\nu_{\ \mu}$ being the idemfactor, which has its four components in the principal diagonal each $=1$, and the other twelve each $=0$.

In empty space

$$\left.\begin{aligned} .\mathrm{L} &= \tfrac{1}{2} g^{(\mu\nu)(\alpha\beta)}.\mathrm{F}_{(\mu\nu)}.\mathrm{F}_{(\alpha\beta)} \\ &= \tfrac{1}{2}\,.[[g\cdot\cdot(.\mathrm{F}\cdot.\mathrm{F}\cdot)]], \end{aligned}\right\}$$

so that

$$.\mathrm{H}^{(\mu\nu)} = g^{(\mu\nu)(\alpha\beta)}.\mathrm{F}_{(\alpha\beta)}$$

or

$$.\mathrm{H}\cdot = .[g\cdot\cdot.\mathrm{F}\cdot]\cdot \quad \ldots \quad \text{(xxvii.)}$$

A further interesting point is the general law that the Grassmann product of $.\nabla.$ into any linear tensor is the same as if $.\nabla_\mu \equiv \dfrac{\partial}{\partial .\mu}$, and is consequently independent of the particular metric or affine relationship by which the covariant derivative may be defined.

The simple form assumed by Stokes's theorem is worth noting:—That whatever the operand may be, and whether the operators be applied in open or Grassmann multiplication, if $d^2\cdot\mathrm{S}\cdot$ be an element of a very small surface, and $d\cdot\sigma\cdot$ one of its bounding curves, the following operations are equivalent:

$$\int d\cdot\sigma\cdot \equiv \iint [d^2\cdot\mathrm{S}\cdot.\nabla.].$$

If the Grassmann product of each of these into a tensor operand of type -1 be formed, we have

$$\int [d\cdot\sigma\cdot.\mathrm{X}.] \equiv \iint [d^2\cdot\mathrm{S}\cdot.\nabla.\,.\mathrm{X}.],$$

which no longer applies only to very small circuits, since both sides are invariant.

Green's so-called "divergence theorem" is capable of similar treatment.

Enough has now been said to make clear the importance of the concept which we have called the Grassmann product. The many forms in which it can arise in the usual tensor notation make some clear indication of this type of product as such almost a necessity if the tensor analysis is to attain to the clarity and vigour of the old vector analyses, such as that of Gibbs; that indicated here is only intended as a suggestion, but it is hoped that it may serve to bring the point into relief more clearly than has formerly been the case.

LXXXIX. *On the Seat of the Electromotive Force in the Galvanic Cell.* *By* J. A. V. Butler, *M.Sc., University College of Swansea**.

ONE of the most disputed and discussed questions of the last century has been the seat and origin of the electromotive force of the galvanic cell and its connexion with the Volta P.D. of metals. Of the reality of the latter there is now no doubt. In the nineteenth century the centre of the controversy was whether the Volta P.D. is an intrinsic property of the metals themselves or due to other causes, *e.g.* chemical action between the metals and air at their surfaces at the moment of breaking contact. The earlier arguments have been summarized in the classical report of Lodge†. The upholders of the intrinsic P.D. view, led by Lord Kelvin‡, could point out that the Volta potential was not markedly affected by replacing air by other gases or in the best vacuum obtainable. They differentiated rightly between the true contact P.D. and the comparatively minute Peltier effect. The chemical theorists, whose position was stated most cogently by Sir Oliver Lodge§, were able to adduce the close correspondence between the Volta series and the heats of oxidation of the metals. They held that the true contact P D. between two metals was merely the equivalent of the Peltier effect. The apparent P.D. in a bath of

* Communicated by the Author.

† B. A. Reports, Montreal, 1884; Phil. Mag. [5] xix. 1835.

‡ Phil. Mag. xlvi. p. 82 (1898); Collected Works, vi. p. 110.

§ Phil. Mag. xlix. p. 351 (1900), and Proc. Phys. Soc. Lond. xvii. p. 369 (1900).

oxygen or other "oxidizing" medium was due to the differential attraction of the metals for the electro-negative oxygen. In the galvanic cell in which the oxygen was replaced by an aqueous solution, an "oxidizing liquid," a very similar state of affairs was supposed to hold.

The chemical theory of the galvanic cell was greatly strengthened by the discovery in the Gibbs-Helmholtz equation of the exact relation between the energy of the chemical process occurring in the cell and the electrical energy produced. The physico-chemical theory of Nernst, in referring the E.M.F. to processes at the electrodes analogous to solubility, served further to focus attention on these junctions as the main seat of the E.M.F., and the success of this theory in accounting for the effect of concentration and the extensive use of the galvanic cell for determining the maximum work of chemical reactions led for a time to an almost universal belief in its sufficiency.

The investigation of photoelectric phenomena has, however, resulted in the complete establishment of the reality of an intrinsic P.D. between metals of substantially the same magnitude as the measured Volta P.D The necessity for taking this into account in photoelectric experiments was first recognized by Richardson and Compton *, and in a series of particularly elegant experiments Millikan and his coworkers † conclusively demonstrated its existence by showing that, provided it is taken into account, the Einstein equation

$$\tfrac{1}{2}mv^2 = \mathrm{V}e = h\nu - \phi$$

universally holds; further, that the contact P.D. measured under the best conditions ‡ closely approximates to the relation:

$$\text{C.P.D.} = \phi_1 - \phi_2 = h(\mathrm{V}_1 - \mathrm{V}_2),$$

where ϕ_1 and ϕ_2 are the "electronic work functions," *i.e.* the amounts of work necessary to remove an electron from the metals, expressed in volts, and V_1, V_2 the "threshold frequencies."

We shall regard the existence of a contact P.D. between metals of substantially this magnitude as established. The contact P.D. does in fact differ from the quantity $\phi_1 - \phi_2$ by an amount corresponding to the Peltier effect. The relation has been discussed in another paper §. But the Peltier

* Phil. Mag. xxiv. p. 592 (1912).
† Phys. Rev. vii. p. 18 (1916); xviii. p. 236 (1921).
‡ Hennings & Kadesch, Phys. Rev. viii. p. 217 (1916).
§ Phil. Mag. October 1924.

effect never exceeds a few millivolts in magnitude and for present purposes may be neglected.

The bearing of the existence of large metal contact P.D.'s on the theory of the galvanic cell has been discussed at some length by Langmuir §. We shall here pursue a different line of thought.

In Table I. are given some representative values of the electronic work functions of the metals, which are taken

TABLE I.

Metal.	ϕ.*	${}_0\epsilon_h$.†	$\phi_{Pt}-\phi_M$.	Heat of solution, kgm. cals.	Heat of solution, volts.	Authority for heat of solution.‡
K	1·45	2·92	2·95	45·4	1·97	Mean.
Na	1·82	2·71	2·6	43·7	1·89	Mean.
Li	2·35	2·96	2·1	51·2	2·22	Mean.
Ca	2·57	2·5	1·8	65	2·82	G
Mg	2·7	1·49	1·7	55·1	2·39	R
Al	3·0	1·34	1·4	42·3	1·83	R
Zn	3·4	·76	1·0	18·2	·79	R
Cd	3·49	·40	·9	8·6	·37	R
Fe	3·7	·44	·7	10·4	·45	R
Sn	3·8	·14	·6	2·3	·10	T
Pb	3·42	·12	1·0			
Cu	4·0	−·34	·4	−8·2	−·36	Ind.
Hg	...	−·80	—			
Ag	4·1	−·80	·3			
Pt	4·4	...	—			

* Langmuir and Hughes, *loc. cit.*

† Lewis and Randall, 'Thermodynamics,' p. 433, except Ca and Mg from Abegg, Auerbach and Luther, 'Messungen Electromotorischen Kräfte'; Al, Heyrovsky, J. Chem. Soc. cxvii. p. 27 (1920).

‡ Mean = mean of values given in Landolt-Börnstein, 4th edition. G = Guntz, R = Richards, T = Thomson. Value for Cu based on reaction $CuSO_4aq+Fe=FeSO_4aq+Cu+37{\cdot}2$ cals. (T).

chiefly from a table compiled by Langmuir ‖ from the measurements available (1916) and in a few cases from Hughes ¶. More recent work has not made it possible to

§ Trans. Amer. Electrochem. Soc. xxix. p. 125 (1916).

‖ *Loc. cit.*

¶ 'Photoelectricity,' p. 40.

undertake a thorough revision of these data *. Owing to the extreme sensitiveness of thermionic and photoelectric effects to minute disturbing causes, the values of this important quantity are still barely known. The figures given can hardly be regarded as numerical data, they give merely a general idea of the order of magnitude of the quantity in question and the trend of its variations.

In the third column are the electrolytic normal potentials of the metals measured against the normal hydrogen electrode. The electrode material in this case is platinum and the metal junction that between the metal and platinum. The fourth column gives the values of this metal contact P.D. estimated from the figures in the first column.

The two sets of values exhibit a very marked correspondence, and if the figures in the first column are anything like correct, it must be concluded that the metal contact P.D. is largely responsible for the E.M.F. of the complete cell. The sum of the electrode P.D.'s, which is equal to the difference between the E.M.F. of the whole cell and the metal contact P.D., appears in most cases to be comparatively small.

It is necessary to reconcile this conclusion with the correspondence between the E.M.F. of the cell and the energy of the chemical reaction at the electrodes. This correspondence is illustrated by the last two columns of Table I., which give the heat of reaction (*i. e.*, of solution of the metal with the liberation of hydrogen) per equivalent, expressed in kilogram calories and in volts.

Now in the cell the reaction $M + H^{\cdot}aq = M^{\cdot}aq + \frac{1}{2}H_2$ is located as follows. At the metal electrode the process is simply the passage of metal ions from the metal lattice into the solution. At the metal junction the transfer of electrons from one metal to the other occurs, and at the hydrogen electrode the electrons discharge hydrogen ions, and the hydrogen atoms so formed yield diatomic hydrogen. Let the total energy changes of these processes be as follows †:

$$M \longrightarrow M^{\cdot}aq \quad , \quad U_1,$$

$$\epsilon_{M_1 \to Pt} \quad , \quad U_3 = (\phi_1 - \phi_2)F,$$

$$H^{\cdot}aq + \epsilon \longrightarrow \tfrac{1}{2}H_2, \quad U_2.$$

* Some recent determinations may be quoted:—
Roy (Phil. Mag. xlvii. p. 561, 1924): Na 2·15 (T), 2·26 (P); Ca 2·86 (T), 3·34 (P); Pt 4·25 (T), 4·42 (P). Young (Proc. Roy. Soc. A, civ. p. 611): K 1·1 (T), 1·98 (P).

T = thermionic measurements.
P = photoelectric measurements.

† Convention as to sign: U is written positive if the total energy increases in the process, *i. e.* heat absorbed.

It may be as well to point out that by the "total energy change" at a junction is meant the heat effect when no electrical work is done. In the galvanic cell only a small part of the energy of the reaction is liberated in the cell as heat.

The sum of the total energy changes throughout the cell is equal to the heat of the reaction Q; *i. e.*,

$$U = -Q = U_1 + (\phi_1 - \phi_2)F + U_2.$$

The sum of the energy changes at the two electrodes ($U_1 + U_2$) might be got by subtracting the electronic work difference of the metals from the whole heat of the reaction. But a partly independent estimate of the energy change in the passage of metal ions into solution can be obtained according to the following scheme :—

The metal is vapourized (heat absorbed S) and the metal vapour thereupon ionized (heat of ionization J). The

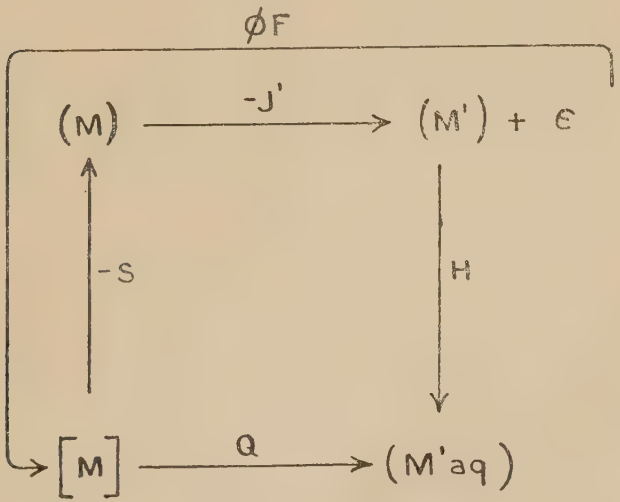

electrons are returned to the metal (heat evolved ϕF) and the metal ions dissolved in water (heat of hydration H).

The total energy change in the passage of metal ions from the metal into the solution is evidently

$$Q_1 = H + \phi F - J - S.$$

Table II. gives the data for the calculation of Q_1 for a number of metals.

TABLE II.

	S.	H.	J.	$n\phi$F.	Q_1+HCl'.
$K\rightarrow K^{\cdot}$	26·9	184	99	33	91
$Na\rightarrow N\dot{a}$.....	30	204	117	42	99
$Li\rightarrow L\dot{i}$	50	237	123·1	54	118
$Ca\rightarrow C\ddot{a}$.....	35	570	411	2×59	$\frac{242}{2}=121$
$Mg\rightarrow M\ddot{g}$ ...	50	672	519	2×62	$\frac{227}{2}=113$
$Zn\rightarrow Z\ddot{n}$.....	35·8	731	666	2×78	$\frac{182}{2}=91$
$Cd\rightarrow C\ddot{d}$.....	31·2	678	634	2×80	$\frac{173}{2}=87$
$Pb\rightarrow P\ddot{b}$.....	57·4	598	548	2×79	$\frac{151}{2}=76$
$Cu\rightarrow C\ddot{u}$.....	83·4	247	177	2×92	$\frac{171}{2}=86$
$Ag\rightarrow A\ddot{g}$.....	63·3	209	173	94	67

The values of J and S are those of Grim* and are the same as those employed in the calculation of H. The heat of hydration of any single metal ion is not known with any certainty, but the sum of the heats of hydration of the two ions constituting a salt can be easily obtained when the lattice energy and heat of solution are known†. The figures given refer to the chloride and differ from the true heat of hydration by a constant amount per equivalent, namely the heat of hydration of the chloride ion.

Owing to the great uncertainties about the value of ϕ the final figures can only be taken as indicating the general order of magnitude of the effect. It has been estimated, assuming that the absolute P.D. of the normal calomel electrode is +·56, that the heat of hydration of the chloride ion is 77. If this value is approximately correct, it will be seen that the energy of the process occurring at metal electrodes is in most cases comparatively small and not in general greater than the heats of solution of metal salts. It may also be observed that the values show a general trend in the direction of the voltaic series.

No stress can be laid on the figures themselves, but it is evident that from the point of view of the energy changes concerned there is no difficulty in regarding the metal metal P.D. as an important contributor to the E.M.F. of the galvanic cell, and the forces operating at the metal electrode

* *Zeits. Phys. Chem.* cii. p. 113 (1922).

† The heats of hydration are taken from a paper by the author which will appear shortly in *Zeits. Phys. Chem.*

essentially the same as those concerned in the solubility of salts.

It remains to coordinate the statistical expressions for the P.D. at the different types of junctions in such a cell as that which has been considered which have been worked out in previous papers.

The Statistical Theory of the Galvanic Cell.

Consider the cell

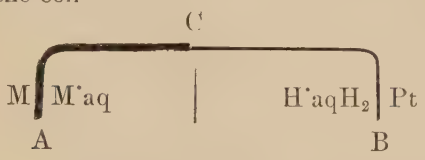

(1) Metal solution junction A. The passage of metal ions from the metal electrode into the solution is regarded as a process in every respect similar and involving similar forces to those coming into play in the ionic equilibrium between a salt crystal and solution. From this point of view * it can be shown that the Nernst conception does not involve any physical impossibility such as has been supposed in connexion with the calculated "solution pressures." The following equation is obtained expressing the P.D. at the surface at equilibrium, *i. e.* when metal ions reach and leave the surface at the same rate :—

$$e_1 = \frac{U_1}{nF} + \frac{RT}{nF}\log_e K_1 + \frac{RT}{nF}\log_e C, \quad . \quad . \quad . \quad . \quad (1)$$

where K_1 = a constant determined by the "statistical conditions,"

C = metal ion concentration in the solution.

(2) Hydrogen electrode B. The mechanism of the interchange of electrons between substances in two states of oxidation has also been considered †, and an analogous equation has been deduced :

$$e_2 = -\frac{U_2}{nF} + \frac{RT}{nF}\log_e K_2 + \frac{RT}{nF}\log_e \frac{c_1}{c_2},$$

where c_2 and c_1 are the concentrations of the reduced and oxidized molecules concerned respectively. The case of gas

* "The Kinetic Interpretation of the Nernst Theory of E.M.F.," Trans. Faraday Soc. xix. p. 729 (1924).

† "A Kinetic Theory of Reversible Oxidation Potentials at Inert Electrodes," Trans. Faraday Soc. xix. p. 734 (1924).

electrodes is rather more complex, involving the dissociation of the diatomic gas, the mechanism of which is obscure. But it is not unreasonable to assume that the relation between the P.D. and the total energy change is of the same form as (2), *i. e.*, we shall write

$$e_2 = -\frac{U_2}{nF} + \frac{RT}{nF}\log_e K_2 + \frac{RT}{nF}\log_e \frac{[H^+]}{[H_2]^{\frac{1}{2}}}. \quad . \quad . \quad (2)$$

(3) Metal-metal junction C. Finally an expression has been deduced * for the P.D. at metal junctions :

$$e_3 = -\frac{U_3}{nF} + \frac{RT}{F}\log_e K_3, \quad . \quad . \quad . \quad . \quad (3)$$

where $U_3 = (\phi_1 - \phi_2)F$, the total energy change in the passage of electrons from the one metal to the other.

Summing the equations for the P.D.'s at the three junctions we obtain for the E.M.F. of the whole cell

$$E = e_1 - e_2 - e_3 = \frac{U}{nF} + \frac{RT}{nF}\log_e C - \frac{RT}{nF}\log_e \frac{[H^+]}{[H_2]^{\frac{1}{2}}} + \frac{RT}{nF}\log_e K, \quad . \quad . \quad (4)$$

which on differentiation gives the Gibbs-Helmholtz equation

$$E - \frac{U}{nF} = T\frac{dE}{dT}.$$

It is thus possible on these lines to reconcile completely the different theories which emerged in the long controversy about the seat of the E.M.F. in the galvanic cell. The "contact" and "chemical" theorists each laid stress on one aspect of the truth, and their conceptions are mutually complementary and in no way inconsistent. The correspondence between the energy of the chemical reaction going on in the cell and the E.M.F. is adequately accounted for, while the Nernst conception of the origin of the E.M.F. remains a fairly accurate representation of the process at soluble metal electrodes.

In conclusion two consequences of this theory may be noted. In the first place the expression (2) for the P.D. of an oxidation-reduction process at an inert electrode involves the electronic work function of the electrode metal †. The

* Phil. Mag. October 1924.

† Since $U_2 = (V - \phi)F + H_{M''} - H_{M'}$, where V = "ionization potential" of reduced substance in solution, $H_{M'}$ and $H_{M''}$ the heats of hydration of the two molecules concerned.

effect of varying the material of the electrode metal on oxidation potentials has not been extensively investigated, although several metals of the platinum group have been employed by various investigators and no difference has been observed. It is evident that when the metal-metal junction is taken into account any variation in the nature of the electrode metal will equally affect the P.D.'s at its two ends. Therefore the E.M.F. of a cell involving a reversible oxidation process at an inert electrode is not dependent on the electrode material *.

Secondly, in attempts which have been made to determine the absolute P.D.'s at electrodes the possibility of metal contact P.D 's between the standard and the experimental electrode metals has not been taken into account. By means of different methods involving the preparation of null solutions at mercury electrodes the P.D. of the normal calomel electrode has been located at about +0·56 volt†. On the other hand, using silver powder in the dropping electrode Billitzer ‡ found a different value, about +0·1 volt. It has been objected that silver in a finely divided form may not exhibit its true electrolytic P.D., but recently Garrison §, making use of a method to which this objection does not apply, has obtained a result in substantial agreement with Billitzer's. It is suggested that the metal contact P.D. between silver and mercury might account for the discrepancy. Unfortunately, it is not possible at present to estimate this P.D. from the available data with any assurance.

Summary.

It is shown that the existence of large metal contact P.D.'s is in no way inconsistent with the correspondence between the E M.F. of a galvanic cell and the energy of the chemical reaction occurring therein. The statistical expressions deduced in previous papers for the different junctions are coordinated, and a theory of a typical galvanic cell is outlined which includes as different aspects of the whole truth (1) the metal contact P.D. theory, (2) the "chemical" theory, (3) the Nernst theory of metal electrode P.D.'s, (4) the relation between E.M.F. and total energy change expressed in the Gibbs-Helmholtz equation.

* Experiments to test this deduction are in progress.

† Ostwald and Paschen, *Zeits. Phys. Chem.* i. p. 583 (1887); Palmaar, *ibid.* lix. p. 129 (1907).

‡ *Zeits. Phys. Chem.* xlviii. p. 513 (1904); li. p. 166 (1905). *Zeits. Electrochem.* viii. p. 638 (1902); also Freundlich and Mäkelt, *Zeits. Electrochem.* xv. p. 161 (1909).

§ J. Amer. Chem. Soc. xlv. p. 37 (1923).

XC. *Contribution to the Kinetic Theory of Vaporization.* *By* Samuel Clement Bradford, *D.Sc., The Science Museum, London, S.W.* 7 *.

MODERN research on the electrical structure of matter has confirmed the view of van der Waals that molecules are surrounded by fields of force. And in previous papers † preliminary attempts have been made to study the properties of solutions in relation to molecular attraction, or cohesion pressure, and motion. Strong evidence has been obtained that solution is due to the diminution of the surface energy of the solute by the counter attraction of the solvent, so that a larger number of solute particles have sufficient energy normal to the surface to enable them to overcome the attraction of the solute and escape into the solvent. A general formula was deduced for the force opposing solution, by means of which, the majority of substances can be arranged in the order of their solubility, and, as a necessary consequence, in the order of all the other properties of solutions. For not only do such properties as solubility, degree of hydration, heat of solution, molecular volume, and compressibility follow the order of cohesion pressures, but so also do the depression of the freezing-point, elevation of the boiling-point, diminution of vapour-pressure, and electrical conductivity. It was possible to calculate the effect, on the freezing-point of aqueous salt solutions, of the altered cohesion pressure due to the different field of force of the solute particles ; and this effect was found to be the same as the observed increase in the depression below the normal depression caused by the presence of a solute with a cohesion not differing greatly from that of water. This appears to be a possible explanation of the so-called anomaly of the strong electrolytes.

It was pointed out that, if the work done by a particle of solute escaping into solution could be calculated, the critical velocity, normal to the surface, necessary to carry it into the solution could be determined. This supposes that it should be possible to calculate the effects of any redistribution of forces between the molecules of the two kinds in a solution, and to allow for any change in the aggregation of the particles of either kind.

Having deduced an expression for the critical velocity, it should be possible to determine the distribution of particles between the solute and its solution and obtain a formula for

* Communicated by the Author.

† Phil. Mag. xxxviii. p. 696 (1919) ; xliv. p. 897 (1922).

the solubility of a given substance in a given solute. This distribution should be of the same nature as the distribution of particles between a liquid and its vapour. However, Dieterici's attempt to deduce a formula for the latter case was unsuccessful, and this simpler equilibrium needs further study before attempting to obtain a formula for solubility. The present paper, therefore, is devoted to the consideration of the vaporization of a liquid.

We will suppose that the liquid, in contact with its vapour only, is maintained within an enclosure at a constant temperature under ordinary laboratory conditions; so that, if heat be abstracted from the liquid by the escaping particles of vapour, it will be supplied immediately from the enclosure, while simultaneously any gain of temperature by the vapour will be compensated.

According to Maxwell's law of the distribution of velocities, the number of particles in unit volume of the liquid that have velocities whose vertical components lie between u and $u + du$ is

$$\frac{n_s}{V_{ps}\sqrt{\pi}} e^{-\frac{u^2}{V_{ps}^2}} du, \quad . \quad . \quad . \quad . \quad . \quad . \quad . \quad \text{(i)}$$

where n_s is the concentration of liquid particles, and V_{ps} Maxwell's most probable speed of the particles. The number of particles in unit volume of vapour in the same condition is

$$\frac{n_l}{V_{pl}\sqrt{\pi}} e^{-\frac{u^2}{V_{pl}^2}} du, \quad . \quad . \quad . \quad . \quad . \quad . \quad . \quad \text{(ii)}$$

n_l being the concentration of the vapour, and V_{pl} Maxwell's constant for the vapour phase. Therefore, the number of liquid particles per unit volume, having velocities normal to the surface between u and du, that strike the surface from below is

$$\frac{n_s}{V_{ps}\sqrt{\pi}} e^{-\frac{u^2}{V_{ps}^2}} u\, du.$$

But, of all the particles that strike unit area of the surface of the liquid from below, only those that have velocities normal to the surface equal to, or greater than, a certain critical velocity, s, will be able to escape from the attraction of the liquid and pass into the vapour. The total number of such particles is

$$\int_s^\infty \frac{n_s}{V_{ps}\sqrt{\pi}} e^{-\frac{u^2}{V_{ps}^2}} u\, du = \frac{n_s V_{ps}}{2\sqrt{\pi}} e^{-\frac{s^2}{V_{ps}^2}} \quad . \quad . \quad \text{(iii)}$$

Now, the total number of particles from the vapour that strike the same area is, from (ii),

$$\int_0^\infty \frac{n_l}{V_{pl}\sqrt{\pi}} e^{-\frac{u^2}{V_{pl}^2}} u\,du = \frac{n_l V_{pl}}{2\sqrt{\pi}}, \quad . \quad . \quad . \quad \text{(iv)}$$

and the greater attraction of the liquid phase ensures that all these return to it.

In equilibrium the number of particles escaping from the liquid must be equal to the number returning, so that, from (iii) and (iv),

$$\frac{n_s V_{ps}}{2\sqrt{\pi}} e^{-\frac{s^2}{V_{ps}^2}} = \frac{n_l V_{pl}}{2\sqrt{\pi}}$$

$$\text{or} \qquad n_l = n_s \frac{V_{ps}}{V_{pl}} e^{-\frac{s^2}{V_{ps}^2}} \quad . \quad . \quad . \quad . \quad \text{(v)}$$

It has been assumed that because the particles in a pure liquid are surrounded on all sides by similar particles, the resultant attraction at any point in the interior of a liquid is zero. From which it has been inferred that the average kinetic energy of a particle in a liquid is the same as in the perfectly gaseous state at the same temperature. However, Kleeman * has shown that this is not the case, because the particles in a liquid do not remain at equal distances apart, and, except when passing through points at which the molecular forces vanish, the particles are under the influence of attraction. Therefore in equation (v) we may not write $V_{ps}=V_{pl}$, but

$$V_{ps}=\lambda V_{pl}, \quad . \quad . \quad . \quad . \quad . \quad . \quad \text{(vi)}$$

where λ is a factor that will vary with the nature of the substance. Let v_l be the volume occupied by the number, N, of molecules in a gramme molecule of the substance in the vapour state, and v_s the volume of the same number of molecules in the liquid condition, then

$$n_l = \frac{N}{v_l - b_l} \quad \text{and} \quad n_s = \frac{N}{v_s - b_s},$$

where b_l and b_s are the apparent volumes of the molecules in either state, defined by Kleeman † as the quantities whose magnitudes affect the external pressure at constant temperature and volume, but not the average velocity of translation of the molecules.

* Phil. Mag. xxiv. p. 101 (1912).

† 'A Kinetic Theory of Gases and Liquids.' New York, 1920.

Equation (v) may then be written

$$v_s - b_s = (v_l - b_l)\lambda e^{-\frac{s^2}{\lambda^2 V_{pl}^2}},$$

or, putting $v_s - b_s = \Phi_s$ and $v_l - b_l = \Phi_l$,

$$\Phi_l = \Phi_s \lambda e^{\frac{s^2}{\lambda^2 V_{pl}^2}} \quad . \quad . \quad . \quad . \quad . \quad . \quad . \quad \text{(vii)}$$

As a first approximation we may take V_{pl}, the most probable speed of the particles in the vapour, as equal to V_p, the most probable speed in a perfect gas, so that

$$V_{pl}^2 = \left(\frac{V}{1{\cdot}23}\right)^2,$$

where V is the average kinetic energy velocity in the gaseous state and fulfils the condition that

$$\tfrac{1}{2}mV^2 = 2{\cdot}012 \times 10^{-16}T,$$

m being the absolute weight of a particle and T the absolute temperature.

To determine s we have

$$\tfrac{1}{2}ms^2 = W,$$

where W is the work done by a particle in passing from the liquid into the vapour. From these relations we find that the index of e in (vii) is

$$\frac{s^2}{\lambda^2 V_{pl}^2} = \frac{7{\cdot}52 \times 10^{15} W}{\lambda^2 T},$$

and, therefore,

$$\Phi_l = \Phi_s \lambda e^{\frac{7{\cdot}52 \times 10^{15} W}{\lambda^2 T}} \quad . \quad . \quad . \quad . \quad . \quad . \quad \text{(viii)}$$

The pressure of the vapour in dynes per sq. cm. is given by the equation

$$p = \frac{V_t}{V} \cdot \frac{RT}{\Phi_l} = 8{\cdot}315 \times 10^7 \frac{V_t T}{V \Phi_l}, \quad . \quad . \quad . \quad \text{(ix)}$$

where V is Kleeman's total average velocity of a molecule in the vapour. Again approximately, we may take $V_t = V$, so that, from (viii) and (ix), and remembering that 1 atmosphere $= 1{\cdot}016 \times 10^6$ dynes per sq. cm., the vapour-pressure in atmospheres is

$$p = 81{\cdot}87 \frac{T}{\lambda \Phi_s} e^{-\frac{7{\cdot}52 \times 10^{15} W}{\lambda^2 T}} \quad . \quad . \quad . \quad . \quad . \quad \text{(x)}$$

We now have to determine W, the work done against the

attraction of the liquid by a particle escaping from the liquid into the vapour.

If all the molecules of the liquid are in continual rapid motion, their rotational velocity will insure that a spherical space of diameter δ is kept clear around the centre of rotation of each molecule. Two molecules collide when their centres come to a distance δ apart *. Since the molecules are electrically neutral, they will repel in some orientations and attract in others. The attractions will preponderate over the repulsions because the duration of the attractive encounters is greater. If we consider a space element dv at a definite position relative to a given molecule, the molecules with their centres within dv will be continually changing their position and attractive forces. In a sufficiently long interval of time, any point within dv will have been occupied by a molecular centre as often as any other point, and the average value of the force at that point will be the same as at any other point. We are concerned, not with the instantaneous values of the attraction, but only with the average attraction during a reasonably long interval of time. The space element dv may be situated at any distance from the attracted molecule equal to or greater than δ. Edser † has shown that the properties of liquids are explained by the assumption that the average attraction between two molecules whose centres are at a distance r is

$$f = \frac{c}{r^8},$$

where $c = \frac{6K\delta^4}{\pi N^2}$, K being the cohesion of the liquid, and N the number of molecules per unit volume.

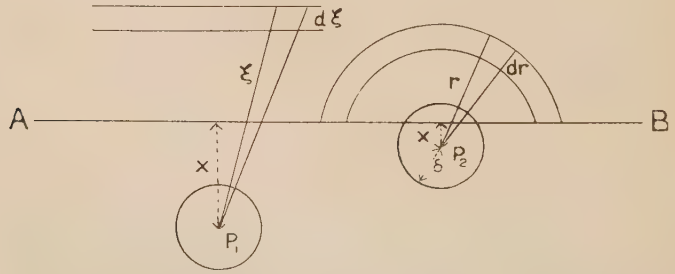

In the figure above, let P_1 represent the centre of a molecule

* Actual collision may not be the rule, and δ may be the mean of the nearest distances of the centres during a considerable number of encounters.

† "Molecular Attraction and the Physical Properties of Liquids," Brit. Assoc. 4th Report on Colloid Chemistry, p. 40 (1922).

at a distance x below the surface AB of the liquid, where $x > \delta$. The attraction of the liquid on P may be taken as equal and opposite to the attraction that would be exerted by a continuous mass of liquid above AB. Describe two planes parallel to AB at distances ξ and $\xi + d\xi$ above AB. Then the molecules whose centres would lie between these planes would exert on P_1 a resultant attraction equal to

$$\frac{2\pi c N d\xi}{(x+\xi)^6} \int_0^{\pi} \cos^6 \sin\theta \, d\theta = \frac{2\pi c N d\xi}{7(x+\xi)^6}.$$

The attraction per unit area exerted on P_1 by all the molecules whose centres would lie above AB would be equal to

$$\frac{2\pi c N}{7} \int_0^{\infty} \frac{d\xi}{(x+\xi)^6} = \frac{2\pi c N}{35 x^5} \quad . \quad . \quad . \quad . \quad \text{(xi)}$$

When the distance below AB of the escaping molecule becomes less than δ, as at P_2, the procedure needs to be modified. Around P_2 describe a sphere of radius δ; the section of this sphere above the plane AB will contain no centres of attracting molecules. With P_2 as centre describe spheres with radii r and $r + dr$, where $r > \delta$. The resultant attraction by molecules whose centres lie between these spheres is

$$\frac{2\pi c N dr}{r^6} \int_0^{\cos^{-1}\left(\frac{x}{r}\right)} \cos\theta \sin\theta \, d\theta = \frac{\pi c N dr}{r^6}\left(1 - \frac{x^2}{r^2}\right),$$

and the total attraction on P_2 by all molecules whose centres would lie above AB is

$$\pi c N \int_{\delta}^{\infty} \left(\frac{1}{r^6} - \frac{x^2}{r^8}\right) dr = \pi c N \left\{\frac{1}{5\delta^5} - \frac{x^2}{7\delta^7}\right\}.$$

The work done by the molecule at P in escaping to the surface of the liquid is, therefore,

$$\frac{2\pi c N}{35} \int_{-\infty}^{-\delta} \frac{dx}{x^5} - \pi c N \int_{-\delta}^{0} \left(\frac{1}{5\delta^5} - \frac{x^2}{7\delta^7}\right) dx = \frac{29\pi c N}{210\delta^4}. \quad \text{(xiii)}$$

An equal amount of work must be done in escaping completely from the surface to infinity. So that, neglecting the small attraction of the vapour, the total work done by a particle of liquid passing into the vapour is

$$W = \frac{29\pi c N}{105\delta^4} \quad . \quad . \quad . \quad . \quad . \quad . \quad \text{(xiv)}$$

Making use of the relations

$$c=\frac{6K\delta^4}{\pi N^2} \quad \text{and} \quad N=6{\cdot}23\times10^{23}\frac{\rho}{M},$$

where ρ is the density of the liquid and M its molecular weight, we have

$$W=2{\cdot}66\times10^{-23}\frac{KM}{\rho},$$

and therefore from (x)

$$p=81{\cdot}87\frac{T}{\lambda\Phi_s}e^{-\frac{2{\cdot}000\times10^{-8}KM}{\lambda^2\rho T}} \quad . \quad . \quad . \quad . \quad (xv)$$

In this formula there is one variable, λ, that is practically unknown. Kleeman has attempted to calculate the ratio of V_t to V_a for CO_2 at 112 atmospheres, and finds it equal to about 1·6. This figure is rather too high for use in the present formula, though probably more accurate analysis would introduce other factors. Moreover, we have to allow for the variation of λ with the nature of the liquid. It is necessary to make an assumption. Accordingly we suppose that, for densities between about 0·6 and 1·0, λ^2 is proportional to the density of the liquid, or

$$\lambda^2=\mu\rho. \quad . \quad . \quad . \quad . \quad . \quad . \quad (xvi.)$$

If μ is given the value 2·012, very good agreement of the calculated with the experimental data is obtained.

There is, then, the further difficulty that different methods of calculating K give values for the same liquid at the same temperature which are altogether incompatible. For instance, the following figures for $K\times10^{-9}$ have been found by different workers to three places of decimals :—

Toluene	1·554
	2·426
	1·710
	2·210
	3·570
Acetic acid	2·977
	1·919
	4·786
	2·100
	5·960
	7·140
Water	6·375
	12·450
	3·645
	11·600
	17·300

Since the cohesion occurs exponentially in the formula, it is obvious that such methods of determining K are useless for the present purpose. Fortunately, however, Edser has obtained a relation between surface tension and cohesion,

$$S = \frac{K\delta}{4},$$

which he has shown to give values of S as near the experimental results as could be expected, considering the uncertainty attaching to the magnitude of the cohesion. And, if surface tension is indeed the outward expression of the internal molecular forces, it is likely that the cohesion of liquids can be calculated with considerable accuracy from the observed values of their surface tensions. Consequently, in the present paper, the cohesion has been determined from the formula

$$K = \frac{4S}{\delta} \quad . \quad . \quad . \quad . \quad . \quad . \quad . \quad . \quad \text{(xvii)}$$

And the figures given in the table at the end confirm the expectation that this is by far the best means known of determining this quantity.

To calculate δ, Edser uses the formula

$$\delta = \left(\frac{3{\cdot}24M}{2{\cdot}016\rho_m}\right)^{1/3} \times 10^{-8} \text{ cm.},$$

where M is the molecular weight, and ρ_m the density near to the freezing-point.

Finally, to reduce the vapour-pressure formula to a form suitable for calculation, the factor A must be introduced to allow for the molecular aggregation of the liquid. Then by making use of the relations (xvi) and (xvii), and putting

$$V = \frac{M}{\rho} \quad \text{and} \quad \delta' = \delta \times 10^8,$$

we obtain

$$p = 56{\cdot}47 \frac{T}{\Phi_s \rho^{1.2} A} e^{-\frac{3{\cdot}806 S V_A^{2/3}}{T\delta'\rho}} \quad . \quad . \quad . \quad \text{(xviii)}$$

In this expression the values of all the variables can be ascertained with tolerable accuracy, excepting those of Φ_s or $(v-b)$ and A. This indicates the need for further research on co-volume and association.

As the former does not occur exponentially, its importance is not so great in the present instance, and it is possible to use a tentative expression for its evaluation, which is

deduced as follows. Kleeman suggests that the apparent molecular volume, v_0, at absolute zero is a superior limit of the apparent volume, b, at higher temperatures. He obtains approximate values of v_0 from the coefficient of expansion. For carbon dioxide and benzene he finds $v_0=25{\cdot}5$ and $70{\cdot}6$ c.c. respectively. The corresponding figures for a single molecule are $v_0'=41{\cdot}1\times10^{-24}$ and 114×10^{-24} c.c. The following table shows the molecular diameters $(v_0')^{1/3}\times10^{-8}$ for these substances as well as for ether and carbon tetrachloride. For comparison, the third column gives Edser's values of δ, and the fourth column the ratio $\dfrac{(v_0')^{1/3}}{\delta}$.

Substance.	$(v_0')^{1/3}\times10^{-8}$.	$\delta\times10^{-8}$.	Ratio.
Carbon dioxide	3·44	4·144	·832
Benzene	4·84	5·192	·932
Ether	4·87	5·277	·925
Carbon tetrachloride	4·88	5·313	·920

It will be seen that δ is somewhat larger than Kleeman's superior limit of b, and that the ratio for the three liquid substances is practically constant at 0·926. It is inferred that $0{\cdot}926\delta$ is the superior limit of b. In another place Kleeman makes an estimate of the actual size of b for carbon dioxide from determinations of n, the number of molecules crossing a square centimetre from one side to the other in a second, and V_t, the total average velocity of a molecule. This second estimate is likely to be more accurate than the former. For carbon dioxide at 0° he finds $b=12{\cdot}2$ c.c. instead of 25·5 as determined from the coefficient of expansion. It is probable, therefore, that 0·926 is about twice the true volume of b for a single molecule, or for a gramme molecule

$$b=\tfrac{1}{2}(0{\cdot}926\delta)^3\times10^{-24}\times6{\cdot}23\times10^{23}$$
$$=0{\cdot}248\delta^3.$$

It does not seem possible yet to allow for change of b with temperature. In the present paper, therefore, the co-volume is taken as

$$\Phi=v-\frac{\delta^3}{4}. \quad . \quad . \quad . \quad . \quad . \quad . \quad . \quad \text{(xix)}$$

Although some modification will be necessary in the light of greater knowledge of the nature of liquids and more capable analysis, it seems probable that the mechanism of vaporization is very much as has been suggested above. On applying the formula (xviii) to substances such as ether, *n*-hexane, and *p*-xylene, which are practically unassociated and for which A is therefore nearly unity, values for the vapour-pressure at any temperature are obtained which agree extraordinarily well with the experimental figures and become equal to one atmosphere at the boiling-point, as shown in columns eleven and twelve of the table which follows. If the calculated and observed vapour-pressures differ, association is indicated. Unfortunately, again, molecular aggregation has been studied very little. Most methods of calculating association have slight theoretical basis, and the various processes give values differing by fifty or a hundred per cent. Since the present formula is particularly sensitive to slight differences in association, the expression may be used as a means of calculating A. This has been done in the table. It will be seen that the values given in column nine differ very little from those calculated by Ramsay and Shields *, or Traube †, which are added in column ten for comparison. For instance, Ramsay and Shields's figure, 1·05, for benzene corresponds to a vapour-pressure of 82 mm. instead of 74, as observed by Young and Regnault, which requires A to be equal to 1·065. This agreement is further confirmation of the truth of the vapour-pressure formula. It may be noted that the figures obtained by Ramsay and Shields were modified subsequently, but it is probable that the earlier values are nearer the truth. The theory will be of use in calculating the effects of the cohesions of salts on the vapour-pressures of their solutions. And it will be possible to ascertain whether the observed increases in the diminution of the vapour-pressure or elevation of the boiling-point, like the increases in the depression of the freezing-point, beyond those due to a neutral solute, are due merely to the cohesions of the salt particles being greater than that of the solvent.

The data for the surface-tensions and densities were taken where possible from Jaeger's ‡ results; the other figures from the new edition of Landolt and Börnstein's *Tabellen*. The higher temperatures given in the third column of the table are the boiling-points of the respective liquids; the densities at these temperatures were extrapolated from Jaeger's data. The rather low boiling-point quoted for toluene suggests that this substance was slightly impure or moist.

* J. C. S. lxiii. p. 1089 (1893). † *Ber.* xxx. p. 265 (1897).
‡ *Zeitsch. anorg. Chemie*, ci. p. 1 (1917).

Substance.	Molecular weight M.	Temperature Centigrade.	Density ρ.	Molecular volume V.	δ'.	Co-volume Φ.	Surface-tension S.	Association calculated		Vapour-pressure.			
										Calculated.		Observed.	
								from vapour-pressure.	by other methods.	Atmo-spheres.	mm.	Atmo-spheres.	mm.
Ether	74·08	34·8	·698	106·13	5·277	69·39	15·9	1·00		1·04		1·00	
		20·5	·758	97·73	5·277	60·99	21·5	1·00			74		c. 68
n-Hexane ...	86·12	20	·660	130·6	5·905	79·10	17·41	1·00			100		120
p-Xylene ...	106·08	136·2	·757	140·13	5·555	97·28	18·1	1·00		1·00		1·00	
		25·7	·857	123·68	5·555	80·83	29·1	1·00			14		—
Toluene	92·06	109·4	·780	111·13	5·383	79·12	19·5	1·00		1·32		1·00	
		26	·860	107·05	5·383	68·06	28·4	1·00			48		48
Benzene	78·05	80·5	·810	96·36	4·946	66·09	20·7	1·065		1·00		1·00	
		20	·878	88·90	4·946	58·63	28·7	1·065	1·05 R & S		75		75
Acetone ...	58·05	56	·710	81·76	4·618	57·14	19·4	1·05		1·02		1·00	
		20	·778	74·61	4·618	49·99	21·9	1·27	1·26 R & S		175		179
Ethyl acetate	88·06	77·1	·816	107·9	5·360	69·4	17·2	1·00		0·95		1·00	
		25·1	·893	98·61	5·360	60·12	22·2	1·43			94		95
Pyridine.....	79·05	114·5	·882	89·73	4·911	63·12	25·2	1·18		1·00		1·00	
Aniline	93·04	184	·867	107·80	5·253	71·60	24·3	1·30		0·99		1·00	
		43·1	1·000	93·04	5·253	56·80	40·8	1·60	1·35 T		1		1
Alcohol	46·05	78·4	·737	62·48	4·641	37·49	17·0	2·17		1·01		1·00	
		25	·786	58·59	4·641	33·60	21·3	2·46	2·43 R & S		60		59
Water	18·02	100	·958	18·80	3·079	11·50	58·92	2·30	2·66 R & S	1·01		1·00	
		20	·998	18·06	3·079	10·76	70·6	2·60	3·44 R & S		16·9		17

Summary.

The kinetic theory has been applied to obtain a quantitative expression for the vapour-pressure of liquids in the form

$$\rho = 56{\cdot}47\,\frac{T}{\Phi\rho^{1/2}A}\,e^{-\frac{3{\cdot}806SVA^{2/3}}{T\delta'\rho}},$$

where

T is the absolute temperature,
Φ the co-volume,
ρ the density,
A the degree of association,
S the surface-tension,
V the volume of a gramme molecule, and
$\delta' \times 10^8$ the nearest distance of approach of the centres of two molecules of the liquid.

Vapour-pressures calculated by means of the formula agree very well with the values observed at given temperatures, and become equal to an atmosphere at the boiling-points of the liquids.

Edser's formula $S = \frac{K\delta}{4}$ may be used to calculate the cohesion of liquids with considerable accuracy.

XCI. *Investigations on the Latent Photographic Image.*—Part I. *The Relation between the Light Frequency and Number of Developable Centres. By* F. C. Toy, *D.Sc., F.Inst.P., and* H. A. Edgerton*.

(Communication No. 39 from the British Photographic Research Association Laboratories.)

THE relation between the number of developable centres (n) in a photographic emulsion and the wave-length (λ) or frequency (ν) of the light which produces them is one of the most important problems in the development of photographic theory. Not many attempts have yet been made along this line. The relationships between n and λ which are vital to the light dart theory as developed by Silberstein (Phil. Mag. xliii. p. 257, xliv. p. 956, 1922; xlv. p. 1062, 1923) have been shown definitely not to hold (Trans. Faraday Soc. xix. p. 290, 1923). The experimental values of n at different values of λ and at constant intensity, all

* Communicated by Dr. T. Slater Price, O.B.E., D.Sc., F.R.S.

other factors being constant, have been shown to be widely different from those which the light dart theory demands, and it seems that the latter can no longer be seriously considered as a basis for theoretical considerations.

In a paper read before the Faraday Society (*ibid.*) it was suggested by one of us that the true relation between n and λ could not be established without a consideration of the quantity of energy which is *absorbed* by the silver halide itself; especially is this so in view of the fact that the light absorption by the silver halides varies enormously with the frequency. Consider for a moment a given intensity of radiation falling on the silver halide grains. Under certain fixed conditions a given number of centres is produced. Now, if the frequency of the radiation is changed without changing anything else, the alteration in the number of centres produced may be due to two causes:—

(1) It is certainly due mainly to the great change in the quantity of energy available for their formation (*i. e.* the amount absorbed).

(2) It may also be due to the change in frequency, *as such*, which would be expected on the quantum hypothesis.

The object of this investigation is to determine whether the observed relation between the frequency and number of centres produced (with incident intensity and all other variables constant) can be explained by these two factors.

The first problem, then, is to find what fraction of the total amount of incident energy of different frequencies is absorbed by the grains when equal intensity of each light is incident on the surface of the single layer photographic plate. This can be calculated, at any rate approximately, since the refractive indices and extinction coefficients of the gelatin and silver halide crystal are known. The problem divides itself into two parts:—

(*a*) The determination of the reflexion and absorption losses due to the gelatin.

(*b*) The reflexion from, and absorption by, the silver halide grains.

We shall consider in this paper only the case of a pure silver bromide emulsion (*i. e.* one containing silver bromide as the only silver halide) with uniform flat grains. The radiations which will be used are the blue, violet, and ultra-violet lines of the mercury arc, with mean wave-length 4358, 4062, and 3650 Å.U. For simplicity all quantities relating

to $\lambda=4358$ will be denoted by suffix 1, those relating to $\lambda=4062$ by suffix 2, and those relating to $\lambda=3650$ by suffix 3. The crystals are assumed to be large enough for the ordinary laws of reflexion and refraction largely to hold.

(a) *Reflexion from and Absorption by Gelatin.*

Let the intensity of all wave-lengths incident at the surface of the gelatin be I_0. The fraction reflected from the surface may then be taken as given by

$$\frac{(\mu-1)^2+K}{(\mu+1)^2+K}, \quad . \quad . \quad . \quad . \quad . \quad . \quad (1)$$

where μ = refractive index from air to gelatin, and K = specific absorption-coefficient of the gelatin. The fraction transmitted is given by

$$4\mu/[(\mu+1)^2+K]. \quad . \quad . \quad . \quad . \quad . \quad (2)$$

For the gelatin used, the absorption from $\lambda=3600$ Å.U. into the visible region was very small; at least it was small enough for any differences in the amounts transmitted to be neglected in our experiments. (This was proved by exposing single-layer plates behind different thicknesses of gelatin and finding no difference in the photographic effect.) The fraction of the incident intensity transmitted through the gelatin layer is therefore

$$4\mu/(\mu+1)^2. \quad . \quad . \quad . \quad . \quad . \quad . \quad . \quad (3)$$

In order, therefore, to ascertain the relative transmissions through the gelatin, we have to determine the values of μ for the three wave-lengths which are used. An approximate determination of this was carried out as follows:—A piece of dry gelatin was taken, and at a certain point on it fine lines were made on both surfaces. The apparent distance between these was then determined for the mercury lines in the yellow, green, blue-green, blue, and violet, using a 1/12 oil-immersion objective. If the apparent relative distances at wave-lengths $\lambda_1 \lambda_2$ etc. are denoted by $a_1 a_2$ etc., then the relative refractive indices are given by

$$\mu_1 : \mu_2 \ldots :: 1/a_1 : 1/a_2 \ldots .$$

Chapman Jones has shown (Phot. Journ. li. p. 163, 1911) that the refractive index of air-dried gelatin for yellow light (sodium) is 1·53. Taking this as a starting-point and using the relative values obtained as above, the actual values of the refractive index at different wave-lengths were obtained.

These were plotted on a graph, and the value for the ultra-violet line found by extrapolation, a procedure which is justified since this wave-length is still remote from the position of the ultra-violet absorption band of gelatin. From this curve we get for the three values of the refractive index which we require

$$\mu_1 = 1{\cdot}539, \qquad \mu_2 = 1{\cdot}543, \qquad \mu_3 = 1{\cdot}549.$$

Applying these values to equation (3), we obtain for the intensities transmitted through the gelatin on to the crystal face :

$$\left.\begin{array}{ll} \text{blue} & = 0{\cdot}955\, I_0 \\ \text{violet} & = 0{\cdot}954\, I_0 \\ \text{ultra-violet} & = 0{\cdot}953\, I_0 \end{array}\right\}, \quad . \quad . \quad . \quad . \quad (4)$$

and these may be regarded as equal to well within the accuracy possible or required.

If, therefore, equal intensities are incident on the plate surface, approximately equal intensities will also be incident on the face of the crystals.

(b) *Reflexion from Crystal Surface and Absorption by Crystal.*

To determine this we must know the refractive index of silver bromide relative to air. This has been determined by Wernicke (Pogg. *Ann.* cxxxix. p. 132, 1870). Plotting a curve of μ against λ, and proceeding in the same way as before, we obtain the following values :

$$\mu_1 = 2{\cdot}35, \qquad \mu_2 = 2{\cdot}40, \qquad \mu_3 = 2{\cdot}48,$$

from which, with the values given above for gelatin, the following values for the refractive index from gelatin to silver bromide are obtained :

$$\mu_1 = 1{\cdot}35, \qquad \mu_2 = 1{\cdot}55, \qquad \mu_3 = 1\ 60.$$

Now, since the silver bromide absorbs all the lights used very strongly, equation (3) cannot be applied to finding the intensities just inside the crystal face without first determining whether K may be neglected or not.

The absorption of silver bromide has been determined by Slade and Toy (Proc. Roy. Soc. A, xcvii. pp. 181–190, 1920), who give the values of k in the equation

$$I_2 = I_1 e^{-kd},$$

where I_1 and I_2 are the intensities at two points d cm. apart

in the silver bromide. The values given are :

$$k_1 = 4{\cdot}86 \times 10^2, \quad k_2 = 16{\cdot}28 \times 10^2, \quad k_3 = 59{\cdot}0 \times 10^2.$$

K and k are connected by the relation

$$K = k\lambda/4\pi,$$

whence by calculation $K_1 = 0{\cdot}0017$, $K_2 = 0{\cdot}0053$, $K_3 = 0{\cdot}0172$. Even in this case K is negligible, the value of the fraction of ultra-violet transmitted with K included being only 0·2 per cent. less than the value calculated if K is neglected. The fractions transmitted through the upper face of the crystal are :

blue 0·956, violet 0·953, ultra-violet 0·945,

so that combining these with (4), we get as the intensities just inside the crystal face (I'), in terms of the incident intensities I_0 :

blue $(0{\cdot}955 \times 0{\cdot}956) \times I_0$,

violet $(0{\cdot}954 \times 0{\cdot}953) \times I_0$,

ultra-violet $(0{\cdot}953 \times 0{\cdot}945) \times I_0$;

that is,

$$I_1' = 0{\cdot}912 \,.\, I_0, \quad I_2' = 0{\cdot}909 \,.\, I_0, \quad I_3' = 0{\cdot}901 \,.\, I_0. \quad . \quad (5)$$

Absorption by the Crystal.

The energy absorbed by a crystal of thickness d cm. on the passage through it of light of wave-length λ and extinction coefficient k is given by

$$I'(1 - e^{-kd}), \quad . \quad . \quad . \quad . \quad . \quad . \quad (6)$$

where I' is the intensity when $d = 0$ (*i. e.* just inside the upper face of the crystal). The expansion of this may be written :

$$I' . kd \left[1 - \frac{kd}{2!} + \frac{k^2d^2}{3!} - \ldots.\right]. \quad . \quad . \quad . \quad . \quad (7)$$

Now, according to Sheppard (' Photography as a Scientific Instrument,' p. 133), the thickness of flat crystals in a photographic emulsion is usually not more than 1/14 of their diameter. The crystals used in the experiments to be described were less than 1 μ in linear dimensions, so that we may take an upper limit for d of about 0·1 μ. This gives a maximum value for kd (taking k for ultra-violet) of $5{\cdot}9 \times 10^3 \times 0{\cdot}1 \times 10^{-4}$, $= 0{\cdot}06$ (approx.). Retaining only two terms in (7) therefore gives an accuracy greater than 1 per cent. at all wave-lengths. With sufficient accuracy

we may therefore put the energy absorbed by the crystal per sec. equal to

$$I'.\frac{kd}{2}(2-kd). \quad . \quad . \quad . \quad . \quad . \quad . \quad (8)$$

If we consider I′ the same for each light used, as they are to within about 1 per cent. (equation (5)), then the relative quantities of energy (E) of different wave-lengths absorbed by the grain are as follows:

$$\left.\begin{aligned} E_2/E_1 &= k_2(2-k_2d)/k_1(2-k_1d), \\ E_3/E_2 &= k_3(2-k_3d)/k_2(2-k_2d). \end{aligned}\right\} \quad . \quad . \quad . \quad . \quad (9)$$

In considering what value to give to d, it must be remembered that the developable centres are, in all probability, formed on the surface of the grain, and it is unlikely that the absorption of energy by atoms in the interior of the crystal has any effect on the latent image formation (a thickness of $0{\cdot}1\ \mu$ corresponds to about 300 layers of atoms). It is therefore improbable that d should be taken as anything like the whole thickness of the grain; rather is it probable that the absorption only by two extremely thin layers at the grain surfaces should be considered. But fortunately the exact value of d is immaterial, for since kd is small compared with 2, the values of E_2/E_1 and E_3/E_2 change very little with large changes in d. Thus, if we assume d so small that kd is negligible compared with 2, we get

$$E_1 : E_2 : E_3 :: 1 : 3{\cdot}35 : 12{\cdot}1,$$

while, if we put $d=0{\cdot}06\ \mu$, we get

$$E_1 : E_2 : E_3 :: 1 : 3{\cdot}35 : 11{\cdot}9\ ;$$

and the difference between these is negligible considering the approximate nature of the calculation. Taking as a sufficiently accurate ratio

$$E_1 : E_2 : E_3 :: 1 : 3{\cdot}35 : 12{\cdot}0,$$

we get

$$E_2/E_1 = 3{\cdot}35 \quad \text{and} \quad E_3/E_2 = 3{\cdot}59. \quad . \quad . \quad (10)$$

These values are calculated on the assumption that the unit of energy is the same in each case—that is, for each frequency. But on the quantum hypothesis it is to be expected that the effectiveness of E, as regards the formation of centres, depends on the number of quanta it contains and not on the total energy. The ratio of the number of quanta

absorbed (q) for equal times of exposure is given by

$$q_1 : q_2 : q_3 : : 1 : 3{\cdot}35 \times \nu_1/\nu_2 : 12{\cdot}0 \times \nu_1/\nu_3 ;$$

i.e.

$$: : 1 : 3{\cdot}12 \quad : 10{\cdot}1$$

or

$$q_2/q_1 = 3{\cdot}12 \quad \text{and} \quad q_3/q_2 = 3{\cdot}24. \quad . \quad . \quad . \quad (11)$$

The object of the experiments now to be described is to determine whether there is any similarity between these figures and the relative number of developable centres produced.

Experimental.

Light through the monochromatic illuminator, indicated by the prism and lens at M in the figure, is brought to a

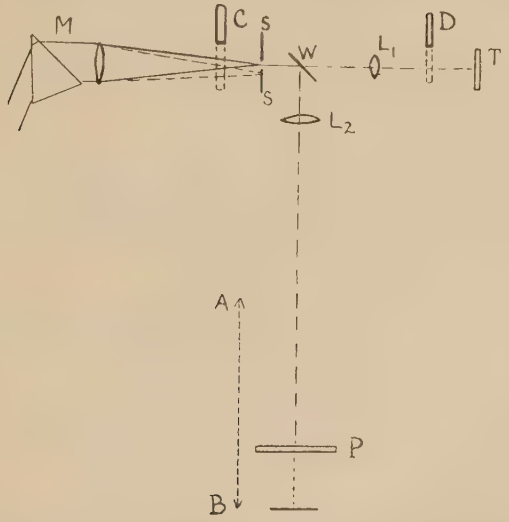

focus at the slit SS. After passing through this slit, the light falls on a parallel plate of fused silica W, which is placed at 45° to the direction of the beam. Part of the latter is reflected through the quartz lens L_2, and forms a very much enlarged image of the face of the prism at P; the other part of the beam, after passing through the quartz lens L_1, forms a very much diminished image of the prism face at T. C and D are shutters, C placed so that all the light can be cut off, and D so that the light reaching T can be cut off without interfering with continuous illumination of P. In the concentrated light at T is placed a Hilger linear thermopile, connected with a suitable moving-coil galvanometer, and at P are placed the single layer photographic plates

used in the experiments. The whole of the apparatus as shown in the figure (except the prism) is movable about the prism as centre, and by this movement any desired colour can be passed through the slit SS. The special carrier for the plates P is movable between the two points A and B, the reason for this being explained in a moment.

Knowing the intensities incident on the thermopile, the intensities in the other beam must be adjustable so that equal intensities of each light shall be incident on the plate. The first step is to find the relation between the intensity of the light measured by the thermopile and the part reflected from the silica plate and used photographically.

Let the total amount of light falling per second on the silica plate = E and the fraction transmitted = α. Then the amount transmitted is αE, and this falls on the quartz lens L_1, which transmits a fraction β of it, and therefore an amount $\alpha\beta$E, part of which is measured by the thermopile. Since the absorption by the silica plate is negligible, the amount reflected is

$$E(1-\alpha),$$

and this is incident upon a quartz lens L_2, the transmission of which is practically identical with that of L_1. Therefore the amount of light in the beam which is active photographically is

$$\beta E(1-\alpha).$$

If the size of the image formed at T is a_1, then the intensity measured by the thermopile (I_t) is given by

$$I_t = \alpha\beta E/a_1.$$

Similarly, the intensity on the plate P (I_p) is

$$I_p = \beta E(1-\alpha)/a_2,$$

where a_2 = size of image at P.

Therefore the ratio I_p/I_t is

$$I_p/I_t = \left(\frac{1-\alpha}{\alpha}\right).\frac{a_1}{a_2}. \quad . \quad . \quad . \quad . \quad . \quad . \quad . \quad (12)$$

By means of this we can find the intensity incident on the plate if the intensity on the thermopile be known.

The next thing is to find how α and the ratio a_1/a_2 vary with the frequency of the light. That very little change of α with ν is to be expected can be shown by calculating the approximate values of α from the theoretical equation

$$F = \tfrac{1}{2}.\frac{\sin^2(i-r)}{\sin^2(i+r)}\left[1+\frac{\cos^2(i+r)}{\cos^2(i-r)}\right],$$

where F = fraction of incident light reflected at a single

surface, and i and r are the angles of incidence and refraction respectively. Taking the angle of incidence on the first surface of the silica as 45° (which was only approximate), a value of $\alpha_1 = 0{\cdot}910$ was obtained for the blue, and $\alpha_3 = 0{\cdot}908$ for the ultra-violet. The experimental values were then found directly by measuring the deflexion of the thermopile with and without the silica in position, and the following values found :—

$$\alpha_1 = 0{\cdot}903, \quad \alpha_2 = 0{\cdot}901, \quad \alpha_3 = 0{\cdot}896.$$

It is sufficiently accurate to take these all as equal to 0·900 for our present purpose, so that the value of $(1-\alpha)/\alpha$ in (12) may be taken as 0·111.

The thermopile was fixed in position as nearly as possible at the focus of the violet light, so that, since the lenses are uncorrected, the blue and ultra-violet were slightly out of focus ; but the want of focus was so small that the edges of the image, area a_1, when photographed appeared almost equally sharp to the eye in each case, and its actual dimensions could be very accurately measured. Similarly, with the enlarged image, area a_2, formed on the photographic plate. The following values of a_1/a_2 were found :

$$[a_1/a_2]_1 = 3{\cdot}91 \times 10^{-3},$$
$$[a_1/a_2]_2 = 3{\cdot}77 \times 10^{-3},$$
$$[a_1/a_2]_3 = 3{\cdot}75 \times 10^{-3}.$$

The violet and ultra-violet values may be taken as each equal to $3{\cdot}76 \times 10^{-3}$, so that we get finally for the relation between the intensity on the thermopile and on the plate

$$\left.\begin{aligned} [I_p/I_t]_1 &= 3{\cdot}91 \times 10^{-3} \times 0{\cdot}111 = 4{\cdot}34 \times 10^{-4}, \\ [I_p/I_t]_2 = [I_p/I_t]_3 &= 3{\cdot}76 \times 10^{-3} \times 0{\cdot}111 = 4{\cdot}17 \times 10^{-4}. \end{aligned}\right\} \quad (13)$$

Now the intensities of the blue, violet, and ultra-violet on the thermopile were not all equal, but were approximately in the ratio 2 : 1 : 1·2, so that, from (13), the ratios which exist at P, on the photographic plate, can be calculated. But what we require is *equal* intensity on the plate, and this is obtained in the following way. As has been said, P is movable between two points A and B, the size of the image of the prism face depending on the position of P. For only one of these positions is the image strictly in focus, but the depth of focus is so large that the image appeared fairly sharply defined at all points between A and B. Thus, by moving P we have a means of varying the intensity on the plate without

altering the total energy in either beam. After exposure of the plate to the blue, in order to make the violet intensity equal to the blue, on the plate, the latter is moved towards A until the area of the patch of light is reduced in the required proportion. Similarly for the ultra-violet.

In order to test whether this method was accurate, the following experiments were carried out, using only one light. With the plate placed at B, an exposure was made and the thermopile deflexion noted. The intensity of the beam passing through the monochromatic illuminator was then cut down by placing a neutral wedge across the original slit, the wedge being adjusted so that the thermopile deflexion was reduced about half—that is, the intensity at B was reduced to half also. The plate was then moved towards A until the area of the image of the prism face formed on the plate was reduced in such a ratio that the intensity should be the same at it was originally at B. Another portion of the plate was now exposed for the same time. On counting the percentage changed, it was found to be the same at both positions of the plate, thus showing that the method adopted was sound.

To get the absolute values of the intensities, the thermopile was standardized by means of a Hefner lamp. According to Coblentz (Bull. Bur. Standards, xi. p. 89, 1915), if a diaphragm 14×50 cm. is placed in front of the Hefner flame at a distance of 10 cm., the intensity of total radiation at a distance of 1 metre from the flame is $23{\cdot}2 \times 10^{-6}$ calorie per square centimetre per second. This radiation produced on the galvanometer a deflexion of 45·0 mm.; and since it was known that over the range used the deflexion was strictly proportional to the intensity, it was very easy to interpret all deflexions in absolute intensities.

The single-layer plates used were $4\frac{1}{2}$ in. long $\times$ 1 in. wide, and by means of a special plate-holder small patches about $1 \times 0{\cdot}75$ cm. were exposed along the centre. The plates were developed for 1·5 minutes in amidol developer consisting of 0·4 gm. amidol, 6 c.c. of 10 per cent. KBr, 100 c.c. saturated Na_2SO_3.

The percentage of the grains changed was determined by direct microscopic counting, the average number of developable centres per grain (n) being calculated from the equation

$$n = \log_e 100/(100-x),$$

where x is the percentage of grains developed. To obtain a very accurate value of x, about 1500 grains were counted in every case. The emulsions used varied greatly in speed, but were all *extremely slow*, even compared with the ordinary

process type of emulsion. This is a very important point, the significance of which will be discussed later.

Table I.

Blue and Violet only.

Plate Reference No.	Time of Exposure in minutes.	Intensity of light falling on plate in calories per sq. cm. per second.	Average No. centres per grain (obs.). n_1.	n_2.	n_2/n_1 (obs.).	n_2/n_1 (calc.).
E 6 (viii)	6	$5{\cdot}25\times10^{-}$	0·043	0·326	7·59	
E 6 (x)	15	4·19 ,,	0·089	0·419	6·14	
E 9 (x)	5	4·06 ,,	0·135	0·683	5·06	
E 15 (v)	10	4·58 ,,	0·301	0·938	3·12*	
E 16 (ii)	10	4·25 ,,	0·281	1·098	3·92	
E 9 (iv)	7	4·19 ,,	0·318	1·195	3·77	
E 9 (ii)	6	4·49 ,,	0·358	1·338	3·74	
E 9 (vi)	10	4·19 ,,	0·344	1·386	4·03*	3·12
E 9 (iii)	8	4·32 ,,	0·532	1·580	2·98*	
E 15 (i)	25	4·04 ,,	0·468	1·690	3·61	
E 9 (v)	10	4·27 ,,	0·533	1·735	3·26	
E 9 (ix)	15	4·35 ,,	0·591	1·815	3·07	
E 15 (vi)	35	4·04 ,,	0·655	2·048	3·14	
E 15 (iii)	35	4·18 ,,	0·710	2·104	2·98	
E 15 (iv)	30	4·58 ,,	0·862	2·440	2·83	

* Irregular, probably due to some experimental error.

Table II.

Violet and Ultra-Violet only.

Plate Reference No.	Time of Exposure in minutes.	Intensity of light falling on plate in calories per sq. cm. per second.	Average No. centres per grain (obs.). n_2.	n_3.	n_3/n_2 (obs.).	n_3/n_2 (calc.).
E 6 (viii)	8	$4{\cdot}52\times10^{-9}$	0·066	0·431	6·53	
E 16 (i)	6	4·10 ,,	0·103	0·623	6·03	
E 6 (xii)	20	4·34 ,,	0·187	1·120	5·99	
E 6 (vii)	6	5·25 ,,	0·328	1·190	3·63	
E 6 (x)	15	4·19 ,,	0·419	1·370	3·27	3·24
E 15 (vii)	8	4·34 ,,	0·821	2·640	3·21	
E 15 (v)	10	4·58 ,,	0·938	2·990	3·20	
E 6 (ix)	20	5·04 ,,	0·942	3·060	3·25	
E 16 (ii)	10	4·25 ,,	1·098	3·550	3·23	

All the experimental data obtained so far are given in the tables. Table I. gives the results for the blue and violet, and Table II. those for the violet and ultra-violet. The first column merely gives the reference numbers of the emulsion used, column 2 the time of exposure in minutes, column 3 the light intensity in calories per square cm. per second falling on the gelatin surface of the plate. Columns 4 and 5 give the observed average number of centres per grain, obtained as shown above, and column 6 the calculated ratio of the number of centres formed, on the assumption that this is proportional to the number of quanta absorbed (equation 11). Now the first thing to notice about these figures is that when the photographic effect (number of centres) is small, the ratios n_2/n_1 and n_3/n_2 are both large, and that as the effect increases, these ratios decrease and tend to become constant at values of n greater than about 0·4 for the less effective light of the pair, *i. e.* about 33 per cent. of the grains changed. The constant value of the ratio can be obtained in each case by taking the average of the last five ratios given, as can be seen by inspection of the tables. On comparing these constant ratios with the relative number of quanta absorbed (see equation 11), we see at once that the agreement is good ; in the case of the violet–ultra-violet the agreement between n_3/n_2 and q_3/q_2 is almost perfect. For convenience these results are given in summarized form below :—

(a) *Blue, Violet.—Equal incident intensity and time of exposure.*

Relative no. of quanta absorbed $= q_2/q_1 = 3{\cdot}12$

Relative no. of centres produced (*if* $n_1 > 0{\cdot}5$) $= n_2/n_1 = 3{\cdot}06$

(b) *Violet, Ultra-violet.—Equal incident intensity and time of exposure.*

Relative no. of quanta absorbed $= q_3/q_2 = 3{\cdot}24$

Relative no. of centres produced (*if* $n_2 > 0{\cdot}4$) $= n_3/n_2 = 3{\cdot}23$

Now these results fit in extremely well with the recent very important work of Eggert and Noddack on the "Proof of the Law of Photochemical Equivalence and the Dry Plate" (*Z. Physik*, xx. p. 299, 1923). They consider that they have proved conclusively that this law holds, and their experiments are certainly very strong evidence in its favour.

There are two important differences between the methods used by Eggert and Noddack and by us :—

(*a*) They used ordinary thick plates, containing many layers of grains, and found experimentally the absorption by the total silver bromide. The values finally obtained for the same three wave-lengths as we have used were very nearly equal, whereas in our case the absorption of the ultra-violet is about twelve times that of the blue. This is because the effective thickness of silver bromide through which the light passed was very much greater in the plates used by Eggert and Noddack than in our single layer plates, and as d increases, E_2/E_1 and E_3/E_2 do decrease towards unity, *i. e.* E_1, E_2, and E_3 become more nearly equal as the thickness of silver bromide increases.

(*b*) They measured what was the "print out" effect, and did not use a developer.

The main conclusions at which they arrived are these :—

(1) The primary elementary process (in the formation of the latent image) consists in the absorption of one quantum of energy by the silver bromide.
(2) For each absorbed $h\nu$ a silver atom is liberated.
(3) The mass of the latent image is determined by the number of absorbed quanta.

These conclusions can be applied at once to explain the results we have obtained above, if we remember that we are detecting the amount of light action, not by measuring directly the mass of silver produced, *but by means of a developer*. Now it is practically certain that the formation of the developable latent image is a *surface* phenomenon, and that any change brought about by the light in the interior of the grain produces no developable effect. Bearing this in mind, we may slightly modify Eggert and Noddack's conclusions, thus :—

(*a*) The primary elementary process (in the formation of the *developable* latent image) consists in the absorption of a quantum of energy by the surface layer or layers of the silver-bromide crystal.

(*b*) The number of silver atoms liberated is proportional to the number of $h\nu$ absorbed by the surface layers.

(*c*) The number of *developable* centres formed is proportional to the number of silver atoms liberated in the surface layers, *i. e.* to the number of $h\nu$ absorbed by the surface layers.

If these are true, then the values obtained for n_2/n_1 and n_3/n_2, when constant, are explained, and there remains the problem of the rapid increase of these ratios with decreasing exposure when the latter is small. A very simple explanation of this follows at once if we accept the idea, originally due to Svedberg (Phot. Journ. lxi. p. 332, 1921), of a minimum area of light-affected silver halide capable of acting as a developable centre. We can then picture the process to be somewhat as follows:—As soon as the light strikes the grains, silver atoms are liberated at isolated points on the grains' surface, the number of atoms formed being proportioned to the time and intensity. Only after a certain interval are there sufficient silver atoms formed within a certain minimum area on which the developer can act. Now, as we have said, the role of the developer is really that of a "detector" of the amount of light action; and since there may be an appreciable light effect without a developable centre being formed, the developer gives a *false record* of the extent of the light action at low exposures, when assumption (*c*) is not true. In other words, the "induction" effect, in the photographic process, is purely a development phenomenon, there being no induction with the true light action, just as there is none in the case of photoelectric substances. The ratios n_2/n_1 and n_3/n_2 begin to increase as soon as the exposure falls low enough for the number of centres formed by the less absorbed light to be within the induction period. In fact, an exposure can be given so that the less absorbed light gives no *developable* effect corresponding to a slight developable effect produced by equal intensity of the light more strongly absorbed, and the ratios n_2/n_1 and n_3/n_2 then become infinite.

The idea that the "induction" period is only a development effect is strikingly supported by Eggert and Noddack's results, that, *at low exposures*, the *total number of silver atoms* produced is directly proportional to the incident intensity.

It must be borne in mind that the conclusions at which we have arrived are not incompatible with the now well-established facts of the great part played by absorption phenomena in controlling the sensitivity of emulsions. For instance, we know that slight "contamination" has an enormous effect on the photoelectric activity of a metallic surface; and Langmuir's work on the catalytic poisoning of thermionic emission by absorbed gases leads us to believe that the light sensitivity of the emulsion is naturally vitally connected with the adsorption processes which have taken place on the grain surface. Thus there is nothing in the conclusions we have

drawn to contradict the statement made by one of us in a previous paper (Trans. Far. Soc. xix. pp. 290–295, 1923) that "the extreme light sensitiveness of the grain is due primarily to the presence of some substance which is not silver bromide."

The results given in this paper have been obtained with *extremely* slow emulsions. Evidence exists that with emulsions of any appreciable speed the values of n_2/n_1 etc. are always much less than the theoretical values given in this paper, and decrease as the speed increases. It is possible that the explanation of this is the occurrence of "reversal" within the normal portion of the characteristic curve, as suggested recently by Svedberg (Phot. Journ. lxiv. pp. 272–274, 1924), and we hope to investigate this question. Further, by using emulsions with larger grains, the ordinary laws of reflexion and absorption will be applicable with less uncertainty.

In conclusion, we wish to express our thanks to Mr. Bloch, of the Ilford Research Laboratories, for much care and trouble in the preparation of suitable emulsions; to the National Physical Laboratory for information regarding the thermopile calibration; and to the Director of Research of the British Photographic Research Association for his interest and advice.

Summary.

1. By applying the laws of reflexion and absorption to the case of a "single layer" photographic plate, the relative quantities of light energy, of different frequencies, absorbed by the grains when equal intensities of each are incident, are calculated: hence the relative number of quanta absorbed is determined.

2. It is shown experimentally that, except at low exposures, the relative number of developable centres produced by different frequencies is equal to the relative number of quanta absorbed.

3. It is suggested that the departure from this equality at low exposures is due to the fact that development does not then give a true record of the extent of the light action.

4. The results are in good agreement with the recent work of Eggert and Noddack on the proof of the Law of Photochemical Equivalence in the case of the photographic dry plate.

XCII. *On the Measurement of the Natural Frequency of an Inductance Coil at Audio-Frequency.* *By* H. NUKIYAMA, *Professor, Tohoku Imperial University, Japan, and* K. KOBAYASHI *.

Abstract.

WE measure the frequency of the alternating current by the known mutual inductance and capacity with Campbell's frequency bridge. The same circuit can be utilized to determine the natural frequency of a coil used as the primary of the mutual inductance, if we know the frequency of the current and the capacity which gives the balance. In the experiment described in this paper the frequency is determined by standard tuning-forks. A theory by which the natural frequency and the self-capacity of the primary coil can be obtained by taking balance at two known frequencies is worked out. The actual method of experiment and the experimental check of this theory are also described. When the sharpness of the balance is greatly affected by the presence of the self-capacity, it can be improved by a simple modification of the circuit as shown in fig. 6.

(1) *Campbell's frequency bridge.*

When an alternating current of the angular velocity $\omega = 2\pi f$ is transmitted to Campbell's frequency bridge, as shown in fig. 1, the condition in which the receiver current disappears is (Bibliography 1, 2, 3, 4)

$$\omega = \frac{1}{\sqrt{MC}}. \quad . \quad . \quad . \quad . \quad . \quad . \quad (1)$$

If the primary coil L of the mutual inductance M is shunted by capacity C_0, as shown in fig. 2, the above conditions must be

$$\omega = \frac{1}{\sqrt{MC + LC_0}}, \quad . \quad . \quad . \quad . \quad . \quad (2)$$

$$\omega C_0 R = 0, \quad . \quad . \quad . \quad . \quad . \quad . \quad . \quad . \quad (3)$$

where L is the self-inductance of the primary coil and R its resistance.

Although condition (2) can be satisfied by adjusting M or C, condition (3) can not be satisfied strictly, and

* Communicated by the Authors.

Fig. 1.

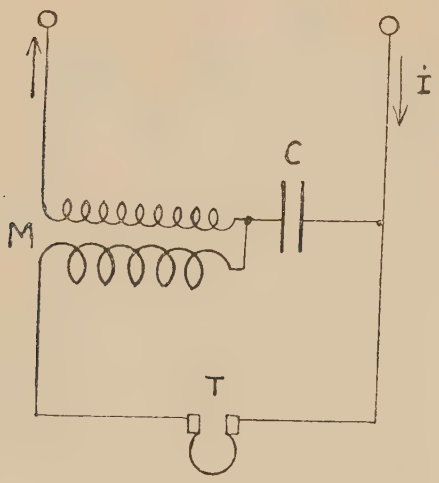

Campbell's frequency bridge.

Fig. 2.

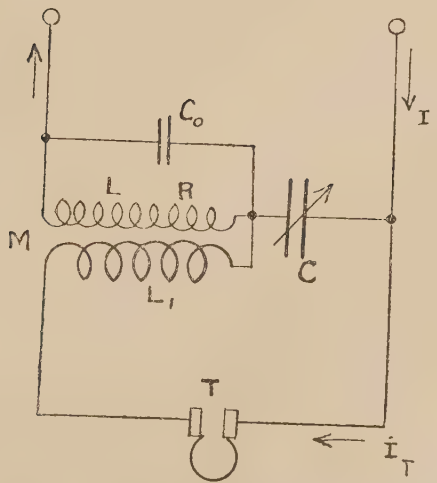

Campbell's frequency bridge with a shunt condenser at the primary.

the balance is not perfect. But in the case of the minimum sound, condition (2) must be satisfied, so that expressing this in the form of eq. (1),

$$\omega = \frac{1}{\sqrt{MC + LC_0}} = \frac{1}{\sqrt{M'C}} \quad . \quad . \quad . \quad . \quad . \quad (4)$$

M′ may be called the "apparent mutual inductance," and

$$M' = M + \frac{C_0 L}{C} \quad . \quad . \quad . \quad . \quad . \quad . \quad . \quad . \quad (5)$$

That is, M may be considered to be corrected by $\frac{LC_0}{C}$ on account of its self-capacity C_0.

(2) *Self-capacity of a coil.*

Considering that the capacity distributed along the conductors of the coil is externally equivalent to the concentrated capacity shunted across the terminals of the coil, we call the latter the "self-capacity" of the coil. By the theory above described, Campbell's frequency bridge can be utilized to determine the self-capacity of the coil.

If the self-capacity of a coil is to be determined, we construct a mutual inductance, using that coil as its primary, and a coil as its secondary of which the self-capacity correction is very slight compared with that in the primary. Campbell's frequency bridge is made of the mutual inductance and a standard condenser; the latter has either a known correction due to frequency, or a negligible percentage of it when compared with the correction of coil L due to its self-capacity. Then, determining the frequency of the current by tuning-forks, we have by (4) at its balance

$$M' = \frac{1}{C\omega^2} \quad . \quad . \quad . \quad . \quad . \quad . \quad . \quad . \quad (6)$$

Thus the apparent mutual inductance can be determined. If the apparent mutual inductances M_1' and M_2' at two known frequencies, and the capacities C_1, C_2 which give the balance, are measured, we have by eq. (5)

$$M_1' = M + \frac{LC_0}{C_1},$$

$$M_2' = M + \frac{LC_0}{C_2},$$

and from these equations we have

$$LC_0 = \frac{M_1' - M_2'}{\frac{1}{C_1} - \frac{1}{C_2}}, \quad \ldots \ldots \quad (7)$$

$$M = M_1' - \frac{LC_0}{C_1}, \quad \ldots \ldots \quad (8)$$

and, finally, the natural frequency of the coil

$$f_0 = \frac{1}{2\pi\sqrt{LC_0}}. \quad \ldots \ldots \quad (9)$$

The self-capacity C_0 may be obtained by a similar experiment to that mentioned above, by shunting the coil by a known capacity C_{01}. In this case, by eq. (5), apparent mutual inductances M_1'', M_2'' and the capacities C_3, C_4 at two known frequencies must satisfy the following condition :

$$M_1'' = M + \frac{(C_0 + C_{01})L}{C_3},$$

$$M_2'' = M + \frac{(C_0 + C_{01})L}{C_4}$$

From these equations

$$(C_0 + C_{01})L = \frac{M_1'' - M_2''}{\frac{1}{C_3} - \frac{1}{C_4}}. \quad \ldots \ldots \quad (10)$$

Eliminating L from both (7) and (10), we have

$$C_0 = \frac{C_{01}}{\frac{(M_1'' - M_2'')\left(\frac{1}{C_1} - \frac{1}{C_2}\right)}{(M_1' - M_2')\left(\frac{1}{C_3} - \frac{1}{C_4}\right)} - 1}. \quad \ldots \quad (11)$$

(3) *Experiments.*

We measured the LC_0 of the primary coil of the mutual inductance as shown in fig. 3. Experiments were worked out on several coils of a different number of turns, of which we shall describe one case as an example. An alternating current was supplied to circuit B, containing Campbell's

frequency bridge, from a triode valve oscillator, as shown in fig. 4. For condenser C, Siemens' standard mica condenser and calibrated dial type air-condenser were used, the latter for fine adjustment. The frequency of the alternating current was determined by tuning the sound of the telephone receiver with Max Kohl's standard tuning-forks, adjusting the condenser C′ of the triode valve oscillator.

Fig. 3.

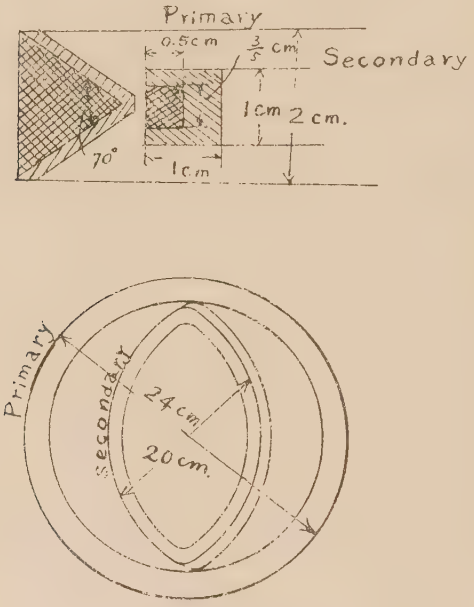

Mutual Inductance.

The secondary of the mutual inductance may be rotated round the common axis of the primary, and the position angle of the secondary coil was measured from the position at which both coils were in the same plane. In Table I. the column marked "degree" denotes this angle, C the capacity which gives the balance, and M′ the apparent mutual inductance calculated by eq. (4) using C and the angular velocity determined by tuning-forks. LC_0 and M calculated by (7) and (8), using the values of M′ and C at

Table I.—Apparent Mutual Inductance.

Degree.	$f=320$.		$f=512$.		$f=704$.		$f=960$.		$f=2048$.	
	C μ.f.	M′ henry.	C μ.f.	M′ henry.	C μ.f.	M′ henry.	C μ.f.	M′ henry.	C μ.f.	M′ henry.
10	0·237	1046·3	0·09154	1059·7	0·04827	1058·3	0·0256	1082	0·00472	1282
20	0·29	855·1	0·10085	961·8	0·05858	874·0	0·0311	891·1	0·00586	1032·6
30	0·355	698·5	0·13892	698·2	0·0729	702·4	0·0387	715·4	0·00720	844·2
40	0·445	557·2	0·17468	555·2	0·0915	559·3	0·0488	567·0	0·00919	658·4
50	0·574	432·0	0·22500	435·9	0·118	433·5	0·0623	444·3	0·0116	521·6
60	0·770	322·1	0·3007	322·5	0·1585	323·0	0 0842	328·0	0·0158	383·0
70	1·135	218·5	0·443	218·9	0·231	221·8	0·1230	225·2	0·0236	256·4
80	2·000	124·0	0·783	123·9	0·413	123·9	0·1284	126·7	0·0413	146·4

Table II.—C_0L and M.

Degree.	$\omega=2\pi\times320$. M_1' henry	$\omega=2\pi\times2048$. M_2' henry.	C_1 μ.f.	C_2 μ.f.	M henry.	C_0L sec^2.
10	1·0463	1·2820	0·237	0·00472	1·052	$11·35\times10^{-10}$
20	0·8551	1·0326	0·290	0·00586	0·853	$10·70\times10^{-10}$
30	0·6985	0·8442	0·355	0·00720	0·697	$10·65\times10^{-10}$
40	0·5573	0·6584	0·445	0·00919	0·550	$9·53\times10^{-10}$
50	0·4320	0·5216	0·574	0·01160	0·4307	$10·6\times10^{-10}$
60	0·3221	0·3830	0·770	0·01580	0·3188	$9·13\times10^{-10}$
70	0·2185	0 2564	1·135	0·02360	0·2106	$9·13\times10^{-10}$
80	0·1240	0 1464	2·000	0·04133	0·1200	$9·45\times10^{-10}$
					Mean	$10·46\times10^{-10}$

$f=320$ and $f=2048$ of Table I., are shown in Table II. The apparent mutual inductances, calculated by (5) using M and the mean value of $LC_0=10{\cdot}46\times10^{-10}$ sec.^{2}, both obtained in Table II., are compared with its actually measured values in fig. 5. Coincidence of both values shows that the

Fig. 4.

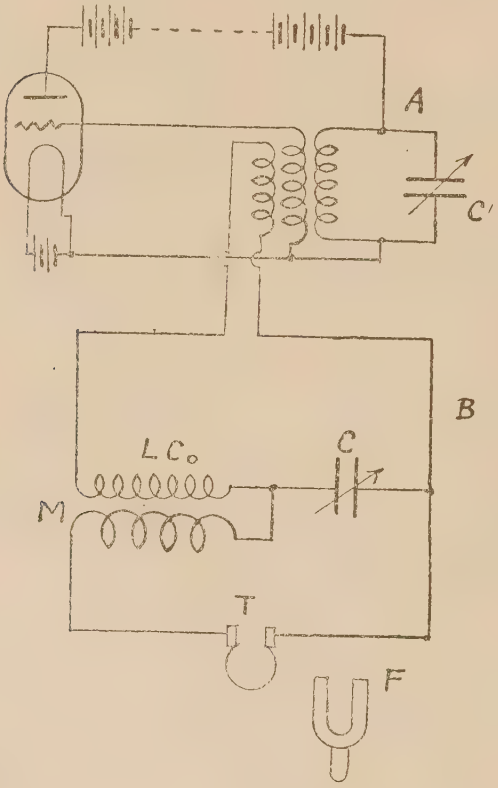

Circuit arrangement.

above-mentioned distributed capacity can be replaced by a concentrated capacity across the terminals in the range of our frequencies. As shown in Table II., the decrease of LC_0 with decreasing M may be the effect of the self-capacity of the secondary coil.

(4) *Method for perfect balance.*

Of the conditions of the balance, eq. (2) and eq. (3), the latter cannot be satisfied in the connexion as shown in fig. 2. When the sharpness of the balance is greatly affected by the resistance of the primary, it can be improved by a simple

Fig. 5.

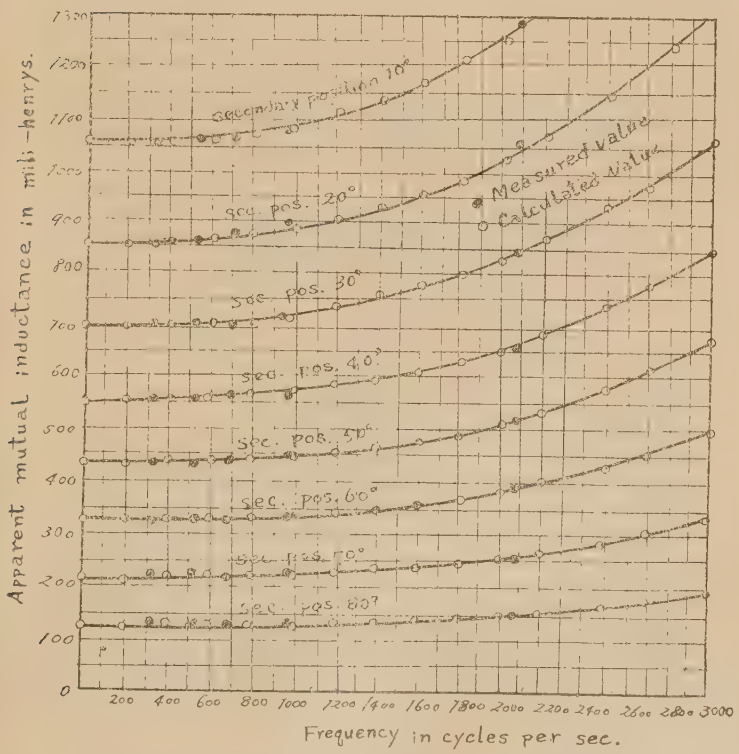

Change of the apparent mutual inductance by the frequency.

modification of the connexion, in which the condenser C is divided into two parts C_1 and C_2, and a non-inductive resistance r is inserted in series with C_2, as shown in fig. 6. (This method was tried by our collaborator, Mr. M. Matsudaira.)

In this circuit, the conditions in which the receiver current

becomes zero are, putting $C = C_1 + C_2$,

$$\omega = \frac{1}{\sqrt{MC + LC_0}}, \quad \ldots \ldots \quad (12)$$

$$C_0R = \frac{C_1C_2Mr}{MC + LC_0}. \quad \ldots \ldots \quad (13)$$

Fig. 6.

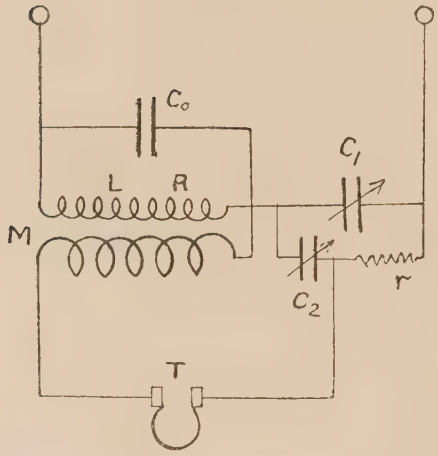

Modification of the Campbell's frequency bridge to obtain a perfect balance.

Then, both equations can be satisfied at the same time by adjusting C_1, C_2, and r, and the balance will be perfect. Yet in this case the method for determining M and LC_0 stands unchanged, as the equation (12) remains the same as eq. (2). Using M and LC_0 obtained by (12), C_0R can be calculated by (13); accordingly the effective resistance of coil R can be determined if we know C_0.

(5) *Conclusion.*

In an ordinary laboratory the greatest difficulty in this method for determining the self-capacity of the coil may be that a standard set of tuning-forks is needed. But if we were trained to calibrate the frequency of the alternating current as a multiple of the frequency of a tuning-fork, only one tuning-fork would be needed. It is a merit of this method that the sources of error due to the change of apparent constants of the circuit element are greatly eliminated by the simplicity of the circuit.

Bibliography.

1. A. Campbell. "On the Use of Variable Mutual Inductances." Phil. Mag. xv. (1908).
2. A. E. Kennelly and Edy Velander. "Rectangular-component, Two-dimensional Alternating Current Potentiometer." Journal of Franklin Institute, July 1919.
3. Edy Velander. "A Frequency Bridge." A. I. E. E., Nov. 1921.
4. S. Chiba. "Modification of Campbell's Arrangement for Measuring Telephone Frequency." *Denki Gakkai Zasshi,* April and Nov. 1922.

XCIII. *The Thermal Conductivity of Bismuth in a Transverse Magnetic Field.* *By* F. A. Ward, *B.Sc.(Lond.), A.Inst.P.**

INVESTIGATIONS of the thermal conductivity of bismuth in a magnetic field when the lines of force are perpendicular to the direction of heat-flow have been made by various observers. Leduc † found a decrease of 5·7 per cent. in a field of 7800 c.g.s. units. Nernst ‡ in 1887 could detect no change. Ettingshausen § found a diminution from 2 to 5 per cent. in a field of 9000 c.g.s. units. Van Everdingen ‖ 5·8 per cent. in a field of 6000, and Blyth ¶ a diminution of 0·05 per cent. in a field of 3500 c.g.s. units. Livens **, assuming the free electron theory, has developed a formula according to which the thermal conductivity of solids should increase in the magnetic field. This is contrary to the experimental results.

The material used in the present investigation was pure bismuth supplied by Messrs. Johnson & Matthey. Some of the metal was powdered and placed in a glass tube about 4 mm. in diameter from which the air was withdrawn. While evacuated, the tube was heated until the whole of the metal was melted. It was then allowed to cool slowly, and on solidification the glass tube was broken, a fairly uniform cast rod being obtained in this way. From a number of rods prepared in this manner two were selected for the investigation.

* Communicated by Dr. L. Lownds.
† *C. R.* cii. p. 358 (1886).
‡ *Wied. Ann.* xxxi. p. 760 (1887).
§ *Wied. Ann.* xxxiii. p. 129 (1888).
‖ *Journ. de Phys.* (3) x. p. 217 (1901).
¶ Phil. Mag. (6) v. p. 529 (1903).
** Phil. Mag. (6) xxx. p. 526 (1915).

The dimensions of the selected rods were: (1) length 7·6 cm., diameter 0·35 cm.; (2) length 7·6 cm., diameter 0·40 cm.

The specific electrical resistance of these rods was 119×10^{-6} ohm-cm. and $119{\cdot}2 \times 10^{-6}$ ohm-cm. respectively.

The rods were fixed between copper blocks A, B, C (fig. 1).

Fig. 1.

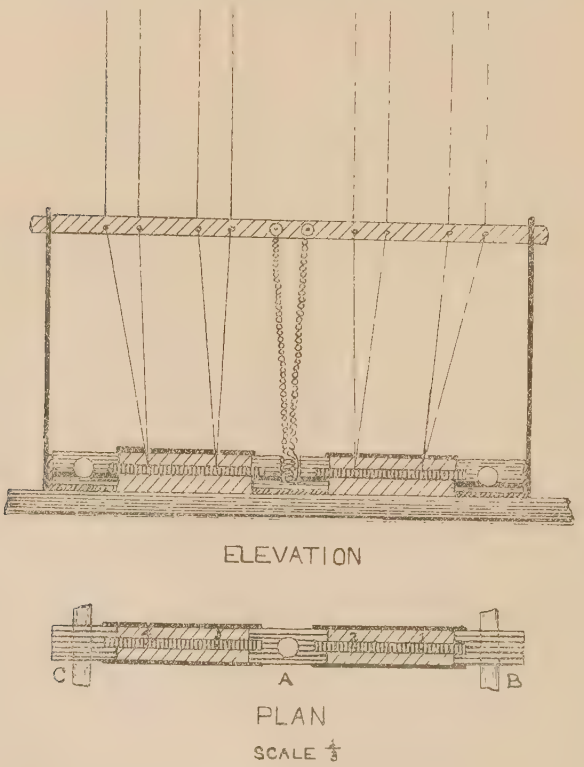

Heat was supplied at a constant rate to the central block A by means of a small coil carrying a current and embedded in the centre of this block. Water circulated through the outer coppers B and C. The whole was well lagged, and when steady conditions obtained, the temperature gradient on each bar was determined by the copper-constantan-thermo-couples (1, 2, 3, 4). The apparatus was mounted so that either of the bars could be placed in an intense uniform magnetic field.

If W denote the rate of supply of heat to the heating coil, K and K_1 the thermal conductivities of bismuth without and with the field ;

A_1 and A_2 the sectional areas of the rods containing junctions (1) and (2), and (3) and (4) respectively ;

g_1 the temperature gradient between the thermo-junctions between the pole-pieces,
g_2 the temperature gradient between the thermo-junctions outside the pole-pieces,
} when there is no magnetic field :

G_1, G_2 the corresponding gradients when the magnetic field is impressed ;

X the heat-losses due to radiation etc., which may be assumed the same in both cases.

Then

$$W = KA_1g_1 + KA_2g_2 + X,$$

$$W = K_1A_1G_1 + KA_2G_2 + X,$$

whence

$$\frac{K_1}{K} = \frac{A_1g_1 + A_2g_2 - A_2G_2}{A_1G_1}.$$

The heating-coil was of nichrome wire (gauge 40), wound on slate and insulated from the copper block. It was firmly cemented in the cavity, and the leads from it, insulated by glass beads, passed through holes in the fibre cross-piece forming the top of the framework which carried the rods and copper blocks. The heating current was supplied by a battery of accumulators, this circuit containing regulating resistance and milliameter. The bismuth rods fitted into holes in the copper blocks, and were secured in position by means of set screws. The thermocouples were of copper constantan (gauge 36). Small holes were drilled in the rods to receive the junctions, and they were soldered in position with a little powdered bismuth to secure good thermal contact.

The distance between junctions (1) and (2) was 1·89 cm., and between (3) and (4) 1·98 cm. The rods were lagged with lightly-packed cotton-wool, which was kept in position by rectangular fibre strips screwed to the copper blocks.

The thermocouple wires passed through slits cut in the upper fibre strips and thence through holes in the fibre cross-piece. The whole was screwed to a brass bar of rectangular section, from which it was insulated. The bar was supported by guides in an outer copper shield, and could move through

these so as to place either bismuth rod between the poles (fig. 2).

To ensure steady conditions, it was found necessary to protect the apparatus from the heating effects of the current circulating in the electromagnet coils. This was done by building round the apparatus a shield of stout sheet copper. This was made in sections (see fig. 2), which could be firmly bolted to one another. The water after circulating through the end coppers was led to the base of the shield, which was a hollow metal box, and thence through copper formers

Fig. 2.

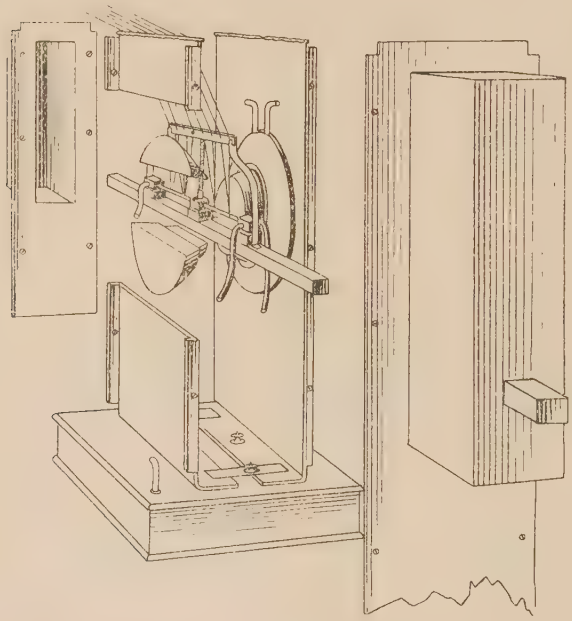

fitting the pole-pieces and in good contact with the vertical sides of the shield. This water, before entering the copper blocks, passed through a metal worm 60 ft. long, contained in a large tank of water to secure uniformity of temperature.

Fig. 3 shows diagrammatically the arrangement for measuring the E.M.F.'s. of the thermocouples. W is a standard cadmium cell, R_2 a resistance of 1013 ohms in series with four accurately adjusted ohm coils and a manganin wire (1 m. long), also adjusted to 1 ohm by a resistance in parallel with it. A is an accumulator. By connecting (1) and (2) to the galvanometer terminals and adjusting R_1,

the potential drop along the manganin wire when no current flows through the galvanometer is made 1 microvolt per mm. E and F are mercury cups connecting to the hot and cold junctions of the several thermocouples. To balance the E.M.F. of a couple, connexions c_1h_1 to E and F are made, (3) and (4) are connected to the galvanometer, and (1) and (2) are broken. The slider on the manganin wire is then adjusted till there is no deflexion in the galvanometer. To avoid disturbing thermal effects at the contact maker a second manganin wire ran alongside the bridge wire, and the contact maker bridging the two wires was of manganin. The apparatus was sensitive to less than 0·5 microvolt.

Fig. 3.

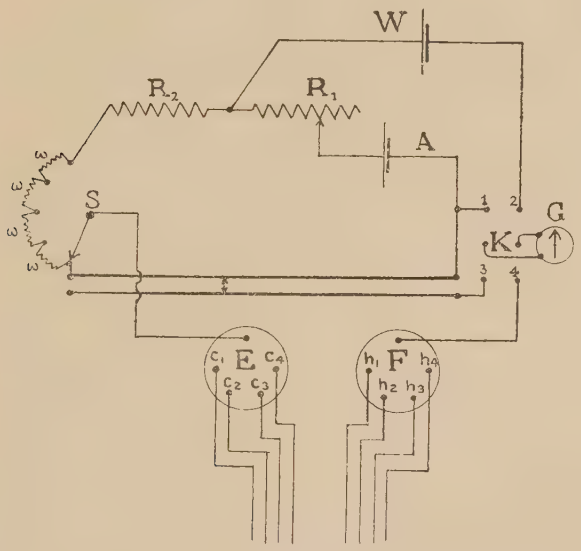

The electromagnet was of the split toroid type, with conical pole-pieces shaped to give a uniform field. The diameter of the pole-pieces was 5 cm., and they were adjusted by means of a distance-piece to a gap width of 2 cm. This was the minimum distance which would accommodate the apparatus. The field strengths were measured ballistically by means of a search coil and standardizing solenoid. The magnetizing field used in the experiments was 5370 c.g.s. units.

The method of a typical experiment was as follows:— The water circuit, heating current, and electromagnet current

were started at about 10 A.M. The magnetizing current at first circulated in opposite directions through the two limbs of the magnet, so that the field was not excited. The ammeters were observed at intervals, and kept at constant values by regulating resistances. Observations were usually commenced after an interval of about 6 hours, after which time conditions were usually steady. Readings of the thermocouples were taken with no field, and then the field was impressed. After about $1\frac{1}{2}$ hours the thermocouple temperatures were again steady and were recorded. The current was again reversed in one of the limbs, and a third set of thermocouple observations taken after a further period of $1\frac{1}{2}$ hours.

Table I. shows a typical set of observations. t_1 is the difference between balance points in mm. on the potentiometer wire for the junctions between the pole-pieces ; t_2 the difference for those outside, when there is no field ; T_1, T_2 the corresponding data when the field is excited.

TABLE I.

Time	4.54.	5.06.	5.15.	5.24.	5.41.	5.52.	6.00.
t_1	212	213	211	210	213	213	213
t_2	211	211	211	211	211	211	211
Time	—	—	6.41.	7.04.	7.16.	7.27.	7.26.
T_1	—	—	216	216	215	215	214
T_2	—	—	216	216	216	215	215
Time	—	—	—	8.36.	8.41.	8.53.	9.14.
t_1	—	—	—	214	214	213	213
t_2	—	—	—	213	211	210	211

In all, sixteen experiments were performed, giving the following average values :—

1*st Series. Junctions* 1 *and* 2 *between the pole-pieces.*

Expt. Nos.	1.	2.	3.	4.	5.	6.	7.	8.	9.	10.
t_1	307·6	219·8	218·8	206·2	205·4	212·6	213·5	298·2	278·2	277·8
t_2	314·8	218·2	219·8	206·3	204·2	211·0	211·2	299·0	280·8	279·8
T_1	313·2	222·9	222·9	209	205·0	215·2	215·2	301·0	280·4	280·4
T_2	317·8	224·5	224·5	210·8	207·6	215·6	215·6	304·1	284·0	284·0

2nd Series. Junctions 3 and 4 between the pole-pieces.

Expt. Nos.	11.	12.	13.	14.
t_1	261·8	261·2	204·5	204·4
t_2	257·0	257·8	202·8	203·4
T_1.....	264·3	264·3	208·2	208·2
T_2.....	260·2	260·2	206·2	206·2

3rd Series. Junctions 1 and 2 between the pole-pieces. Field reversed.

Expt. Nos.	15.	16.
t_1	272·0	289·6
t_2	211·7	224·5
T_1.....	277·7	295·2
T_2.....	215·5	226·8

These numbers were converted into values for g_1, g_2, G_1, G_2 by dividing by the distance between the junctions concerned, and the average value of K_1/K deduced by combining the observations as follows :—

Expt. Nos. 1 to 6	96·28		
2 to 7	96·20		
3 to 8	96·55	.....96·52	.....96·78
4 to 9	97·05	.....96·95	
5 to 10.....	97·01		
Expt. Nos. 11, 12, 13, 14	.....	.....	96·80
Expt. No. 15, 16	.....	.....	96·70
		Mean.....	$K_1/K = 96·78$

The average diminution of the thermal conductivity of bismuth is 3·22 per cent. in a transverse magnetic field of 5370 c.g.s. units. With a field of 6260 c.g.s. units the heating of the electromagnet became excessive, so that prolonged observations could not be carried through. The decrease in this case was of the order 5 per cent.

My thanks are due to Dr. Lownds for suggesting this work to me and for his advice and help during its progress.

Physics Department,
Chelsea Polytechnic,
June 1924.

XCIV. *Low-Voltage Glows in Hydrogen.* *By* G. Stead, *M.A., Reader in Physics in the University of London, and* B. Trevelyan, *B.A., Yarrow Research Student, Girton College, Cambridge* *.

Introduction.

THE type of discharge-tube employed in the present investigation, and described in a previous paper †, shows peculiarities not found in the more usual forms of two- and three-electrode thermionic tubes. The essential features are (1) the use of a very open grid close to the filament, (2) the absence of an anode, and (3) the large volume on the side of the grid remote from the filament. Under these conditions a large emission can take place from the filament when the difference of potential between the grid and the filament is quite low, and a considerable proportion of the emitted electrons passes through the grid into the space beyond, giving rise to intense ionization in a large volume of gas. Some of the positive ions so formed are drawn into the region between the grid and filament, some are repelled by the grid to the walls of the tube, which may thus become charged to a considerable potential, whilst others must recombine before reaching either the filament or the walls. It is only those positives which reach the neighbourhood of the filament before recombining that are effective in reducing the negative space-charge and causing an increase in the filament-grid current.

The present investigation is concerned chiefly with hydrogen. The results obtained seem to indicate (1) some kind of action between hydrogen and a glowing tungsten filament : (2) the formation in the discharge-tube of a substance which shows no evidence of ionization below 40–50 volts, whereas ordinary hydrogen in the same tube ionizes at 20–27 volts ; (3) the formation of some compound, [possibly identical with (1)], which is condensable in liquid air, but unstable at ordinary temperatures.

The large-volume ionization in the region beyond the grid renders this type of tube particularly suitable for studying chemical actions. It also seems likely that this form of tube would favour the formation of negative ions, and these would probably show considerable chemical activity. It is known (from J. J. Thomson's experiments on positive rays) that hydrogen is capable of forming H_2 and H.

* Communicated by the Authors.

† Stead & Stoner, Proc. Camb. Phil. Soc. xxi. p. 66 (1922).

Electro-positive elements, such as mercury, nickel, and tungsten, would perhaps be more likely to combine with negative hydrogen ions than with positive ions, and also a molecule such as H_3 might be produced by a combination of $\overset{-}{H_2}$ with $\overset{+}{H}$.

The following investigations were a continuation of the work of Stead and Stoner * on low-voltage glows obtained in mercury vapour by means of a thermionic tube of special design.

Cadmium.—Preliminary experiments were performed with cadmium vapour in a tube of the same form as that used for mercury (fig. 1). The grid was an open one of zigzag

Fig. 1.

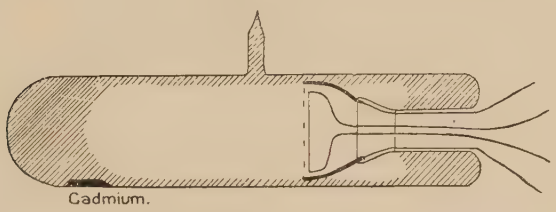

pattern, with about three turns, and of length just less than the diameter of the tube ; there was no anode, the grid being connected to the positive end of the high-tension battery. The tungsten filament (about ·0089 cm. diameter) was about 1·5 mm. from the grid. A small stick of pure cadmium was placed in the tube, which was evacuated and baked in the usual way ; the pressure on sealing off, as measured by the McLeod gauge, was less than ·0001 mm. of mercury. Different pressures of cadmium vapour could be maintained in the tube by keeping it as nearly as possible at different constant temperatures by means of an electric furnace.

Observations.

The same type of characteristic curve was obtained as in the case of mercury vapour (fig. 2). The following points were observed :—

(1) The sudden jump to saturation again occurred, synchronous with the appearance of the glow, and the corresponding fall of current from the saturation value occurred at a lower voltage than the rise.

* *Loc. cit.*

(2) The striking potential again decreased with increasing pressure till an optimum pressure was reached, at which the striking potential was a minimum (it increased with further increase of pressure).

(3) At the point of minimum striking potential, the area of the hysteresis loop was a maximum, and with sufficiently high pressure the hysteresis loop disappeared entirely and the currents were very small.

(4) The glow, as before, could be made to move up and down the tube by increasing or decreasing the voltage within limits; the spectrum of the glow was not examined in detail, but the ordinary line spectrum of cadmium was prominent.

Fig. 2.

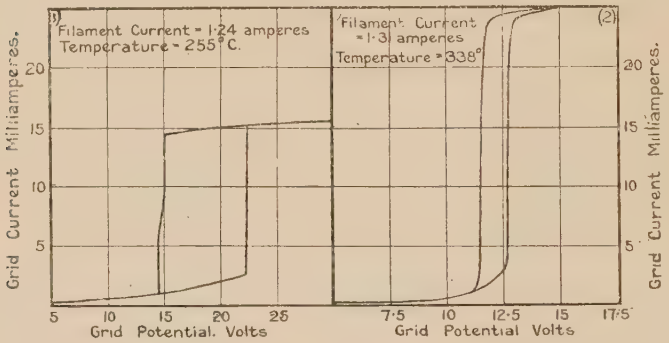

It seems likely that, since cadmium and mercury show similar results under similar conditions, other monatomic gases and vapours would behave in the same kind of way.

Hydrogen.—The valve used in the experiments on hydrogen was identical in design with the cadmium and mercury valves, except that it had two outlet tubes, one attached to the evacuating apparatus, and the other to the source of hydrogen, which was, at first, a strong solution of phosphorus pentoxide in water. This was electrolyzed, and the hydrogen was passed over dry phosphorus pentoxide and through a trap immersed in liquid air. In later experiments a palladium tube was used as a source of hydrogen, but it was found that the change did not affect the observations. The discharge-tube was baked out as usual, and was evacuated each day before experimenting: a trap immersed in liquid air was placed between the main tube and the pump, to condense as much mercury vapour as possible.

Observations.

I. Oscillations.

A small amount of hydrogen at a pressure of about 0·5 mm. was let into the main tube, and the characteristic curve, grid current/grid potential, was plotted. The type of curve obtained was quite different from that shown by the monatomic vapours. There was no sudden jump to saturation, but the curve appeared quite continuous, giving a gradual increase of current till a potential of about 30 volts was reached. At this point a small jump occurred in the current, and then a curious instability was observed. Instead of remaining at a steady value for constant voltage, the current rose slowly and regularly to a maximum, and then fell again to a minimum, then increased again, and so on with a regular oscillatory movement of definite period.

Fig. 3.

Filament current 1·16 amp. Pressure ·057 mm. Filament current 1·0 amp. Pressure ·05 mm.

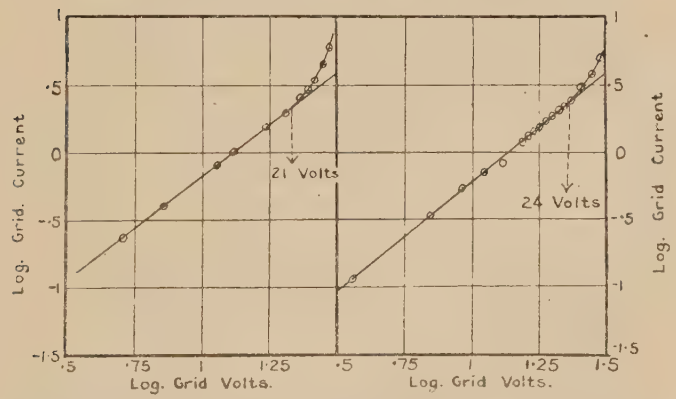

The rise and fall of the current corresponded to a motion of the glow up and down the tube. The small jump at the minimum voltage for this oscillatory condition (about 27–30 volts) probably coincided with the first appearance of the glow, though it was difficult to observe the latter, as it was very faint at first, the intensity increasing gradually with the extension of the glow along the tube. On plotting the logarithms of the current and potential up to the oscillating point, it was seen that a rise in the power curve occurred at about 20–25 volts; the exact point varied with the conditions (filament current, pressure, etc.) (fig. 3).

Preliminary experiments indicated that in general the time of oscillation decreased with increasing voltage. Under favourable conditions, with an optimum pressure of about ·04 mm., oscillations could be observed up to at least 80 volts on the grid, but to obtain oscillations at these higher potentials it was essential to perform a step-up process. The oscillatory state was first produced at a low potential, *e. g.* at about 40 volts, and the voltage then increased by steps of about 2 volts, the system being allowed to settle into the oscillatory state at each step, which it would do if left alone for a few minutes. The oscillations were followed by watching the pointer of the milliammeter, and on some occasions it was possible, by means of the step-up process, to observe an oscillation (at a grid potential of about 80 volts) which was so rapid that it was only shown by a trembling of the pointer. If a high voltage was applied to the grid at first, without the step-up process, a fairly steady current was shown with no oscillations.

Rough observations made on the spectrum of the glow by means of a Hilger spectroscope showed that in the latter case the Balmer lines were the most prominent and the secondary spectrum faint; but when the glow grew to a maximum at low voltages, there was a corresponding gradual increase in intensity of the secondary spectrum. If the glow was thus allowed to grow to a maximum, and the high voltage then applied to the grid, without any intermediate steps, a momentarily very large current was obtained, with a brilliant secondary spectrum, but this decreased very rapidly to a minimum, and the secondary spectrum again became faint, leaving the Balmer lines prominent.

The oscillations were studied in more detail, and the following results were obtained :—

(1) *The frequency of oscillation* increased regularly with increasing voltage. If the logarithm of the time of oscillation is plotted against the logarithm of the grid voltage, the points seem to lie approximately on a straight line (fig. 4 *a*). The extreme values for high and low voltages are somewhat off the line, but it was impossible to keep the pressure constant during a series of observations extending over any length of time. The three lines corresponding to the three series taken gave a mean slope of 3·9. The frequency of oscillation was therefore approximately proportional to the fourth power of the grid voltage. Pressure changes during the oscillations could not be investigated, as there was a general pressure decrease all the time, which made observations on a slow oscillation unreliable, and it was

impossible to follow the rapid oscilliations with the McLeod gauge, but changes of pressure accompanying similar changes of current were observed (see later) with another form of tube.

Fig. 4 *a*.

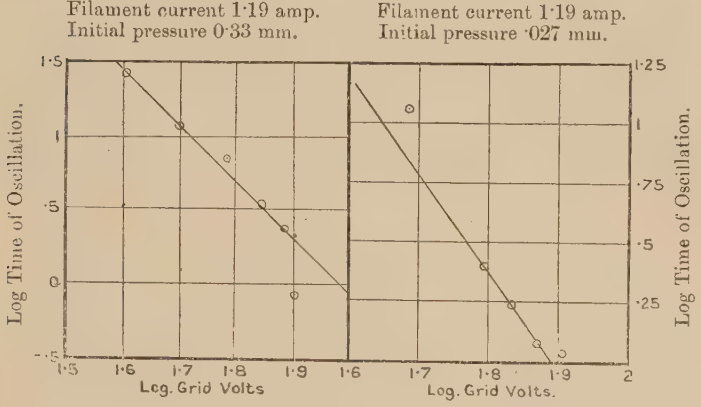

(2) *Variation of Current with Time.*—During the fall of one oscillation from maximum to minimum, the current decreased with the time ; the curve was approximately exponential in form, but with irregularities near the maximum and minimum (fig. 4 *b*). The maximum currents often reached several hundred milliamperes.

Fig. 4 *b*.

Fig. 4 *c*.

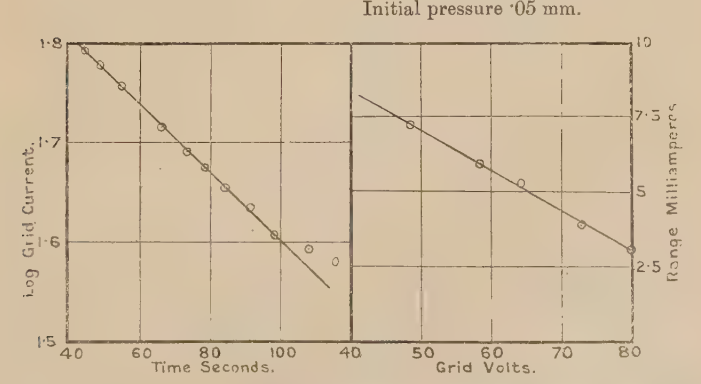

(3) *The range of oscillation* varied directly with the grid voltage when the oscillation had reached a steady condition (fig. 4 *c*). Each time the grid potential was increased, the range of oscillation was at first rather irregular, but settled

down to a fairly constant value. This was most easily seen with slow oscillations of large amplitude, the range decreasing from the initial value, while the time of oscillation showed a slow increase, and may probably be largely accounted for by the general pressure decrease due to absorption of hydrogen into the walls. With rapid oscillations the steady condition was reached more quickly, though there was a subsequent slow increase in the time of oscillation, again probably due to change of pressure; for instance, an oscillation of approximately constant period was maintained for ten minutes, and the change of period was only appreciable after this time.

Table I.

Initial pressure.	Final pressure.	Fil. current.	Grid volts.
·0385 mm.	·033 mm.	1·2 amps.	80

Number of oscillations in successive intervals of 10 seconds.

11, 10, 11, 11, 11, 12, 12, 12, 12, 12, 12, 12, 11, 11, 11, 11, 11, 11, 12, 12, 10, 10, 10, 11, 10, 10, 10, 11, 9, 9, 10, 10, 10, 10, 10, 10, 11, 10, 11, 10, 10, 10, 11, 10, 12, 14, 13, 12, 12, 12, 11, 12, 12, 11, 10, 11, 11, 11, 11, 8, 10, 12, 8, 9, 10, 9, 10, 9, 8, 9, 9, 10, 10, 8.

There is not much change here for at least ten minutes. It may therefore be assumed that the time of oscillation would be constant for constant pressure. Greater changes of pressure had a marked effect on the time of oscillation.

(4) *The form of oscillation*, when fairly rapid, was a gradual rise, then a jump to the maximum, then a gradual fall and a jump to the minimum.

(5) An attempt to obtain an oscillatory glow with a stream of hydrogen passing through the tube was unsuccessful.

In case the oscillatory phenomena were due to the periodic charging up and discharging of the walls of the tube, the experiments were performed with a tube whose walls were silvered internally and connected to the negative end of the filament, but it was still possible to obtain the oscillating glow under these conditions.

An attempt was made to exclude mercury as far as possible by baking the main tube, with liquid air round traps on either side, till the mercury lines were no longer visible in the spectrum of the glow. The oscillations could still be obtained, though not so easily as before. Of course it was impossible to remove all the mercury by this means, but the experiments seemed to indicate that mercury was not an essential factor for the production of the oscillations.

Later experiments with other tubes of as nearly as possible the same design, and used under approximately the same conditions, were unsuccessful in producing regular oscillations, though at low pressures irregular oscillations were shown. It seems likely, therefore, that in the first case an optimum spacing of the grid wires had occurred accidentally. The same electrodes were used for the silvered and unsilvered tubes, but were afterwards unfortunately broken. Further attempts will be made to reproduce the oscillations with grids of various spacings. It is also probably necessary to have carbon vapour present (from tap grease) to produce the oscillations, but this alone is not sufficient.

II. Effect of Liquid Air.

Another tube of slightly different design was prepared, with a collecting tube at right angles to the main tube below the filament (fig. 5). This collecting tube was immersed in

Fig. 5.

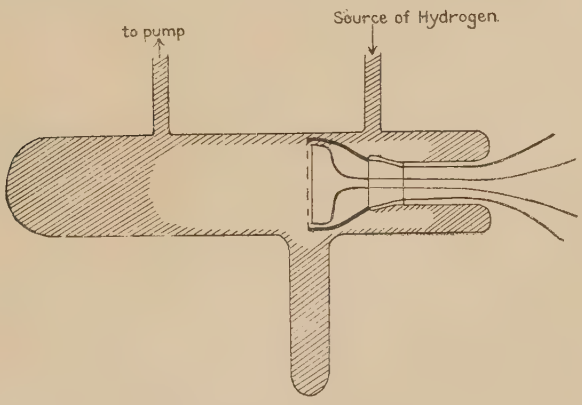

liquid air, in order to collect any condensible gases. At the same time another McLeod gauge was attached near the main tube, so that the gauge and tube could be shut off by taps from the rest of the apparatus. The main results with this tube were as follows :—

(1) *Disappearance of Hydrogen.*—Very brilliant glows were obtained ; these showed intense secondary spectra, and very large currents up to 700 milliamps. The glow did not oscillate, but grew to a maximum, and gradually increased

in brightness, then fell back slowly and disappeared when close to the filament; it could not be produced again by increasing the filament current, and it was found that nearly all the hydrogen had disappeared into the collecting-tube. The process could be repeated any number of times. Sometimes the glow could be temporarily regenerated by a slight decrease in filament current, but would soon disappear again.

(2) *Appearance and Disappearance of the Glow.*—When the glow had run back, it could also be regenerated by increasing the grid potential, and by a step-up process be made to disappear at successive increasing grid potentials.

(3) *Variation of Pressure with Current.*—Oscillations could not be obtained with this tube, either with or without liquid air on the collecting-tube. The nearest approach to the oscillating condition was shown by allowing the glow to grow and the current to increase while there was a low potential on the grid, say 35 volts, and the pressure noted at the maximum; a high potential, say 80 volts, was then put on the grid, the current diminished rapidly, and it was found that the pressure rose. A typical example is shown in the following table.

Table III.

Pressure. (300 mark of gauge.)	Position of glow.	Grid volts.	Grid current. (milliamps.)
277	max.	30·5	grows to 55
281·5	min.	81·5	falls to 6
268·5	max.	30·5	grows to 46
274	min.	81·5	falls to 6·25
256·5	max.	32	grows to 42
263	min.	82	falls to 6·1

(4) *Return of Pressure.*—Yet another pressure effect was observed. Readings of the McLeod gauge when the filament was put on showed the usual fall of pressure, but on switching off the filament a rise in pressure took place, sometimes to nearly the initial value. This was a very definite effect, usually more marked the greater the current to the grid. Several series of readings were taken, of which one is given below. The pressure readings were taken as quickly as the McLeod gauge would allow, so that about one minute elapsed between P_2 and P_3. The time between P_1 and P_2 varied, but was generally of the order of 10 to 60 seconds.

TABLE IV.

Grid volts.	Initial pressure. P_1 mm.	Pressure on switching off. P_2 mm.	Pressure on standing. P_3 mm.
(*a*) 29	·0545	·0475	·0505
	·0505	·046	·05
	·05	·046	·049
	·049	·046	·053
(*b*) 49	·055	·0495	·055
	·055	·050	·053
(*c*) 60	·057	·051	·059
	·059	·052	·059
(*d*) 90	·063	·059	·063
(*e*) 127	·064	·060	·064

a, *b*, *c*, *d*, *e*, are examples selected from a longer series; some intermediate voltages are not given, so that for a change of voltage in the table the pressure readings are not consecutive.

This return of pressure must be distinguished (as quite different) from the changes of pressure observed during the variation of the glow. For the latter effect it was essential that the filament should be on continuously; but the former effect was not apparent unless the filament was switched off, and the tube allowed to stand for at least half a minute.

(5) *The gas liberated on removing the liquid air* from the collecting-tube was investigated. The method first employed was that of sparking in a quartz capillary tube substituted for the glass capillary above the bulb of the second McLeod gauge. External tinfoil electrodes were used, and the discharge from the secondary of an induction coil passed through the gas trapped in the gauge. The observations were made on the change of pressure at constant volume. Very irregular results were obtained; the ratio of the volume after sparking to the volume before sparking varied between extremes of about seven and one. The spectrum of the discharge showed strong carbon bands in addition to the hydrogen spectrum. Control experiments with ordinary hydrogen gave a ratio less than one, though carbon lines were still present in the spectrum, probably due in this case to impurities on the surface of the gauge and mercury, but they were much less prominent. Control experiments with hydrocarbons such as methane and ethane gave an increase in volume on sparking, and bright carbon and hydrogen lines.

It seems probable that in these experiments very active hydrogen was formed in the tube, and this combined readily with carbon impurities. The most likely source of the latter was tap grease; although it has a small vapour-pressure, it could distil over into the main tube at night. Another source might be the carbonates of the glass itself. The taps were replaced by mercury barometer columns, and after running the tube for some time under these conditions, the sparking ratio decreased and was sometimes less than one. The hydrogen also did not disappear so readily; but even after prolonged use it did not seem possible to eliminate the carbon lines from the glow and spark spectrum of the liberated gas, part of which appeared to be non-recondensible.

III. Quartz Tube.

In order to eliminate the carbon impurities as far as possible, a quartz tube was constructed. It was similar to the glass tube, except that it had one outlet only, opposite the collecting-tube, and the electrodes were so arranged that the axis of the filament was in a straight line with the axis of the collecting and outlet tubes. The quartz was heated red hot every day, with liquid air surrounding a trap between it and the pump and nearest mercury cut-off, so that it might be assumed that after prolonged use there was very little carbon left; a large part of the mercury present would also be removed by heating, though a certain amount would still be left on the electrodes etc.

With liquid air round the collecting-tube, the glow did not run back as before, except at very low pressures. In the latter case a faint secondary glow was left after the bright primary one had disappeared; this secondary glow had also been seen with the glass tube. At higher pressures large currents were obtained up to about 500 milliamperes. They were accompanied by bright glows, showing a marked secondary spectrum of hydrogen. The optimum pressure for this condition was of the order of ·07 mm., and the optimum voltage about 38 volts; a definite time was required for the glow to grow to a maximum. Further points were observed on experimenting with this tube:—

(1) *Disappearing Glow.*—In place of the run back and disappearance of the glow, which were obtained easily with the glass tube, another type of disappearing glow was seen. Under favourable conditions of pressure, and when the current had been allowed to grow slowly to a maximum, if the potential lead was removed from the battery for a few

seconds and then replaced, the current was smaller than before, and the glow had disappeared. If the potential was then increased by a few volts, the glow and large current would appear again, and could once more be made to disappear, and the process could be repeated up to the limit of the battery. This effect is similar to that observed with the glass tube (2). It seems that this "artificial disappearance" is not a simple pressure effect, for though it is more easily produced at low pressures, it can also occur at pressures quite sufficient to show the ordinary ionization glow under ordinary conditions. Of course at low pressures the glow is very faint, and might then appear to be absent, but other evidence supports the conclusion that the gas in the tube is in an abnormal condition.

(*a*) The disappearance cannot occur without liquid air round the collecting-tube. Without it, a somewhat similar effect could sometimes be produced at very low pressures, but only up to about 47 volts. In this case the pressure was probably diminished by absorption into the walls, and became too low to maintain a glow at the lower voltages. With liquid air round the tube the glow would disappear easily at higher pressures and up to at least 80 volts. The experiments were not usually carried further, though it was possible at low pressures to carry it up to at least 180 volts on the grid; the upper limit of disappearance was apparently higher the lower the pressure.

(*b*) When the glow had disappeared, it could be regenerated by removing the liquid air from the collecting-tube, though this involved very little general pressure change.

(*c*) When the glow had disappeared at one voltage, and was regenerated at a higher, if the lead was put back in the first position, the glow would sometimes appear again, the next removal causing it to disappear once more, so that the first disappearance could not have been simply due to a fall of pressure.

(*d*) If the characteristic curve for the tube (grid current/grid voltage) was plotted when liquid air was not on the collecting-tube, the upward bend in the log curve due to ionization occurred at about 20–27 volts (the exact point depending on filament current, pressure, etc.) (fig. 6*a*). If, however, the characteristic was plotted for the tube in the "disappeared" condition, at the same order of pressure, the upward bend did not occur until the grid potential had a much higher value, such as 40, 50, or 60 volts, the position of the bend depending upon the potential at which the glow had been made to disappear (fig. 6*b*).

Fig. 6 *a*.

Ordinary hydrogen.
Quartz tube.

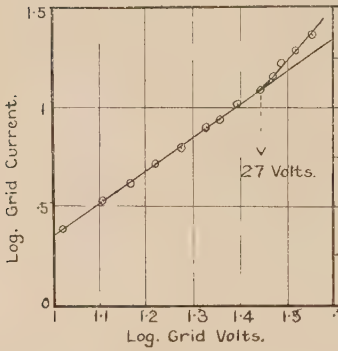

Fig. 6 *c*.

Ordinary hydrogen. Quartz tube.
(Low pressure.)

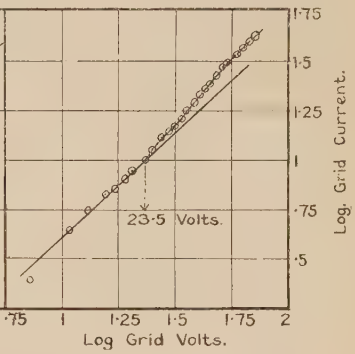

Fig. 6 *b*.

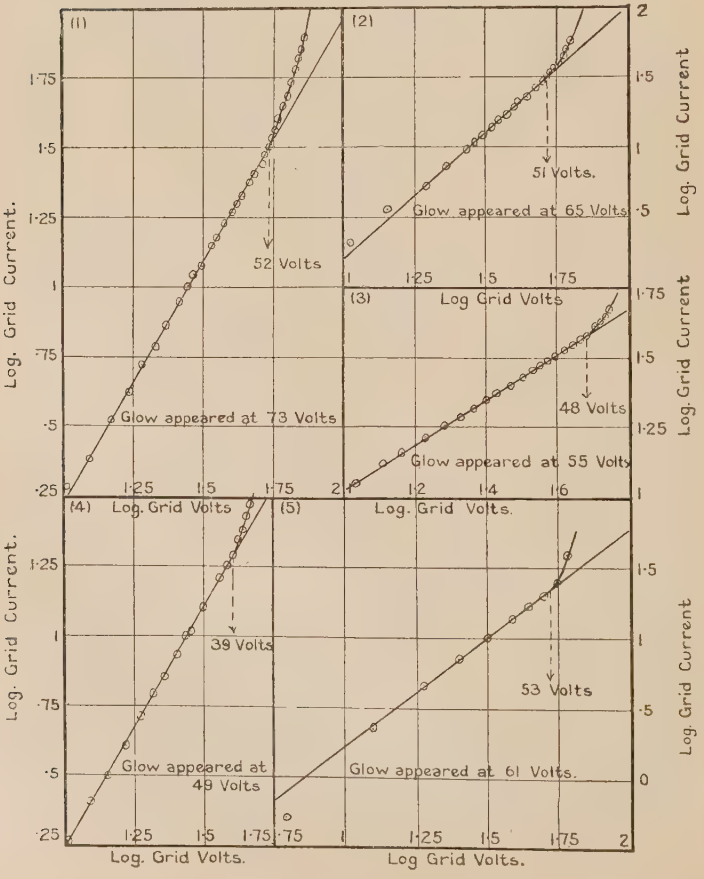

In general the bend occurs at a higher value for a higher appearing potential. Table V. gives the position of the ionization bend in a series of curves, and in each case the corresponding potential at which the glow appeared. The

TABLE V.

Ionization break. Volts.	Appearing Voltage.
51	63
39	49
52	73
54	—
50	57
53	63
48	55
58	72
49	55
53	57
59	80
General order of pressure	·01–·05 mm.

average value for the upper limit lies between 48 and 54 volts; there are two higher values at 58 and 59 volts, corresponding to high appearing voltages, but in both cases the pressure was low. It is impossible to say, from the curves already obtained, whether there is a definite upper limit to the voltage at which ionization takes place, since the position of the bend can be shifted through two or three volts by changes of pressure, filament current, etc.; it would be necessary to perform experiments with a linear source of constant velocity electrons to establish this point. Table V., however, indicates that possibly there is such an upper limit.

When the glow finally did appear, the currents were large: often about 180 milliamperes. Characteristic curves at the same order of pressure for the tube in the ordinary conditions, with or without liquid air near the filament, showed quite a different form of curve (fig. 6*c*). Even at very low pressures, the potential at which ionization was detectable was much lower than that observed for the "disappeared" state.

(*e*) The disappearance was much more easily obtained when the level of the liquid air was high round the collecting-tube, and when there was therefore a sharp temperature gradient near the filament. Also the current could be made to increase by pressing cotton-wool soaked in liquid air on to the outside of the main tube next to the upper end of the filament; this sometimes caused an increase of about 10 milliamperes. The cooling was more effective the nearer the cold spot was to the filament.

(*f*) Before disappearance the glow was much fainter over the liquid air than behind the filament.

(*g*) With this type of disappearance the secondary glow was never seen.

(*h*) The "disappeared" state would persist for hours unless the liquid air was removed.

(*i*) The characteristic curve showed the hysteresis effect in the region of the glow striking potential.

(*j*) The difference between the currents before and after the disappearance of the glow was greater the greater the ionization; for instance, a current of 100 milliamperes would drop to about 10 milliamperes.

(2) *Absorption of Gas.*—Gas was absorbed into the walls of the tube even when there was no potential on the grid, but this was more marked the greater the ionization. A certain amount was restored on heating to red heat, and, when tested, behaved like ordinary hydrogen. The discrepancy between the amount disappeared and the amount restored was always greater with large ionization currents. The following table gives an example:—

Table VI.

Ratio of gas disappeared/gas returned.	Grid volts.	Ionization current. (milliamps.)
255/87	up to 75	up to 450
125/71	34	—
67/59	32	30
191/80	up to 80	200

(3) *Fluorescence of the Quartz.*—After experiments in which an intense glow had been in the tube for some time, on switching off the filament the tube glowed with a whitish phosphorescence, and when heated gave out a bright green fluorescence, which was destroyed by heating to red heat and was only recovered by leaving the glow on again. It was an internal effect, and not due to the flame with which the tube was heated, as it also showed on the small quartz tubes covering the electrodes inside the main tube. A similar effect has been noted by other workers with quartz tubes, and has been shown by Ludlam and West * to be due to small impurities in the quartz, which absorb radiation from a glowing gas and show an accelerated phosphorescence on heating. It was probably strong ultraviolet radiation that was absorbed in this case; as far as could be seen with a direct-vision spectroscope, the spectrum of the fluorescent light was a continuous band in the green.

* Ludlam and West, 'Nature,' March 15, 1924.

(4) *Return of Pressure.*—The return of pressure on switching off the filament (as with the glass tube (II. 4)) was very marked in the quartz tube. It occurred with or without liquid air on the collecting-tube, and also, though to a less extent, when there was no potential on the grid.

The filament in the quartz tube burnt out, and was replaced by another, arranged so that it was just behind the collecting-tube instead of immediately over it. Though the results observed before were all reproduced, they were on a smaller scale, and the currents were not so large. It was not so easy to get the disappearing glow, and a lower pressure, of the order of ·01 mm., was necessary to observe it at the higher voltages. The green fluorescence was not visible, but by this time there was a considerable metallic deposit on the walls.

(5) *Effect of charging the Walls.*—This deposit was examined, and was found to consist in part of a fine layer of tungsten, and in part of a flaky metallic deposit all round the tube just behind the grid. On analysis this proved to be chiefly nickel with perhaps just a trace of mercury. The grid must therefore have been sufficiently hot to drive out any occluded gas. Connexion was made to the deposit by inserting a stranded copper wire with a brush of wires at the end down the outlet tube ; the wire was bent so that the brush pressed against the upper wall of the main tube. The end of the wire was sealed in through a T-piece above the outlet tube. The deposit was very uniform, and formed an efficient internal metallic coating. Experiments were then carried out to see how far the foregoing results were affected by a positive or negative potential on the walls.

(*a*) The return of pressure was not affected by either earthing or putting a negative potential on the walls ; it also occurred when the glow was in a "disappeared" state. With a positive potential on the walls, it was shown up to a certain point when the nature of the discharge changed, and nearly all the current went to the walls ; on switching off the filament then, the pressure either remained the same or decreased.

(*b*) Curves were plotted showing the relation between grid current and wall potential, and current to the walls and wall potential, for constant grid potential (fig. 7*a*).

With the grid above the ionizing potential, as would be expected, one curve is the mirror image of the other. Very little effect is observed on charging the walls negatively ; both the grid and wall currents have practically constant values, the latter negative, (observed by interchanging the

grid and wall leads and reversing the connexions to the milliammeter). The negative current is obviously due to the accumulation of positive ions. The kink in the curve at 0 volts shows the potential acquired by the insulated walls. When the walls are charged positively, with increasing charge they take more and more positive current from the grid. The potential on the insulated walls may be read off the curve by drawing a horizontal line from the point giving the current for insulation to the curve on the positive side,

Fig. 7 *a*.

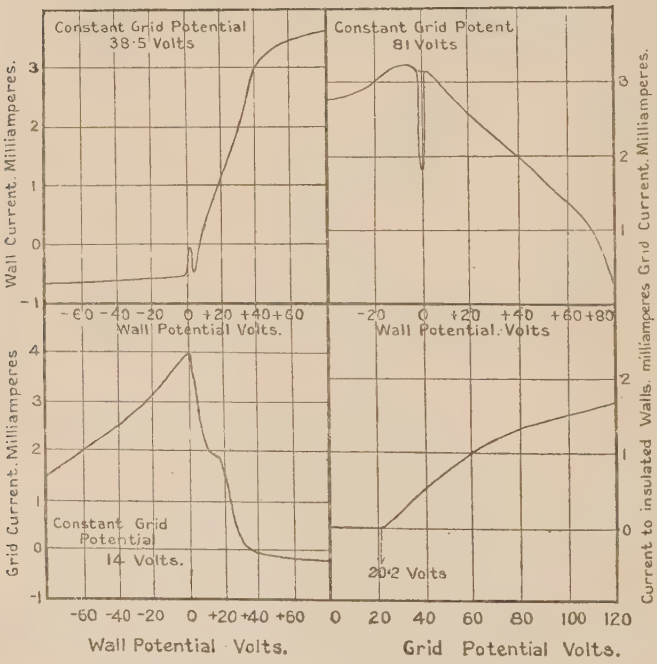

Fig. 7 *b*.

Fig. 7 *c*.

and the point at which the curve cuts this line corresponds to a certain potential, which is also that of the insulated walls. The same type of curve was shown whether liquid air was on or off the collecting-tube.

With the grid below the ionizing potential, the tube acts as a three-electrode valve. The curves are of the form shown in fig. 7 *b*. The grid current gradually increases as the wall potential is increased from a negative value. With a positive potential on the walls, the grid current approaches

a saturation value, but decreases again at about 19 volts, owing to the production of positive ions. A second saturation is shown later ; the grid current is then negative, as positive ions are driven into it.

The apparatus was arranged at one time so that the potential of the insulated walls could be read for increasing grid potential. Fig. 7*c* shows this relation. There is zero current to the walls till ionization takes place. The point where the curve breaks away from the line of zero current indicates the potential at which positive ions appear. A current of ·001 milliampere could be detected by the milliammeter, and a sensitive galvanometer could be deflected by much less. With sufficient increase of grid potential, the current to the insulated walls and the potential of the walls reached constant values. When the glow was bright and there was a large current to the grid, for instance about 120 milliamperes, the potential of the insulated walls was small, of the order of 2 or 3 volts ; when the grid current was small (4 or 5 milliamperes) the potential of the insulated walls was large (15, 20, or even on one occasion 40 volts) ; the grid voltage in the latter case was 80 volts. The potential on the walls was increased by putting liquid air on the collecting-tube. Just before the glow disappeared, the wall potential fell slowly and then gave a jump to zero.

(*c*) Earthing the walls or charging them negatively did not prevent the disappearing glow, nor did a positive charge up to a certain limit at which a very large proportion of the electrons went to the walls instead of the grid. If the glow was first made to disappear and a sufficient positive potential then put on the walls, it would reappear, and on removing the lead from the walls, the grid current increased above its former value.

(6) *Spectroscopic Observations.*—Rough observations were made on the spectrum of intense glows which accompanied large currents at low voltages ; a Hilger spectroscope was used. The most prominent lines in the secondary spectrum were those placed by Fulcher * in Group I. of his classification—those which do not show the Zeeman effect. No photographs have yet been taken.

(7) *Liberated Gas.*—The products condensed in the collecting-tube by liquid air were again examined. The following methods were used :—

(*a*) On sparking the liberated gas in the McLeod gauge, it decreased in volume.

* Fulcher, Astrophys. Journ. xxxvii. p. 65 (1913).

(*b*) On the examination of the glow spectrum of the liberated gas as it passed the filament, the momentary flash showed bright hydrogen lines and bands, and in the case of the glass tube strong carbon bands as well, but these were not noticeable in the quartz tube.

(*c*) The gas was also investigated by means of the Pirani gauge *. An Osram lamp was sealed on to the aparatus near the main tube; the lamp filament formed one of four arms of a Wheatstone bridge. When gas was liberated from the collecting-tube, the resistance of the lamp filament altered, and the balance was regained by adjusting the total potential round the bridge. The temperature of the collecting-tube

Fig. 8.

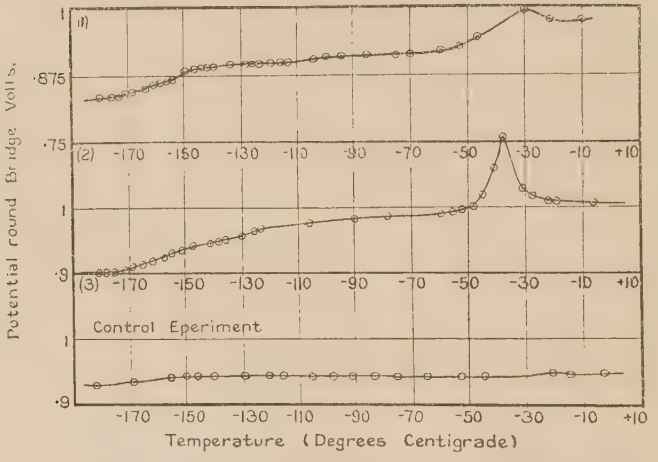

was roughly determined by means of a direct-reading thermopile inserted in a tube of ether round the collecting-tube, the whole being immersed in liquid air. The temperature was plotted against the total potential round the bridge. When no gas was being given off, the curve had a slight upward slope, since the volume of the collecting-tube was comparable to the volume of the part of the apparatus into which the gas could expand. When gas was given off, the curve rose more steeply till all the particular gas had been given off; it then continued nearly horizontal till the next gas was liberated. The curves obtained with the glass tube were irregular, and showed that several gases were present. The curves for the quartz tube (fig. 8) showed that certainly one, and possibly

* General Electric Co., Proc. Phys. Soc. 1921, p. 287.

two, non-recondensible gases were present, besides a certain amount of mercury which could not be removed, and was recondensible in the upper liquid-air trap, as the fall at the end of the curve shows. The other product or products were given off between the temperature of $-174°$ and $-140°$ centigrade. The exact temperature could not be determined, as the position of the thermopile varied, and only gave a rough approximation of the temperature of the collecting-tube ; also this form of gauge takes about a minute to settle for each reading, so that it is very difficult to get an accurate continuous series. Fig. 8 also shows the results of a control experiment in which ordinary hydrogen in the collecting-tube was warmed up from the temperature of liquid air.

(*d*) The characteristic curve for the liberated gas was plotted from readings taken in the quartz tube when there was an insulated rod electrode opposite the grid (see below). The curve (fig. 9) was very similar indeed to one taken for hydrogen at very much the same low pressure.

(8) *Effect of extra Electrode.*—Various experiments were performed when the tube had this extra electrode. The main results noted were as follows :—

(*a*) The currents were not nearly so large as had been observed in the tube before.

(*b*) At no time was the secondary spectrum any more than faint ; the Balmer lines were always the most prominent.

(*c*) The disappearing glow could not be produced except at very low pressure, when it is probable that there was not enough gas to maintain the ionization current.

(*d*) The return of pressure with the filament off was unaffected.

(*e*) The characteristic curve was somewhat altered in form. It showed a sharp rise at about 18 volts, which was marked even at a pressure of ·003 mm. ; with the tube in its former condition no noticeable rise could be seen at this order of pressure.

(*f*) The hysteresis effect was well marked.

Summary of Results.

(1) The cylindrical tube with open grid and no anode is favourable for the production of large currents and glows showing intense secondary spectra ; these show a time-effect in their growth to a maximum.

(2) With an optimum spacing of grid wires and in the presence of carbon vapour, the glow shows regular oscillations.

(3) In the presence of carbon vapour, a very large proportion of the hydrogen present can be made to condense at a temperature of liquid air. If carbon is eliminated as far as possible by using a quartz tube etc., a small but definite amount of the hydrogen still condenses, either by itself or in the form of a compound. The liberated gas is non-recondensible and behaves like ordinary hydrogen.

(4) When there is a sharp fall of temperature close to the filament, by suitable treatment the gas in the tube may be brought to a condition where there is no detectable ionization, even though the grid potential is above the ionizing potential of hydrogen. This condition is stable for at least an hour, probably longer. The gas may be brought back to the ionized condition by removing the liquid air or by giving a sufficient positive charge to the walls of the tube.

(5) When the filament is bright, hydrogen is absorbed by the walls whether there is a potential on the grid or not, though more is absorbed in the first case. The absorption also occurs whether the walls are earthed, charged positively or negatively. Only part of the gas is liberated on heating the walls to red heat.

(6) When the walls are insulated they acquire a considerable positive charge, which is greater for small grid currents and less for large grid currents.

(7) On heating the filament there is a decrease in pressure, but there is a certain return of pressure on switching off the filament and allowing the tube to stand for about half-a-minute. This effect is independent of the charge on the walls, the potential on the grid, and the presence of another insulated electrode; provided the nature of the discharge does not change, the magnitude of the effect is in general greater for greater ionization.

(8) The insertion of an insulated-rod electrode opposite the grid modifies the characteristic curves, reduces the currents, and prevents the occurrence of the disappearing glow. It also intensifies the Balmer lines in comparison with the secondary spectrum.

Discussion of Results.

(1) *Return of Pressure.*

The pressure changes described in paragraphs II. 4, III. 4, and III. 5*a* seem to be chiefly an effect due to the filament, since they occur when the grid potential is not on. The pressure is smaller when the filament is glowing than when it is cold, and this probably indicates absorption of gas by the

hot filament with subsequent re-emission when the filament current is cut off. This may be associated with the fall of current from the initial value observed when the filament is switched on, if there is a sufficient potential on the grid to make a considerable quantity of positive ions. There is at first a definite decrease of current from the initial value, independent of any subsequent growth; the fall-back can be reproduced after allowing the tube to stand for a short time with the filament off.

It appears likely that this is due to the formation of an endothermic compound of hydrogen and tungsten which depresses the emission of the filament. Such a compound might be quite stable at 2500° K. and extremely unstable at ordinary temperatures. Langmuir* states that all the atomic and 65 per cent. of the molecular hydrogen which strikes a heated tungsten filament is absorbed by it, and that further dissociation of the hydrogen takes place within the filament. The increase of pressure occurs more readily when there has been a positive potential on the grid sufficient to ionize the hydrogen, so that probably hydrogen ions (H^+ or H_2^+) combine with tungsten more readily than neutral hydrogen molecules. The electric field in the tube will cause the filament to be bombarded by positive ions. The only condition so far observed under which the return of pressure does not occur, is when there is a large positive potential (considerably larger than the grid potential) on the walls of the tube. In this case the grid current has either a negative or a very small positive value, which indicates that positive ions are being driven into it. Normally the field in the tube drives the positive ions into the filament, but under these conditions, since the grid has a much larger surface area and is at a considerably lower potential than the walls, it probably collects most of the positive ions and acts as a screen to the filament. Calculation of the mean free path in hydrogen showed that it was of the order of the distance between the filament and grid (about 1·5 mm.) at a pressure of about ·08 mm. The mean free path of an electron is certainly greater; and as the experiments were generally carried out at a pressure less than ·08 mm., the grid would effectively screen the filament from most of the positive ions formed.

(2) *Nature of the liberated Gas.*

In the glass tube there can be little doubt that the gas released when the liquid air is removed from the collecting-tube consists largely of compounds containing carbon and

* Langmuir, Journ. Amer. Chem. Soc. xxxvii. p. 451 (1915).

hydrogen. This is shown by (*a*) the presence of strong carbon-monoxide bands along with hydrogen lines in the spectrum of the gas; (*b*) the large, but irregular, increase in volume when the gas is sparked. It seems probable that hydrocarbons would be formed by the action of hydrogen ions on carbon compounds from the glass, and it is known that such compounds as ethane are decomposed by an electric discharge.

The curve obtained with the Pirani gauge shows that a number of different substances are present in the collecting-tube, and that these substances evaporate one by one as the tube is allowed to warm up after the liquid air is removed.

In the quartz tube it is unlikely that carbon compounds can exist in appreciable quantities after the tube has been in

Fig. 9.

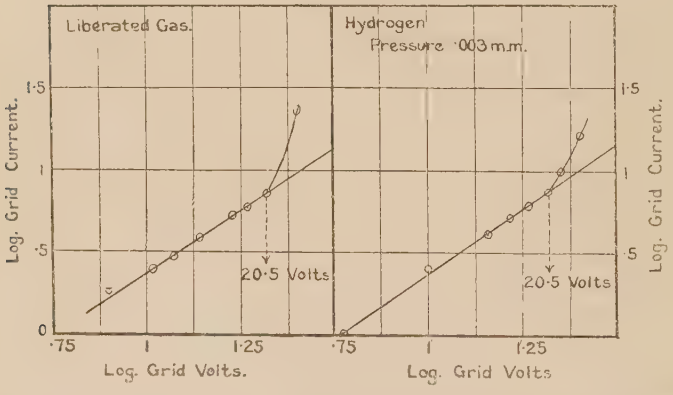

use for some time. The quartz was heated red hot by a blow-pipe each morning before experiments were started, and the liberated gas was pumped out by a Gaede pump and by charcoal and liquid air. The electrodes constituted the only other available source of carbon, and these were always at a high temperature when the tube was in use, the grid being kept at red heat by electron bombardment. Any carbon originally present would probably disappear in a few hours under these conditions.

The spectrum of the gas liberated from the quartz tube showed only hydrogen lines and bands, though this by itself cannot be taken as a proof of the absence of carbon. The characteristic curve of the liberated gas closely resembled that obtained under similar conditions with hydrogen at low pressure (fig. 9). Also the liberated gas, like hydrogen in

control experiments, showed a diminution in volume when sparked in a quartz capillary tube, whereas hydrocarbons give a large increase in volume. The Pirani gauge experiments showed that the gas in the collecting-tube came off when the temperature was between $-174°$ C. and $-140°$ C., and was non-recondensible in liquid air. It therefore seems very probable that the liberated gas is hydrogen, and three possible hypotheses suggest themselves :—

(*a*) That hydrogen in the atomic state is absorbed by the walls of the collecting-tube. This would correspond to Langmuir's * NR gas.

(*b*) That a condensed form of hydrogen, such as H_8, is present in the collecting-tube, stable at the temperature of liquid air, but dissociating at higher temperatures.

(*c*) That active hydrogen forms a compound with mercury, nickel, or tungsten, and that this compound is unstable except at very low temperatures.

The fact that the gas is non-recondensible is satisfied by all three possibilities.

The first hypothesis does not seem consistent with the form of the Pirani gauge curves. If the gas was absorbed by the walls of the collecting-tube, the amount absorbed would be greater the lower the temperature. Some gas would be given off directly the liquid air was removed, and the curve would immediately show an upward slope ; whereas the initial part of the curve is nearly horizontal, and the spot of light on the galvanometer scale was practically steady until the thermopile, which was inserted next to the coldest part of the collecting-tube, read about $-170°$ C. The spot of light then moved on the scale, and the curve took a definite upward bend. On either of the other two hypotheses, the liberation of the gas on removal of the liquid air is a dissociation, and not simple evaporation. The glow spectrum of the liberated gas, obtained as it passed the filament, showed at first marked hydrogen secondary lines and bands ; these gradually faded away, leaving the Balmer lines most prominent. This change may have been simply due to lowering of pressure as the gas diffused into the other parts of the apparatus, but it is unlikely that atomic hydrogen would show a marked secondary spectrum immediately on liberation into a practically evacuated tube. Also the pressure during the experiments was higher than that (·001–·01 mm.) at which Langmuir found that the atomic form of hydrogen (NR gas) was present in large quantities near a glowing filament, so that these conclusions are not necessarily in conflict with his.

* Langmuir, Journ. Amer. Chem. Soc. xxxiv. p. 860 (1912).

It does not seem possible to differentiate between hypotheses (*b*) and (*c*) without further data.

(3) *The disappearing Glow.*

Any theory of the disappearing glow must account for (*a*) the necessity of having liquid air close to the filament; (*b*) the step-up process; (*c*) the marked difference in the potential at which ionization appears in ordinary hydrogen, and in hydrogen in which the glow has been made to disappear; (*d*) the time factor.

The gradual hardening-up of the tube during the discharge is not capable of accounting for (*a*) or (*c*), since ordinary hydrogen at approximately the same pressure behaves normally (fig. 6 *a*). The discrepancy between the two voltages at which ionization takes place in the two cases is much too great to be accounted for by changes of pressure, filament current, etc. The ionization potential observed in the ordinary case is probably the critical potential that exists at about 16 volts, since the fall of potential down the filament was from 4 to 6 volts. The corrected potential at which the abnormal gas is ionized would be roughly between 42 and 51 volts. Smyth * has deduced from his experiments that under certain conditions H_2^+ is formed at 16·5 volts and is not accompanied by disssociation. Horton and Davies† also assign a critical potential at 15·9 volts to the molecule, though Olmstead ‡ considers that the molecule is dissociated and one atom ionized at this point. It seems, however, quite certain that we are here dealing chiefly with a molecular action. The growth of the glow is accompanied by a gradual intensification of the secondary spectrum. Other workers have found similar phenomena at liquid-air temperatures, and all ascribed it to some kind of molecular action §.

The change in the form of the characteristic on inserting a third insulated electrode shows that the latter modifies the field in the tube and shifts the region where $\frac{dV}{d.x}=0$ nearer the filament, thereby reducing the negative space-charge; with the tube in this condition it was impossible to obtain the large currents and disappearing glow.

* Smyth, Proc. Roy. Soc. cv. pp. 116–128 (1924).
† Horton & Davies, Phil. Mag. Nov. 1923.
‡ Olmstead, Phys. Rev. p. 613 (1922).
§ Wendt & Landauer, Journ. Amer. Chem. Soc. xliv. p. 510 (1922); Lemon, Astrophys. Journ. xxxv. p. 109 (1912).

We have therefore, as essentials for the production of the abnormal condition, (*a*) the presence of liquid air near the filament, (*b*) a very dense electron stream resulting in a large negative space-charge, (*c*) a considerable time factor.

These conditions result in the growth of very large currents, sufficient to maintain the grid at red heat and to cause a large amount of nickel to sputter on the walls, and the gradual intensification of the secondary spectrum, especially the Fulcher Group I. bands. This state must first be acquired at a low potential, but may be observed at a high potential by a step-up process; it does not occur if the high potential is applied in the first place.

We put forward the following tentative explanation :—

The conditions seem favourable for the formation of some substance with a large molecule, such as either H_3 or a compound of hydrogen with mercury, nickel, or tungsten, or they may all be formed. The very dense electron stream would increase the chances of production of negative atoms or molecules, and the presence of these would probably favour the formation of such compounds. The gradual growth of the current and the time-effect involved indicate that the chief action of the liquid air is to slow down the heavy positive ions which tend to collect near the filament and in some way form larger neutral molecules by combination with negative ions, the process of accumulation taking a considerable time. This will reduce the partial pressure of H_2 so that when the grid potential is momentarily disconnected and then put on again, the glow is unable to start up until the potential has been raised a few volts. The heavy neutral molecules continue to accumulate, and the partial pressure is again reduced. In this way the appearing voltage of the glow is gradually stepped up, until the accumulation is very considerable. This idea of the gradual reduction of the partial pressure of H_2 is supported by the fact, frequently observed, that when the glow has been on for some time in the quartz tube, the portion of the glow over the liquid air just in front of the grid is definitely fainter than the part at the back of the tube behind the electrodes. When the step-up process has been accomplished, the gas is then in the curious condition in which the characteristics show no evidence of ionization below 42–51 volts.

It seems that there are two possible explanations of the high ionizing potential :—

(*a*) The substance which accumulates is a neutral molecule which posseses considerable stability, and the upper limit of the values found for the high ionizing potential represents

the voltage required to decompose it, when the partial pressure of H_2 is too low to produce an appreciable number of positive ions at a lower voltage.

(*b*) In some way the emission of the filament is depressed, either by increasing the negative space-charge or by action on the filament itself, and that to overcome this condition, electrons of much higher velocity are required. It appears that the only way of increasing the negative space-charge would be by the accumulation of a large number of negatively-charged molecules or atoms which are known to be sometimes present in hydrogen subjected to discharges of various kinds *. However, the abnormal condition is not destroyed by switching off the filament ; so that it does not seem likely that this hypothesis is the right one. It also seems improbable that the emission of the filament can be seriously impaired by chemical action, since there are enough electrons emitted to give considerable grid currents, up to 30 milliamperes, before there is any detectable ionization, when the tube is in the abnormal state. We therefore conclude that (*a*) is the more likely explanation.

It remains to decide whether the large neutral molecule is an aggregate of hydrogen, such as H_3, or a compound of hydrogen with one of the metals present—nickel, mercury, or tungsten.

The abnormally large currents are similar to those obtained by Compton and Duffendack † in their experiments on nitrogen. They found a very active form of nitrogen at 70 volts or more ; this condition was accompanied by a large clean-up and by very big currents up to 4 amperes, which caused the appearance of globules of nickel ; the electrodes finally fused. They suggest the possibility that nickel is a catalytic agent in an action of this sort. Gauger ‡ finds indication of the existence of a nickel-hydrogen complex by observation of the critical potentials of hydrogen in the presence of nickel, and so accounts for the catalytic influence of nickel in the chemical reactions of hydrogen.

Compton and Turner § have found spectroscopic evidence of the existence of a mercury hydride in a discharge-tube containing mercury and hydrogen.

It seems most probable that the gas which collects in the liquid air is to be identified with some kind of hydrogen-metal

* J. J. Thomson, 'Rays of Positive Electricity'; Foote & Mohler, Bureau of Standards, 400, p. 669, vol. xvi.

† Compton & Duffendack, Phys. Rev. May 1924, p. 85.

‡ Gauger, Journ. Amer. Chem. Soc. March 1924.

§ Compton & Turner, Phil. Mag. August 1924.

compound, and is stable at low temperatures, but dissociates spontaneously when the temperature is raised, for the gas which is liberated appears to be ordinary hydrogen. It is not likely that an unstable compound of this description would show the definite ionization effects seen in the tube; also gas is condensed in the collecting-tube in the absence of the disappearing glow effect. It therefore seems reasonable to conclude that several actions occur in the tube simultaneously:—

(*a*) Hydrogen acts on the filament to form an endothermic compound with tungsten, stable at high temperatures. (Return of pressure.)

(*b*) The conditions favour the production of negative ions, which combine with

(1) one or several of the metals present, to form a compound or compounds stable at liquid-air temperature but unstable at ordinary temperatures (possibly identical with (*a*)) ;

(2) positive hydrogen ions, to form a large hydrogen molecule such as H_3, which is not ionized until the grid potential reaches a value between 42 and 51 volts. On this view, H_3 must be considerably stable under these conditions, and must be more difficult to ionize than H_2. This is surprising, but is in accordance with the deductions of H. S. Allen * from his static models of H_2 and H_3. He calculates that a potential of 46 volts would be necessary for the complete disintegration of a molecule of H_3. Smyth †, in his recent work on positive rays, has found under certain conditions a preponderance of H_2^- ions, and at the same time distinct evidence of a considerable number of H_3^+ ions.

(4) *Oscillations.*

It does not seem possible at present to find a satisfactory explanation of the oscillations with only the results we have so far obtained ; further investigations are necessary. It is certain that large quantities of carbon compounds are in the oscillating-tube, since they show their presence in the other glass tube by their condensation in liquid air and decomposition by a high voltage, giving an increase in gas-pressure (Table III.). The slow oscillation at low voltage would suggest that it was due to the periodic formation and decomposition of such substances, but it is difficult to reconcile this hypothesis with the very rapid oscillations at high

* H. S. Allen, Proc. Roy. Soc. Edin. xliii. No. 13 (1922–23).

† H. D. Smyth, 'Nature,' July 26th, 1924.

voltage. The latter suggest some kind of oscillation due to the fall of potential between the grid and filament as a result of the large current, but again it is difficult to apply such a hypothesis to a slow oscillation with a period of several minutes, when the glow is already present. It seems necessary to investigate more fully the conditions for the production of these oscillations, and why they were only produced with one set of electrodes. We shall be glad if other investigators can throw light on their mechanism.

Cavendish Laboratory,
Cambridge,
August 1924.

XCV. *On the Coefficient of Performance of Refrigerating Machines employing Throttle Expansion.* *By* Alfred W. Porter, *D.Sc., F.R.S., F.Inst.P., Professor of Physics in the University of London* *.

WHEN comparison is made between two cases of mechanical refrigeration in one of which the cooling is produced by cylinder expansion and in the other by throttle expansion but in which all else is the same in both, the coefficient of performance is less in the throttle case than in the other for two reasons :

i. More work is required to keep the fluid in circulation.

ii. Less heat can be removed from the cold stores.

This can be explained by aid of pressure-volume and temperature-entropy diagrams.

Sketch diagrams are shown in figs. 1 and 2. The points in fig. 2 which correspond to points in fig. 1 are marked with accented letters.

When cylinder expansion is used the refrigeration per cycle is $\frac{DA}{EF} \times$ latent heat at T_2 or $D'A' \times T_2$ where D′ is vertically below C′ ; while the work required for circulation is

area DABC or D′A′B′C′.

Hence the coefficient of performance is

$$\frac{D'A' \times T_2}{\text{Area } D'A'B'C'}.$$

If, however, expansion through a throttle takes place at

* Communicated by the Author.

C the state after expansion is indicated by a point H′ (or H) where H′ and H are to the right of D′ and D, since the entropy increases in the expansion, although the change is

Fig. 1.—Pressure-volume diagram.

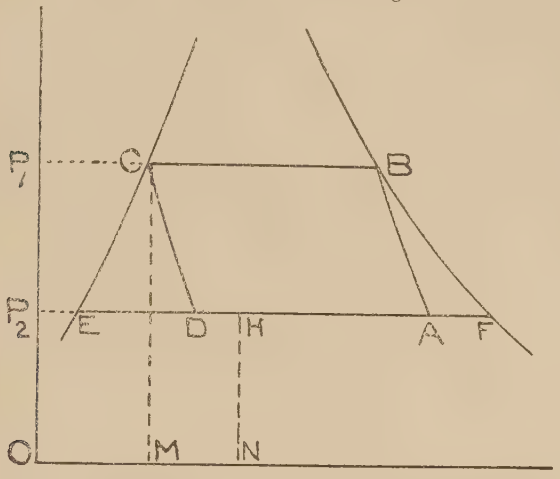

Fig. 2.—Temperature-entropy diagram.

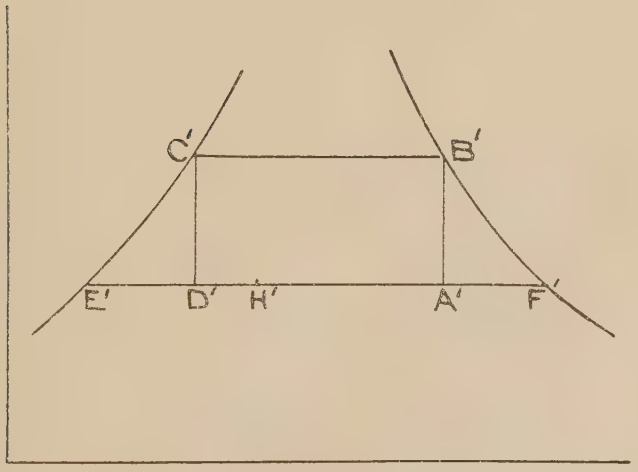

adiabatic, by an amount calculable from the frictional heat in the throttle. The refrigeration per cycle is now only

$$\frac{HA}{EF} \times \text{latent heat at } T_2$$

or $H'A' \times T_2$.

It is not quite so obvious how the work of circulation is increased, but an examination of the heat entry round the cycle will make it clear.

Let the heat given out to the condenser in each case be H_1 while the refrigeration is H_2 in the cylinder case and H_2' when the throttle is used. Then by applying the law of the conservation of energy to the complete cycle we have, since the paths AB and CD or CH are adiabatic:

Cylinder case: W = work of circulation $= H_1 - H_2$.
Throttle case: $W' =$,, ,, ,, $= H_1 - H_2'$.

But H_2' being less than H_2 it follows that W′ is greater than W by an equal amount. If this excess $W' - W = w$ (say) we have

	Cylinder case.	Throttle case.
Coeff. of performance ...	$\frac{H_2}{W}$	$\frac{H_2 - w}{W + w}$.

Thus it appears that w plays a two-fold function detrimental to effectiveness.

Calculation of w.

The principal part of this note is concerned with the exact calculation of w. It is usually stated that the point H′ can be determined by making $D'H' \times T_2$ equal to the approximately triangular area E′C′D′. In a contribution which I made to Hal Williams' 'Mechanical Refrigeration' (Whittaker & Co., 1903) I indicated that this is not correct and may only give about half the true value of the correcting term w. No proof was given of this and I now supply this proof.

The characteristic of adiabatic throttle expansion is that $E + pv$ is the same before and after the expansion, where E is the internal energy, p the pressure, and v the specific volume. The external work done in the expansion is therefore $p_2v_2 - p_1v_1$. In the cylinder case, the external work is represented by the area underlying the path traversed on the p,v diagram. Hence

	External work.
Cylinder ...	CDHNM
Throttle ...	$p_2v_2 - p_1v_1 = P_2HNO - P_1CMO$.

The difference w equals

$$CDHNM + P_1CMO + ONHP_2 = P_1CDP_2.$$

Now this is greater than ECD (the value usually taken) by the area P_1CEP_2. Hence to determine the point H_1 on the

entropy diagram we must make $D'H' \times T_2 =$ area P_1CDP_2 on the p–v diagram. This area is bounded on one side by the cylinder adiabatic CD. To avoid calculating the form of such an adiabatic the area can be represented as

$$P_1CEP_2 + CDE.$$

But CDE = C′D′E′ because both these areas correspond to the work done in the same possible reversible cycle. But the path C′D′ on the entropy diagram is vertical and consequently the point D′ is easily determined.

The area P_1CEP_2 must however be obtained from a p,v chart. Using Behn's values for the border curve of carbon dioxide I obtain the following values for the area, reckoning from 0° F. as origin. The values are given both in British and in C.G.S. units.

Area P_1CEP_2.

Temp. F.	B.T.U. / lb.	Temp. C.	Gram. Cal. / gram.
70	1·85	20	·98
60	1·48	15	·81
50	1·19	10	·67
40	·87	5	·50
32	·65	0	·35
30	·61	− 5	·22
20	·36	−10	·12
10	·15	−15	·06
0	0	−20	0

The area P_1CEP_2 corresponding to any particular range of temperature is obtained from the above by taking the difference of the values for the extreme temperatures. For example :—

Condenser temp. ... 70° F.
Refrigerator „ ... 5° F.
} Area = 1·85 − ·075 = 1·775 B.T.U. per lb.

Condenser temp. ... 20° C.
Refrigerator „ −15° C.
} Area = ·98 − ·06 = 0·92 gr.cal. per gr.

To the value calculated in this way must be added the thermal equivalent of the area C′D′E′ which is the area usually taken into account. From the temperature-entropy chart of Jenkins and Pye (Trans. Roy. Soc. Lond. A, 215. p. 361) this can be calculated with sufficient accuracy for any

fall of temperature lying between $+20°$ C. and $-20°$ C. (or $+70°$ F. and $0°$ F.) by the following simple formulæ:

Area C′D′E′ { in cal. per gram ... ·00106 (fall of temp. C.)². in B.T.U. per lb. . ·00059 (fall of temp. F.)².

Example:

Condenser temp. 70° F. Refrigerator temp. 5° F.

Area P_1CEP_2	1·775	B.T.U. per lb.
Area C′D′E′	2·493	„ „
Total w	4·268	

Cylinder coefficient of performance $\frac{460+5}{65}=7·15$,

or $\frac{H_2}{W}=\frac{53}{7·41}=7·15$,

as read off an entropy chart.

In the case of throttle expansion we have instead

$$\text{coeff. of performance}=\frac{H_2-w}{W+w}=\frac{53-4·27}{7·41+4·27}=4·2.$$

The usual calculation would give 5·1 instead, that is 21 per cent. in excess of the true value.

XCVI. *Quantum Defect and Atomic Number.*—II. *The Ionizing Potentials of the Rare Gases and of the Halogen Acids. By* Louis A. Turner, *M.A., Ph.D., Charlotte Elizabeth Procter Fellow in Physics, Princeton University* *.

IF ν is the value of a spectroscopic term, the quantity x defined by the equation $\nu=R/x^2$, where R is the Rydberg constant, is called the effective quantum number, by analogy with Bohr's theory of the hydrogen atom. If n be the total quantum number of the electron orbit corresponding to the term, the difference $n-x=q$ is defined as the quantum defect.

In a previous paper † I have shown that the asymptotic value of this quantum defect, which it approaches for the smaller term values of a series of terms, is a linear function of the atomic number for corresponding series of elements of the same chemical sub-group, provided that the quantum

* Communicated by the Author.

† Louis A. Turner, Phil. Mag. xlviii. p. 384 (1924).

numbers assigned by Bohr be increased for elements of high atomic number. An approximate relationship of the same sort holds for the quantum defects computed from the largest terms of the series, since these do not differ greatly from the asymptotic value and the deviation is usually in the same direction. These largest term values are the ones, however, which are proportional to the ionizing potentials of the elements considered. The value of x, the effective quantum number for the largest term, can be computed from the relation $V_i = 13{\cdot}53/x^2$, V_i being the ionizing potential, and 13·53 being the value of the Rydberg constant expressed in volts, *i.e.* the ionizing potential of the hydrogen atom.

Recent measurements of the ionizing potentials of the rare gases by Hertz * and Déjardin † present the opportunity for a further test of the linear relation between the quantum defects. Their results for the ionizing potentials are given in Table I.

TABLE I.

Ionizing Potentials.

	Hertz.	Déjardin.
Ne.....	21·5±0·12	
Ar.....	15·3±0·12	15·2±0·2
Kr.....	...	12·7±0·2
Xe.....	...	10·9±0·2

The values of x and q computed from these data are given in Table II. Bohr's quantum numbers are used for Ne and Ar, but that for Kr has been increased by 1 and that for Xe by 2, in accord with the changes made in the quantum numbers for the neighbouring elements, discussed in the previous paper.

TABLE II.

Element.	At. No.	V.	x.	n.	q.
Ne	10	21·5±0·12	0·792±0·003	2	1·208±0·003
Ar	18	15·2±0·2	0·942±0·006	3	2·058±0·006
Kr	36	12·7±0·2	1·030±0·009	5	3·970±0·009
Xe	54	10·9±0·2	1·111±0·010	7	5·889±0·010

These values of q are plotted in the diagram, the line AA′ being drawn through them. It has the slope 1·065. The corresponding line obtained from the asymptotic values of the quantum defect of the series of the alkali metals has the slope 1·068. A point corresponding to the ionizing potential of

* G. Hertz, *Zeit. f. Phys.* xviii. p. 307 (1923).
† G. Déjardin, *C. R.* clxxviii. p. 1069 (1924).

helium does not lie on the line, as would be expected. By extrapolation the ionizing potential of Nt of atomic number 86 can be predicted. The quantum defect predicted is $9{\cdot}30 \pm 0{\cdot}02$, which corresponds to an ionizing potential of $27{\cdot}5 \pm 1{\cdot}5$ volts if the quantum number is taken to be 10 in agreement with the quantum number of 11 found to be best for the valence electron of Ra. If the quantum number for Nt is taken to be 11 the ionizing potential predicted is $4{\cdot}66 \pm 0{\cdot}11$ volts. An experimental determination of this

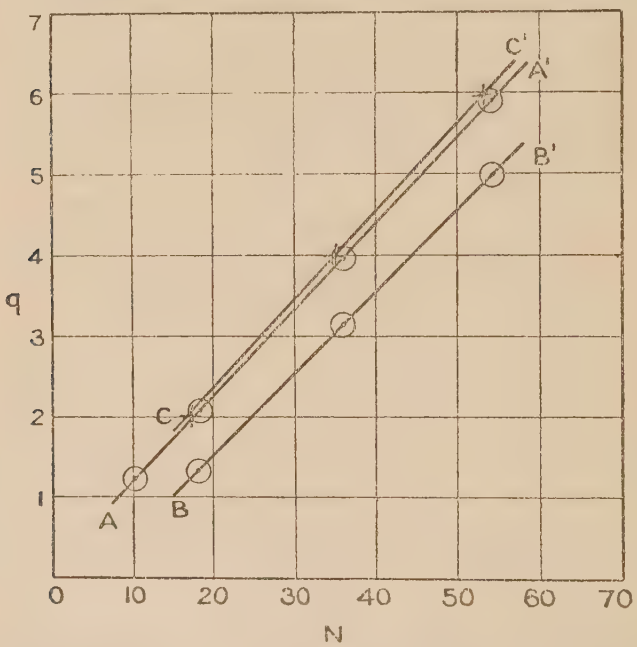

quantity is greatly to be desired. It would show whether or not this great extrapolation of the linear relation is valid.

Radiating potentials for these elements have been determined by Hertz * and Sponer †. The difference between the ionizing potential and a radiating potential of an element gives the value in volts of the spectroscopic term corresponding to the upper level involved in the radiating potential transfer. I have tried to find relations between the quantum defects calculated for these higher levels, but without success. Apparently the transitions are not entirely analogous for all these atoms. It should be noted that experimental errors would introduce very large relative discrepancies in these

* G. Hertz, loc. cit.

† H. Sponer, *Zeit. f. Phys.* xviii. p. 249 (1923).

term values because of the relatively small differences between the radiating and ionizing potentials.

Déjardin has also determined the critical potential for the appearance of the blue spectrum of Ar, and for the analogous phenomena with Kr and Xe. He attributes the production of these spectra to the double ionization of the atoms. If that hypothesis be correct, the difference between this second critical potential and the ionizing potential of the atom gives the ionizing potential corresponding to the removal of the second electron after the first has already been removed. Table III. gives the data and the quantum defects computed from them. In this computation a value of the Rydberg constant four times that for neutral atoms has been used.

TABLE III.

Element.	Second critical potential.	Second V_i.	x.	n.	q.
Ar	34·0±0·5	18·8±0·5	1·691±0·020	3	1·309±0·020
Kr	28·2±0·5	15·5±0·5	1·866±0·030	5	3·134±0·030
Xe	24·2±0·5	13·3±0·5	2·041±0·046	7	4·986±0·046

These data are plotted in the figure, the line BB′ being drawn through the points. The slope of the line BB′ is slightly less than that of AA′. It comes much further below AA′ than was the case with similar pairs of lines from the spectrum data discussed in the previous paper.

By extrapolation the second ionizing potential of Ne is predicted to be 23·7±1·2 volts, and the potential for double ionization or appearance of a second spectrum 45·2±1·2 volts. Déjardin points out that this second critical potential is within experimental error equal to 2·22 times the first ionizing potential for Ar, Kr, and Xe. Using that relation, one can predict a value of 47·7±0·5 for Ne. Experiment will have to decide whether either of these predicted values is correct.

C. A. Mackay * has recently determined values of the ionizing potentials of the halogen acid molecules HCl, HBr, and HI. His data and the quantum defects computed from them are given in Table IV.

TABLE IV.

Molecule.	Atomic No.	V_i.	x.	n.	q.
HCl	17	13·8±0·2	0·989±0·008	3	2·011±0·008
HBr	35	13·2±0·2	1·010±0·008	5	3·990±0·008
HI	53	12·8±0·2	1·027±0·008	7	5·973±0·008

* C. A. Mackay, Phil. Mag. xlvi. p. 828 (1923).

The quantum numbers are the same as those used for the corresponding rare gases. The values of q are plotted in the figure and the line CC′ drawn through the points. The fact that the line lies so close to the line AA″ for the noble gases may be taken to be one more bit of evidence favouring the hypothesis that the ionization of one of these molecules consists in the removal of one of the electrons of the halogen atom rather than the splitting up of the molecule into a positive H ion and a negative halogen ion. By extrapolation the ionizing potential of HF is computed to be $17{\cdot}9 \pm 0{\cdot}5$ volts.

Summary.

It is shown that there is a linear relation between the atomic number and the quantum defects computed from the ionizing potentials of the rare gases, from the second ionizing potentials of the rare gases, and from the ionizing potentials of the hydrogen halide molecules.

The following critical potentials are predicted on the basis af these relations: ionizing potential of Nt, $27{\cdot}5 \pm 1{\cdot}5$ volts; appearance of a "blue" spectrum of Ne, $45{\cdot}2 \pm 1{\cdot}2$ volts; ionizing potential of HF, $17{\cdot}9 \pm 0{\cdot}5$ volts.

Palmer Physical Laboratory,
Princeton, New Jersey, U.S.A.
May 28, 1924.

XCVII. *The Effect of a Hole in a Bent Plate.* *By* W. G. Bickley, *M.Sc., Lecturer in Mathematics, Battersea Polytechnic* *.

1.

In a recent paper † the effect of a circular hole in a tension member on the distribution of stress is studied experimentally, and it is found that the stresses are considerably enhanced (to about three times the average) at points on the boundary of the hole. In an appendix, a mathematical investigation, limited to the case of an infinitely wide plate, is given, and the experimental results are in close agreement with this, notwithstanding the use of members of finite width. It occurred to the author that a corresponding mathematical investigation of the stresses near a hole in a *bent* plate might also be of some importance as similarly enhanced values of the stresses are to be expected, and some indication of their amount would be obtained. The present paper contains the results of this investigation.

* Communicated by the Author.

† Coker, Chakko, and Satake, Trans. Inst. of Engineers and Shipbuilders in Scotland, 1919.

2.

Referred to polar coordinates, r, θ, in the plane of the plate, and denoting by z the distance from the central surface, the equations for the stresses, in terms of w, the displacement of the central surface, are * :—

$$\nabla^2 w = 0, \quad . \quad . \quad . \quad . \quad . \quad . \quad . \quad . \quad . \quad . \quad . \quad . \quad (2.1)$$

$$-\widehat{rr} = \frac{Ez}{1-\sigma^2}\left[\left\{\frac{\partial^2}{\partial r^2} + \sigma\left(\frac{1}{r}\frac{\partial}{\partial r} + \frac{1}{r^2}\frac{\partial^2}{\partial \theta^2}\right)\right\} - \left(h^2 - \frac{2-\sigma}{6}z^2\right)\left(\frac{1}{r}\frac{\partial}{\partial r} + \frac{1}{r^2}\frac{\partial^2}{\partial \theta^2}\right)\nabla^2\right] w, \quad (2.21)$$

$$-\widehat{\theta\theta} = \frac{Ez}{1-\sigma^2}\left[\sigma\frac{\partial^2}{\partial r^2} + \frac{1}{r}\frac{\partial}{\partial r} + \frac{1}{r^2}\frac{\partial^2}{\partial \theta^2} - \left(h^2 - \frac{2-\sigma}{6}z^2\right)\frac{\partial^2}{\partial r^2}\cdot\nabla^2\right] w, \quad (2.22)$$

$$-\widehat{r\theta} = \frac{Ez}{1-\sigma^2}\frac{\partial}{\partial r}\left[(1-\sigma)\frac{1}{r}\frac{\partial}{\partial \theta} + \left(h^2 - \frac{2-\sigma}{6}z^2\right)\frac{1}{r}\frac{\partial}{\partial \theta}\nabla^2\right] w, \quad . \quad (2.23)$$

$$-\widehat{rz} = \frac{E(h^2-z^2)}{2(1-\sigma^2)}\frac{\partial}{\partial r}(\nabla^2 w), \quad . \quad . \quad . \quad . \quad . \quad . \quad . \quad (2.24)$$

$$-\widehat{\theta z} = \frac{E(h^2-z^2)}{2(1-\sigma^2)}\frac{1}{r}\frac{\partial}{\partial \theta}(\nabla^2 w), \quad . \quad . \quad . \quad . \quad . \quad . \quad . \quad (2.25)$$

$$N = -D\frac{\partial}{\partial r}(\nabla^2 w), \quad . \quad . \quad . \quad . \quad . \quad . \quad . \quad . \quad . \quad . \quad . \quad (2.31)$$

$$G = -D\nabla^2 w + D(1-\sigma)\left(\frac{1}{r^2}\frac{\partial^2}{\partial \theta^2} + \frac{1}{r}\frac{\partial}{\partial r}\right)\left(w + \frac{8+\sigma}{10(1-\sigma)}h^2\nabla^2 w\right), \quad . \quad . \quad . \quad . \quad (2.32)$$

$$H = D(1-\sigma)\frac{\partial}{\partial r}\left\{\frac{1}{r}\frac{\partial}{\partial \theta}\left(w + \frac{8+\sigma}{10(1-\sigma)}h^2\nabla^2 w\right)\right\}, \quad . \quad (2.33)$$

where

E = Young's Modulus,
σ = Poisson's ratio,
$2h$ = thickness of plate,
$D = 2Eh^2/3(1-\sigma^2)$.

* Love, 'Mathematical Theory of Elasticity,' 3rd ed., p. 479.

These formulæ assume that the plate is bent to a state of "generalized plane stress," *i.e.* that $\widehat{zz}$ vanishes everywhere, and that $\widehat{rz}$ and $\widehat{\theta z}$ vanish at the surface, $z=\pm h$. They are not sufficiently general to ensure that the cylindrical boundary is *entirely* free from stress; but these residual stresses are small, and it *is* possible to obtain a solution which makes the resultant force and couple on any small element of the boundary, standing on an arc $\delta\theta$, vanish. To secure this, the boundary conditions are

$$\left.\begin{aligned} \mathrm{G}&=0,\\ \mathrm{N}-\frac{1}{r}\frac{d\mathrm{H}}{d\theta}&=0.\end{aligned}\right\} \quad . \quad . \quad . \quad . \quad . \quad . \quad (2.4)$$

If the plate is complete, and bent so that the curvature of the x axis is k, the y axis will, in the absence of any bending couple in the yz plane, have an "anticlastic" curvature σk. (x and y are rectangular coordinates.) We shall then have for w the formula

$$\left.\begin{aligned} w_1&=\tfrac{1}{2}k(x^2-\sigma y^2)\\ &=\tfrac{1}{4}kr^2\{(1-\sigma)+(1+\sigma)\cos 2\theta\},\end{aligned}\right\} \quad . \quad . \quad (2.5)$$

and then

$$\widehat{xx}=-k\mathrm{E}z, \quad \widehat{yy}=0=\widehat{xy},$$

so that the maximum tensile or compressive stress is $k\mathrm{E}h$. The contour lines of the bent middle surface given by (2.5) are a family of hyperbolas with the common asymptotes $x=\pm\sqrt{\sigma}y$.

We may also consider the case of a plate bent into a cylinder of curvature k, in which case

$$w_1=\tfrac{1}{2}kx^2=\tfrac{1}{4}kr^2(1+\cos 2\theta). \quad . \quad . \quad . \quad (2.51)$$

This necessitates a couple in the yz plane as well as in the xz plane. Both cases may be included in the formula

$$w'=\tfrac{1}{4}kr^2(\alpha+\beta\cos 2\theta) \quad . \quad . \quad . \quad . \quad . \quad (2.52)$$

3.

Denoting the radius of the hole by a, we have a solution of 2.1 which tends to 2.52 when r is large,

$$\begin{aligned} w&=w_1+w_2\\ &=\tfrac{1}{4}k\left[\alpha r^2+\mathrm{A}a^2.\log r/a+\cos 2\theta\left(\beta r^2+\mathrm{C}a^2+\mathrm{F}\frac{a^4}{r^2}\right)\right], \end{aligned}$$

$$. \quad . \quad . \quad . \quad (3.1)$$

from which we derive, by equations 2.3 ...

$$G=-\tfrac{1}{4}kD\left[\alpha(1-\sigma)-(1-\sigma)A\frac{a^2}{r^2}+\cos 2\theta\,.\left\{2\beta(1-\sigma)\right.\right.$$
$$\left.\left.-4C\left(\sigma\frac{a^2}{r^2}+\frac{3(8+\sigma)}{5}\frac{h^2a^2}{r^4}\right)+6F(1-\sigma)\frac{a^4}{r^4}\right\}\right], \quad . \quad (3.21)$$

$$N-\frac{dH}{r\,.\,d\theta}=\tfrac{1}{4}kD\frac{\cos 2\theta}{r}\left[4\beta(1-\sigma)\right.$$
$$\left.-4C\left\{(3-\sigma)-\frac{6(8+\sigma)}{5}\frac{h^2a^2}{r^4}\right\}-12F(1-\sigma)\frac{a^4}{r^4}\right].$$
$$. \quad . \quad . \quad . \quad (3.22)$$

The identical vanishing of these when $r=a$ leads to :—

$$\left.\begin{aligned}&2\alpha(1-\sigma)-(1-\sigma)A=0,\\&2\beta(1-\sigma)\\&\quad-4C\left\{\sigma+\frac{3(8+\sigma)}{5}\frac{h^2}{a^2}\right\}+6F(1-\sigma)=0,\\&4\beta(1-\sigma)\\&\quad-4C\left\{(3-\sigma)-\frac{6(8+\sigma)}{5}\frac{h^2}{a^2}\right\}-12F(1-\sigma)=0.\end{aligned}\right\}\ .\ (3.31)$$

Solving these, we obtain :—

$$\left.\begin{aligned}A&=\frac{2\alpha(1+\sigma)}{1-\sigma}, \qquad C=\frac{2\beta(1-\sigma),}{3+\sigma}\\F&=-\frac{\beta(1-\sigma)}{3+\sigma}+\frac{4\beta(8+\sigma)}{5(3+\sigma)}\frac{h^2}{a^2}.\end{aligned}\right\}\ .\ .\quad (3.32)$$

Thus the displacement due to the hole is :—

$$w_2=\tfrac{1}{4}k\left[\frac{2\alpha(1+\sigma)}{1-\sigma}a^2.\log r/a+\left\{\frac{2\beta(1-\sigma)}{3+\sigma}a^2\right.\right.$$
$$\left.\left.-\frac{\beta(1-\sigma)}{3+6}\frac{a^4}{r^2}+\frac{4\beta\ 8+\sigma)}{5(3+\sigma)}\frac{h^2a^2}{r^4}\right\}\cos 2\theta\right]. \ .\quad (3.4)$$

Some concern may be felt upon noticing that this makes w_2 infinite at infinity ; but a moment's reflexion will show that our formula also makes w_1 infinite there, and that w_2 is small compared with w_1, for moderate or large values of r/a ; the formula may be relied upon near the hole, and the stresses derived from it accepted as valid.

By means of this formula, the "relative contours" ($w_2=$ constant) may be plotted, and they are given in figs. 1 and 2 for the anticlastic and cylindrical cases respectively. The value of σ used in the calculations is 0·28 (*i. e.* a common value for steel), and the unit chosen is the displacement at

$(a, 0)$ in the absence of the hole; $\frac{1}{2}ka^2$. The actual contour lines, w=constant, are given in figs. 3 and 4 respectively, and the values of w along the x and y axes are plotted in fig. 5. In the last, curves I. are for a complete plate, II. for the anticlastic case, and III. for the cylindrical case.

Fig. 1.

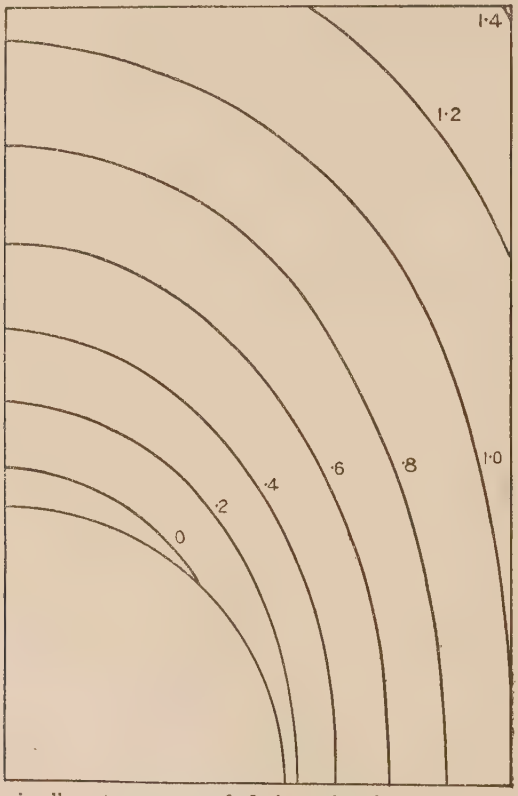

"Relative" contours near a hole in a plate bent anticlastically.

4.

We now turn to the consideration of the stresses as calculated from these displacement formulæ. For the anticlastic case, using the appropriate values of α and β in (3.4) and inserting in equations (2.2) ...., we get

$$\widehat{rr} = -kEz\left[\tfrac{1}{2}(1-\frac{a^2}{r^2}+\cos 2\theta\left\{\tfrac{1}{2}-\frac{2\sigma}{3+\sigma}\frac{a^2}{r^2}\right.\right.$$
$$\left.\left.-\frac{3(1-\sigma)}{2(3+\sigma)}\frac{a^4}{r^4}-\frac{6(2-\sigma)}{3+\sigma}\frac{a^2}{r^4}\left(\frac{h^2}{5}-\frac{z^2}{3}\right)\right\}\right], \quad . \quad (4.11)$$

$$\widehat{\theta\theta} = -kEz\left[\tfrac{1}{2}\left(1-\frac{a^2}{r^2}\right) - \cos 2\theta\left\{\tfrac{1}{2}+\frac{2}{3+\sigma}\frac{a^2}{r^2}\right.\right.$$
$$\left.\left.+\frac{3(1-\sigma)}{2(3+\sigma)}\frac{a^4}{r^4}+\frac{6(2-\sigma)}{3+\sigma}\frac{a^2}{r^4}\left(\frac{h^2}{5}-\frac{z^2}{3}\right)\right\}\right], \quad . \quad (4.12)$$

Fig. 2.

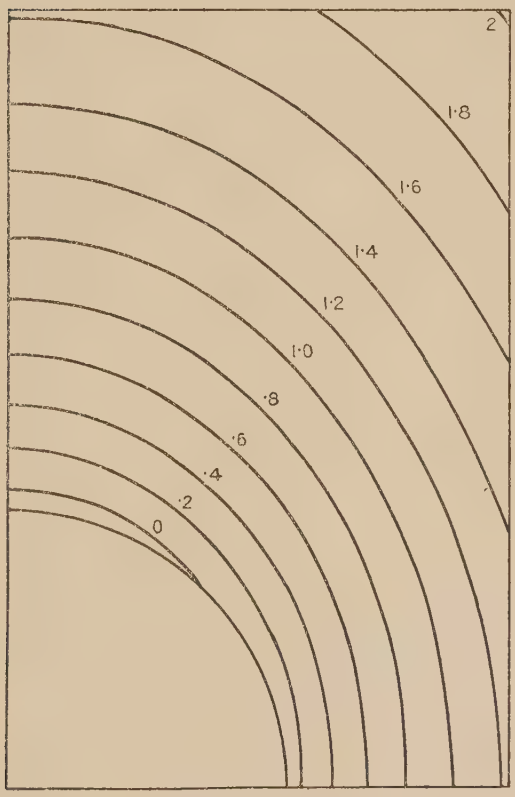

"Relative" contours near a hole in a plate bent into a cylinder.

$$\widehat{r\theta} = kEz \,.\, \sin 2\theta\left[\tfrac{1}{2}-\frac{1-\sigma}{3+\sigma}\frac{a^2}{r^2}+\frac{3(1-\sigma)}{2(3+\sigma)}\frac{a^4}{r^4}\right.$$
$$\left.+\frac{6(2-\sigma)}{3+\sigma}\frac{a^2}{r^4}\left(\frac{h^2}{5}-\frac{z^2}{3}\right)\right], \quad . \quad (4.13)$$

$$\widehat{rz} = -\frac{2kE(h^2-z^2)}{3+\sigma}\frac{a^2}{r^2}\cos 2\theta, \quad . \quad . \quad . \quad . \quad . \quad . \quad . \quad (4.14)$$

$$\widehat{\theta z} = -\frac{2kE(h^2-z^2)}{3+\sigma}\frac{a^2}{r^2}\sin 2\theta. \quad . \quad . \quad . \quad . \quad . \quad . \quad . \quad (4.15)$$

These stresses do not vanish identically when $r=a$, *i. e.* at

the edge of the hole. In fact, the values there are :—

$$\widehat{rr}_e = kEz\frac{6(2-\sigma)}{3+\sigma}\left(\frac{h^2}{5}-\frac{z^2}{3}\right)\frac{\cos 2\theta}{a^2},$$

$$\widehat{\theta\theta}_e = -kEz\left[1-\frac{5-\sigma}{3+\sigma}\cos 2\theta - \frac{6(2-\sigma)}{3+\sigma}\left(\frac{h^2}{5}-\frac{z^2}{3}\right)\frac{\cos 2\theta}{a^2}\right],$$

Fig. 3.

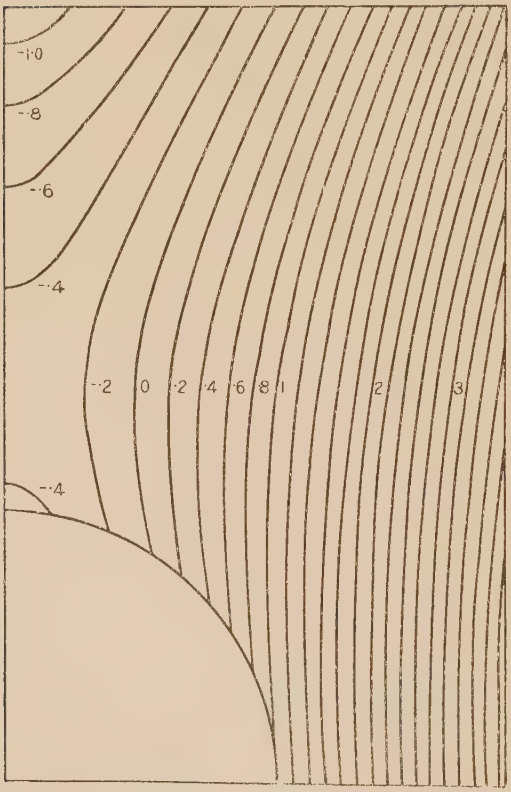

Contours near a hole in a plate bent anticlastically.

$$\widehat{r\theta}_e = kEz\sin 2\theta\left[\frac{2}{3+\sigma}+\frac{6(2-\sigma)}{3+\sigma}\left(\frac{h^2}{5}-\frac{z^2}{3}\right)\frac{1}{a^2}\right],$$

$$\widehat{rz}_e = -\frac{2kE(h^2-z^2)}{3+\sigma}\frac{\cos 2\theta}{a}$$

$$\widehat{\theta z}_e = -\frac{2kE(h^2-z^2)}{3+\sigma}\frac{\sin 2\theta}{a}$$

From an examination of these formulæ, the general effect of the hole can be obtained, and also the limitations of the solution which are, of course, due to the simplifying assumption of a state of "generalized plane stress."

$\widehat{rr}$ is seen to be of the order h^2/a^2, compared with the stress in the absence of the hole. In fact, its greatest value, which occurs on the boundary of the hole where $\theta=0$,

Fig. 4.

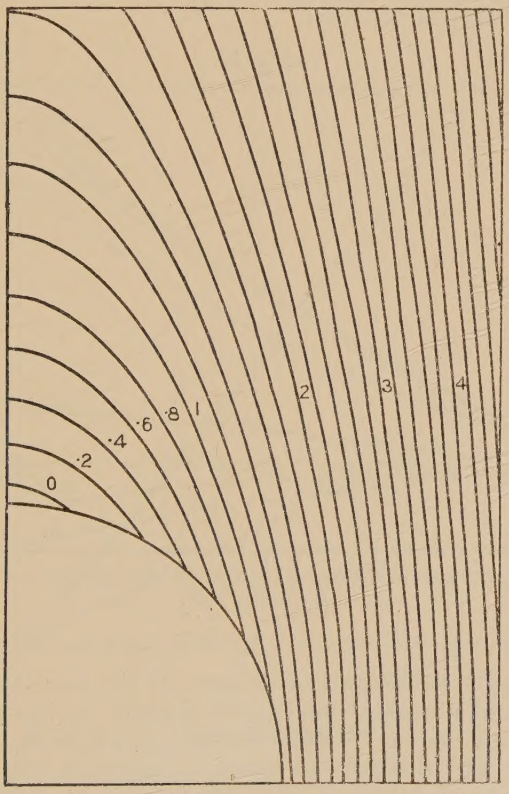

Contours near a hole in a plate bent into a cylinder.

and on the surface, is $0{\cdot}308\ h^2/a^2$ times this. ($\sigma=0{\cdot}28$, as before.)

$\widehat{\theta\theta}$ is comparatively large when $\theta=\pm 90°$. There, neglecting the h^2 term, its value is $-8k\mathrm{E}z/(3+\sigma)$, *i. e.* more than twice (2·44 times, if $\sigma=0{\cdot}28$) the stress in the absence of the hole. For a plate of finite width this value would probably be modified, but it is certain that the maximum

stress would still be much greater at the edge of the hole than that calculated upon the assumption of a uniform distribution along the radius perpendicular to the straight edges. In fig. 6 the values of $\widehat{\theta\theta_e}$ for values of z/h are plotted (I.) without taking into account the hole, (II.) neglecting h/a, and (III.) for $h/a=\frac{1}{2}$, *i. e.* radius of hole equal to thickness of plate. The effect of the h^2 term is seen to be very small. In fig. 7 the maximum stresses along the axes, neglecting the h^2 term, are given as fractions of the maximum stress, $k\mathrm{E}h$, in the absence of the hole.

Fig. 5.

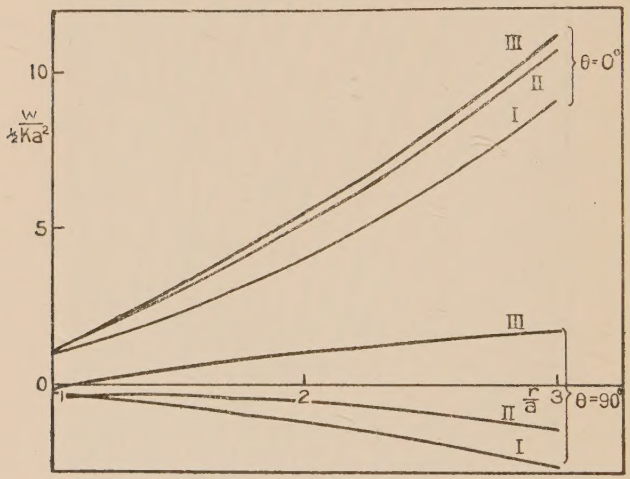

Displacements of the central surface of bent plates containing a circular hole.

5.

It remains to devote a small space to the consideration of the residual stresses at the edge of the hole, and to show that they form a system of zero resultant, to which St. Venant's Principle may therefore be applied. Consider the resultant tractions on an element $\delta\theta$ of the boundary. It is easy to verify that :—

$\int \widehat{rr_e}.dz=0$, *i. e.* there is no resultant radial traction.

$\int \widehat{rr_e}.z.dz=0$, *i. e.* there is no bending couple about a tangent to the circumference.

$\int -\widehat{r\theta_e}.dz=0$, *i. e.* there is no resultant tangential traction.

$\int -\widehat{r\theta_e} \,.\, z \,.\, dz = -2\mathrm{D}kh(1-\sigma^2)\sin 2\theta/(3+\sigma)$. This is a torsional couple, of amount $\mathrm{H} = -2\mathrm{D}kh(1-\sigma^2)\sin 2\theta/(3+\sigma)$ per unit length.

$\int \widehat{rz_e} \,.\, dz = -4\mathrm{D}kh(1-\sigma^2)\cos 2\theta/(3+\sigma)a$. This is a resultant shearing force per unit length. Now the torsional

Fig. 6.

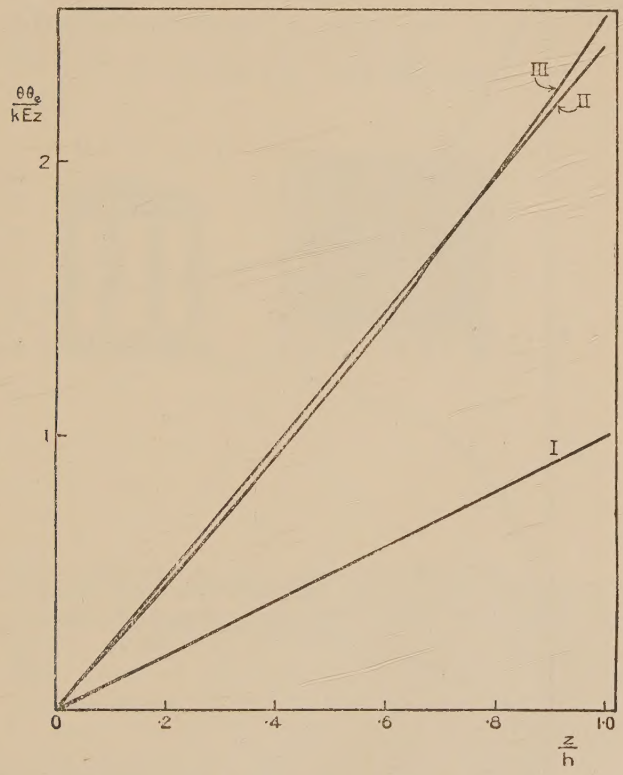

Stress $\theta\theta_e$ at 90°.

couple H can be considered as applied * by a distribution of shearing force

$$\mathrm{N}' = -d\mathrm{H}/a \,.\, d\theta = +4\mathrm{D}kh(1-\sigma^2)\cos 2\theta/(3+\sigma)a$$

per unit length. This exactly neutralizes N. We thus see that the residual tractions form a system in equilibrium for *any* small element $\delta\theta$ of the boundary, and consequently their effect is negligible at a small distance from the edge.

* See, for instance, Love, *loc. cit.* p. 466.

A further investigation, eliminating these residuals, might be interesting mathematically, but would be of little practical importance.

Fig. 7.

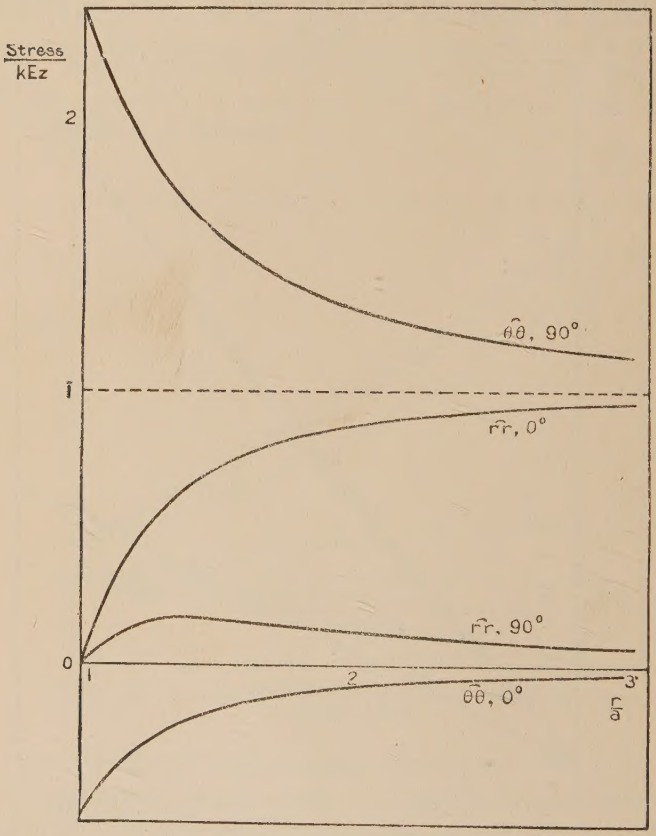

Maximum stresses along the axes.

A similar detailed treatment of the plate bent into a cylinder would lead to similar results, but we content ourselves with the contours and displacements along the axes, already given.

London,
February 1924.